ENHANCED SOIL STRUCTURING BENEATH WHITE CLOVER AND ITS IMPACT ON NUTRIENT TRANSPORT

Thesis submitted to the University of Plymouth in partial fulfilment for the degree of

DOCTOR OF PHILOSOPHY

Deborah Anne Lydia Holtham

Environmental and Fluid Modelling Group

School of Earth, Ocean and Environmental Sciences

University of Plymouth

Soil Science and Environmental Quality

North Wyke Research Station

Institute of Grassland & Environmental Research

July 2006

ABSTRACT

Deborah Anne Lydia Holtham

Enhanced soil structuring beneath white clover and its impact on nutrient transport

Previous work at IGER has revealed that soil structural differentiation under white clover is phenomenally rapid and enhanced when compared with ryegrass. White clover is one of the most nutritious and widely distributed forage legumes. Its use is advocated in sustainable systems of livestock production because of its ability to acquire atmospheric N through biological fixation in the root nodules. It thus provides an economically viable alternative to the N-demanding conventional system, and a possible solution to reduce the environmental impacts of nitrate leaching from agricultural land.

There are, however, potentially negative impacts associated with improving soil aggregation through the use of clover that need further investigation. It appears that legume-based systems are not environmentally benign: similar amounts of N and P are leached from beneath grass-clover swards as those leached from beneath fertilised grass operating at the same level of production. In some circumstances, clover rich swards can give rise to very high levels of nitrate leaching. Thus, this observation of clover induced soil aggregation has important implications for the pollutant transport qualities of soils and for the organic/conventional agriculture debate.

Re-packed soil columns of four soil series and 0.5 m intact monoliths of the Crediton series were planted with white clover, perennial ryegrass and a mixture of the two species, and managed according to an organic and conventional farming regime.

Visual observations revealed a rapid enhancement in soil structure beneath white clover compared to ryegrass and unplanted soil. A novel technique to determine oxygen diffusion as an indicator of soil porosity, gave a diffusion rate that was nearly nine times greater than that of the grass treatments and fifteen times greater than the unplanted control soil, with intermediate values for the mixed treatment. Thus enhanced structural differentiation beneath white clover was supported by greater permeability to air and freer drainage to water. Structural stability tests suggested that white clover improved the ability of the soil to maintain its structure under the action of water, and was estimated to be three times more stable than ryegrass. There was also evidence which implied improved shear strength and resistance to mechanical forces.

Differences in soil structure were verified with water retention measurements, which showed a greater proportion of macropores. The void structure was simulated with the 3D Pore-Cor network model, which also suggested a number of larger pores and a saturated hydraulic conductivity which was four times greater than ryegrass. This also highlighted inadequacies in the current standard ISO protocol for water retention.

The solute transport studies showed elevated levels of nitrate and phosphate leaching. Concomitant transport of bromide inferred structural differentiation and changes in leaching dynamics. In addition, white clover allowed the passage of greater volumes of water. Most importantly, this was manifested at the soil profile scale and therefore likely to be of consequence in the field.

The implications of the research are that enhanced soil structure beneath white clover alters the transport of gases, water, nutrients and other dissolved substances. Further understanding of these soil processes are needed before advocating the use of forage rich legumes in sustainable systems, and for the development of management strategies.

LIST OF CONTENTS

CHAPTER ONE – INTRODUCTION

CHAPTER TWO – METHODS AND MATERIALS – EXPERIMENTAL DESIGN

CHAPTER THREE – CHARACTERISATION OF SOIL PROPERTIES & SOIL STRUCTURE

CHAPTER SIX – SUMMARY, OVERVIEW & FUTURE WORK

LIST OF FIGURES

LIST OF TABLES

CHAPTER ONE

1. Introduction

1.1. Overview of thesis chapters

Chapter One – Introduction to the research.

This chapter introduces the research and its relevance. The aims, objectives and hypotheses are presented. Fundamental issues and theories discussed in literature are also presented.

Chapter Two – Methods, materials and experimental design.

The details on how the experimental systems were set-up are explained. The growth and maintenance of plants are presented.

Chapter Three – Soil characterisation and structural differentiation.

The first part of this chapter presents routine soil classification methods and results for soils prior to re-packing and plant growth. The second part of this chapter presents methods and results for the characterisation of changes in soil structure in re-packed soil columns after plant growth.

Chapter Four – Modelling water retention release data.

This chapter presents the methods and results of soil water retention characteristics, and the simulation of void structure and hydraulic conductivity using a 3-dimensional network model.

Chapter Five – Water release, nutrient and tracer transport.

This chapter presents detailed methods and results for water release and tracer transport studies in soils, both at the re-packed column and intact monolith scale.

Chapter Six – Summary, overview and future work

In this brief overview, the findings of this project that disprove or support each hypothesis are summarised. Suggestions for further work are also included.

1.2. Introduction to the research

There is great concern about the environmental impacts of agriculture and the consequent pressure for de-intensification throughout Western Europe. Achieving an effective balance between environmental protection and agricultural production requires understanding and management of soil processes. Soil structure strongly influences plant growth (Angers and Caron, 1998) and agricultural sustainability. Good soil structure is the basis of good agricultural production and for agriculture to be sustainable it is important that the soil resource is not degraded.

The factors associated with good soil aggregation include improved aeration and drainage leading to an active aerobic microflora, as well as improved root penetration, water holding and organic matter incorporation. These factors lead to improved nutrient availability to the plant and to improved plant yield. There is also evidence that in well structured soils nitrate leaching is reduced (Scholefield *et al.*, 1996) and that the soil's capacity to buffer watercourses is enhanced (Scholefield *et al.*, 1998).

However, many agricultural practices, such as high rates of fertilisation, use of heavy machinery and long term monocropping degrade soil aggregation and soil microbial diversity. In addition, inappropriate management can cause damage at a larger scale, e.g. eutrophication of surface water, impairment of water quality, destruction of aquatic habitats and emission of greenhouse gases (Ball *et al.*, 1997). Therefore, a plant-based system that can repair and rebuild soil aggregation has great potential benefit to sustainable systems.

Sustainable agriculture must also be economically viable. Unfortunately the economic targets of farmers cannot easily be reconciled with reduced use of fertilizers in conventional grassland systems. This has prompted a marked swing to 'organic'

2

production, which is based principally on the acquisition of nitrogenous compounds through biological fixation in the root nodules of legumes, notably white and red clover (*Trifolium*) species.

White clover is one of the most nutritious and widely distributed forage legumes (Duke, 1981). Its behaviour and contribution to pasture has been extensively studied but there has been relatively little interest in its below-ground behaviour (Cresswell *et al.*, 1999). Previous work at IGER has revealed that structural differentiation under white clover is phenomenally rapid and enhanced when compared with ryegrass (Mytton *et al.*, 1993). Figure 1.1 illustrates this effect. Although the mechanisms of aggregation are poorly understood, Scholefield *et al.* (2005) hypothesise two biological mechanisms driving the soil physical effects: (i) the nodal roots of white clover exert considerable force as they contract towards the soil causing soil particle movement and (ii) the enhanced *rhizobia* in presence of clover increases polysaccharide gum production and acts as a binding agent.

There are potentially negative impacts associated with improving soil aggregation through the use of clover that need further investigation. It appears that legume-based systems are not environmentally benign, as similar amounts of N and P are leached from beneath grass-clover swards as those leached from beneath fertilised grass operating at the same level of production (Tyson *et al.*, 1997; Cuttle *et al.*, 1998). In some circumstances, clover rich swards can give rise to very high levels of nitrate leaching (MacDuff *et al.*, 1990; Loiseau *et al.*, 2001).

Leaching of nitrogen (N) and phosphorus (P) species is determined not only by factors that control accumulation in the soil, but also by those that control transport during the leaching process (Scholefield *et al.*, 1993; Haygarth *et al.*, 1998a). Soil structural differentiation is thus a major control of both the proportion of accumulated nutrient that actually leaches

and the concentration at which it enters water bodies (Scholefield *et al.*, 1996). In general, nutrients that reside within the inter-aggregate micropores are likely to be relatively conserved by structural development, whereas nutrients that enter the soil in in-coming water are likely to be lost by leaching more readily.

Figure 1.1. Illustration of the potential effect of white clover on soil structure, in comparison with ryegrass (Mytton *et al.*, 1993).

1.3. Relevance of the research

The observation of clover induced soil aggregation (Mytton *et al.*, 1993) has received little further study to date. However, the significance of this novel observation is also being realised as part of the increasing appreciation of the importance of soil quality in the grassland sector. The focus of this research is the grass/clover-based pasture system. The research is novel in that it proposes mediation of soil processes by the plant and/or its

symbiont, and has relevance for soil management strategies in agricultural systems. The environmental modelling aspect of this project utilises an innovative three-dimensional network model and highlights the importance of high quality experimental data. The project promotes basic, strategic and applied research relevant to grassland and extensive agricultural systems whilst minimising adverse environmental consequences, and investigates the mechanisms of nutrient cycling at a range of scales (from the aggregate (mechanical stability), the re-packed soil core (structural visualisation, nutrient leaching and modelling) to the monolith lysimeter (leaching through intact soil profiles)). The project supports and promotes integrated, multidisciplinary research.

Much work has been done on aggregate stability, but the actual process of aggregation is poorly understood. This suggests that there is a major gap in our understanding of the dynamic processes of soil structuring that this study would help to fill. In addition, chemical movement through soil has generated much interest due to the concern about the quality of surface and ground waters. Agricultural practices involve significant chemical inputs over large landscape units; however, there is a poor understanding of water and solute transport in field soils (Quisenberry *et al.*, 1993). The importance of soil structural units in water and solute transport is recognised, yet describing these units in a way that would be useful for modelling transport is difficult (Quisenberry *et al.*, 1993). Thus, the knowledge gained from this research will improve our ability to describe transport phenomena in field soils, and has important implications for pollutant transport qualities of soils and for the organic/conventional agriculture debate.

1.4. Overall aims and context of the research

This research aimed to demonstrate that soil structure formation is more pronounced and rapid under white clover than under grass swards, and to assess the impact of such rapid re-structuring on water and nutrient transport. This study also aimed to assess the concomitant changes in nutrient leaching in order to achieve a balanced insight into the sustainability and environmental consequences of manipulating soil structure in agricultural systems.

This study has wider implications and effects beyond the scope of the present work, for example: the impacts of a well developed and stable soil aggregate structure in relation to other soil functions, such as fertility; buffering watercourses from pollutants and pathogenic organisms; storing and transmitting water to offset risk of land flooding; acting as a sink rather than source of biogenic greenhouse and pollutant gases; and, acting as a resilient bio-reactor and initiating biodiversity in the landscape.

The success of the research relied on producing and maintaining a supply of healthy, actively growing clover and grass plants established under replicated, controlled experimental conditions in well-characterised soil. The work was conducted by the author at both IGER and the University of Plymouth. Water retention data was obtained by the National Soils Resources Institute (NSRI) at Cranfield.

The project has also benefited from alignment with research conducted by Scholefield *et al.* (2005), where molecular microbiology and root studies were carried out to test hypotheses that structuring under white clover was due to forces exerted by contractile roots and stability of structure imbued by enhanced polysaccharide gum formation by rhizobium. Scholefield *et al.* (2005) also performed experiments to test hypotheses that impacts of enhanced structuring on nutrient leaching, soil organic matter accumulation and microbial diversity would all be beneficial.

1.5. Hypotheses

The project aimed to test the following hypotheses:

i.   White clover will enhance structural differentiation relative to perennial ryegrass and a fallow control.

ii. This enhanced soil structuring will increase both the amount and concentration of nitrate and phosphate leaching below the root zone.

iii. Nitrate, phosphate and bromide will have different transport behaviour and therefore elution profiles through the soil.

iv. The elution behaviour of nitrate, phosphate and bromide will depend on soil saturation conditions and the initial distribution of the eluting species prior to simulated rainfall.

v.   Analysis of the leaching results can be carried out semi-quantitatively by characterising the elution profiles.

vi. Differences will be identified at the core scale compared to the monolith scale; thus a spectrum of useful information will be obtained by using a wider range of samples at the core scale and studying detail of some samples at the monolith scale.

vii. Enhanced soil structuring under white clover will be detectable by changes in oxygen diffusion rates.

viii. Enhanced soil structuring under white clover will alter soil stability.

ix. Enhanced soil structuring under white clover will cause differences in water retention characteristics.

x.   The precise nature of soil structuring under white clover, in terms of the changes to the void network can be discovered by modelling water retention curves with the void network simulator Pore-Cor.

1.6. Objectives

The objectives of the project, designed to allow testing of the hypotheses, were as follows:

i. To demonstrate and characterise enhanced soil structural differentiation beneath white clover swards

- Produce and demonstrate enhanced soil structuring beneath white clover under controlled conditions.

- Characterise the resulting soil structure relative to that beneath perennial ryegrass, a mixture of the two species as found in a grassland system, and unplanted control soil.

- Conduct water retention measurements to indicate soil structure.

- Simulate soil structure using water retention data and the Pore-Cor 3-dimensional network model.

- Measure oxygen diffusion through soil using a novel electrochemical technique and hence infer soil porosity.

- Evaluate the stability of the aggregates to the action of internal and external forces.

ii. To evaluate and explain the impacts of such soil structure formation on the transport of gases, water and dissolved N and P compounds

- Conduct water retention measurements.

- Conduct water and nutrient flux studies.

- Compare the transport of nitrate and phosphate to that of the non-reactive tracer bromide.

- Calculate simulated hydraulic conductivity using the Pore-Cor 3-dimensional network model.

- Measure oxygen diffusion through soil using a novel electrochemical technique.

iii. To ascertain whether any of these impacts were manifested at the scale of the whole soil profile, rather than merely within the rhizosphere

- Compare re-packed soil core lysimeters to precision automated intact monolith lysimeters.

iv. To assess the implications for the sustainability of organic farming systems

- To comment on the consequences of manipulating soil structure in agricultural systems.

1.7. Background to the research

1.7.1. Soil structure

The term soil structure refers to the internal configuration of the soil matrix, and expresses a qualitative concept rather than a directly quantifiable property, as there is no truly objective or universally applicable method for its determination (Hillel, 1980, 1998; Niewczas and Witkowska-Walczak, 2005). In general, three broad categories of soil structure are recognised: single grained (loose or unconsolidated), massive (tightly packed cohesive blocks) and aggregated (quasi-stable small clods). The traditional descriptive methods for characterising the structure of soils are illustrated in Figure 1.2.

			1. **Angular blocky** – peds with sharp angular corners with flat, convex or concave faces, fairly tightly packed, middle horizons.
1 Angular blocky	2 Columnar	3 Crumb	2. **Columnar** – large, vertically elongated peds with vertical faces, middle horizons. 3. **Crumb** – irregular shaped peds with rough surfaces, form loose porous mass in upper horizons beneath grassland.
4 Granular	5 Lenticular	6 Massive	4. **Granular** – subspherical peds, form loose porous mass in upper horizons. 5. **Lenticular** - convex peds which overlap each other, common in compacted horizons. 6. **Massive** – coherent, with or without peds and pore space, lower horizons and underlying material.
7 Prismatic	8 Subangular blocky	9 Wedge	7. **Prismatic** – vertically elongated peds with vertical faces, medium or fine textured soils. 8. **Subangular blocky** – peds with convex or concave faces and rounded corners, middle horizons. 9. **Wedge** – wedge shaped peds with inter-sections of planer pores, middle horizons.

Figure 1.2. Some types of soil structure (after Fitzpatrick, 1986).

A well-developed and stable aggregated structure is the most desirable condition. These are important features of the soil tilth, an elusive agronomic qualitative description of a highly desirable physical condition in which soil is optimally loose, friable and contains a porous assemblage of stable aggregates, that permits free entry and movement of air and water, growth of roots and easy cultivation (Hillel, 1980, 1998; Niewczas and Witkowska-

Walczak, 2005). Poor soil structure and low aggregate size and stability enhance compaction of the soil surface, reduce infiltration rate and increase the potential for soil erosion (Sarah, 2005).

Thus, favourable soil structure and high aggregate stability are important factors for maintaining soil fertility and biodiversity, agronomic productivity and environmental quality control (Bronick and Lal, 2005). Soil structure has been the subject of much research. The literature abounds with reports of studies of aggregation and soil stability, but few studies have tried to explain the underlying mechanisms involved (Six *et al.*, 2004; De Gryze *et al.*, 2006).

Definitions of soil structure (Table 1.1) generally refer to the size, shape and distribution of the solid mass and pore space. However, definitions ignore the dynamic biological component (Jastrow and Miller, 1991) and should accommodate the many different aspects which exist at different size scales (Dexter, 1988). As noted by Bartoli *et al.* (1999), soil is a complex multiscale and hierarchical porous medium with aggregates ranging from nano- to micro- and macroscale. Figure 1.3 illustrates the magnitude of some soil structural features.

Perhaps newer definitions of soil structure will extend to the additional functions of the soil resource and its role in the moderation of environmental quality. Soils are now required to fulfil several additional functions, as mentioned above (Section 1.4), namely: buffering watercourses from pollutants and pathogenic organisms; storing and transmitting water to offset risk of land flooding; acting as a sink rather than source of biogenic greenhouse and pollutant gases; and, acting as a resilient bio-reactor and initiating biodiversity in the landscape. However, a well developed and stable soil aggregate structure may not be optimal for fulfilling all of these functions (Scholefield *et al.*, 2005).

Table 1.1. Definitions of soil structure.

Definition	Reference
The arrangement and organization of the particles in the soil.	Hillel (1980)
The size and arrangement of particles and pores in soils.	Oades (1984)
The degree and type of aggregation and the nature and distribution of pores and pore space.	Fitzpatrick (1986)
The spatial heterogeneity of different components or properties of soil.	Dexter (1988)
The spatial arrangement of the solid, liquid and gas phases.	Angers and Caron (1998)
The size, shape and arrangement of solids and voids, continuity of pores and voids, their capacity to retain and transmit fluids and organic and inorganic substances, and ability to support vigorous root growth and development.	Lal (1991)
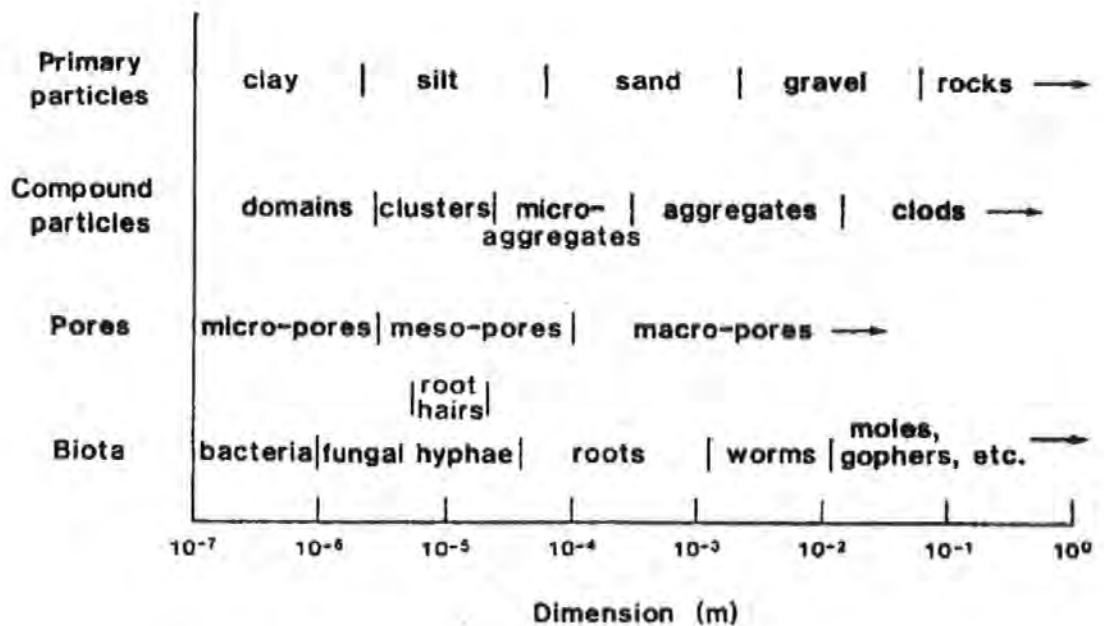
Figure 1.3. Approximate dimensions of some soil structural features (Dexter, 1988).

Soil structure is essential in maintaining soil physical properties, such as porosity, gas exchange and water infiltration, and in facilitating biogeochemical cycling (Diaz-Zorita *et al.*, 2002) and is also crucial to the success of sustainable agriculture and erosion resistance (Piotrowski *et al.*, 2004). Soil structure influences a range of soil processes from the physical to the biogeochemical, as listed in Table 1.2, thus creating the habitat of interactive soil biota (Jastrow and Miller, 1991), an important agronomic resource and a vector of environment quality.

Table 1.2. Some major soil processes influenced by soil structure (Jastrow and Miller, 1991).

PHYSICAL PROCESSES	NUTRIENT CYCLING	CARBON CYCLING
Erosion	Immobilization	Respiration
Runoff	Mineralization	Carbon inputs
Infiltration	Gaseous fixation	Root turnover
Hydraulic conductance	Gaseous losses	Root exudation
Fast drainage	Leaching	Turnover of microbial biomass
Aeration	Weathering of minerals	Microbial by-products
	Ion exchange	Decomposition
		(aerobic vs. anaerobic)
		Carbon accumulation
		Humification
		Physical protection of carbon

While good structure is usually associated with pasture plants (Robinson and Jacques, 1958) and found in soils under long-term grass swards (Tisdall and Oades, 1979), a previous study has revealed that structural differentiation under white clover is phenomenally rapid and enhanced (Mytton *et al.*, 1993). There is also a small body of evidence that suggests other legumes enhance the soil aggregation process (Angers and Carter, 1996). Papadopoulos *et al.* (2006) demonstrated enhanced soil macroporosity beneath red clover (*Trifolium pratense*) and red clover/ryegrass swards, and reported that the effect was not lasting.

1.7.2. Soil aggregation and structural formation

1.7.2.1. Mechanisms of aggregation

Aggregates are secondary compound particles, and are grouped by size: microaggregates (<250 μm) and macroaggregates (>250 μm) (Tidsall and Oades, 1982). They are formed through the complex dynamics of aggregation, in which mineral particles combine with organic and inorganic substances. Aggregation is the result of a rearrangement, flocculation and cementation of particles (Duiker *et al.*, 2003; Bronick and Lal, 2005) and is mediated by both biotic and abiotic factors (Tisdall & Oades, 1982), such as soil carbon, cations, clay, and biota (Bronick and Lal, 2005).

According to the conceptual model of aggregate hierarchy of Tisdall & Oades (1982), primary particles and aggregates of various sizes are arranged in a hierarchical order. Soil structural features of a given hierarchical order may be produced either by the combination of particles of a lower order or by the fragmentation of higher order particles (Tidsall and Oades, 1982; Dexter, 1988).

The lowest hierarchical order is the combination of single mineral particles, like clay, to form compound particles of 1-2 μm, such as quasi-crystals, domains or assemblages (Tidsall and Oades, 1982). The next hierarchical order is that of larger compound particles of 2-20 μm such as clusters of primary particles or clusters of quasi-crystals, domains or assemblages, or clay particles adhered to mucilage and decomposing matter (Tidsall and Oades, 1982). Clusters are bound into microaggregates of 20-250 μm by organic molecules, polyvalent cations and other inorganic constituents, to form the next hierarchical order (Tidsall and Oades, 1982; Dexter, 1988; Angers and Caron, 1998).

Microaggregates (<250 μm) are enmeshed by fungal hyphae and fine roots, which exude binding agents such as polysaccharides to form macroaggregates >250 μm (Tidsall and

13

Oades, 1982; Bronick and Lal, 2005). This hierarchical order continues, and clods >25 mm are formed by compaction of smaller structural units. (Tidsall and Oades, 1982; Dexter, 1988; Angers and Caron, 1998). However, not all hierarchical orders are necessarily present.

Fragmentation of a higher hierarchical order to produce smaller structural units of a lower order is the result of mechanical stress (Tidsall and Oades, 1982). The stress may be applied externally (e.g. tillage implements) or internally (e.g. action of water, roots and soil fauna) and will cause fragmentation either by shear or tensile failure (Dexter, 1988). The use of tillage implements can cause shattering of the soil structure (Dexter, 1988), whilst rapid wetting of a dry soil may cause slaking into microaggregates by entrapped air, mechanical breakdown, or the formation of micro-cracks by differential swelling (Dexter, 1988; Zhang & Horn, 2001). Wetting and drying cycles also form macroaggregates: when soils dry they shrink and cracks appear, upon wetting the soil swells and consolidates the aggregates, although the cracks remain planes of weakness (Tidsall and Oades, 1982; Dexter, 1988; Angers and Caron, 1998).

It is well recognised that soil biota play an important role in the formation and stabilisation of soil structure (Davidson and Grieve, 2006). Many insects, earthworms, nematodes and larger macro-organisms influence soil structure; they ingest and egest soil material, relocate plant material and form biogenic structures (Bronick and Lal, 2005). These macro-organisms increase the macropore volume and continuity and thus improve aeration, porosity and infiltration. They improve aggregate stability, organic matter mixing, and N and C stabilization (Bronick and Lal, 2005; Davidson and Grieve, 2006).

The reciprocal relationship between fauna and structure is of crucial importance in influencing microbial activity (Young and Crawford, 2004). Root exudates stimulate microbial activity in the rhizosphere (Czarnes *et al.*, 2006; Davidson and Grieve, 2006).

Microbial activity varies with aggregate size, seasons, cropping activities, management, residue quality and quantity and soil type (Bronick and Lal, 2005).

Bacteria, fungi and roots enhance aggregation by enmeshing soil particles and providing extracellular polysaccharides that bind particles together (Czarnes *et al.*, 2006). The arbuscular mycorrhizal fungi (AMF) is one of the most important biotic influences on soil aggregation (Jastrow *et al.*, 1998; Bronick and Lal, 2005), due to the release of glomalin, a glycoprotein, which is present in soils at high concentrations and is an important factor in stablizing aggregates (Wright and Upadhyaya, 1998; Rillig *et al.*, 2002). It is possible that the hydrophobic, recalcitrant nature of the glomalin molecule may protect other aggregating agents (Wright and Upadhyaya, 1998).

Tisdall and Oades (1982) suggest that fungal activity dominates in macroaggregation while bacterial activity may dominate in microaggregate formation. Other theories suggest that macroaggregates can form around a nucleus of particulate organic matter (POM) (Puget *et al.*, 1995) and bacterial colonies (Bronick and Lal, 2005), and in turn macroaggregates decompose or breakdown to form microaggregates (Six *et al.*, 2000; Bronick and Lal, 2005; Pulleman *et al.*, 2005). The concentric theory of aggregation (Santos *et al.*, 1997) proposes a concentric accumulation of primary particles as layers on the external surface of aggregates, so that the aggregate interior contains older soil organic carbon (SOC) which is protected against microbial decay.

The possible scenarios of aggregation are represented in Figure 1.4. Aggregates are probably formed through a combination of the above processes, as summarised by Bronick and Lal (2005): microaggregates form by the bonding of primary particles (clay, organic matter and cations), or by the breakdown macroaggregates; macroaggregates may form from the combination of microaggregates, around POM or bacterial cores, or by the concentric accumulation of primary particles as external layers on aggregates.

```
        ┌─────────────────────────┐
        │    Primary Particles    │
        │  Clay – OM – Cations    │
        └─────────────────────────┘

clay – particle – OM      /        \    Concentric
                         /          \   Accumulation

  ┌──────────────────┐   Hierarchical   ┌──────────────────┐
  │ Microaggregates  │ ───────────────► │ Macroaggregates  │
  │                  │ ◄─────────────── │                  │
  └──────────────────┘   Bacterial or   └──────────────────┘
                          POM core
```
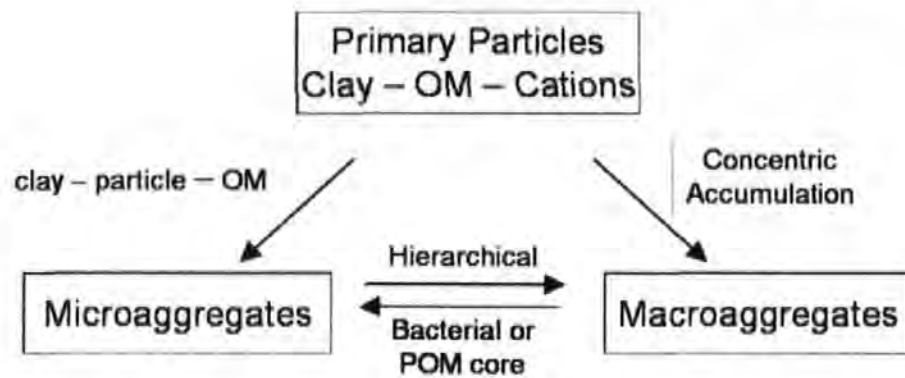
Figure 1.4. Possible scenarios of aggregation (after Bronick and Lal, 2005). Organic matter (OM), particulate organic matter (POM).

The process of aggregation is possibly driven by two mechanisms: a force must be exerted to move the soil particles into close proximity and there must be a physico-chemical means of holding them together. As illustrated in Figure 1.5, the complex dynamics of aggregation are influenced by many interacting processes that include physical, chemical, biological, pedological, hydrological, pedogenic, environmental factors and soil management practices (Bronick and Lal, 2005).

Reports and studies of processes that influence aggregation and aggregate stability include wetting and drying (Czarnes *et al.*, 2000; Denef *et al.*, 2001), Fe (hydr)oxides (Duiker *et al.*, 2003), soil fauna (Juma, 1994; Pulleman *et al.*, 2005), root penetration (Angers and Caron, 1998; Oades, 1993), organic matter decay (Tidsall and Oades, 1982), microbial activity (Aspiras *et al.*, 1971, Denef *et al.*, 2001), rhizosphere microbial biomass (Caravaca *et al.*, 2002), polysaccharide gum production (Traoré *et al.*, 2000), plant and microbial mucilage (Czarnes *et al.*, 2000), microflora (Molope *et al.*, 1987), mycelial fungi (Beare *et al.*, 1997) humic substances (Piccolo *et al.*, 1997), water repellencey and soil texture (De Gryze *et al.*, 2001), water infiltration (Franzluebbers, 2002), climate (Boix-Fayos *et al.*, 2001), seasonal variations (Plante and McGill, 2002; Papadopoulos *et al.*, 2006) and agricultural management (Beare *et al.*, 1997; Six *et al.*, 2000; Pagliai, 2004; Pulleman *et al.*, 2005; Wright & Hons, 2005).
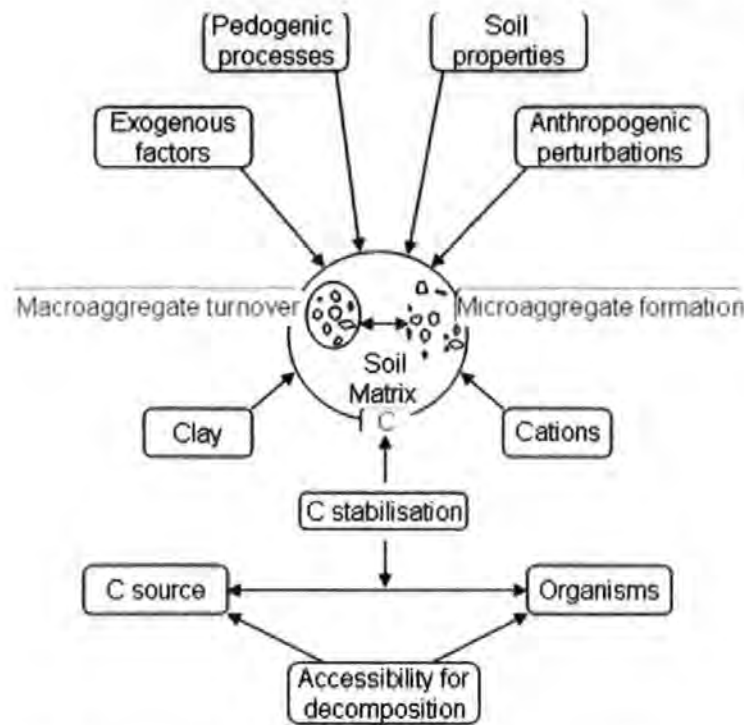
Figure 1.5. Factors affecting soil aggregation (after Bronick and Lal, 2005).

1.7.3. Soil structural stability

Dexter (1988) defined stability as the ability of soil structure to persist, and reviewed the two principal types of stability: under the action of water and external mechanical stress. The ability of soil to retain its structure under external mechanical stresses depends on the soil structure and stress applied (Dexter, 1988). Soil structural resiliency, which is the ability of the soil to recover once the mechanical stress has been removed, has received much less attention than stability (Angers and Caron, 1998).

Soil structural stability is an important aspect of soil quality; it determines root penetration and organic matter stabilization (De Gryze *et al.*, 2006), and influences several aspects of a soil's physical behaviour, in particular water infiltration, soil erodibility and susceptibility to compaction (Legout *et al.*, 2005). The dynamics of soil aggregation and stability have gained increasing attention because of the potential role in carbon sequestration (Plante and

McGill, 2002; Lal, 2004). Organic matter is an important driving force in environmental global change as it acts as both a source and sink of atmospheric carbon.

Generally, aggregate stability depends on soil properties such as organic matter, clay and oxide contents (Zhang & Horn, 2001). The stability of clayey soils depends on its physical-chemical properties (e.g. smectitic clays are more dispersible than kaolinitic and illitic soils) (Zhang & Horn, 2001). Soil organic matter content is generally positively correlated with the clay content of the soil, which can be attributed to increased surface adsorption (Balabane and Plante, 2004). Free and weakly bound carbon and carbon combined with clay are the dominant organic cementing material in aggregates. Clay-associated organic matter is confirmed as an important sink of long-term stabilized soil carbon, and appears to have been increasingly preserved when in increasingly larger aggregates (Balabane and Plante, 2004).

Different pools of soil organic matter (SOM), with varying stability and turnover rates, have been identified (Spaccini *et al.*, 2004), classified as inorganic carbon (carbonates) and organic carbon, which can consist of both labile and stable fractions (particulate organic matter (POM), carbohydrates, polyschacarides, phenols, lignin, lipids and humic substances) (Bronick and Lal, 2005). However, not all of the SOM is involved in the formation and stabilization of aggregates.

While many studies have concluded that soil aggregate turnover is a significant control on organic C turnover, few have made direct links between the observed organic matter dynamics and the dynamics of soil aggregates (Plante and McGill, 2003). A comprehensive understanding of the factors that control the long-term stabilization of organic matter in soil still needs to account for the specific role of soil aggregation in the whole process better than it does at present (Balabane and Plante, 2004).

Tisdall and Oades (1982) demonstrate the well known relationship between water-stable aggregates and organic carbon in soils in a red-brown earth under different cropping regimes, where the mean weight diameter (MWD) of water-stable aggregates increased with increasing organic matter and microbial biomass. They suggest that the water-stability of higher hierarchical orders is a function of various binding agents (Figure 1.6). They concluded that macroaggregates (>250 μm diameter) derive their water-stability from roots and hyphae and are therefore influenced by soil management. Microaggregates (<250 μm diameter) are influenced by organic carbon and soil management to a lesser extent as they derive their stability from organo-mineral complexes or polysaccharide mucilages. Furthermore, microaggregates exhibit greater stability than macroaggregates (Tisdall and Oades, 1982, De Gryze *et al.*, 2006).

The microbial biomass and soil biota are important factors in rendering aggregates more resistant and in establishing a stable structure, especially in soils which are poor in stabilizing media of physico-chemical nature (Oades, 1993). The different mechanisms by which microorganisms interact with the soil structure, the entanglement of particles by fungal hyphae and the polysaccharide mediated aggregation or stabilization by bacteria are well understood (Niewczas and Witkowska-Walczak, 2005). The effects of changes in animal diversity on soil physical structure may influence the pathways and magnitude of carbon transfers, but our understanding of the links between carbon fluxes, soil animal diversity and soil architecture remains poor (Grieve *et al.*, 2005).

Sarah (2005) reported that a positive feedback mechanism exists, in which soil aggregate size and stability affect the infiltration of water and solutes into the soil and their movement within it, overland flow generation and soil erosion, which in turn affects soil fauna and flora. Thus, a change in an external factor, such as climate or land use, will sharply influence soil structure and degradation.
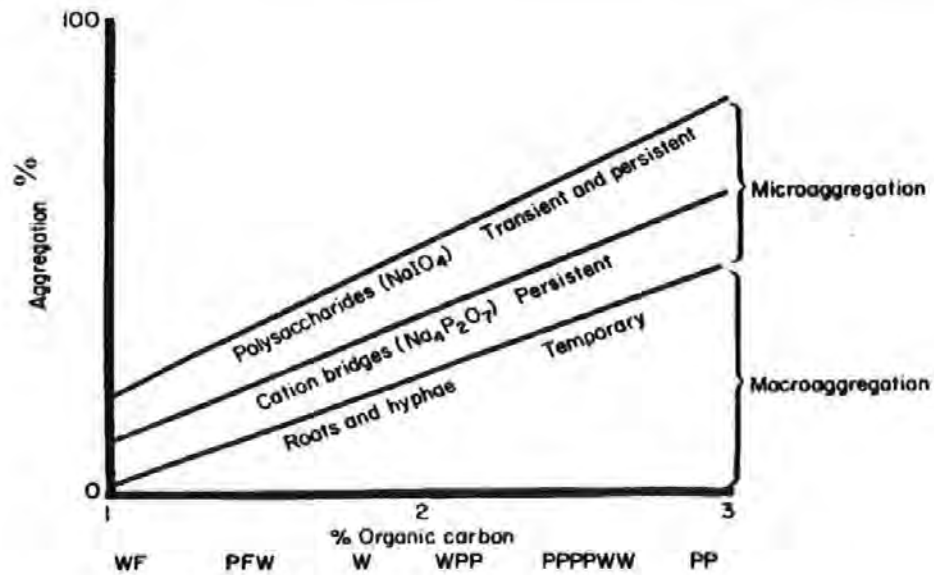
Figure 1.6. Relationship between water-stable aggregates and organic carbon content of various cropping regimes. P = pasture, W = wheat and F = fallow (multiple letters refer to combinations) (Tisdall and Oades, 1982).

1.7.4.   Organic binding agents

The diverse organic materials involved in stabilising aggregates have been the focus of much research. Tisdall and Oades (1979, 1982) and Oades (1984, 1993) proposed three main groups of organic binding agents (transient, temporary and persistent) and classified them according to their age and degradation, not chemical composition. Tisdall and Oades (1979, 1982) hypothesised that the various binding agents not only influence the stability of aggregates, but also their age and size.

1.7.4.1. Transient binding agents

Transient binding agents are those rapidly produced and decomposed. Polysaccharides are the most important and are associated with roots and microbial activity. These binding agents are responsible for binding transiently stable microaggregates (<250 μm diameter) which persist for a few weeks (Tisdall and Oades, 1979, 1982; Oades, 1984, 1993).

1.7.4.2. Temporary binding agents

Temporary binding agents are plant roots and fungal hyphae (living or decomposed) which physically enmesh soil particles. Theses agents are responsible for binding macroaggregates (>250 μm diameter), which can persist for several months and are affected by soil management (Tisdall and Oades, 1979, 1982; Oades, 1984, 1993).

1.7.4.3. Persistent binding agents

Persistent binding agents are composed of strongly humified organic matter and complexes of organic colloids with polyvalent metal cations and clay. These binding agents are responsible for binding stable microaggregates (<250 μm diameter) which persist months or even years (Tisdall and Oades, 1979, 1982; Oades, 1984, 1993).

1.7.5. Measurement of soil structure

Numerous methods for characterising soil structure have been proposed and generally involve separate or simultaneous analysis of the solid mass and pore space. The method used will differ with the question asked (Jastrow and Miller, 1991) and will depend on the scale of the structural feature of interest. Methods should also assess the stability of the structure under the action of water and mechanical stresses (Dexter, 1988).

Soil structure variables proposed by Sarah (2005) are: aggregate stability, aggregate mean weight diameter (MWD), micro-particles percentage, and macro-particles percentage, organic matter content (OM), electrical conductivity, and sodium and potassium adsorption ratio. Ball *et al.* (1997) assessed soil structure by measuring soil properties that affect fluid storage and transport to identify soil qualities indices to assist with soil management. Parameters included: bulk density, shear strength, cone resistance, macroporosity, relative diffusivity, air permeability and water infiltrability. Visual assessment of soil structure and interpretation is given by Hodgson (1974) and the Agricultural Advisory Council (1970).

1.7.5.1. Measurement of soil aggregation

Soil aggregation and aggregate stability are used as indicators of soil structure (Six *et al.*, 2000; Bronick and Lal, 2005). Soil aggregation is frequently evaluated in terms of the size distribution and stability of the particles (Dexter, 1988; Jastrow and Miller, 1991), which is not a measurement of whole soil structure (Six *et al.*, 2000). The mean weight diameter (MWD), on the other hand is an index that characterizes the structure of the whole soil by integrating the aggregate size class distribution into one number, and has often been used to indicate the effect of different management practices on soil structure (Six *et al.*, 2000). Determination of the state of soil aggregation and the stability of soil aggregates has been performed using various indices, but no universal technique is employed (Niewczas and Witkowska-Walczak, 2005).

Aggregate size distribution is readily determined in wet or dry samples using a series of oscillating sieves. Wet sieving the aggregates provides a disruptive force and therefore tests aggregate stability (Jastrow and Miller, 1991). There are two main types of wet sieving which measure different properties and vary as to the intensity of the force applied. The first is rapid, disruptive wetting when slaking may occur, and determines the amounts of water-stable aggregates and microaggregates (Tidsall and Oades, 1982). The second type applies a minimally disruptive force by slowly saturating the aggregates with water vapour and indicates the stability when no slaking occurs (Dexter, 1988).

Dry soil is regarded as the most sensitive indicator of variability of aggregate stability (Zhang & Horn, 2001). The stability of drier soil provides information on the soil's workability and its ability to withstand force applied (Dexter, 1988). Large aggregates and clods are assessed by the drop-shatter test, whilst the crushing test is used to determine tensile strength of smaller and stronger aggregates (Dexter, 1988). Various other techniques have been used to evaluate aggregate stability and size distribution: the single-

sieve method, turbidimetry, sedimentation, elutriation, permeability, dispersion and disruption by ultrasound (Jastrow and Miller, 1991).

Soil strength varies with water content and so simultaneous determinations must be made. Dexter (1988) reported an inverse linear relationship between water content and the logarithm of soil strength. In a disturbed soil, the relationship is assessed using Atterberg consistency limits, which are measured by the drop-cone and rolling-out methods (Sowers, 1965). For undisturbed field soils, a penetrometer is used to indicate soil strength with depth (Dexter, 1988).

A difficulty in characterising soil aggregation is that it depends on the method used (Diaz-Zorita *et al.*, 2002; Balabane and Plante, 2004). The yield of aggregates from any given soil depends strongly on the energy applied to the sample during the procedure used to isolate the aggregates (Balabane and Plante, 2004). Measurements of aggregate-size distributions are sensitive to sampling conditions, pre-treatment, sieving technique (e.g. wet versus dry) and the duration of sieving (Balabane and Plante, 2004).

To test aggregate stability, soil physicists generally subject aggregates to artificially induced forces designed to simulate phenomena that are likely to occur in the field. Most frequently, the concept of aggregate stability is applied in relation to the destructive action of water (Niewczas and Witkowska-Walczak, 2005). Aggregate stability is also affected by the method of determination, initial soil water content, rate of wetting, and initial aggregate size (Zhang & Horn, 2001).

The most common protocol to measure aggregate stability is wet-sieving aggregates after rapid immersion in water (Balabane and Plante, 2004). Le Bissonnais (1996) proposed a comprehensive protocol to describe aggregates based on the nature of the binding; the method consists of three treatments applied to 3–5 mm aggregates, and differentiates between the various mechanisms of breakdown: slaking due to fast wetting, microcracking

due to slow wetting and mechanical breakdown by stirring of pre-wetted aggregates. The results are expressed as the resulting fragment size distribution and as the mean weight diameter (MWD). Niewczas and Witkowska-Walczak (2005) proposed the index of soil aggregates stability (ASI), which is a new tool for comparing soil aggregation changes caused by the destruction factor or process no matter which method is used for the soil aggregate stability determination.

1.7.5.2. Measurement of pore space

Several authors argue that a more appropriate way to study soil structure is to focus on the arrangement of voids and the properties these voids confer to soils (Letey, 1991; Baveye, 2005). Pore space measurements are being increasingly used to characterise soil structure (Pagliai *et al.*, 2005), and have been combined with solute transport and dye tracer studies to understand flow mechanisms, both in the laboratory (Aeby *et al.*, 1997; Morris and Mooney, 2004) and the field (Droogers *et al.*, 1998; Ewing and Horton, 1999a, b; Forrer *et al.*, 2000; Papadopoulos *et al.*, 2006).

Pore space is quantified by either indirect or direct measurement (Jastrow and Miller, 1991), using physical and morphological techniques (Ersahin *et al.*, 2002), and through the use of simulation models. Each method will give different estimates (Ersahin *et al.*, 2002). Indirect laboratory estimates of the size distribution of pores <300 μm (equivalent pore diameter) can be determined from the drying limb of the water-retention curve using the Laplace equation (Peat *et al.*, 2000) and pores < 150 μm by mercury-intrusion porosimetry (Bartoli *et al.*, 1999). In the field, a tension infiltrometer is used to indirectly assess the porosity of macro- and mesopores (Dexter, 1998).

Methods for the direct quantification of soil pores have improved with technological and theoretical advances (Moran and McBratney, 1992). Direct observations are made using

morphometric techniques, in which images from sections of impregnated soil provide information on pore geometry, orientation and spatial distribution additional to that from indirect liquid displacement methods (Jastrow and Miller, 1991). Sections are cut from impregnated samples using a diamond saw and are polished until smooth (McBratney *et al.*, 1992). Thick and thin sections are the two main types used, and are viewed by reflected and transmitted light respectively (Dexter, 1998). Digital images for visualising and measuring soil structure have been processed using computerised image-analysis systems (McBratney *et al.*, 1992). These digital image processors render rapid counting procedures and allow standardization of the method (Vogel and Roth, 2001). With recent technological advancements, high-resolution images are captured using digital cameras (Morris and Mooney, 2004; Papadopoulos *et al.*, 2006).

The one-dimensional binary transect method records the presence or absence of pores at specific points along a linear line (Deeks *et al.*, 1999; McBratney and Moran, 1990) and provides information on pore size distribution. For quantification of pore size, shape and orientation, two-dimensional scanning is employed (Murphy *et al.*, 1977a,b; Ringrose-Voase and Bullock, 1984; Ringrose-Voase, 1987). Many improvements have been made since the 1970s Quantimet system; preparation techniques are much improved and computer processing power has now increased. Three-dimensional analysis of soil structure is extremely complex and still its use is still in its infancy due to cost, availability and resolution (Mooney, 2002). However, it is possible to gain quantification about important parameters, such as pore connectivity and tortuosity, which affect many important transport processes in soils (Pagliai *et al.*, 2005).

Three-dimensional analysis of soil structure can be inferred from two-dimensional information using stereological methods (Ringrose-Voase, 1996) and the technique of serial sectioning, in which the 3D-geometry of the pore space is reconstructed from the

digitized images of a series of thin sections (Vogel and Kretzschmar, 1996; Vogel, 1997; Vogel and Roth, 2001; Morris and Mooney, 2004).

A more advanced, non-intrusive and non-destructive imaging technique is X-ray Computed Tomography (CT). This novel technology provides three-dimensional visualization and characterization of soil morphology from two-dimensional images. These images map the variation of X-ray attenuation within objects. The attenuation relates closely to density (Ketcham and Carlson, 2001), thus enabling segmentation of the air, water and solid phases (Mooney, 2002). The imagery is analogous to data that would be obtained more tediously and laboriously with serial sectioning (Ketcham and Carlson, 2001). CT provides spatial information on soil structure at less than millimeter scales, while high-energy Synchrotron-source X-ray computerized microtomography (CMT) is capable of spatial resolution on the order of a few micrometers (Ketcham and Carlson, 2001). CT scanners can be generally grouped into four categories, based on their spatial resolution and the size of objects they are most suitable for scanning (Table 1.3).

Table 1.3. General classification of computed tomography (Ketcham and Carlson, 2001)

Type	Example	Scale of observation	Scale of resolution
Conventional	Medical scanners	m	mm
High-resolution	Medical and industrial scanners	dm	100 μm
Ultra-high-resolution	Industrial scanners (e.g. tandem scanner)	cm	10 μm
Microtomography	Synchrotron X-ray scanner	mm	μm

Recent utilisations of X-ray CT in soil science include characterization of soil and pore-space morphology (Pierret *et al.*, 2002; De Gryze *et al.*, 2006) and direct imaging of fluid-flow observation of water through macropores. These developments have enabled the visualization of real time water movement (Mooney, 2002), thus enabling more detailed research into solute and tracer transport description and modelling (Ketcham and Carlson, 2001). The activity of macrobiota, such as earthworms and plant roots, has also been

detected and measured (Pierret *et al.*, 1999). Nunan *et al.* (2006) report the potential of CMT as an appropriate scale for quantifying and understanding the soil microbial physical habitat and soil-microbe interactions.

Gamma ray computed tomography (GCT) is another non-invasive imaging technique used to investigate possible modifications in soil structure and other soil physical properties (Pires *et al.*, 2005). Advances in the techniques of Nuclear Magnetic Resonance (NMR) and Magnetic Resonance Imaging (MRI) also open up the opportunity for direct quantification of the internal architecture of soil (Nunan *et al.*, 2006).

Once digital images are available, arithmetic and morphologic manipulations can be carried out with ease (Dathe, 2001). Images have been processed using various software packages, such as analySIS (Morris and Mooney, 2004) and Image Tool (Papadopoulos *et al.*, 2006). As the data are digital, the method lends itself more easily to both quantitative analysis and widespread dissemination (Ketcham and Carlson, 2001). Other techniques using image analysis to describe and classify soil structure include fractal analysis (Pachepsky *et al.*, 1996; Hallett *et al.*, 1998; Young *et al.*, 2001; Papadopoulos *et al.*, 2006), distance transform data (Holden, 2001) and dynamic programming analysis (Eggleston & Peirce, 1995). Such techniques use micromorphological observations from which transport pathways can be determined (Quisenberry *et al.*, 1993).

Over the last decade significant advances have also been made in simulating the complex spatial structure of soil, attempting to link the geometry of soil structure to soil function (Nunan *et al.*, 2006), such as the three-dimensional Pore-Cor network model (Peat *et al.*, 2000; Johnson *et al.*, 2003a), and the behaviour of soil biota (Young and Crawford, 2001). Furthermore, studies involving micromorphology and soil ultrastructure have greatly contributed to our knowledge of soil structural dynamics and can provide information on the mechanisms of soil structural formation (Jastrow and Miller, 1991).

1.7.6. Water and solute transport in soils

Knowledge of the dynamics of water in and below the root zone is paramount for many disciplines. The transport, storage and interactions of both water and solutes in soils has generated much attention due to the rapid transport of agrochemicals from non-point agricultural sources to surface and ground waters. The processes include, phosphorus loss (Sharpley, 1995; Hawkins and Scholefield, 1996; Haygarth *et al.*, 2005), nitrate leaching (Jarvis, 2000; Schröder *et al.*, 2004), transport of pesticides (Bergström, 1990; Ghodrati and Jury, 1992, Flury, 1996), herbicides (Flury *et al.*, 1995; Zehe and Flühler, 2001), pathogens (Oliver *et al.*, 2005) and veterinary antibiotics (Kay *et al.*, 2005).

A better understanding of the soil processes and properties that favour preferential water pathways is essential for developing integrated management and regulatory strategies to reduce the environmental impacts of non-point agricultural pollutants (Zehe and Flühler, 2001; Williams *et al.*, 2003). Research has been directed at both the nature of the pathways themselves, the generation of runoff and the transport of pollutants (Williams *et al.*, 2003). Numerous laboratory and field experiments are reported in the literature that demonstrate the impact of soil physical, biological, and chemical interactions on water flow in both saturated and unsaturated soils, and at a range of scales.

It is well recognised that morphological properties of the soil control the infiltration and transport of water, the space which is filled with air, the movement of solutes and gases and even the movement of micro-organisms through the soil (Bouma, 1991; Li and Ghodrati, 1995), and in turn soil formation, soil erosion, and many other important processes. Modifications in the soil morphology, such as voids and aggregates produced by soil structural development, or impermeable inclusions like stones and roots, are highly significant for water and solute transport (Diestel, 1993).

Overall, the impact of macropores on soil transfer properties is directly related to their geometrical and topological characteristics, among which continuity and pore-size distribution are of prime importance (Pierret *et al.*, 2002). There is rising evidence that macropores provide easy pathways through the soil as well as improved exposure to preferential flows of oxygen, water and nutrients (Pierret *et al.*, 2002). Water that moves slowly through the soil matrix is distinguished from faster routes; such transport behavior is known as channel, rapid, macropore, bypass, fingering, or preferential flow (Langner *et al.*, 1999; Williams *et al.*, 2000, 2003).

There is no universally agreed definition of preferential flow (Williams *et al.*, 2003). Morris and Mooney (2004) defined it as the deep movement of water through a fraction of available pore space. Like many authors, they indicate that the phenomenon implies a large flux or velocity of flow through a limited number of pathways, such as macropores or worm channels, thus bypassing regions of immobile water (Bouma *et al.*, 1977, Larsson *et al.*, 1999; Williams *et al.*, 2000, 2003). The phenomenon of preferential flow in soil has been known for many years, and has been studied in detail more recently (Gjettermann *et al.*, 1997).

Preferential flow is particularly important in agricultural soils because the rapid movement of agrochemicals from the soil surface to significant depths in the vadose zone increases the probability of groundwater contamination (Langner *et al.*, 1999; Williams *et al.*, 2000, 2003). Solutes bypass most of the unsaturated zone, and so the interaction between potential pollutants and the soil matrix and is limited. Thus, the opportunity for amelioration and retention, through processes of adsorption, immobilisation and degradation, is reduced (Flury *et al.*, 1995; Larsson *et al.*, 1999; Zehe and Flühler, 2001; Williams *et al.*, 2003). In addition, agricultural practice of subsurface drainage increases the potential of rapid breakthrough of pollutants to surface waters (Larsson *et al.*, 1999; Zehe and Flühler, 2001).

The success of any management measure to prevent losses of water-borne contaminants from agroecosystems to the aquatic environment depends on the understanding of the mechanisms of transport of water and solutes in soil (Gjettermann *et al.*, 1997) and the methodologies to determine and predict large scale flow (Javaux and Vanclooster, 2006). Luxmoore (1991) and Flury (1996) summarized many research results from field experiments indicating that chemicals can be rapidly transported through certain pathways into the groundwater. Kung *et al.* (2000) suggest that preferential pathways make unsaturated field soils behave like a perforated filter, and state that the impact of macropore flow on contaminant transport under field conditions can not be accurately replicated and examined in laboratory studies. The movement of air, water and solutes at the field scale are governed by mechanisms that differ from voids between aggregates (inter-aggregate), which also differ considerably to the dynamics of voids within aggregates (intra-aggregate) (Diestel, 1993).

To obtain a better understanding of preferential flow mechanisms in the field, it is obviously beneficial to carry out in-situ experiments at a more representative scale (Gjettermann *et al*, 1997). However, many studies of the transport of solutes through re-packed laboratory soil columns and small blocks have been reported. These studies are limited as they do not necessarily represent the heterogeneity of the soil in the field, and do not take into account spatial and temporal resolution (Gjettermann *et al.*, 1997; Williams *et al.*, 2000). This has led to several methods which propose up-scaling of local hydraulic properties for describing large scale-flow (Javaux and Vanclooster, 2006) and to the development of mechanistic models (Larsson *et al.*, 1999; Javaux and Vanclooster, 2006), and predictive models of hydraulic functions (Mualem, 1976; Van Genuchten, 1980), which also have their limitations (Greco, 2002; Logsdon, 2002, Vogel and Roth, 2003).

The framework for further development of mathematical transport models is assisted by other techniques concerned with water, gas and solute transport governed by soil structure,

such as the classification system based on selected soil properties proposed by Quisenberry *et al.* (1993), and the indices of Geeves *et al.* (1998). Such systems help to identify those soil properties that most affect transport processes to predict behaviour, and highlight the plethora of dynamic processes occurring at a range of temporal and spatial scales.

1.7.7. Tracer studies

It is well understood that the conventional approach of using simple parameters to describe macropores is not sufficient to predict preferential transport of water and solute (Allaire-Leung *et al.*, 2000). Tracer studies have been utilised both in the field and the laboratory to gain valuable information on flow and transport processes in soils (Kasteel *et al.*, 2000). Transport experiments have been conducted with both re-packed and undisturbed soils (structured and structureless), under both saturated and unsaturated conditions and at a range of scales.

The most common chemicals used as water tracers are chloride, bromide, tritium and uranine, and are infiltrated into soil to indicate where the water has moved and to what depth (Bouma *et al.*, 1977). These are examples of non-reactive tracers, which behave conservatively, bromide and uranine are well-established groundwater tracers. (Ammann *et al.*, 2003). The Br anion, though observed to have some anionic repulsion, has been used successfully as a tracer of water and nitrate movement in soil (Stutter *et al.*, 2003).

Ammonium and strontium tracers are used for their reactive behaviour in cation exchange processes. Strontium is involved exclusively in the cation exchange process, whereas ammonium is a nutrient cation and therefore subject to microbial transformations (Ammann *et al.*, 2003). Ethanol, hexanol, and benzoate are used as biodegradable tracers. Labelled compounds are also used, such as ^{15}N, and ^{14}C which is a biotracer biodegraded by microbes (Alter *et al.*, 2003). Pesticide tracers are commonly used, such as atrazine, napropamide and prometryn (Ghodrati and Jury, 1992).

Dyes are also used as substitutes for certain pesticides in pesticide transport studies or as water tracers (Stutter *et al.*, 2003). The most suitable is Brilliant Blue FCF dye, which has exceptional properties in terms of mobility, visibility and toxicity, which is anionic and not strongly adsorbed by negatively charged soil particles (Mooney and Nipattasuk, 2003; Morris and Mooney, 2004). Other commonly used include the cationic methylene blue and the fluorescent naphthionate, which is assumed to behave conservatively.

Dye tracer studies combined with image analysis techniques and computed tomography are used to investigate soil heterogeneity on preferential flow through the visualization of stained active transport pathways (Gjettermann *et al*, 1997; Droogers *et al.* 1998; Mooney and Nipattasuk, 2003; Morris and Mooney, 2004). These can be subjected to semi-quantitative analysis (Mooney and Nipattasuk, 2003; Morris and Mooney, 2004).

The concentrations at which tracers are applied are based on dilution factors and background concentrations in the soil, and detection limits of the specific instrumentation used for analysis (Ammann *et al.*, 2003). The application of tracers is generally as a slug followed by irrigation at the top boundary; leachates are collected at the bottom.

Breakthrough curves (BTC) are plotted to characterize the presence or absence of macropores and can indicate pore-connectivity and tortuosity (Allaire-Leung *et al.*, 2000). BTC can show if a significant proportion of the soil volume is bypassed when water flows preferentially through macropores; these data describe the behaviour of bulk volumes of soil (Bouma *et al.*, 1977).

A non-reactive tracer at uniform flow will yield a symmetrical BTC, indicating a low dispersion coefficient of advective velocity and an equilibrium in solute transport (Ersahin *et al.*, 2002). Macropore flow on the other hand, is reflected in a highly asymmetric BTC showing early breakthrough, and a tailing due to intra-aggregate diffusion, i.e. conditions

that are non-equilibrium with a high dispersion coefficient (Ersahin *et al.*, 2002). Numerous experiments have been conducted at various soil matrix potentials to determine microscopic flow (Ersahin *et al.*, 2002).

1.7.8. Soil structure and nutrient leaching

There is evidence that suggests that in well-structured soils nitrate leaching can be reduced (Scholefield *et al.*, 1996) and that the soil's capacity to buffer watercourses is enhanced (Scholefield *et al.*, 1998). Levels of nitrate leaching are determined by the factors that control accumulation and generation in the soil, and transport during the leaching process (Scholefield *et al.*, 1993). Both the proportion of accumulated nutrient that actually leaches and the concentration at which it enters watercourses are determined by soil structural differentiation (Scholefield *et al.*, 1996). In general, nutrients that reside within the inter-aggregate micropores are likely to be relatively conserved by structural development, whereas nutrients that enter the soil with the incoming water are likely to be lost by leaching more readily.

The transport of potential pollutants, particularly nitrate, is further complicated by the enhanced soil structuring observed with the growth of certain legume roots, notably white clover (Mytton *et al.*, 1993). Highly differentiated soil structure from beneath white clover systems could give rise to strong concentrations of nitrate in surface and ground water due to preferential macropore flow, or even from small volumes of highly concentrated drainage water. Alternatively, the enhanced structuring may result in relative protection from nitrate leaching due to inter- and intra-aggregate diffusion and retention in micropores (Scholefield *et al.*, 1996). An important consideration is the site of nitrate prior to leaching. In the field, nitrate is produced and accumulated during the summer and homogeneously distributed through out the soil matrix. However, the onset of the autumn rain will result in drainage and nitrate leaching (Scholefield *et al.*, 2001).

1.7.9. Legumes and sustainable agriculture

A fundamental shift has occurred in both agricultural research and production; whilst the main driving force is to maximise productivity, there is an increasing appreciation of the need for sustainability (Peoples *et al.*, 1995a). The objectives of economic, environmental and social sustainability have led towards alternatives to conventional farming systems (Stockdale *et al.*, 2000). These alternatives include organic (biological/ecological) farming systems and low-input systems referred to as 'sustainable', 'alternative' and 'integrated' (Stockdale *et al.*, 2000) and seek to achieve an effective balance between agriculture production and environmental protection.

Legumes are considered by some to be an essential part of sustainable agriculture; the most obvious benefit is their potential to fix atmospheric N by symbiotic associations with their root nodule bacteria (*Rhizobium* spp.) and therefore reducing the need for fertiliser application (Miller and Jastrow, 1996). Legumes provide a renewable source of N (Peoples *et al.*, 1995b), replenishing N removed and lost from the soil (Condron *et al.*, 2000). The main grassland and forage legumes in western Europe are *Trifolium repens* (white clover), *Trifolium pratense* (red clover) and *Medicago sativa* (lucerne and alfalfa) (Sprent and Mannetje, 1996).

White clover is an important forage legume of high nutritive value and is widely distributed throughout humid and temperate regions of the world (Pederson, 1995). In the UK, the area annually sown with white clover was estimated to be 184 Kha^{-1} in 1982, declining to 144 Kha^{-1} in 1989 (Sprent and Mannetje, 1996). Boller and Nosberger (1987) estimate N fixation by white clover to be 227-283 kg N ha^{-1} in mixed pasture swards, whilst Wood (1996) suggests that white clover has the potential to fix only 100-200 kg N ha^{-1}. Annual production from white clover based pastures can equal that of grass based pasture fertilized with 400 kg N ha^{-1} a^{-1} (Sprent and Mannetje, 1996). When grown in

mixed pastures, white clover can release N to soil and transfer N to associated grasses (Peoples *et al.*, 1995a). Boller and Nosberger (1987) estimate this transfer of N to grasses to be 11-52 kg ha^{-1} and Ledgard (1991) reports the greater amount of 70 kg N ha^{-1}.

White clover is more nutritious than perennial ryegrass (*Lolium perenne*). Animals produce more milk and liveweight gain when fed pure clover or grass/clover mixtures compared to pure grass and are therefore more profitable (Sprent and Mannetje, 1996). However, too much clover can cause fatal bloat (tympanitis) in cattle (Sprent and Mannetje, 1996). Furthermore, the ruminant uses clover-N in feed less efficiently than grass-N, and so a greater portion of clover ingested N is recycled to the soil in excreta, resulting in greater leaching losses and emissions (Scholefield *et al.*, 2001).

The performance of white clover is inconsistent and it has a poor persistency in pastures (Sprent and Mannetje, 1996). If legumes are to be used efficiently, and used to meet the demand for N in agriculture that is increasing with world population (Herridge and Danso, 1995), their N-fixing potential must be optimised (Sprent and Mannetje, 1996). Suggestions include improving the effectiveness of the rhizobia-host plant symbiosis through breeding and selection (Herridge and Danso, 1995), by improving plant and soil management (Peoples *et al.*, 1995b), or by simply increasing the area sown with clover. However, this enhances the potential downside, as increased inputs of N will lead to greater emissions to the environment.

Most studies of nitrate leaching from beneath forage legumes involve white clover in combination with grasses under grazing management (Scholefield *et al.*, 2001). Parsons *et al.* (1991) found that nitrate leaching from grass-white clover is generally much smaller than highly fertilised grass. The same was found by Eriksen *et al.* (2001, 2004), who showed that nitrate leaching from grazed unfertilised grass/clover was always considerably

lower than from grazed fertilised ryegrass. Such research suggests that legume-based systems are environmentally benign. However, it is believed that the N loss is smaller because the level of production is lower in the grass-clover system than the pure grass (Scholefield *et al.*, 2001). Eriksen *et al.* (2001, 2004), attributed the higher leaching losses from fertilised grass than from unfertilised grass-clover systems to both a reduction in N_2-fixation in grass-clover over time, and a reduction in dry matter production in grass-clover over time lowering the grazing intensity and the recycling of grassland N via animal excreta.

Several studies have shown that legume-based systems are not environmentally benign, and N from clover is just as likely to leach to the environment as fertiliser N, particularly under grazing (Mannetje and Jarvis, 1990). Similar amounts of N and P are leached from beneath grass-clover swards as those leached from beneath fertilised grass operating at the same level of production (Tyson *et al.*, 1997; Cuttle *et al.*, 1998). In some circumstances, clover rich swards can give rise to very high levels of nitrate leaching (MacDuff *et al.*, 1990; Loiseau *et al.*, 2001; Scholefield *et al.*, 2001).

A large scale study of twelve sites across northern Europe over three years compared nitrate leaching beneath five forage legumes grown in pure strands and in combination with a companion grass as the basis for economically and environmentally sustainable systems of livestock production (Scholefield *et al.*, 2001). Although nitrate leaching varied considerably with site, the greatest leaching potential was from beneath red clover (32 kg N ha^{-1}) and white clover (36 kg N ha^{-1}). The lowest potential was from grass without fertiliser N (17 kg N ha^{-1}), whilst fertilised grass receiving 200 kg N ha^{-1} had a leaching potential slightly below that of red and white clover (29 kg N ha^{-1}).

Loiseau *et al.* (2001) reported leaching losses over six years from lysimeters sown with pure white clover as 28-140 kg N ha^{-1}, compared to 1-19 kg N ha^{-1} for grass-white clover. A three year study from a dairy farm in the Netherlands reported slightly higher nitrate leaching from grass-white clover systems (28 mg L^{-1}) compared to fertilised N grass systems (26 mg L^{-1}), and that the nitrate leaching was positively correlated with clover content in the sward (Schils *et al.*, 2000).

1.7.10. Agriculture, environmental pollution and protection

There has been a growing concern about the pollution of fresh water by excess nutrients from agricultural land. Diffuse water pollution from agricultural sources cannot be attributed to a precise point or incident, with the exception of, for example, the spillage of a farm slurry store into a river. It is the cumulative affect of day to day activity over a large area. Although other activities contribute to diffuse pollution, agriculture is a major polluter of water; and also a significant emitter of gaseous emissions to the atmosphere (Powlson, 2000). In agriculture, diffuse pollutants include silt from soil erosion, nutrients from the application of fertiliser or spreading of manure, the transport of pathogens, and pesticides from the handling and application of the chemicals (DEFRA, 2002). Surface water, ground water, drinking water, estuarine and coastal waters are all at risk; as well as detrimental effects to the aquatic ecosystem and human health, the costs of remediation are expensive.

Of the total N and P emitted to surface waters in Western Europe, agriculture contributes 37-82 % of N emissions and 27-38 % of P emissions (Isermann, 1990). In English waters alone, over 70% of nitrates and 40% of phosphates originate from agricultural land (DEFRA, 2002). Grassland agriculture covers more than 5 x 10^6 ha of the land surface in England and Wales (Jarvis, 2000). The average application rate of N on fertilized grassland in this area is about 145 kg N ha^{-1}, compared to the higher rate of 281 kg N ha^{-1} to dairy

farms (Jarvis, 2000). The average application rate of P fertilizer for all grassland in England and Wales is 14 kg P ha^{-1}, and large quantities of P are provided in feeds and manure (Haygarth *et al.*, 1998a).

N and P compounds are both essential macronutrients, required by both plants and living organisms, but they are also pollutants, with potentially harmful consequences if present at certain concentrations under specific conditions. N and P species are key determinants in environmental monitoring programmes (Kramer, 1998) because of their role in eutrophication of waterbodies (Neal *et al.*, 2000) due to the excess flux from agricultural practices.

P transfer from agricultural land to surface waters can contribute to freshwater eutrophication (Haygarth & Jarvis, 1999; McDowell *et al.*, 2001); both issues are of major environmental concern (Withers *et al.*, 2001). The role of P has been well documented and only a small increase in P (20 μm L^{-1}) is needed for a eutrophic waterbody to stimulate excessive populations of undesirable biota (Haygarth & Jarvis, 1999), which is one of the most serious and widespread environmental problems.

Although nitrate pollution also contributes to eutrophication, the addition of P to freshwaters is of more importance; phosphate is the main cause in freshwater eutrophication because P is often the limiting nutrient for algae growth (Harrison, 1990). The uptake of these nutrients occurs in the approximate ratio of C:N:P 100:16:1 and P concentrations in natural waters are much lower than C and N (Radojević and Bashkin, 1999). The contribution to freshwater eutrophication from agriculture varies from catchment to catchment (DEFRA, 2002). However, eutrophication of lakes and reservoirs is increasing worldwide, and is accelerated in subtropical and tropical climates (Harrison, 1990; Radojević and Bashkin, 1999).

Nitrate is the limiting factor in marine eutrophication in estuarine and coastal waters, which arises primarily in relation to the North Sea. Another concern associated with nitrate is public health. Limits for nitrate in drinking water are based on its effect on the infant blood disease, methaemoglobinaemia (Packham, 1996). The 1980 EU Drinking Water Directive (80/778/EEC) included a Maximum Admissible Concentration of 50 mg NO_3^- L^{-1} (Packham, 1996). Water draining from agricultural land often exceeds the EC nitrate limit (Scholefield *et al.*, 1993), and so Europe adopted the 1991 Nitrates Directive (91/676/EC) to reduce the level of surface and groundwater pollution caused by nitrates from agriculture. To comply with this, the UK applied the agricultural *Action Programme* measures within discrete *Nitrate Vulnerable Zones* (NVZs) (DEFRA, 2002).

In 1996, 66 NVZs, covering some 600,000 hectares (8%) of England, were designated to protect drinking waters from nitrate pollution in catchments where nitrate levels in water exceed, or were likely to exceed, the legal limit (DEFRA, 2002). In a NVZ, farming practices must be modified to reduce the inputs of nitrate and to protect against pollution of surface and groundwater (DEFRA, 2002). However, a judgment by the European Court of Justice in December 2000 ruled that the UK had failed designate sufficient areas to protect surface and groundwaters against diffuse nitrate agricultural pollution (DEFRA, 2002). By October 2002, a total of 55% of England was designated as a NVZ (Figure 1.7).

The use of clover is promoted in such environmentally sensitive areas and areas designated for nature conservation in combination with farming (Sprent and Mannetje, 1996). Thus this research has major implications for the sustainability of agricultural systems, water quality control and environmental management.
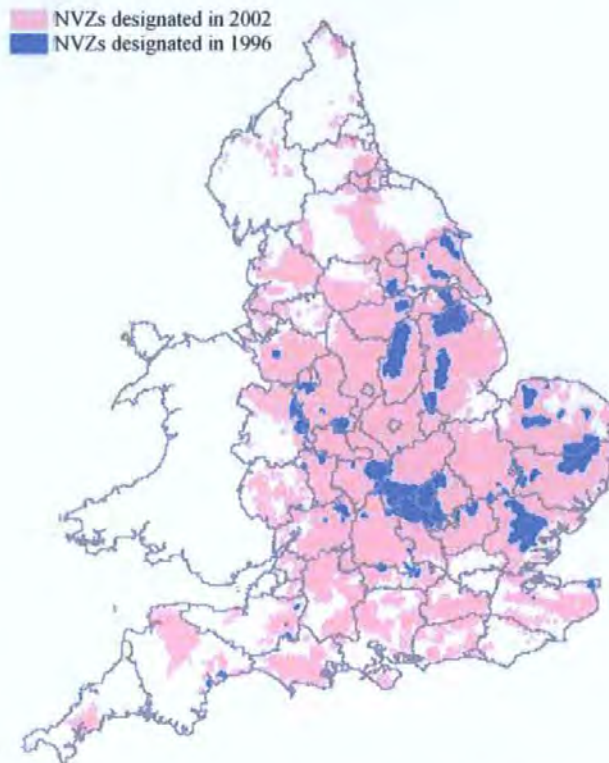
Figure 1.7. Designation of Nitrate Vulnerable Zones (NVZs) in England (DEFRA, 2002).

The General Quality Assessment scheme (GQA) is the Environmental Agency's national method for classifying water quality in rivers and canals. The scheme provides a way of comparing river quality from one river relative to another, and for monitoring changes. The Environment Agency (EA) assesses water quality in four separate ways: chemistry, biology, nutrients, and aesthetics. Table 1.4 refers to the nutrient assessment, and gives the limits for each grade and descriptors that relate to the nitrate and phosphate concentrations. For nitrate, 'High' concentrations refer to average concentrations above 30 mg L^{-1}, which roughly correspond to a 95 percentile of the 50 mg L^{-1} limit used in the EC Drinking Water Directive and the EC Nitrate Directive. For phosphate, 'High' descriptions are used where concentrations are above 0.1 mg L^{-1}, which is considered indicative of possible existing or future problems of eutrophication. However, 'High' concentrations do not necessarily mean that the river is eutrophic; other factors such as the amount and type of algae present, flow rates, and dissolved oxygen concentrations also have to be considered.

As part of the government's Strategic Review of diffuse water pollution from agriculture, the concentrations of nitrate and phosphate in UK rivers was determined. Water samples were collected each month for three years (1998-2000); 36 samples were analysed from each of the 8,000 monitoring sites, representing over 40,000 kilometres of rivers and canals. The concentrations of these nutrients are represented in Figure 1.8. Based on these concentrations, the environment agency developed a General Quality Assessment scheme (GQA) for classifying nutrient status in rivers and canals, from which a classification and grade is given to rivers based on the nitrate and phosphate concentrations, and is used to make decisions on developments that may affect water quality, Table 1.4 (DEFRA, 2002).

The Water Framework Directive (2000/60/EC) is the most substantial piece of EC water legislation. The directive came into force in December 2000, and requires all inland and coastal waters to reach 'good status' by 2015. This will be achieved by establishing a river basin district structure, each having a management plan with demanding environmental objectives (DEFRA, 2006).

Table 1.4. The Environment Agency's General Quality Assessment scheme (GQA) for classifying nutrient status in rivers and canals. Classification and grade given to rivers based on the nitrate and phosphate concentrations, and is used to make decisions on developments that may affect water quality (DEFRA, 2002).

| Grade | Nitrate (total oxidized nitrogen) | | Phosphorus (orthophosphate) | |
	Description	Grade limit (mg NO_3 L^{-1}) Average	Description	Grade limit (mg P L^{-1}) Average
1	Very low	<5	Very low	<0.02
2	Low	>5 to 10	Low	>0.02 to 0.06
3	Moderately low	>10 to 20	Moderate	>0.06 to 0.1
4	Moderate	>20 to 30	High	>0.1 to 0.2
5	High	>30 to 40	Very high	>0.2 to 1.0
6	Very high	>40	Excessively high	>1.0
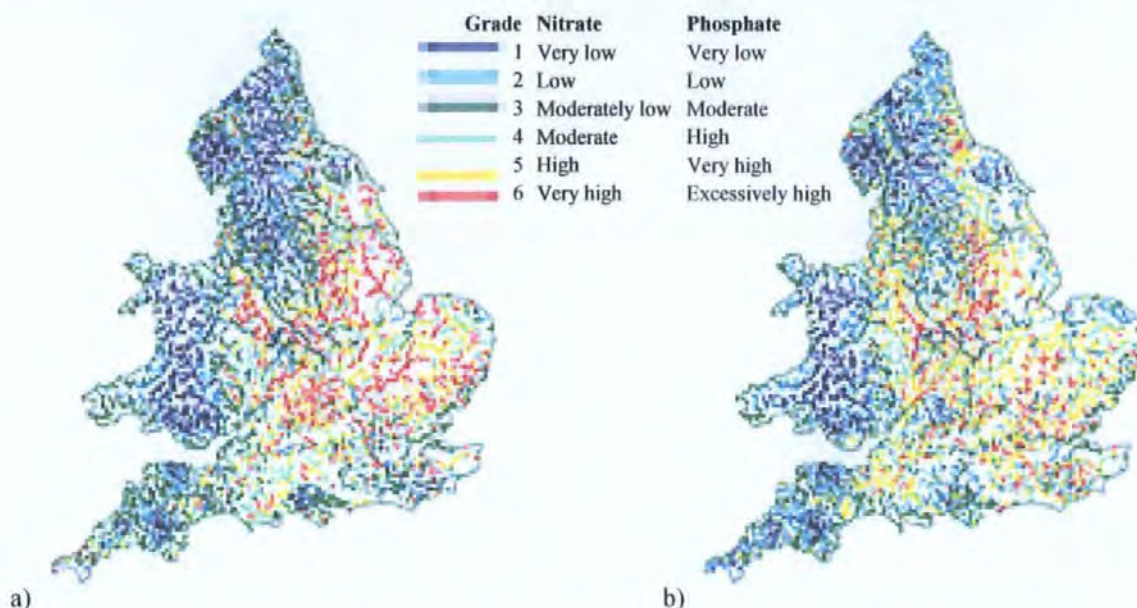
Figure 1.8. a) nitrate and b) phosphorus concentrations in UK rivers, 2000. Numerical values corresponding with the grade classification are listed in Table 1.4 (DEFRA, 2002).

1.7.11. Nutrient cycling

1.7.11.1. Nitrogen abundance and properties

N is a non-metallic element and a major component of the global ecosystem and exists in a wide range of organic and inorganic forms. N readily combines with itself to form a colourless, odourless and tasteless gas (dinitrogen, N_2) that is relatively inert under typical atmospheric conditions and only slightly soluble in water (Williams, 2001). Some physical and chemical properties of N are given in Table 1.5.

N is the most abundant chemical element in the atmosphere and as a consequence this constitutes its main reservoir (Figure 1.9). The predominant atmospheric species is N_2, but N also exists as oxidised gases (e.g. nitrous oxide, nitric oxide and nitrogen dioxide), reduced gases (e.g. ammonia) and in aerosols (e.g. nitrates, nitrites, nitric acid) (Williams, 2001). Small concentrations of N occur in natural waters; the most important nitrogenous species are inorganic (e.g. ammonium, nitrate and nitrite ions), although small concentrations of organic-N are also present. N is an essential macronutrient incorporated

into all plant and animal tissues as amino acids and proteins, and is excreted as urea $((NH_2)_2CO)$. N is the 31st most abundant element in the Earth's crust, and is rarely found within mineral ores (Williams, 2001).

Table 1.5. Physical and chemical properties of nitrogen (after Williams, 2001).

Property	Value/Example
Atomic number	7
Atomic weight	14.0067
Naturally occurring isotopes	^{14}N (99.63%), ^{15}N (0.37%)
Radioactive isotopes	^{12}N, ^{13}N, ^{16}N, ^{17}N, ^{18}N, ^{19}N, ^{20}N
Oxidation states	
-3	Ammonia (NH_3); ammonium ion (NH_4^+)
-2	Hydrazine (N_2H_4)
-1	Hydroxylamine (NH_2OH)
0	Dinitrogen (N_2)
+1	Nitrous oxide (N_2O)
+2	Nitric oxide (NO); nitrogen (II) fluoride (N_2F_4)
+3	Nitrite ion (NO_2^-); nitrous acid (HNO_2); nitrogen (II) chloride (NCl_3)
+4	Nitrogen dioxide (NO_2); dinitrogen tetroxide (N_2O_4)
+5	Nitrate ion (NO_3^-); nitric acid (HNO_3)

1.7.11.1.1. Global nitrogen cycle

The depicted N cycle is, by necessity, greatly simplified (Figure 1.9) using the six most commonly-depicted forms of N for the entire eight electron range of oxidation/reduction that N can undergo. N is present in many chemical forms, both organic and inorganic, as a gas, liquid (dissolved in water) and solid, and is transformed by biological, chemical, and physical processes through the atmosphere, biosphere, hydrosphere, and geosphere (Williams, 2001). Environmental cycling and chemistry of N is complex, as it can exist in

various different oxidation states (Table 1.5 and Figure 1.10). There are also many intermediate oxidation/reduction forms that N can assume, and the oxidation/reduction reactions of the N cycle are carried out in all four spheres during its biogeochemical cycling.
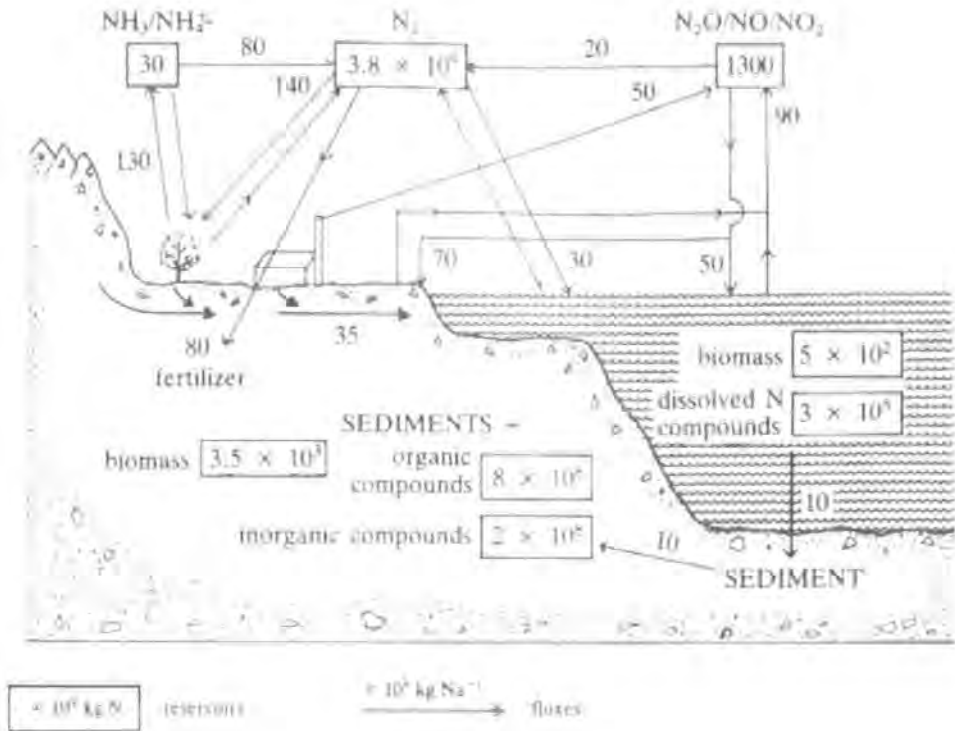
Figure 1.9. Simplified schematic representation of the global biogeochemical nitrogen cycle, illustrating quantification of some fluxes and reservoirs (O'Neill, 1993).

Important inorganic species include N_2, nitric acid (HNO_3), nitrate (NO_3^-), nitrite (NO_2^-), nitrous oxide (N_2O), nitric oxide (NO), N dioxide (NO_2), ammonium (NH_4^+), and ammonia (NH_3). Organic-N species exist in solution and as particulates, most organic-N species are important biomolecules. The sum of organic and inorganic species of N in both dissolved and particulate forms is often reported as total N (Williams, 2001).

N is a vital component of proteins, peptides, enzymes, genetic material (RNA and DNA), NO_3^-, energy-transfer molecules (adenosine triphosphate (ATP), adenosine diphosphate (ADP)), and substances that are vital to all organisms. Although the amount of N needed by animals, micro-organisms and plants varies considerably, the amounts of N required are

always great enough to make N fall into the category of being an essential macronutrient (needed in large amounts relative to other important essential nutrients such as: calcium, phosphorus, potassium, sulfur, and magnesium). In all cases, the nutritional requirements for N are exceeded only by those of carbon, hydrogen and oxygen (Williams, 2001).
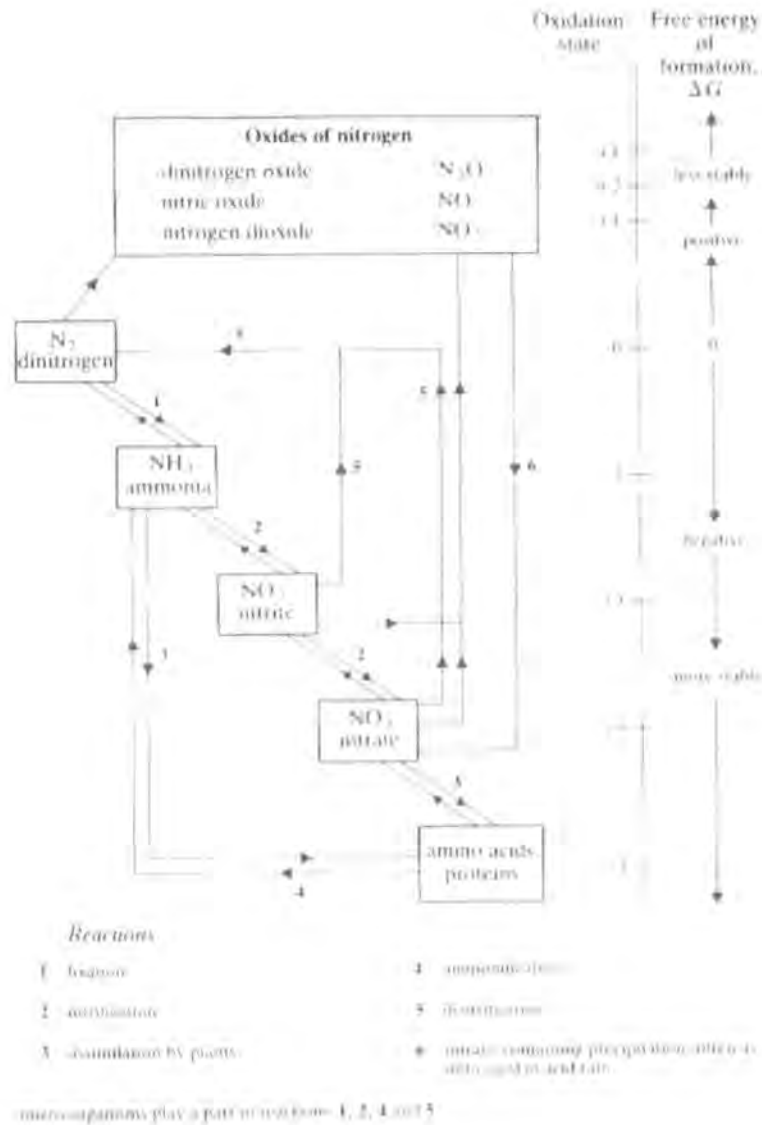
Figure 1.10. Simplified schematic representation of the chemical species of the nitrogen cycle, illustrating changes in oxidation states and relative stability (O'Neill, 1993).

1.7.11.1.2.   Soil nitrogen cycle

Soil-N is continuously transferred from one form to another through a variety of complex processes that either enhance or deplete the soil-N pool. Figure 1.11 illustrates the main

components and processes in soil-N cycle. Some of these processes are well understood, other less so; thus a better knowledge of soil N dynamics will assist in decreasing losses to the environment (Hofman and Cleemput, 1992).
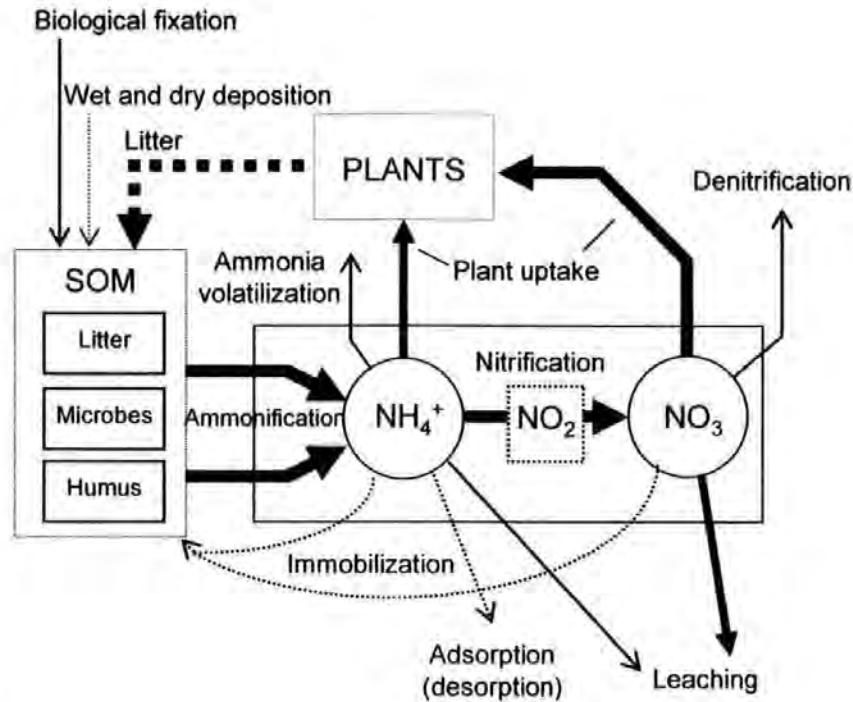
Figure 1.11. Simplified schematic representation of the soil nitrogen cycle. The dimension of the arrows indicates the relative importance of the various fluxes in the cycle; the continuous lines refer to processes wherein the impact of soil moisture is more relevant. (Porporato *et al.*, 2003).

Most N in soil is organic and is primarily derived from atmospheric N_2; both free living soil micro-organisms and those symbiotically associated with plants fix N_2 to produce organic-N in the form of amino groups in proteins ($-NH_2$), which becomes part of the SOM (Rowell, 1994; Porporato *et al.*, 2003). The decomposition of SOM converts organic-N into mineral-N (nitrate (NO_3^-), nitrate (NO_2^-) and ammonium (NH_4^+)). Mineral-N is taken up by plants and micro-organisms and transformed into organic-N. This internal cycling involves only plants and micro-organisms and dominates the N turnover at daily to seasonal time scales (Porporato *et al.*, 2003). Other fluxes, of N_2 gas and wet and dry deposition, are important in the long term balance (Porporato *et al.*, 2003). Biogeochemical

cycling of N has been extensively studied in different ecosystems (Radojević and Bashkin, 1999). The complex soil nitrogen transformation processes involving plants and micro-organisms are simplified in Table 1.6.

Table 1.6. Soil nitrogen transformation processes involving plants and micro-organisms (after Rowell, 1994; Porporato *et al.*, 2003).

Process	Description	Simplified reaction
Mineralization	microbial conversion of organic-N into mineral-N	$organic\text{-}NH_2 \rightarrow NH_4^+$
Nitrification	oxidation of ammonium-N to nitrite and nitrate by nitrifying bacteria	$NH_4^+ \rightarrow NO_2^- \rightarrow NO_3^-$
Immobilization	conversion of mineral-N to organic-N, and occurs when micro-organisms can not obtain enough organic-N from SOM	NH_4^+ and $NO_3 \rightarrow$ organic-NH_2
Volatilisation	loss of ammonia gas by conversion of ammonium ions to ammonia molecules in solution under alkaline conditions	$NH_4^+ + OH^- \rightarrow$ $NH_3 + H_2O$
Denitrification	reduction nitrite and nitrate to dinitrogen and nitrous oxide gas by denitrifying bacteria under anaerobic conditions and subsequent loss of these gases from the soil	NO_2^- and $NO_3^- \rightarrow$ $NO_2^- \rightarrow NO \rightarrow N_2O \rightarrow N_2$
Fixation	conversion dinitrogen gas to ammonium by nitrogen-fixing bacteria	$N_2 \rightarrow NH_4^+$
Assimilation	conversion of ammonium by micro-organisms to organic-N	$NH_4^+ \rightarrow$ organic-NH_2
Ammonification	conversion of organic-N to ammonia	$organic\text{-}NH_2 \rightarrow NH_3$

The degree of nitrogen transformation and cycling involving the processes listed in Table 1.6 depends on numerous factors. Figure 1.12 shows the relative fate of nitrogen fertilisers applied to soils. However, this is hugely generalised, as within soils, there are also temporal changes both with the changing demand by crops and with the seasonal soil conditions. For example, only small amounts of N are needed in the autumn, and in the winter crops are almost dormant. Uptake slowly increases in spring, and during the

summer months, the rapid growth of crops demands on average 1.6-3 kg N ha^{-1} d^{-1}, although this can be as much as 6 kg N ha^{-1} d^{-1} (Rowell, 1994). Ideally, the supply of N should match the demand. However, the N surpluses in the UK can range from 63-667 kg N ha^{-1} in dairy farms (Jarvis, 2000). The efficiency is low under intensive grassland management because of extra losses from the cycling of crop N through livestock (Davies, 2000).

Mineralization occurs during the growing season, and leaching occurs with the onset of rain (Rowell, 1994). Whether the concentration of nitrate increases as a result of mineralization or fertiliser application, there is potential for increased loss by leaching. Nitrate moves freely in soil solution and although nitrate leaching is a serious cause for concern, Figure 1.12 shows that loss by leaching is not the greatest pathway. N is also liable to loss as gaseous ammonia (Rowell, 1994).
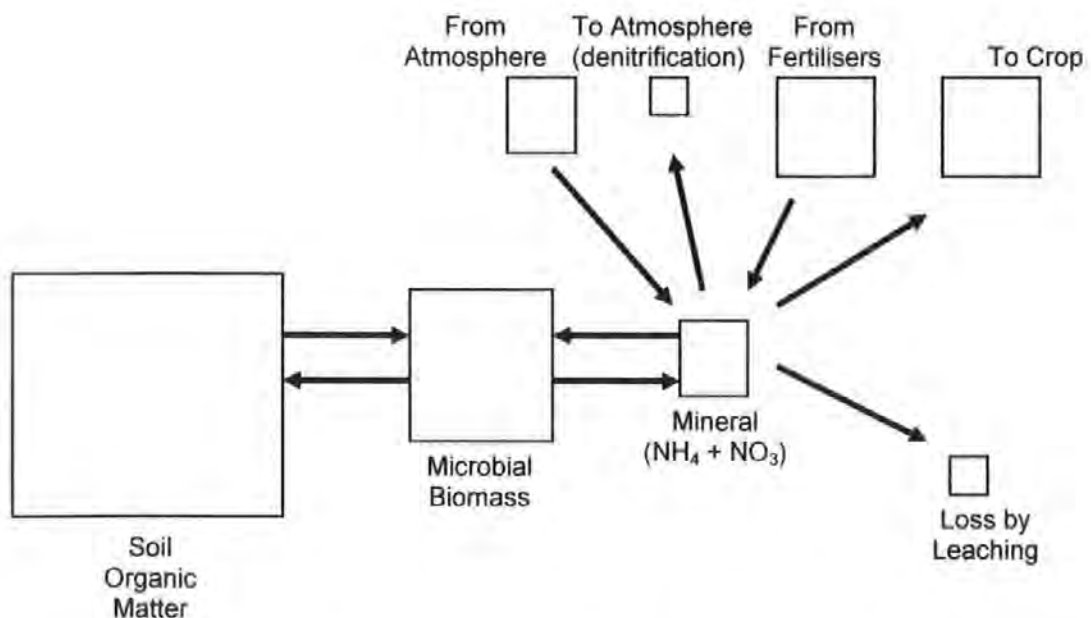
Figure 1.12. Nitrogen pathways in soils from artificial nitrogen fertilisers. The quantities of nitrogen likely to be in each form are proportional to the areas of the squares. (Schröder *et al.*, 2004).

1.7.11.1.3. Aquatic nitrogen

Nitrate is the most common form of nitrogen found in natural oxic waters. It can be biologically reduced to nitrite, which in turn can be oxidised to nitrate. Nitrates are highly soluble and readily leached to aquatic systems via surface and sub-surface flow to ground waters. In unpolluted freshwaters levels of NO_2^--N, NO_3^--N and NH_4^+-N are <1 mg L^{-1}, and this can limit plankton growth. Some fresh waters have harmful, elevated levels of both ions due to agricultural runoff and waste water discharge. Atmospheric deposition of nitrate to surface waters is elevated with various emission processes (5-10 mg L^{-1} NO_3^--N). Industrial, domestic and agricultural effluents can introduce large amounts of nitrate into surface and ground waters (50-100 mg L^{-1} NO_3^--N); this can reach water supplies, and control is expensive but monitored for human health. Agriculture is a major source of nitrate pollution due to N fertilizers and runoff from animals; these sources are very difficult to control because of their diffuse nature. Even if agricultural source controls are implemented, the response times in ground waters may be too long to make control effective. In addition, nitric acid in rain water and acid runoff from N fertilisers causes acidification of lakes, streams and groundwater that is also a concern (Radojević and Bashkin, 1999).

The separation of dissolved and particulate N is operationally defined based on filtration using 0.45 or 0.2 μm membrane filters (Robards *et al.*, 1994; Estela and Cerdà, 2005). The filtered fraction is referred to as dissolved (Figure 1.13). The main components of dissolved inorganic nitrogen (DON) are the ions referred to by their chemical speciation: nitrate [NO_3^-], nitrite [NO_2^-] and ammonia/ammonium [NH_3/ NH_4^+]. Dissolved organic nitrogen (DON) includes naturally occurring urea, vitamins and peptides. Particulate organic nitrogen (PON) refers to both biotic compounds such as proteins, peptides and nucleic acids, and abiotic humic substances and synthetic compounds.
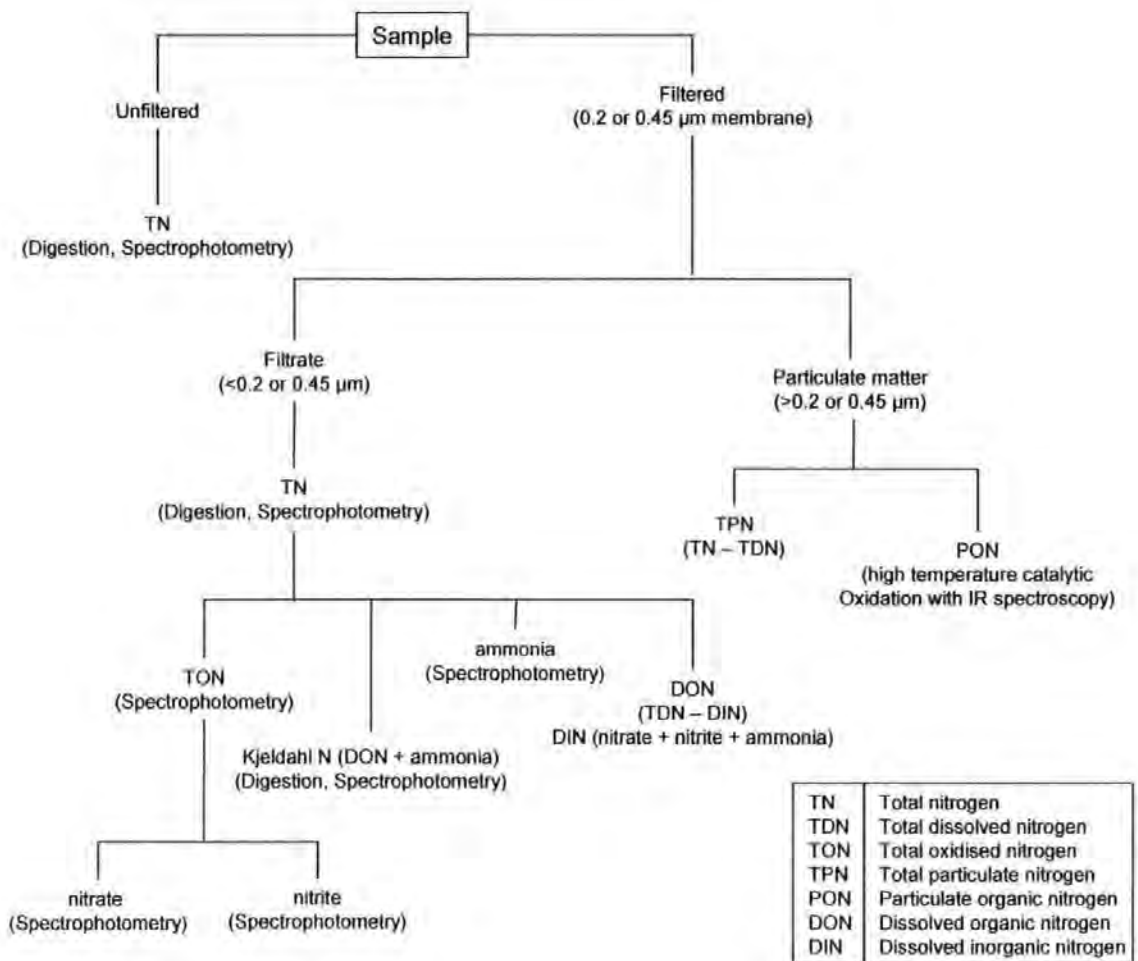
Figure 1.13. Operationally defined aquatic N fractions (after Robards *et al.*, 1994).

1.7.11.2.   Phosphorus abundance and properties

P is a non-metallic element that occurs both in organic and inorganic forms. It exhibits allotropy as it exists in several physically different but chemical identical forms (Williams, 2001). P is highly reactive, but its reactivity depends on its physical structure. Unlike N, P only forms compounds in one oxidation state that is stable (+5) (Williams, 2001). Some physical and chemical properties of P are given in Table 1.7. In the environment, P occurs in rocks, in marine sediments, as suspended solids in water and as dust particles in the atmosphere. It is the 11th most abundant element in the Earth's crust, and is mainly present as calcium phosphate minerals (apatites) and inorganic phosphates of aluminium, calcium and iron (Williams, 2001). P is an essential macronutrient for plant growth and a vital component of energy transfer molecules (ATP, ADP) in biological systems (Williams,

2001). It is a trace element in living organisms and a main constituent of DNA, bones, teeth and nerve and brain tissues (Williams, 2001).

Table 1.7. Physical and chemical properties of phosphorus (after Williams, 2001).

Property	Value/Example
Atomic number	15
Atomic weight	30.97376
Naturally occurring isotopes	^{31}P (100%)
Radioactive isotopes	$^{29}P, ^{30}P, ^{32}P, ^{33}P$
Oxidation states	
0	Red phosphorus (P_4)
+2	Phosphorus (II) chloride (P_2Cl_4); phosphorus (II) bromide (P_2Br_4)
+3	Phosphorus (III) fluoride (PF_3); phosphorus (III) hydride (PH_3); phosphorus (III) oxide (P_4O_6)
+5	Phosphate (PO_4^{3-}); phosphorus (v) oxide (P_4O_{10}); phosphorus (v) iodide (PI_5)

1.7.11.2.1. Global Phosphorus cycle

The simplified P cycle given in Figure 1.14 illustrates some fluxes and reservoirs. P is transported through the biosphere, hydrosphere and geosphere, and apart from dust transfer, there is relatively little circulation between the atmosphere and the other environmental compartments (Williams, 2001). Naturally occurring P compounds have low solubilities and volatilities; thus the mobility of P is low, and the biogeochemical cycling mainly occurs through transfer of suspended solids (Williams, 2001). The concentration of P in the oceans is characteristic of a biolimiting element: it is low at the surface and increases with depth due to decreasing photosynthesis and biological uptake (Figure 1.14).
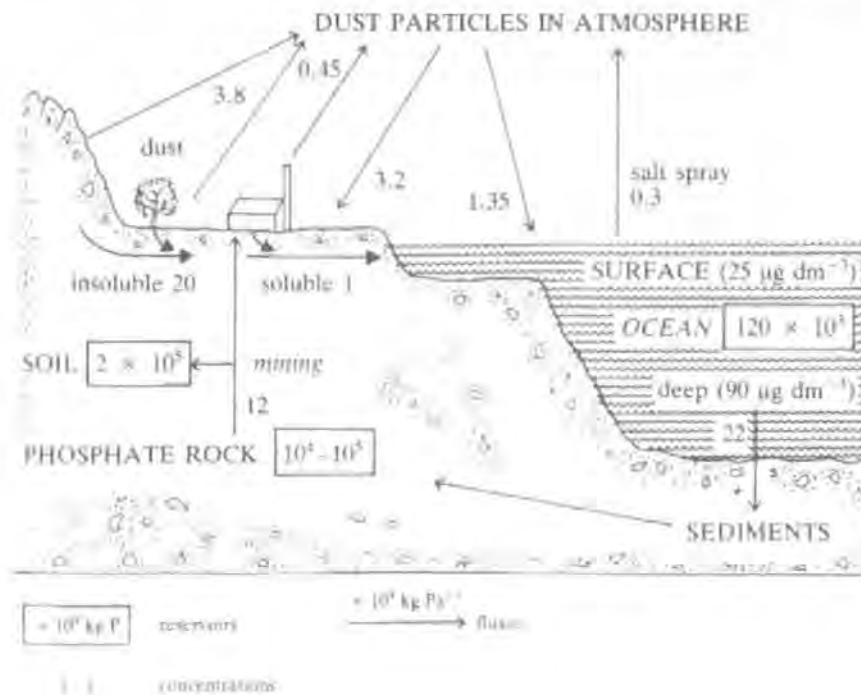
Figure 1.14. Simplified schematic representation of the global biogeochemical phosphorus cycle, illustrating quantification of some fluxes, reservoirs and concentrations (O'Neill, 1993).

1.7.11.2.2. The soil phosphorus cycle

Soil P exists in organic and inorganic forms (Figure 1.15). These forms are characterised by chemical extractions and relative lability (Sharpley, 1995). However, the forms generalized in Figure 1.15 are not discrete entities, as intergrades and dynamic transformations continuously occur to maintain equilibrium conditions (Sharpley, 1995). Extractable forms of P in soil are more widely studied than extractable forms of most other elements (Radojević and Bashkin, 1999).

Inorganic P species are dominated by hydrous sesquioxides, amorphous, and crystalline alumimium and iron compounds in acidic, noncalcareous soils and by calcium compounds in alkaline, calcareous soils (Figure 1.15). Organic P forms include relatively labile phospholipids, inositols and fulvic acids, while more resistant forms are comprised of humic acids (Figure 1.15). Soil microbial processes are important in the cycling of P (Williams, 2001) as a dynamic intermediary between inorganic and organic forms (Sharpley, 1995).
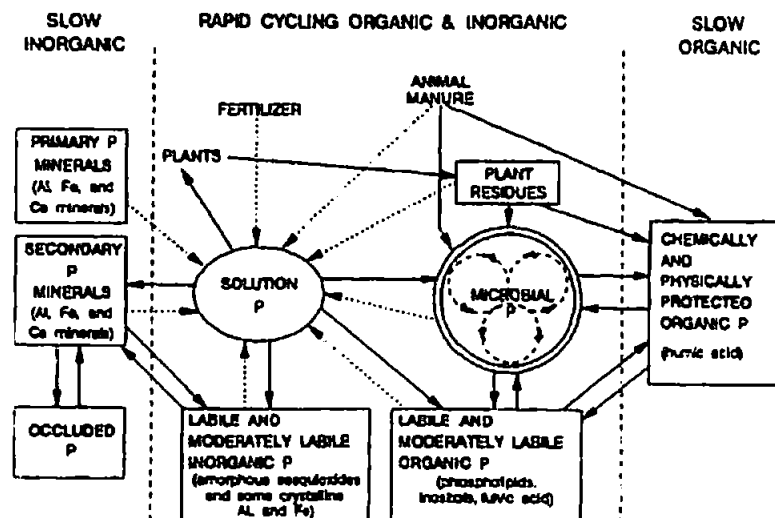
Figure 1.15. Simplified schematic representation of the soil phosphorus cycle, illustrating its components and measurable fractions (Sharpley, 1995).

Soil P content varies with parent material, texture, and management factors, which in turn influence the relative amounts of inorganic and organic P (Sharpley, 1995). In most soils, the P content of surface horizons is greater than subsoil due to the sorption of added P and greater biological activity and accumulation of organic material (Sharpley, 1995). However, many soils are deficient in bio-available phosphate, as like N, it must be present in an inorganic form before it can be utilised by plants (Williams, 2001). In most soils, 50 to 75% of the P is inorganic, although this fraction can vary from 10 to 90% (Sharpley, 1995). Soil phosphorus transformation processes involving plants and micro-organisms are given in Table 1.8.

Table 1.8. Soil phosphorus transformation processes involving plants and micro-organisms (from Rowell, 1994; Sharpley, 1995)

Form	Description
P-minerals	primarily aluminium, iron and calcium phosphates
P-particles	primarily bound to sesquioxides, clay minerals and humic substances to form very small particles, or absorbed to calcite in calcareous soils
Soil solution	predominantly as $H_2PO_4^-$ and HPO_4^{2-} over usual soil pH range
Plant-P	predominantly as organic esters
Organic matter	primarily as esters, speciation of organic-P depends on nature of plants and micro-organisms

The main P species in soils are orthophosphate (PO_4^{3-}), hydrogenphosphate (HPO_4^{2-}) and dihydrogenphosphate ($H_2PO_4^-$) (Williams, 2001). Orthophosphate is relatively insoluble and is difficult to remove with water due to its triple charge and strong affinity for cations. Hydrogen phosphates are more soluble as they have lower charges, and are commonly used as nutrient fertilisers (e.g. triple superphosphate ($Ca(HPO_4)_2$), although this soluble phosphate rarely migrates far from a fertiliser particle (Williams, 2001).

P, like N, is indispensable for the sustainability of agriculture (Schröder *et al.*, 2004). The use of both inputs has increased dramatically in recent decades, but so have the nutrient losses (Isermann, 1993; Schröder *et al.*, 2004). Throughout the 1950s to 1970s, soil P was subject to intensive research when crop response was the dominant interest. In the 1990s there was renewed interest because of the environmental consequences of its movement to aquatic systems (Powlson, 1998). An increasing proportion of P in receiving surface waters is derived from agricultural land, and the majority of farms in Europe operate on a P surplus (Edwards and Withers, 1998). Withers *et al.* (1998) estimate the UK surplus as 16 kg ha^{-1} a^{-1}, which is high considering the average field application in England and Wales is 14 kg ha^{-1} and 16 kg ha^{-1} to grassland and dairy farms, respectively (Haygarth *et al.*, 1998b).

In the past, it was perceived that phosphate, unlike nitrate, was strongly held by soil particles and that movement to the aquatic system was minimal (Powlson, 1998). It is now recognized that the phenomenon of preferential flow occurs in a wider range of soils than previously thought (Flury *et al.*, 1994; Powlson, 1998; Morris and Mooney, 2004). Thus P from fertilizer or manure applications can escape adsorption, and very low concentrations (20 µg P L^{-1}) can significantly enrich surface waters (Powlson, 1998). There is also greater recognition of surface runoff and soil erosion as mechanisms of P transport (Powlson, 1998). Figure 1.16 illustrates phosphorus loss from land to surface and ground waters.
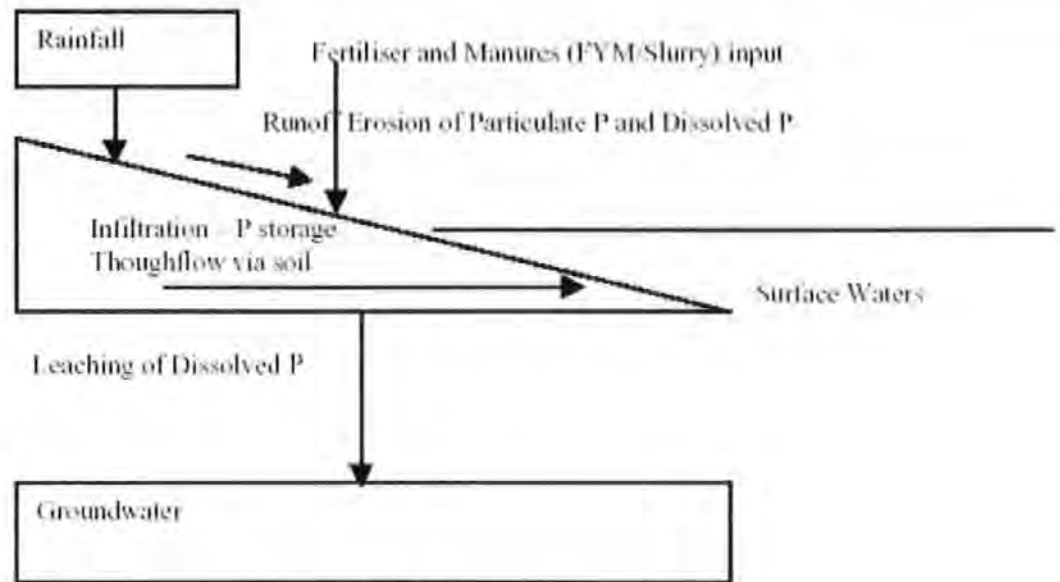
Figure 1.16. Simplified diagram illustrating phosphorus loss from land. (Schröder *et al.*, 2004)

1.7.11.2.3. Aquatic phosphorus

Aquatic P can be found in the form of different inorganic and organic species which in turn can be present in either the dissolved, colloidal or particulate form. However, the dominant species is always orthophosphate (Estela and Cerdà, 2005). The concentration of naturally occurring P compounds in unpolluted water is generally very low and P is the most common limiting nutrient in water (Williams, 2001).

Excess phosphates enter the aquatic system from industrial sources (sewage treatment, detergents and water softeners) and agricultural sources (soil erosion, animal manure, fertilisers and pesticides) (Williams, 2001). Aquatic microbial processes are significant in the cycling of P, particularly with the growth of photosynthetic algae, resulting in the undesirable process of eutrophication when the aquatic ecosystem receives an excessive enrichment of soluble phosphates (Williams, 2001), as discussed in Section 1.7.10.

As shown in Figure 1.17, the distinction between particulate (<0.45 μm) and dissolved (>0.45 μm) P is operationally defined based on filtration (Estela and Cerdà, 2005; Worsfold *et al.*, 2005). The term 'total' refers to the whole or unfiltered sample, 'filterable' indicates that the sample has been filtered, whereas 'reactive' is associated with P species that react with molybdate (Jarvie *et al.*, 2002; Estela and Cerdà, 2005). The term acid-hydrolysable phosphorus refers to the required acidic hydrolysis for the conversion of condensed phosphates to orthophosphate (Estela and Cerdà, 2005). Each fraction contains a range of P species (Jarvie *et al.*, 2002).

The dissolved fraction is defined as the filtered fraction and typically contains compounds such as orthophosphates (Peat *et al.*, 1997). In the literature, this filtered fraction is indistinctively used together with the words dissolved or soluble. Parameters determined on the filtered fraction are namely: filterable reactive phosphorus (FRP), total filterable phosphorus (TFP) and filterable acid-hydrolysable phosphorus (FAHP) (Estela and Cerdà, 2005). The filterable organic phosphorus fraction (FOP = TFP - (FAHP + FRP)) consists of nucleic acids, phospholipids, inositol phosphates, phosphoamides, phosphoproteins, sugar phosphates, aminophosphonic acids, phosphorus-containing pesticides (Estela and Cerdà, 2005) as well as organic condensed phosphates (pyro-, meta- and other polyphosphates) (Radojević and Bashkin, 1999).

Filterable condensed phosphates (FCP) are equal to acid-hydrolysable phosphorus (FCP = FAHP) and if the reaction of molybdate is used, FRP + FAHP is obtained (Estela and Cerdà, 2005). The parameters obtained from the whole sample (without filtration) are namely: total reactive phosphorus (TRP), total acid-hydrolysable phosphorus (TAHP), total phosphorus (TP) and total organic phosphorus (TOP) and are equivalent to those previously mentioned. However, this also considers the particulate fraction (Estela and Cerdà, 2005).

Total particulate phosphorus (TPP = TP - TFP), particulate reactive phosphorus (PRP = TRF - FRP), particulate acid-hydrolysable phosphorus (PAP = TAHP - FAHP) and particulate organic phosphorus (POP = TOP - FOP) related to the contents of phosphorus in the particulate phase and are determined by the transformation into orthophosphate and the reaction of molybdate (Estela and Cerdà, 2005). Determination of FOP, TFP, TP or TOP requires a previous digestion of the sample for the conversion of the organic phosphates into the orthophosphate reactive specie.
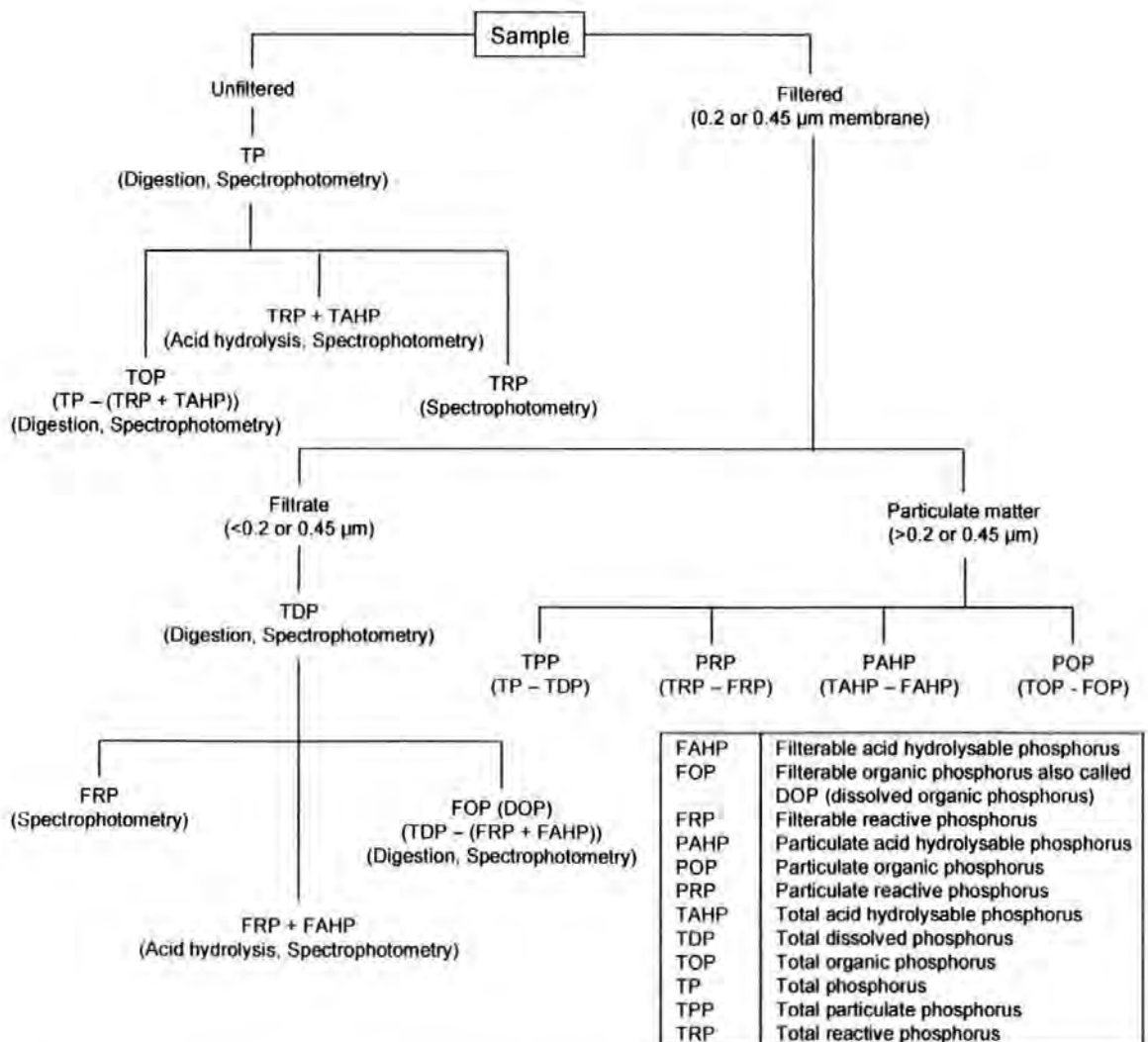
Figure 1.17. Operationally defined aquatic P fractions (after Worsfold *et al.*, 2005)

1.7.12. Analytical determination of nutrients and tracers

The most widely used methods for determination of nitrate (after reduction to nitrite) are spectrophotometric and based on the Griess reactions. A variety of analytical methods such as chromatographic, fluorimetric, amperometric, voltammetric, chemiluminescence, and capillary electrophoresis have also been developed for the determination of nitrate (Haghighi and Farrokhi Kurd, 2004).

The molybdenum blue reaction is almost universally used for phosphate determinations (Peat *et al.*, 1997). Combined with spectrophotometric flow methods the technique has been applied to a wide range of samples (Estela and Cerdà, 2005). Determination of phosphorus can be carried out by classical analysis methods, namely: gravimetric methods (precipitation) and volumetric methods (titration).

Instrumental techniques include, optical methods based on molecular spectroscopy techniques (visible photometry, thermal lens spectroscopy, chemiluminiscence and fluorescence), atomic spectroscopic techniques (atomic absorption spectrometry, inductively coupled plasma-atomic emission spectrometry) and electrochemical techniques (potentiometry, amperometry and voltametry) (Estela and Cerdà, 2005). Chromatographic methods such as high-performance liquid/ion chromatography, gel filtration/exclusion chromatography and capillary electrophoresis together with the use of several detection systems have enabled carrying out speciation. (McKelvie, 2000; Estela and Cerdà, 2005).

CHAPTER TWO

2. Methods and Materials – Experimental Design

2.1. Overview of experimental design

The phenomenon of enhanced structural differentiation in soils beneath white clover and its impact on nutrient transport was studied at various scales. The dimensions of the different scales of study are given in Table 2.1. Note that the dimensions are of the soil not the container. The dimensions of the rhizotrons are given to illustrate the scales of study, however, the results are not reported because of unsuccessful growth of plants and roots, and the rapid colonization of algae on the glass plates and soil surface.

Table 2.1. Dimensions of the scales of study.

Dimension	Column	Monolith	Rhizotron
Surface Area (cm^2)	83.3	2700	5.25
Volume (L or dm^3)	1.17	140	0.116
Height (cm)	14.0	52.0	22.0
Length (cm)	-	52.0	10.5
Width (cm)	-	52.0	0.50
Diameter (cm)	10.3	-	-

2.1.1. Column Experiments

Column Experiment 1 was set-up using soil from two different horizons of the Crediton soil series. The Crediton series was selected due to its availability (it is a local North Wyke soil), because the soil has been well characterized at IGER (Williams *et al.*, 2000), and because it was used in previous PhD research (Peat, 1998; McDonald, 2000; Johnson, 2004) for similar transport studies and modelling with Pore-Cor. Soil was extracted from two soil horizons, with high and low carbon content, and are referred to as topsoil (0-200 mm) and subsoil (200-650 mm) respectively. The variable carbon content was intended to assess the degree of structural differentiation related to the carbon substrate for microbes.

Preliminary results were obtained from Column Experiment 1. The number of treatments and replicates were increased in Column Experiment 2 (from 12 treatments and 64 samples to 22 treatments and 199 samples). The number of replicates was increased to accommodate for destructive sampling techniques. Treatments were extended to include soil of the Crediton series dried at 85°C to suppress biological activity, and intact samples in their original field state. Re-packed soil was also selected from three additional soil series with different textures. The soil of the Denbigh series was used in the original study of enhanced structural differentiation in soils beneath white clover (Mytton *et al.*, 1993). The soil of the Frilsham series was selected because of its calcareous nature and soil of the Greinton series was of similar texture to the other soil series but under arable management. The soil series, treatments and number of replicates for Column Experiments 1 and 2 are summarized in Table 2.2 and Table 2.3 respectively.

Table 2.2. Column Experiment 1: treatments and number of replicates.

Soil	Ryegrass	White clover	7:3 mixture	Unplanted	Total
Crediton series re-packed topsoil	7	7	7	3	24
Crediton series re-packed subsoil	7	7	7	3	24
Crediton series re-packed clear pots	4	4	4	4	16
Total	18	18	18	10	64

Treatments from Column Experiment 1 (Table 2.2) were used for the following experiments: samples in clear pots were used for assessing changes in soil structure; re-packed topsoil and subsoil were used for observations and photography, oxygen diffusion rates/porosity, soil structural stability, and preliminary nitrate leaching experiments; and soil water retention and modelling using Pore-Cor was performed on re-packed subsoil in parallel to a PhD study (Johnson, 2004), which compared subsoil from four different soil series.

Treatments from Column Experiment 2 (Table 2.3) were used for monitoring changes in soil structure, oxygen diffusion rates, and nutrient leaching/tracer experiments. Samples of the Crediton series re-packed heated topsoil were not used due to time limitations. Samples of the Crediton series undisturbed topsoil were not used as they contained a high proportion of large stones.

Table 2.3. Column Experiment 2: treatments and number of replicates.

Soil	Ryegrass	White clover	7:3 mixture	Unplanted	Total
Crediton series re-packed topsoil	25	25	25	25	100
Crediton series re-packed subsoil	6	6	-	6	18
Crediton series re-packed heated topsoil	3	3	-	3	9
Crediton series undisturbed topsoil	6	6	-	6	18
Greinton series re-packed topsoil	6	6	-	6	18
Frilsham series re-packed topsoil	6	6	-	6	18
Denbigh series re-packed topsoil	6	6	-	6	18
Total	58	58	25	58	199

2.1.2. Half-meter lysimeters

Due to time constraints of analysis and costs involved in extracting large soil monoliths, only one soil type was extracted and prepared for one replicate for each plant treatment. These four lysimeters were used for the study of nutrient and tracer transport.

2.2. Re-packed Column Experiments

2.2.1. Sample containers and growth tables

The purpose-built cylinders used as sample containers for all Column Experiments are shown in Figure 2.1. UPVC pipe with an internal diameter of 103 mm was cut into sections

of 170 mm. Twelve 2 mm holes were drilled into a polyethylene tube end and used as a base. The base was attached to the bottom of the container with epoxy resin and the inside sealed with silicone. The containers were thoroughly cleaned in 20% (v/v) nutrient-free detergent Decon90® (Decon Laboratories, UK) to remove contaminants, such as plasticizers and adhesives, which interfere with soil structuring (Meneffe & Hautala, 1978). A nylon mesh was used to cover the base of the container to prevent loss of soil particles.

UPVC pipe: 170mm x 103 mm diameter
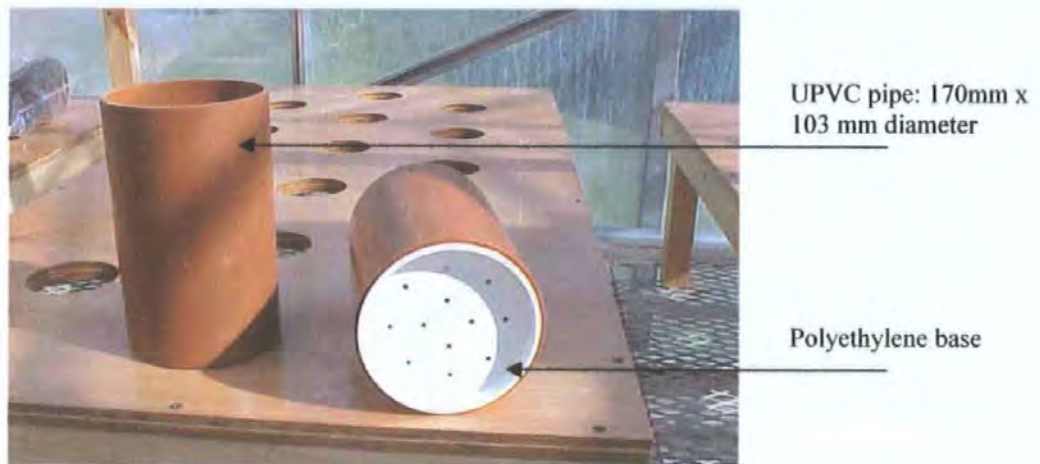
Polyethylene base

Figure 2.1. Sample containers made from UPVC pipe and a polyethylene base.

The stands shown in Figure 2.2 were built as growth tables. A sheet of marine plywood (1.2 m x 0.6 m) was attached to a timber frame (0.3 m tall). Sixteen holes (78 mm diameter) were made in each table. A polypropylene funnel designed to sit inside the base of each container was placed in each hole for drainage.

Sample container

Polypropylene funnel

Growth table with holes for funnels
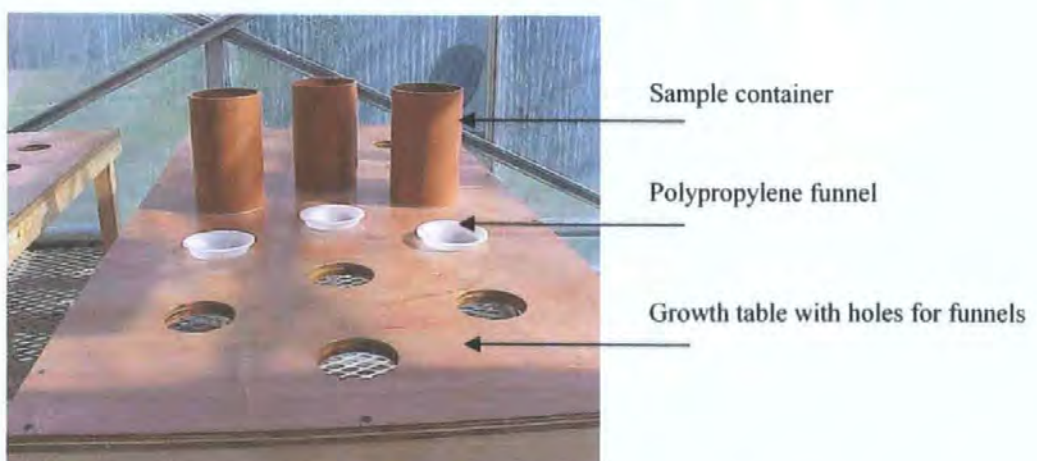
Figure 2.2. Sample containers and polypropylene funnels in position on growth table.

2.2.2. Soil excavation

Soil was taken from beneath a pasture managed by the Institute of Grassland and Environmental Research (North Wyke) which is located 10 km north of Dartmoor National Park and 10 km north-east of Okehampton, Devon, UK. The soil is of the Crediton series 'DeBathe' (Dystric Eutrocrept [FAO]), classified as a well drained reddish, stony, loamy brown earth (Clayden & Hollis, 1984). During May 2001, soil was manually excavated from a profile that had been previously exposed to a depth of 2 m (Figure 2.3). The soil profile was weakly differentiated into two horizons. Samples were taken from a depth of 0-200 mm (with high carbon content) and 200-650 mm (with low carbon content), and are referred to as topsoil and subsoil respectively. The soil was transported in pre-washed black plastic bins to a glasshouse at North Wyke. This soil was used for the treatments in Column Experiment 1 (Table 2.2).

Figure 2.3. Manual excavation of topsoil (0-200 mm) and subsoil (200-650 mm) of the Crediton series.

During spring 2002, a second sample of topsoil and subsoil of the Crediton series was taken as described above. In addition, three other soil series were collected from England and Wales (details are given in Table 2.4). The turf layer (<50 mm) was removed and soil was taken from a depth of 0-200 mm, referred to as topsoil. The soil was transported in plastic bins/bags to a glasshouse at IGER, North Wyke. These soils were used for the treatments in Column Experiment 2 (Table 2.3).

Table 2.4. Four different soil series used: soil type, classification, land use and location.

Soil Series	Texture	Classification	Drainage	Land Use	Location	Grid Reference	Reference
Crediton	Sandy loam	Reddish, stony, loamy typical brown earth	Well-drained	Long ley pasture	IGER, North Wyke, Devon	SS 677 018	Clayden, 1971
Greinton	Fine sandy loam	Loam from sandstone	Slow-draining	Arable	Long Ashton Research Station, Bristol	ST 539 697	Donaldson (pers. comm.)
Frilsham	Sandy loam or clay loam	Loamy head over chalk, typical argillic brown earth	Well-drained	Permanent grass	Berkshire College of Agriculture, Berkshire	SU 833 821	Mackney, 1986
Denbigh	Silty clay loam	Silt loam acid brown earth	Slow-draining to moderate	Long ley pasture	IGER, Trawsgoed Farm, Ceredigion	SN 683 739	Rudeforth, 1970

2.2.3. Soil sample preparation

2.2.3.1. Drying

The soil was spread across individual tables in the glasshouse (Figure 2.4) and allowed to air-dry for an hour at an ambient temperature of 30°C. During the drying period, large aggregates were broken by hand and soil turned frequently to ensure even drying. Latex gloves were washed in water and worn at all times to minimise the risk of contamination from the skin.

Figure 2.4. Drying and de-structuring of soil, prior to sieving and repacking.

2.2.3.2. Sieving

Soil was initially sieved through a 5 mm mesh to remove large stones, plant debris and macro fauna (mostly worms). It was subsequently homogenized by passing it through a 2 mm sieve; particles remaining in the sieve were gently crushed using a mortar and pestle and re-sieved. Soil (<2 mm) was stored in labelled plastic bins. Soil moisture content was determined at 105°C for 24 hours and organic matter content by loss-on-ignition at 450°C for 4 hours (see Chapter Three, Section 3.3.2.2).

2.2.3.3. Re-packing

Using a method adapted from Didden *et al.* (1991), a reproducible soil structure with uniform soil physical characteristics was obtained by compressing a pre-determined amount of soil to a specific volume (1.167 m^3) in purpose-built sections of UPVC pipes with an internal diameter of 103 mm to a height of 140 mm. Various bulk densities (Table 2.5) were achieved by applying a 22 kg weight for 5 minutes to each of 4 equal soil layers. Preliminary test showed that the bulk density was evenly distributed rather than layered. The six soil treatments (Figure 2.5) were conditioned to 15% or 30% moisture content (Table 2.5).

Table 2.5. Mean bulk density, moisture content, porosity and pore-volume of the six soils after re-packing.

Soil Type	Mean Bulk Density (g cm^{-3})	Moisture Content (%)	Adjusted Moisture Content (%)	Mean Porosity (%)	Mean Pore Volume (cm^{-3})
Crediton Topsoil	1.18	14.2	15.0	55.5	646.7
Crediton Subsoil	1.30	11.7	15.0	51.0	595.0
Crediton Dried	1.36	1.0	15.0	48.7	568.2
Greinton series	1.17	13.5	15.0	56.0	653.0
Frilsham series	1.18	11.5	15.0	55.7	648.9
Denbigh series	0.91	27.7	30.0	65.5	763.8

Crediton dried

Crediton subsoil

Denbigh series

Frilsham series

Greinton series

Crediton topsoil

Figure 2.5. The six re-packed soils used in Column Experiment 2.

2.3. Intact Column Experiment

2.3.1. Sample containers

The same UPVC containers were used as in the re-packed Column Experiment as detailed in Section 2.2.1. The base was attached to the container after sample extraction, as described below.

2.3.2. Sample extraction

During summer 2002, intact soil cores of the Crediton series topsoil were manually excavated. The turf layer (50 mm) was removed and sample containers were hammered carefully into the exposed soil (Figure 2.6). Soil was removed from the outside of the container with a trowel and the base roughly trimmed with a knife. Cores were transported to the glasshouse at North Wyke, where the base of the soil removed to give a core height of 140 mm. Samples were weighed and the time taken for 100 ml to drain from the soil surface assessed to identify differences between cores.

Figure 2.6. Extraction of intact cores of topsoil from the Crediton series.

2.4. Undisturbed 0.5 m cube lysimeters

2.4.1. Lysimeter casing

The lysimeter casings were made from marine ply-wood (540 mm wide x 540 mm high x 18 mm thick) held together along the four sides with angle iron (50 mm wide x 600 mm high x 5 mm thick). The angle iron stood 60 mm proud of the wooden sides and two holes were drilled into each piece of angle iron to enable passage of a lifting-strap for handling (Figure 2.7). Interior wood was preserved with polyurethane varnish, exterior wood sealed

with preservative, and edges and holes covered with silicone sealant (the chemical components of materials were researched for their possible interference on soil structure).

An external cutting plate was made from four pieces of angle iron (5 mm thick x 50 mm high) and attached to the base of the casing (Figure 2.8). The edge to be in contact with the soil surface was slightly sharpened to assist with the cutting of the soil and so to aid ease of extraction.

Figure 2.7. Assembly for lifting the lysimeter casing.

Figure 2.8. Metal cutting plate attached to the base of the lysimeter casing.

2.4.2. Soil block extraction

A suitable site for extraction was identified; the site was an un-grazed pasture managed by the IGER (North Wyke) and was reseeded in 1999. Soil beneath a long-term pasture has some soil structuring, but this was preferred over a de-structured arable soil with possible contamination of herbicides. The site is located 10 km north of Dartmoor National Park and 10 km north-east of Okehampton, Devon, UK. The soil is of the Crediton series classified as DeBathe (Dystric Eutrocrept [FAO]), and is a well drained reddish, stony, loamy typical brown earth (Clayden & Hollis, 1984). Topsoil is subject to summer cracking, overlaying a B/C horizon of in-*situ* weathered regolith (Holden *et al.*, 1995). Stone content was variable, increasing with size and frequency at depth. This soil series was also used for some Column Experiments (Sections 2.2 and 2.3).

The extraction processes is shown in schematically in Figure 2.9 and sequentially in Figure 2.10 (A to I). This is preferable to the extraction method of Shan *et al.* (2005), where lysimeters of 700 mm height x 386 mm internal diameter were obtained by removing the surrounding soil to leave a cylindrical intact column; the column was carefully chiselled to size and inserted into a PVC tube coated with paraffin.
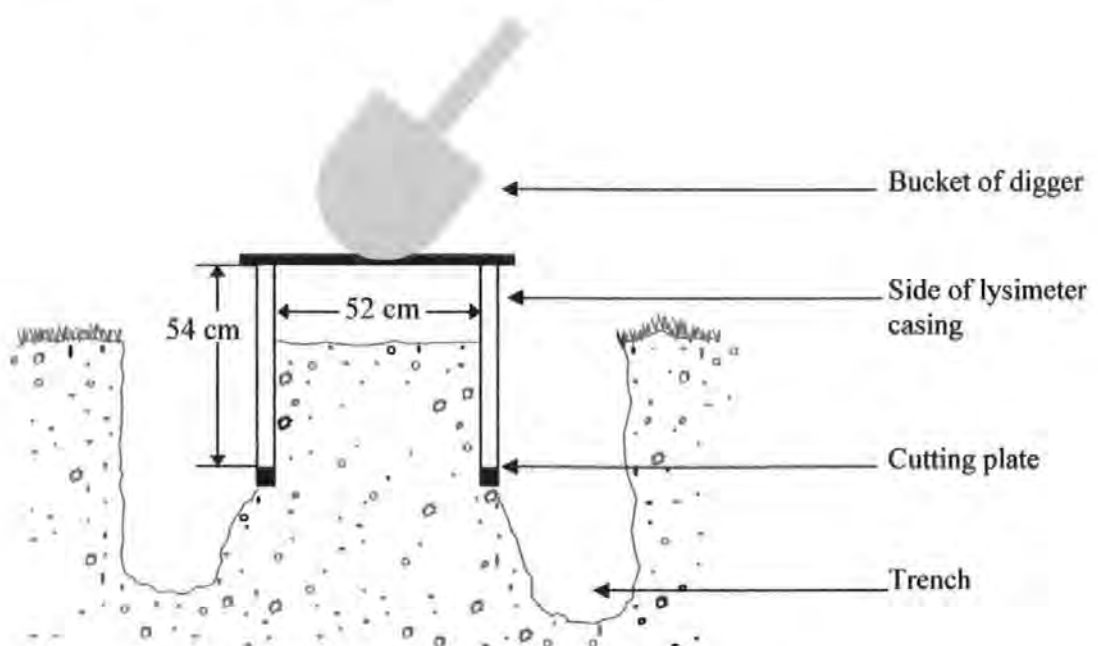
Figure 2.9. Diagrammatic representation of soil monolith extraction.

The lysimeter casting was placed on the soil surface and the sample area was marked leaving an extra 500 mm of soil around the outside of the casing to reduce the risk of collapse and fractures of the monolith. A hydraulically operated digger was used to excavate a trench (500 mm x 500 mm) around the sample monolith (Figure 2.10.A). The turf, topsoil and subsoil were kept separately for later replacement and restoration of the land.

The turf layer (50 mm) was removed from the sample area and the lysimeter casing placed on the exposed monolith (Figure 2.10.B). The bucket of the digger was used to gently apply weight to the top of the casing, which was kept level. As the casing filled, soil and large stones were manually removed from around the cutting plate (Figure 2.10.C). Once the soil had reached the desired level inside the casing (Figure 2.10.D), scaffolding poles were hammered into the soil beneath the monolith. The monolith was freed from the bulk soil by lifting the scaffolding poles with the digger (Figure 2.10.E).

The soil block was then gently tipped onto its side, the cutting plate removed and the base roughly trimmed until level with the casing (Figure 2.10.F). A nylon mesh and a metal grid were attached to the base of the block (Figure 2.10.G) and the block was returned upright. Lifting hooks and ropes were attached to holes on the top of the angle iron frame. The lysimeter was lifted from the pit with the digger (Figure 2.10.H), placed on a trailer and transported to North Wyke (Figure 2.10.I).

Figure 2.10. Lysimeter extraction: (A) trench dug around monolith; (B) lysimeter casing placed on monolith and gently pushed with bucket of digger; (C) soil and large stones removed from around cutting plate; (D) lysimeter casing filled; (E) lysimeter detached from bulk soil; (F) base of monolith trimmed; (G) nylon mesh and metal grid attached to base of casing; (H) intact lysimeter extracted with digger; (I) lysimeters placed on trailer for transportation.

The monoliths were unloaded with a fork-lift truck. Six holes (20 mm diameter) were drilled into each side of the lysimeter casing (Figure 2.11.A) and injected with inert polyurethane expanding foam (Figure 2.11.B). The foam was observed to flow freely from the delivery points completely surrounding the sides of the soil, thus creating a solid water-tight seal to prevent edge effects. Excess foam was removed and trimmed level with the soil surface, injection holes were sealed with silicone. The lysimeter casing was subsequently cladded with Celotex® to provide insulation (Figure 2.11.C).

Figure 2.11. Lysimeter preparation: (A) six holes drilled into each side of lysimeter casing; (B) expanding foam injected into holes to prevent water flow between soil monolith and casing; (C) insulation attached to outside of the casing.

2.5. *Rhizobium* inoculation

To ensure effective nodulation in the roots of white clover and subsequent nitrogen fixation, all treatments and samples (pots, lysimeters and rhizotrons) were inoculated with a mixture of IGER's *Rhizobium leguminosarum* bv. *trifolii* strains 502, 505, 509, 511 and 515. These symbionts were applied in liquid form to the soil surface at approximately 2×10^{11} *rhizobia* ha^{-1}. This is typical of agricultural legume inoculation practice and represents about 1% of the 10^4 g^{-1} *rhizobia* naturally present in topsoil (Amarger, 2001).

2.6. Treatments

Treatments are given in Section 2.1 (Table 2.2 and 2.3). The various soil types and soil horizons used for the rhizotrons and Column Experiments were dried, sieved and re-packed. Undisturbed soil was extracted from the field at the 0.5 m cube scale, at the pot scale and smaller, but from only one soil type. Re-packed samples will differ from intact soils in physical properties and microbial activity (Schjønning *et al.*, 1999). However, re-packed soil provides an initial reproducible and uniform structure for characterising changes.

Fertilized ryegrass treatments were used to represent conventional farming systems. Mixed treatments represented a realistic value of 30% clover in a mixed sward under organic grazing management. Pure white clover treatments assessed the impact of the extreme effect of soil structuring and provided an extreme comparison with ryegrass. Unplanted soils served as controls and simulated fallow conditions.

2.7. Planting Densities

The samples (various soil types and scales) were sown with seeds of perennial ryegrass (*Lolium perenne* L. cv. AberAvon), white clover (*Trifolium repens* L. cv. AberHerald), or

a mixture of the two species (7:3 grass:clover) at various planting densities (Table 2.6). Unplanted controls were also included.

The Column Experiment soils were sown with 10 seeds per pot at a uniform spacing of 1 seed per 8.3 cm^2 (Figure 2.12). This was selected for maximum effect after Mytton *et al.*, 1993. Using a template (Figure 2.12), a small hole was marked for the position of each seed. Seeds were lightly covered with 1 mm of soil. The pots were covered with polythene sheeting to ensure adequate moisture and humidity levels during germination. Plants were maintained at 10 per pot.

The soil block lysimeters were sown according to realistic field seed rates, which are 20-30 kg ha^{-1} for perennial ryegrass and 2-4 kg ha^{-1} for white clover (Rhodes, 2001). The upper limit of each recommended range was used (Table 2.6). This corresponded to a lower planting density than for the Column Experiments, the planting density would be too high if up-scaled from pot to block. In a mixed sward, the recommended seed rates are 3.5 kg ha^{-1} clover plus 22-25 kg ha^{-1} grass (Frame and Newbould, 1986) and 4 kg ha^{-1} clover plus 25-30 kg ha^{-1} grass (DEFRA, 2002). The mixed blocks were sown according to Rhodes (2001), who reports that the initial clover to grass ratio must be sufficient to sustain a 30% clover content. The above seed rates would have given less than 30% clover.

The soil surface of the blocks were prepared to an undulating fine tilth, roots were removed. The seeds were weighed, evenly sprinkled over the soil surface and lightly covered with 1 mm of soil. The blocks were covered with polythene sheeting to ensure adequate moisture and humidity levels during germination.

For the rhizotrons, a single seed was placed on the undulating surface of each soil to enable comparison between root and soil structural development.

Table 2.6. Plant/seed density and surface area.

		Column	Monolith	Rhizotron
Surface Area (cm^2)		83.3	2700	5.25
Number of Seeds	Grass	10	203	1
	Clover	10	180	1
Mixture	Grass	7	74	-
	Clover	3	180	-
Planting Density	Grass	48	30	76
(Kg ha^{-1})	Clover	7	4	11
Mixture	Grass	34	11	-
	Clover	2	4	-

1 grass seed = 4 mg; 1 clover seed = 0.6 mg.
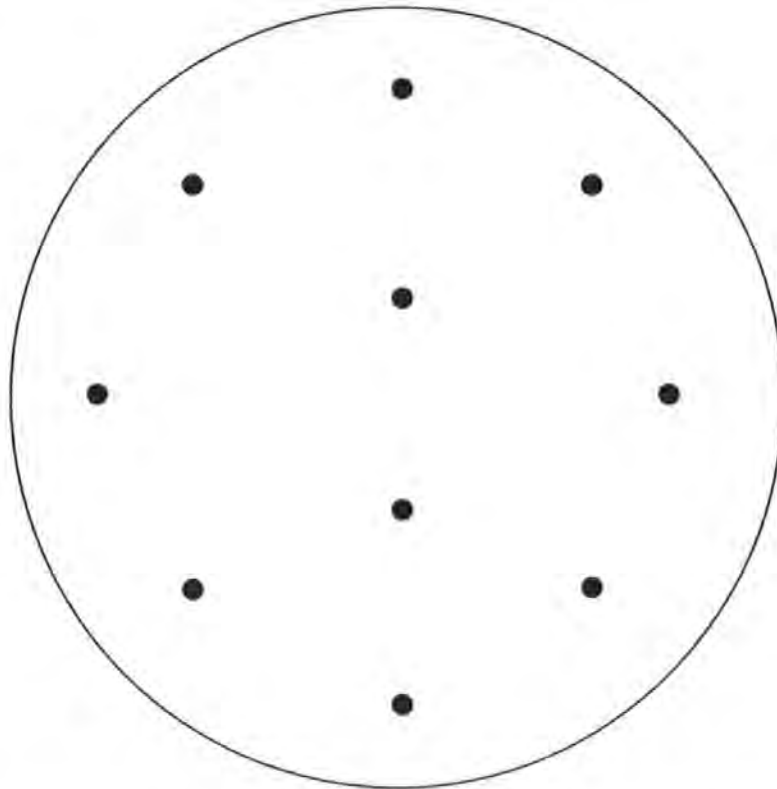
Figure 2.12. An actual-size diagram for the planting position of 10 seeds per pot, at a uniform spacing of 1 seed 8.3 cm^{-2}, equivalent to a planting density of 48 Kg ha^{-1} and 7 Kg ha^{-1} for mono-treatments of perennial ryegrass and white clover, respectively.

2.8. Controlled growing conditions

Samples were grown in a glasshouse under natural illumination during the summer, whereas supplementary horticultural lighting was provided for 12 hours a day during the autumn and winter months. The ambient temperature reached a maximum of 50°C during

summer and a minimum of 15°C by night. After 2 weeks, 10 seedlings were established in each pot (Figure 2.13) and the samples were randomly placed in their growing positions. Figure 2.14 and Figure 2.15 show the plants after weeks 4 and 13 respectively. The block lysimeters were placed inside the glasshouse for the winter (Figure 2.16), to encourage plant growth, prevent frost damage to the plants and to avoid the freeze-thaw mechanism of soil structuring. In spring, the half-meter lysimeters were positioned outdoors to receive natural illumination and rainfall.
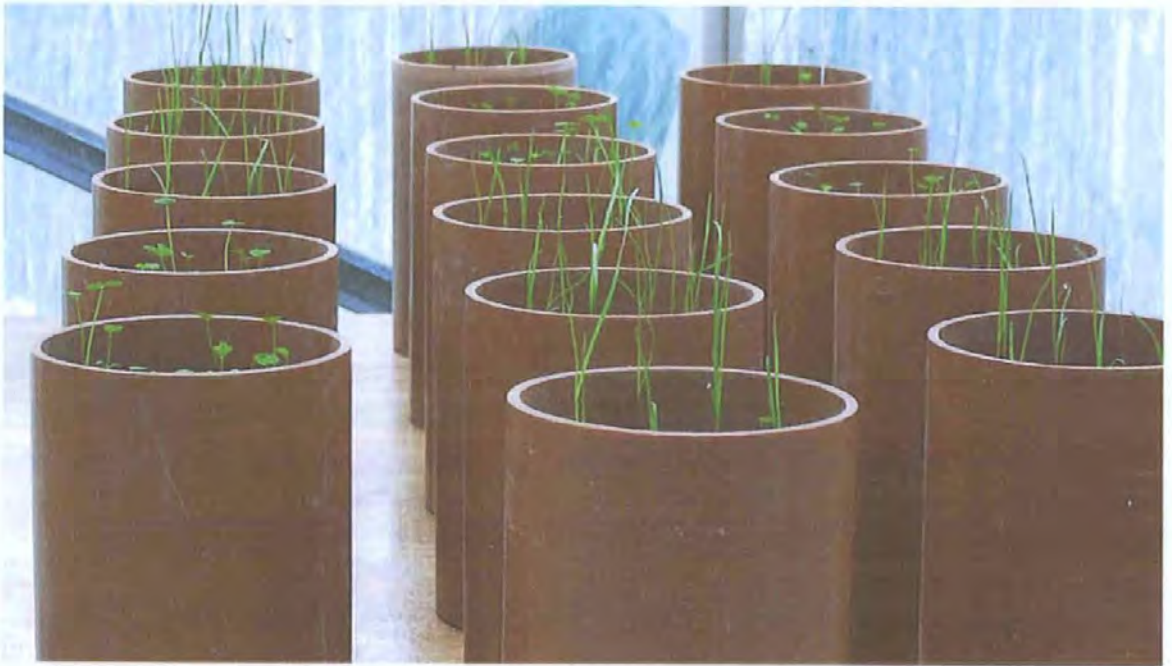
Figure 2.13. Seedlings after 2 weeks of growth.

Figure 2.14. Plants after 4 weeks growth in a glasshouse.

Figure 2.15. Plants after 13 weeks growth in a glasshouse.

Figure 2.16. Planted lysimeters inside glasshouse during winter.

2.9. Water regime

The regime adopted for supplying water to the samples changed during the experiment according to various criteria. The main aims were to apply a non-limiting volume for plant growth and a volume that would not promote leaching. Samples were watered frequently to minimise intense wetting and drying cycles. To determine the volume of water to apply, samples were weighed before irrigation. The change in weight was determined from the weight of the sample before watering minus the weight after the previous watering. This change in weight was caused by various possible processes, namely a positive change due to an increase in water content or biomass or a negative change due to evapotranspiration. The relative rates of these processes were not measured, but as shown below, nearly all changes were negative, indicating the dominance of evapotranspiration.

For Column Experiment 1, the treatments received an equal volume of tap water during the first 128 days of growth. Figure 2.17 and Figure 2.18 show the mean decrease in weight of each treatment, measured as the change in weight between each irrigation event. The difference in weight loss between all treatments was small during the first 35 days of growth. After 39 days, the difference in weight loss between the planted treatments increased but continued to show similar trends; the unplanted controls increased in weight as they reached field capacity (Figure 2.17). From day 129, treatments received differential amounts of water so that all samples were of similar weight and near field capacity. Weight loss from clover treatments was greater than grass during the winter months; this was attributed to a faster rate of evapotranspiration, as plant growth was low.

For Column Experiment 2, treatments were watered every day to 15% water content (w/w) during the initial weeks of growth, with the exception of the Denbigh series, which had a higher initial water content and so was maintained at 30% (w/w). Water loss from clover treatments was greater than that of the grass treatments, attributed to a faster rate of

evapotranspiration due to a greater surface area of clover biomass. To reduce the difference
in water demand between treatments, the plants were trimmed at regular intervals.
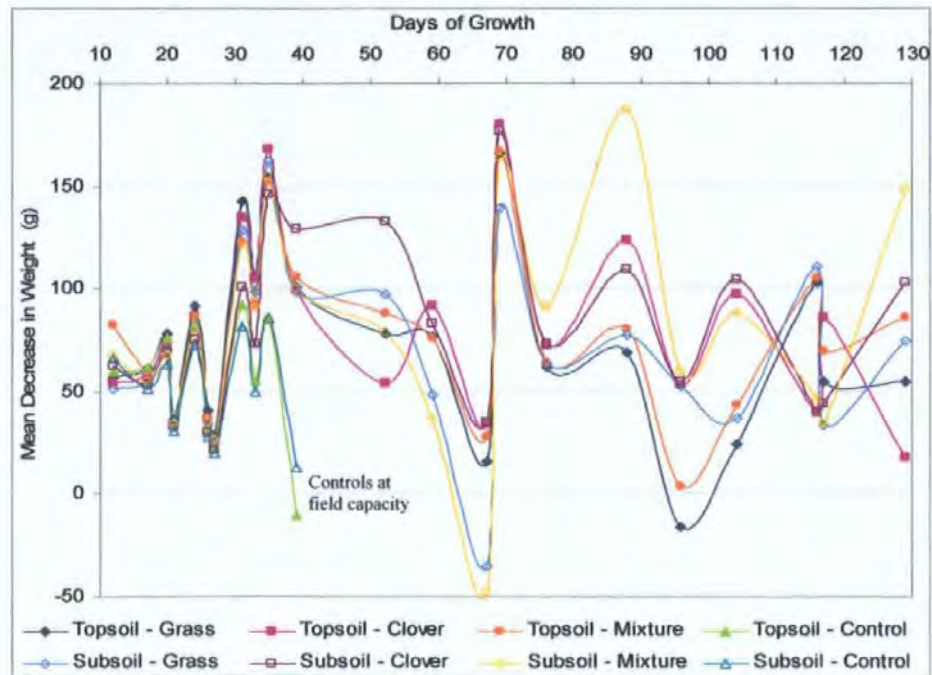
**Figure 2.17. Mean decrease in weight between irrigation events of all treatments in Column
Experiment 1 for the first 129 days of growth. Negative values represent an increase in
weight. The greater the decrease, the greater the rate of evapotranspiration relative to
biomass increase. (n = 7, except control where n = 3).**
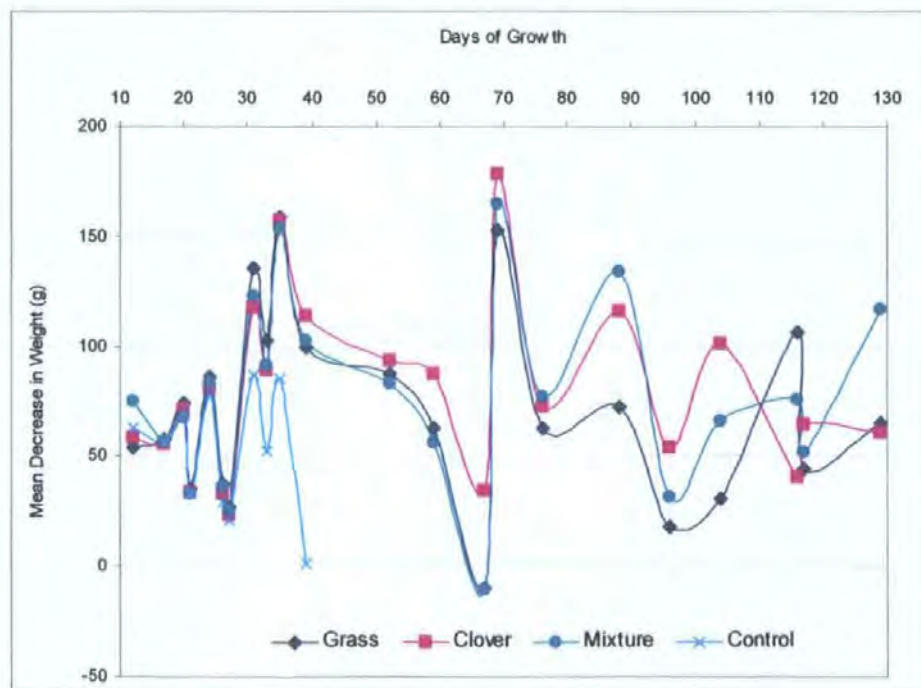
**Figure 2.18. Mean decrease in weight between irrigation events for plant treatments in
Column Experiment 1 for the first 129 days of growth. Negative values represent an increase
in weight. The greater the decrease, the greater the rate of evapotranspiration relative to
biomass increase. (n = 14, except control where n = 6).**

2.10. Biomass Yield

After day 129, plants were cut to 30 mm high and the off-take reported as fresh biomass yield (Figure 2.19). White clover and the mixed treatments gave a greater yield than the grass treatments. The one-way analysis of variance (ANOVA) and least significant difference (LSD) procedures indicated that the plant biomass yield showed statistically significant differences at the 95% confidence interval ($p < 0.05$).
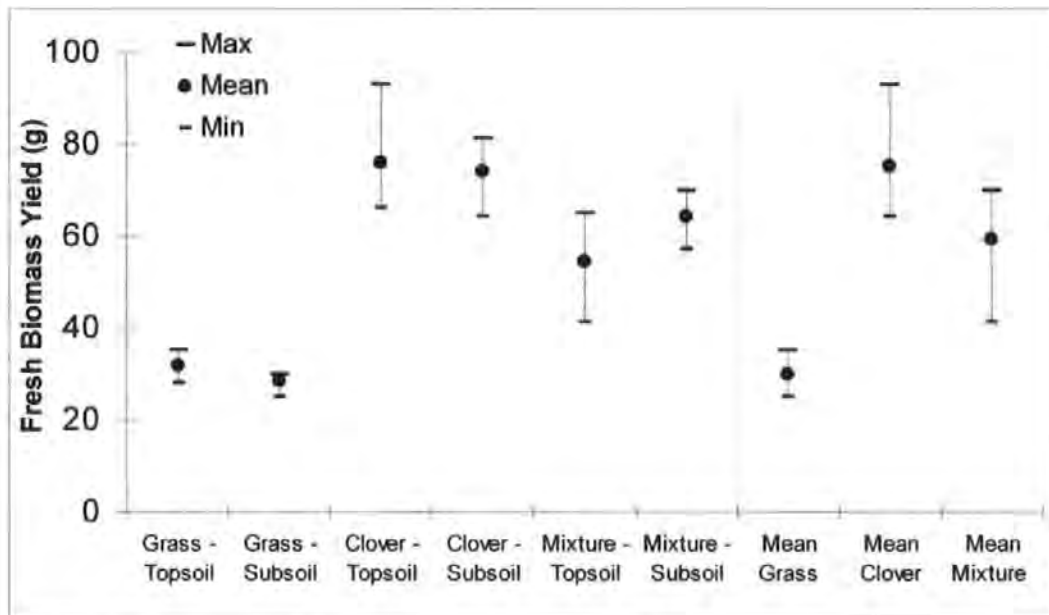
Figure 2.19. Fresh biomass yield (g) of all treatments in Column Experiment 1 after 129 days of growth. n = 7, except mean values where n = 14. p<0.05.

2.11. Nutrient application

Arnon's nutrient solution (Table 2.7) was used to supply the nutritional requirements of the plants (Hoagland & Arnon, 1950, Hewitt, 1966). Stock solutions were prepared in dark bottles and stored at 4°C when not in use. The major elements were prepared in individual bottles to prevent coagulation (N, P & Ca, K, Mg) whilst the trace elements (B, Mn, Cu, Zn, Mo, Co) and Fe were prepared and stored the same bottle. The stock solutions were diluted as stated in Table 2.7 to the concentration of the applied nutrient solution. The

relative concentration of each species represents the ratio required by the plants and should remain constant. The principal function of molybdenum in the legume is as a component of the nitrogenase enzyme complex required for nitrogen fixation (Baker & Williams, 1987). Mo was added at a similar concentration to the other trace nutrients.

Table 2.7. Modified Arnon's nutrient solution. Major and trace nutrients required for growth (Hewitt, 1966). Molybdenum was included for nodulation in the roots of white clover.

Compound	Formula	Concentration of stock solution (g L^{-1})	Volume of stock solution per litre (ml)	Concentration of applied nutrient solution (mg L^{-1})
Ammonium nitrate	NH_4NO_3	11.43	50	572
Calcium tetrahydrogen di-orthophosphate	$CaH_4(PO_4)_2.H_2O$	2.52	50	126
Potassium sulphate	K_2SO_4	6.687	66.7	446
Magnesium sulphate heptahydrate	$MgSO_4.7H_2O$	9.86	50	493
Iron (II) sulphate heptahydrate	$FeSO_4.7H_2O$	14.94	1	14.94
Boric acid	H_3BO_3	2.86	1	2.86
Manganese (II) chloride tetrahydrate	$MnCl_2.4H_2O$	1.81	1	1.81
Zinc sulphate heptahydrate	$ZnSO_4.7H_2O$	0.22	1	0.22
Cobalt (II) chloride hexahydrate	$CoCl_2.6H_2O$	0.09	1	0.09
Copper (II) sulphate pentahydrate	$CuSO_4.5H_2O$	0.08	1	0.08
Sulphuric acid	H_2SO_4	0.50	1	0.50
Molybdic acid	$H_2MoO_4.H_2O$	0.09	1	0.09

The total application of nutrients is given in Table 2.8, based on the application rate of 110 kg N ha^{-1}, which was representative of a conventional grassland system (Dawoudu, 2004). Other nutrients were supplied according to the ratio suggested by Hewitt (1966), which

gave an N:P:K ratio of 6:1:6 (17 kg P ha^{-1} and 110 kg K ha^{-1}). The pure grass treatments received a 10 x concentration of nitrogen equivalent to 110 kg N ha^{-1}. The pure clover, mixed species and fallow treatments received nutrient solution at 0.1 x concentration of nitrogen (equivalent to 11 kg N ha^{-1}). Other nutrients were applied at the same concentration to all treatments as listed in Table 2.8. Plants of the Column Experiments and the lysimeters received three doses of nutrient solution. The first dose was 0.1 x the total application and was applied to the seedlings during the first week of growth (Table 2.9). The aim of giving the pure grass treatments a greater application of N was to simulate conditions akin to a conventional grassland system.

Table 2.8. Total application of major and trace nutrients.

Major Nutrient	kg ha^{-1}	Trace Nutrient	g ha^{-1}
N	11*	Fe	1657
P	17	Mn	277
K	110	B	276
		Zn	28
Ca	11	Mo	26
Mg	27	Co	12
		Cu	11

*pure grass treatments received 10 x strength N.

Table 2.9. Initial diluted application of major and trace nutrients applied to seedlings.

Major Nutrient	kg ha^{-1}	Trace Nutrient	g ha^{-1}
N	1.1*	Fe	165.7
P	1.7	Mn	27.7
K	11.0	B	27.6
		Zn	2.8
Ca	1.1	Mo	2.6
Mg	2.7	Co	1.2
		Cu	1.1

*pure grass treatments received 10 x strength N.

2.12. Pest Control

Plants grown in artificial conditions of the glasshouse are susceptible to disease and prone to pests in the absence of natural predators. The clover plants suffered a short infestation of the western flower thrip (*Frankliniella occidentalis*). Figure 2.20 shows the leaf damage caused by the pest: leaf surfaces are speckled with yellow spots, a silvery metallic sheen and black specs of feces (thrips do not damage roots of plants). The plants were sprayed with *Fenitrothion* and fumigated with *Pirimiphos-methyl*; both are contact organophosphate insecticides (Whitehead, 1999). Yellow-sticky traps were deployed (Figure 2.21); the traps reflect light at the 550 nm that attracts thrips and other flying pests.

Thrip

Figure 2.20. Leaf damage caused to white clover by the western flower thrip (*Frankliniella occidentalis*).
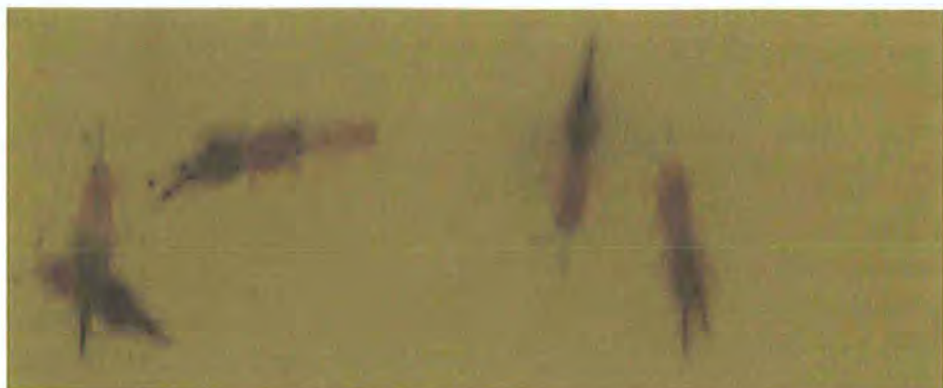
Figure 2.21. Adult western flower thrips (*Frankliniella occidentalis*) on a yellow-sticky trap.

The thrips were very resilient to the chemicals used and therefore attempts were made to reduce the population using the predator mite (*Amblyseius cucumeris*) shown in Figure 2.22 (supplied by Koppert UK Ltd., Suffolk, UK). The predators were supplied at all stages of their life cycle (eggs, larva, nymphs and adults) in small sachets, which were hung from the pots (Figure 2.23). The adults and nymphs actively search the immature stages of thrips (hatching eggs and larva). Biological control had not been previously utilized at IGER, North Wyke, but proved a successful method.

Figure 2.22. Adult predator mite (*Amblyseius cucumeris*).

Figure 2.23. Predator mite (*Amblyseius cucumeris*) supplied in small sachets.

Aphids (Figure 2.24) were also a problem and were rapidly treated to minimize the risk of viral diseases, of which aphids are prime vectors. There are approximately 4,000 aphid species in the world, so identification of the infesting species was not possible. Plants were initially sprayed with the systemic insecticide *Pirimicab*, which was not harmful to the predator mite population. Biological control was then introduced; the use of green lacewings (*chrysoperia carnea*) as predators for the control of aphids was not as rapid as the eradication of thrip by the predator mite. The green lacewings shown in Figure 2.25 were supplied as larva (Koppert UK Ltd., Suffolk, UK), which prey on adult aphids and their eggs. An alternative predator is the ladybird (*Hippodamia convergens*), which were not used as they are very demanding of their environment and will depart if the humidity is not high enough. Gall-midge (*Aphidoletes aphidimyza*) are the most effective for controlling aphid populations, however they were not used as larva of up to 3 mm burrow into the soil to pupate.

Figure 2.24. Adult aphids (*aphididae*).

Figure 2.25. Green lacewing (*chrysoperia carnea*), adult and preying larva.

2.13. Chemicals, solutions, water and equipment

All chemicals were of analytical-reagent grade (AnalaR or Spectrosol), and were used as received. Chemicals were purchased from BDH Chemicals (Merck), Poole, UK, unless otherwise stated. Brij[®] 35 and FFD6 were supplied by Skalar UK Limited, UK. For stock solutions, standards, reagents and dilutions, the diluent was ultra-pure water (distilled, double deionised and UV irradiated), purified using an Elga Maxima[®] (Elga Lab Water Global Operations, Buckinghamshire, UK) that produces water with 18 MΩ resistance. Deionised water (18 MΩ resistivity), purified with a distilling unit followed by a Millipore Super-Q Plus Water System (Milli-Q, Millipore Corporation), was also used. Water was used on the day of purification. The use of ultra-pure water was particularly important in the analysis of phosphate, as distilled water and tap water were analysed and contained 20 μg P L^{-1} and 1 mg P L^{-1}, respectively (i.e. the lowest standard in the analytical range and five times greater than the highest of 200 μg P L^{-1}).

Containers, bottles and glassware used in experiments, sampling and storage were washed in 10% (v/v) nutrient-free detergent (Decon90[®] or Neutracon[®], Decon Laboratories, UK) and rinsed three times with ultra-pure water. Those required for nutrient and tracer analysis were additionally soaked in 10% (v/v) hydrochloric acid (HCl) for at least 24 h, rinsed three times with ultra-pure water and air-dried at room temperature.

2.14. Experimental Analysis

Experimental techniques and methods of analysis are presented in the Chapters Three to Five.

2.15. Analytical quality control

Analytical chemistry at IGER's Selborne Laboratory is monitored for accuracy and precision. Within-run and within-lab precision is monitored by IGER's analytical quality

control and laboratory accreditation scheme Analytical results are entered into a database by IGER's Selborne Laboratory Manager and must fall within an acceptable range to pass analytical quality control; thus they can be reported as reliable results. Between-lab precision was determined by regular participation in the *'Aquacheck'* quaterly inter-comparison study. Nitrate values determined using segmented flow analysis at IGER passed all quality control tests, and when compared to *'Aquacheck'* results from various laboratories across the country, showed a low %RSD (Relative Standard Deviation) and mid-range mean results.

Segmented flow analysis at the University of Plymouth was a lengthy procedure due to the large throughput of samples, and so quality control was essential. Within-run precision was standard procedure and maintained with automatic drift correction; between-run precision was constantly monitored by changes in absorbance values of known standards. Between-lab precision of the instrument has previously been determined by participation in the 2002 *'NOAA/NRC 2nd annual inter-comparison study for nutrients'* (Clancy and Wille, 2003), whereby two seawater samples, a certified reference material and a control sample were analysed for orthophosphate and nitrite/nitrate.

Treatments and samples were run at least in triplicate, with the exception of soil leachates by segmented flow analysis, and unless otherwise stated. Good laboratory practice was adopted and awareness of contamination maintained.

2.16. Statistical analyses

Data were statistically analyzed using either StatsGraphics Plus or GenStat. The tests used varied with experiments, details of which are given in the relevant sections.

CHAPTER THREE

3. Characterisation of soil properties and soil structure

3.1. Overview of chapter and objectives

The first part of this chapter presents routine soil classification methods and results performed on soils prior to re-packing and plant growth. It is important to note that these characterisation techniques were performed on the initial soils and not at the end of the experimentation period. The second part of this chapter presents methods and results for the characterisation of changes in soil structure.

The objectives were:

1. to identify suitable experimental protocols for the characterisation of soil properties,

2. to characterise the initial soil properties in terms of soil pH, organic matter content and soil texture,

3. to determine the bulk density and porosity of the re-packed soils

4. to develop suitable experimental protocols for the classification of changes in soil structure,

5. to characterise the changes in soil properties after the growth of white clover and perennial ryegrass in terms of soil structural formation and stability,

6. to compare the changes of soil structural formation and stability induced by white clover and perennial rye grass against an unplanted control.

3.2. Overview of analytical techniques

Certain techniques used (soil classification, water retention, nutrient/tracer transport, structural stability and soil structural characterization) were traditional approaches. Other methods were novel (oxygen diffusion as an indicator of soil porosity, and the 3-D Pore-Cor network model as a simulation of soil structure and permeability). The methods presented in this chapter are only those used in this study. For a discussion on other

available techniques, please refer to the relevant section in Chapter One. Water retention and 3-D network modelling is presented in Chapter Four and nutrient/tracer transport studies in Chapter Five.

Standard soil classification measurements (soil pH, organic matter, moisture content, texture, bulk density, porosity, shear strenght) and some nutrient/tracer transport studies were conducted on all four soil series (Crediton, Greinton, Frilsham, Denbigh) from Column Experiments 1 and 2. Other techniques were only performed on soil of the Crediton series (soil structural characterization, water retention, 3-D network modelling, oxygen diffusion and structural stability to water) from Column Experiment 1. The half-meter lysimeters were only used for nutrient/tracer transport studies, and are discussed in Chapter Five.

3.3. Soil Classification

3.3.1. Soil pH of initial soil

In this research, the pH of soils was determined before the soils were re-packed and prepared for plant growth. This was performed as routine soil classification. The pH was not determined after or during experimentation. However, many soil processes will influence the end pH of the soils studied. For example, the physiological constitution of legumes induces a net efflux of protons at the root–soil interface that is significantly higher than that observed under non-nitrogen fixing species (Lesturgez *et al.*, 2006). The addition of protons results in the displacement of exchangeable bases and subsequently lowers the soil pH. Acidification of soils is also controlled by the removal of cations associated with nitrate leaching (Lesturgez *et al.*, 2006). Additional background information on soil pH can be found in Appendix I.

3.3.1.1. Theory

Methods for the determination of soil pH are either colorimetric (by use of colour indicators) or electrometric (an electrode monitored by a potentiometer). Measurements are made in a suspension by diluting the soil with water or a salt solution. The latter gives a lower result than obtained with water but enables standardisation of the conditions (Allen *et al.*, 1974). There are numerous limitations of the method that will all affect soil pH readings, such as the interference of hydrated ions (e.g. Al), the difference between fresh material and air-drying the soil, and the ratio of diluent to soil (Allen *et al.*, 1974).

3.3.1.2. Procedure

Soil pH was determined using a method described by Allen *et al.* (1974). Fresh, sieved soil (<2 mm, ~10g) was placed in a 100 ml beaker to the 30 ml line and filled to 50 ml with deionised water. Solutions were stirred rapidly for 5 min and left to stand for 15 min. Soil pH measurements were taken with a Jenway 3320 pH meter (Barloworld Scientific Ltd., Essex, UK) calibrated with solutions of pH 4.0, 7.0 and 10.0 ('Colourkey' buffer solutions, BDH/Merck). The pH electrode was immersed in the soil solution, when the reading stabilized pH was recorded to one decimal place. After each measurement, the probe was rinsed with deionised water. Each soil type was triplicated and the mean values calculated. Samples of known pH were included as part of IGER's analytical quality control and laboratory accreditation scheme.

3.3.1.3. Results

These results show that all of the soils were acidic (Figure 3.1), ranging from pH 4.9 – 6.1. The Crediton series topsoil was the most acidic (pH 4.9) and the Denbigh series the least acidic (pH 6.1). The Frilsham series was expected to have the greatest pH due to its calcareous bedrock, but this was not detected (pH 5.8). As expected the soil pH of the

Crediton series increased with depth (subsoil (pH 5.5) > topsoil (pH 4.9)) due to the decreasing organic matter content and concentration of basic cations.
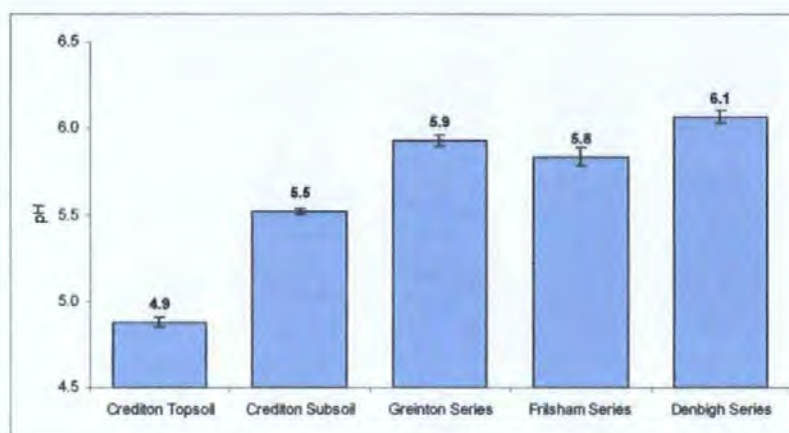
Figure 3.1. Mean pH of five soils under investigation (subsoil and four topsoils). (n=3).

3.3.2. Moisture content

3.3.2.1. Theory

The determination of soil water content is important, and several direct or indirect methods have been developed for both field and laboratory use. Direct methods involve removing the water from the soil and indirect methods involve measurement of soil properties that are affect by water content (Gardner, 1965). In the laboratory, determining physical and chemical properties necessitates knowledge of water content. Gravimetry with thermal drying is a common direct method; however, there is a problem in defining the 'dry' state, as soil is a complex matrix of lattice bound structural water, adsorbed water and free water (Gardner, 1965).

It is generally recommended to dry between 100°C and 110°C, so as not to drive off structural water from minerals, and to minimise volatilization, oxidation and partial breakdown of organic matter (Allen *et al.*, 1974). Thus, the drying time and temperature must be specified. Non-destructive indirect techniques that enable rapid, reliable, and

routine measurements of water content using simple sensors have been developed and are applicable to field conditions, such as Time-Domain Reflectometry (TDR).

3.3.2.2. Procedure

The moisture content was determined by four methods as specified:

i. The gravimetric method after thermal drying described by Allen *et al.* (1974), in which, dried, sieved soil (<2 mm) was placed in an air-circulation oven at 105°C for 24 hours until dried to a constant weight. The water content is reported on a wet-mass (Equation 3.1) or a dry-mass basis (Equation 3.2).

ii. The fresh moisture content was determined by weighing fresh soil relative to its original dry-weight (Equation 3.3.).

iii. Water retention measurements were determined gravimetrically at specific matrix potentials (Chapter Four), and converted to volumetric water contents (Equation 3.4 or Equation 3.5).

iv. Time-Domain Reflectometry (TDR) probes were used to determine the *in-situ* volumetric water content by means of an electromagnetic pulse (Chapter Five).

The moisture content of the initial soils was determined for the calculation of organic matter content, soil texture and bulk density. The results are not reported here, as they are not relevant to the classification of soil in the context of this Chapter. However, moisture content is an important property in field soils, and in studies of water and solute transport (Quisenberry, 1993).

$$\text{Moisture content (\%)} = \frac{\text{weight loss on drying (g)}}{\text{initial wet weight (g)}} \times 100$$

Equation 3.1.

$$\text{Moisture content (\%)} = \frac{\text{weight loss on drying (g)}}{\text{dry weight (g)}} \times 100$$

Equation 3.2.

$$\text{Fresh moisture content (\%)} = \frac{\text{fresh weight - original dry weight (g)}}{\text{original dry weight (g)}} \times 100$$

<div align="right">**Equation 3.3.**</div>

$$\text{Volumemetric water content} (cm^3 \, cm^{-3}) = \frac{\text{volume of water} (cm^3)}{\text{sample volume} (cm^3)}$$

<div align="right">**Equation 3.4.**</div>

$$\text{Volumemetric water content} (g \, cm^{-3}) = \text{moisture content} (g \, g^{-1}) \times \text{bulk density} (g \, cm^{-3})$$

<div align="right">**Equation 3.5.**</div>

3.3.3.   Organic matter content of initial soil

3.3.3.1.   Theory

The loss-on-ignition method by quantitative ashing of soil is a rough indication (not a true measure) of organic matter content, and multiplication of the result by a factor gives an approximate measure of the organic carbon (OC) content of the soil (Allen *et al.*, 1974). The crude correction factor was not used as it assumes that organic matter contains 58% carbon. The ratio of OM:OC has long been accepted as 1.72; however, this varies for different soils (Allen *et al.*, 1974).

The method does not distinguish between the organic and inorganic species (Davies *et al.*, 1993). In calcareous soils, this presents more of a problem due to the combustion of carbonates present in the soil (Allen *et al.*, 1974). However, a hydrochloric acid digest will disperse carbonates, and so correct for inorganic carbon (Allen *et al.*, 1974). Automated instruments, such as the C-H-N analyser, are generally used to determine total carbon content, which give the additional benefit of providing useful C/N ratios.

Another limitation of the method is the choice of a suitable combustion temperature; ignition at 375°C eliminates weight loss of structural water from clay, where as

temperatures over 500°C will result in loss of volatile minerals. Allen *et al.* (1974) tested a wide range of soils and reported satisfactory results at 450°C. Additional background information on organic matter content can be found in Appendix I.

3.3.3.2. Procedure

The organic matter content was determined by the loss-on-ignition method described by Allen *et al.* (1974). Dried, sieved soil (<2 mm, 20 g) was accurately weighed into a pre-weighed crucible and placed in a drying oven at 105°C for 24 hours. Samples were cooled to room temperature in a desiccator and dried to a constant weight to determine the moisture content (Section 3.3.2.2). The material was subsequently placed in a muffle furnace at 450°C for 4 hours and cooled in an oven at 105°C. Samples were then cooled to room temperature in a desiccator until constant weight was achieved. The percentage loss-on-ignition was calculated from the weight loss during combustion (Equation 3.6) and is an indication of the amount of organic matter present in the soils. Each soil type was replicated three times and the mean value is reported.

$$\text{Loss - on - ignition (\%)} = \frac{\text{weight loss (g)}}{\text{dry weight (g)}} \times 100$$

Equation 3.6.

3.3.3.3. Results

Figure 3.2 shows that the Denbigh series soil had significantly more organic matter (6.8%) and the Crediton subsoil has the least (1.9%). Similar amounts were determined in the Greinton (3.7%), Frilsham (3.4%) and Crediton series topsoil (3.6%). The Crediton series topsoil contained nearly twice as much organic matter than the subsoil; such decrease would be expected between soil horizons.
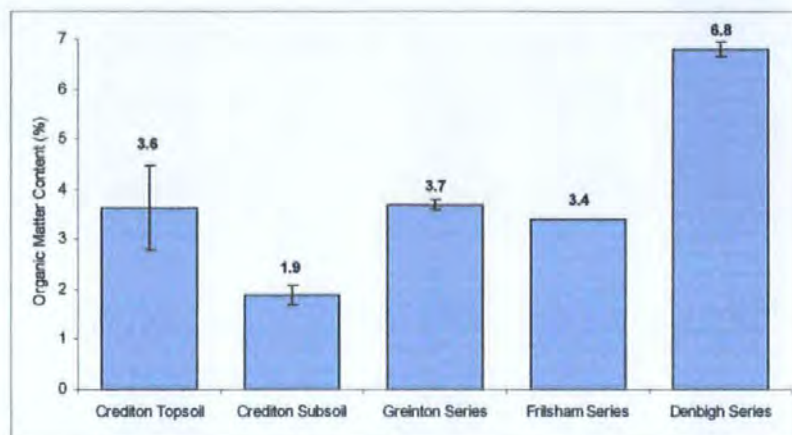
Figure 3.2. Mean organic matter content determined by the loss-on-ignition method of five soils under investigation (four topsoils and a subsoil). (Error bars indicate the standard deviation). (n=3).

3.3.4. Soil texture of initial soil

3.3.4.1. Introduction

The size limits of the clay, silt and sand fraction vary from country to country; Figure 3.3 gives the class intervals of the major systems in use. Additional background information on soil texture can be found in Appendix I.

Figure 3.3. Particle size classes adopted internationally. The systems differ in the upper limit for silt and the subdivision of the sand fractions. (White, 1997).

3.3.4.2. Theory

A successive sieving technique to determine particle size is not possible, as particles below 0.1 mm cannot be separated in this way. The hydrometer method introduced by Bouyoucos (1926) enables the classification of soil texture by separating and calculating the concentration of different size particles in suspension. This method of fractionation is based on the dispersion and settlement of particles in water according to Stoke's law (Equation 3.7) by calculating the time for a spherical particle to fall a definite distance through a suspension (Day, 1965).

$$v = Kr^2$$

Equation 3.7.

where the velocity (v) of the fall of a particle through a liquid has a direct relationship to the square of the particle radius (r). The compound factor (K) is constant for a fixed or corrected temperature.

The method is however limited, as the law assumes that all particles behave as perfect spheres and that they all have the same density (Allen *et al.*, 1974). A more reliable and accurate technique is that of particle size distribution using a Laser Diffraction Analyser (Malvern Instruments, Worcestershire, UK).

3.3.4.3. Procedure

Soil moisture content was determined at the start of the experiment (Section 3.3.2.2). Soil texture was determined using the method described by Allen *et al.* (1974). Sodium hexametaphosphate (($NaPO_3$)$_6$) (50 g) was dissolved in deionised water, diluted to 1 L to give 50 g L^{-1} and adjusted to pH 8.5 with sodium carbonate (Na_2CO_3). Sodium hexametaphosphate solution (25 ml of 5% w/v) and tap water (400 ml) were added to dried, sieved soil (<2 mm, 50 g) in a polythene bottle. The sample solutions were shaken

for 15 min, transferred to cylinders and diluted to 1 L. The solutions were stirred until no soil was left unmoved.

After 4 min 48 s a soil hydrometer was placed into the cylinder to determine the density of the soil/water mixture (g L^{-1}) and the concentration of silt and clay particles (< 20 µm) and was recorded. The temperature of the suspension was also recorded (0.3 hydrometer units were added/subtracted for every degree above/below 19.5°C). This was repeated after 5 h to determine the concentration of clay particles (< 2 µm). Calcareous soils should be pre-treated with hydrochloric acid to allow dispersion of carbonates, and organic matter removed with hydrogen peroxide. The fractions of clay (<0.002 mm / 2 µm), silt (<0.02 mm / < 20 µm) and sand (<2 mm) were calculated as percentages (Equation 3.8 - Equation 3.11). The experiment was replicated and the mean values reported.

$$\text{Clay (\%)} = \frac{A\,(\text{g L}^{-1}) \times 100}{(\text{soil weight - moisture weight}) \,(\text{g})} - 1$$

Equation 3.8.

$$\text{Clay + silt (\%)} = \frac{B\,(\text{g L}^{-1}) \times 100}{(\text{soil weight - moisture weight}) \,(\text{g})} - 1$$

Equation 3.9.

where soil weight = 50 g; A = hydrometer reading (g L^{-1}) after 4 min and 48 s; B = hydrometer reading (g L^{-1}) after 5 h; (A and B are corrected against temperature); 1 = sodium hexametaphosphate correction factor.

$$\text{Silt (\%)} = (\text{silt + clay})\,(\%) - \text{clay}\,(\%)$$

Equation 3.10.

$$\text{Sand (\%)} = 100 - (\text{silt + clay})\,(\%)$$

Equation 3.11.

3.3.4.4. Results

Experimentally determined particle size (Table 3.1 and Figure 3.4a & c) does not show the same distribution as values reported by the Soil Survey of England and Wales for the typical corresponding horizon of each of the four soil series (Table 3.2 and Figure 3.4b & d). Table 3.3 shows that the experimental results do not even follow the same trends as literature values. When the experimental data are plotted on the triangle diagram (Figure 3.5), soils are classified as either sandy loams or loamy sands. However, Table 3.2 shows that the soils are of different textural classes (sandy, silt and clay loams). Thus, the amounts of clay and silt were underestimated, and therefore, the proportion of sand was overestimated. This was confirmed when handling the soil and through observation. Although the hydrometer method did not prove a very reliable method in this study, other authors have reported satisfactory results (Gülser, 2006). A Laser Diffraction Analyser is recommended for future studies.

Table 3.1. Particle size distribution of soils under investigation (four topsoils and a subsoil). Fractions according to the International Classification System.

Soil Type	% Clay (<0.002 mm)	% Silt (0.002 - 0.02 mm)	% Sand (0.02 - 2 mm)
Crediton Topsoil	8.1	14.3	77.6
Crediton Subsoil	6.7	13.7	79.7
Greinton Series	5.3	11.6	83.2
Frilsham Series	7.5	15.1	77.4
Denbigh Series	5.6	17.6	76.8

Table 3.2. Soil texture according to the Soil Survey of England and Wales for a typical corresponding horizon of each of the four soil series.

Soil Type	% Clay (<0.002 mm)	% Silt (0.002 - 0.02 mm)	% Sand (0.02 - 2 mm)	Depth (cm)	Soil Texture
Crediton Topsoil[a]	16	43	42	0-23	Very stony course sandy loam
Crediton Subsoil[a]	12	33	55	23-71	Very stony course sandy loam
Greinton Series[b*]	12	49	39	0-18	Fine sandy loam/sandy silt loam
Frilsham Series[c]	20	46	34	0-25	Moderately stony clay loam
Denbigh Series[d]	23	57	20	0-22	Slightly stony clay loam

[a] Findlay *et al.* (1984); [c] Jarvis *et al.* (1984); [d] Rudeforth *et al.* (1984).

[b*] Donaldson (pers. comm.), experimental values not Soil Survey data.

Table 3.3. Ranking (low to high) of the relative proportions of clay, silt and sand determined experimentally compared to data of the Soil Survey of England and Wales.

Clay		Silt		Sand	
Literature	**Experimental**	**Literature**	**Experimental**	**Literature**	**Experimental**
Crediton Subsoil	Greinton Series	Crediton Subsoil	Greinton Series	Denbigh Series	Denbigh Series
Greinton Series	Denbigh Series	Crediton Topsoil	Crediton Subsoil	Frilsham Series	Frilsham Series
Crediton Topsoil	Crediton Subsoil	Frilsham Series	Crediton Topsoil	Greinton Series	Crediton Topsoil
Frilsham Series	Frilsham Series	Greinton Series	Frilsham Series	Crediton Topsoil	Crediton Subsoil
Denbigh Series	Crediton Topsoil	Denbigh Series	Denbigh Series	Crediton Subsoil	Greinton Series
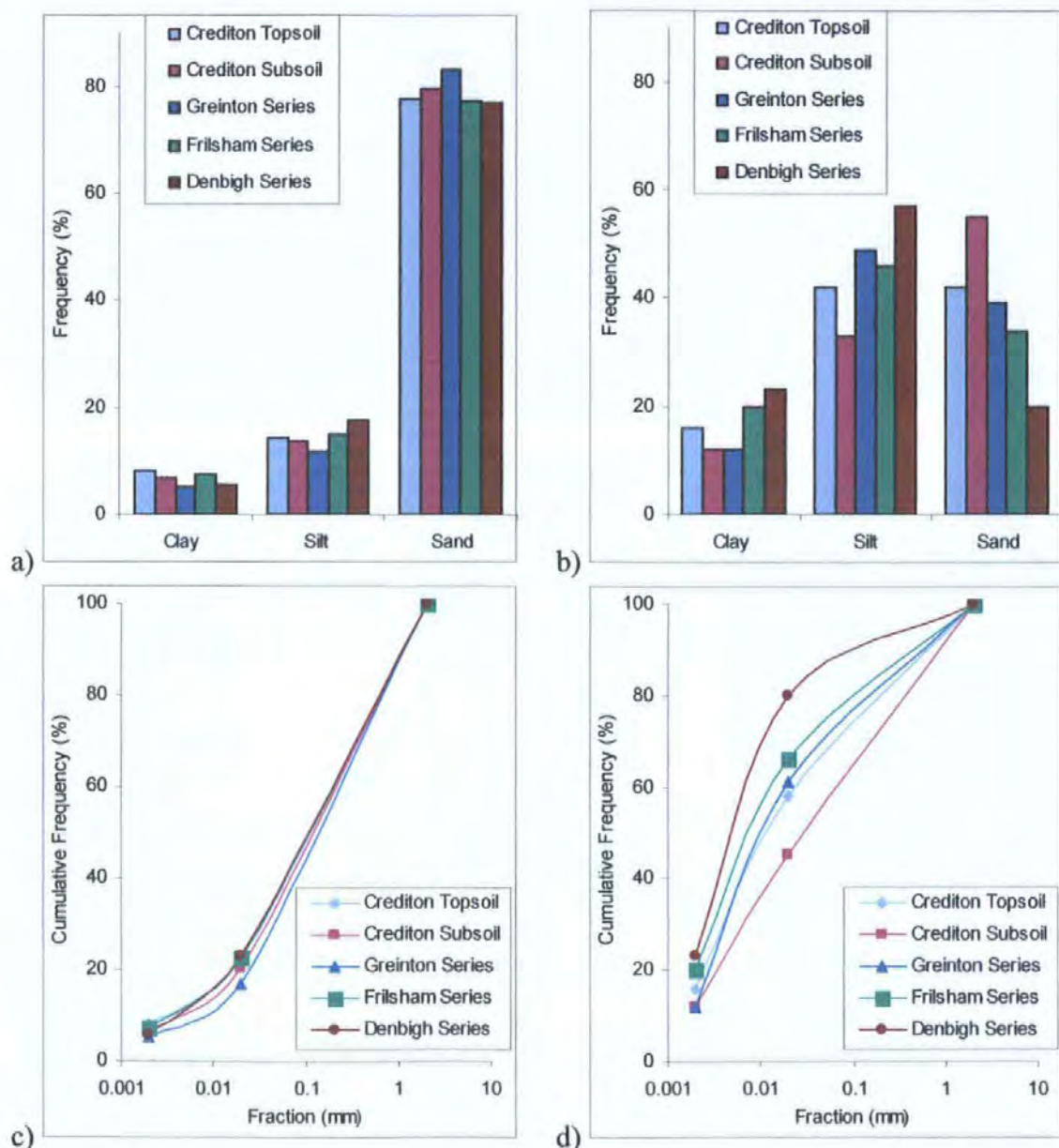
Figure 3.4. Particle size distribution of soils under investigation (four topsoils and a subsoil). a) relative and c) cumulative frequency of experimental results given in Table 3.1. b) relative and d) cumulative frequency of literature values given in Table 3.2 from the Soil Survey of England and Wales. Fractions according to International Classification System: Clay (<0.002 mm); Silt (0.002 – 0.02 mm); Sand (0.02 – 2 mm).
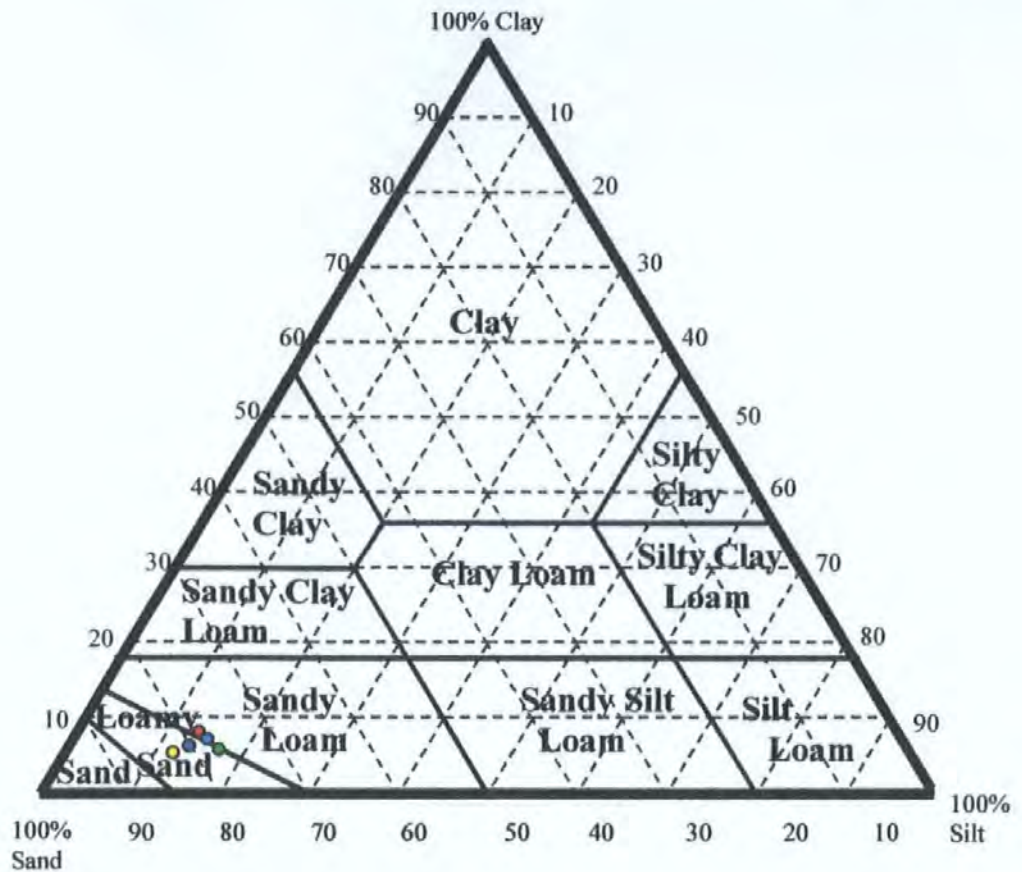
Figure 3.5. Triangle diagram of soil textural classes adopted in England and Wales.

Experimental classification of soils:

⬤ Crediton topsoil;   ⬤ Crediton subsoil;   ⬤ Greinton series;   ⬤ Frilsham series;   ⬤ Denbigh series.

3.3.5. Bulk density and porosity of re-packed soils

3.3.5.1. Introduction

Bulk density is defined as the ratio of the mass of dry soil to its total volume (Equation 3.12). The bulk density of a sandy soil (1.6 g cm^{-3}) is higher than that of a clay soil (1.1 g cm^{-3}) (Marshall *et al.*, 1996). Porosity is an index of the relative pore volume in the soil (Equation 3.13). Porosity is often expressed as a percentage and typically varies from 30–60%; clays are more porous than sandy soils. Porosity can be calculated from the particle and bulk densities (Equation 3.14) (Hillel, 1980). The average density of particles is 2.5–2.8 g cm^{-3}, and a value of 2.65 g cm^{-3} is commonly used. However, the density of organic matter is less than this (Marshall *et al.*, 1996).

$$\text{Bulk Density} = \text{mass of dry soil} / \text{total volume}$$

<div align="right">Equation 3.12.</div>

$$\text{Porosity} = \text{total volume of pores} / \text{total volume}$$

<div align="right">Equation 3.13.</div>

$$\text{Porosity} = (\text{particle density} - \text{bulk density}) / \text{particle density}$$

<div align="right">Equation 3.14.</div>

3.3.5.2. Results

Table 3.4 lists the bulk density achieved for each re-packed soil and the calculated porosity (particle density assumed to be 2.65 g cm^{-3}). The bulk density achieved for the Denbigh series was lower than the other soils. The Denbigh series is shown to be more porous than the other soils. However, this soil series has a significantly higher organic matter content and so the particle density and therefore the porosity may have been overestimated.

Table 3.4. Bulk density and porosity of the re-packed soils.

Soil	Bulk Density (g cm^{-3})	Porosity (%)
Crediton Topsoil	1.18	55.5
Crediton Subsoil	1.30	51.0
Crediton Dried	1.36	48.7
Greinton Series	1.17	56.0
Frilsham Series	1.18	55.7
Denbigh Series	0.91	65.5

3.3.6. Discussion of soil classification results

The experimental result of soil classification are collated in Table 3.5. The Crediton series topsoil is classified as a very strongly acidic soil (pH 4.9) (FitzPatrick, 1986). Compared to its moderately acidic soil subsoil (pH 5.5), the topsoil has a greater organic matter content (1.9% and 3.6%, respectively). This increase in pH and decrease in organic matter is

expected with depth (FitzPatrick, 1986), and although the values are slightly different, the trend is consistent to those reported in the literature for this soil series (Table 3.6). There should also be a difference in particle size distribution, and although the Crediton series subsoil contained more sand and less clay than the equivalent topsoil, the values were different to those given in Table 3.6, as the results appear to be inaccurate (Section 3.3.4.4).

The Greinton and Frilsham series are also classified as moderately acidic (pH 5.9 and 5.8, respectively) (FitzPatrick, 1986). The pH of the Frilsham is lower than the pH of 8.3 reported by the Soil Survey of England and Wales (Table 3.6). The Greinton (3.7%) and Frilsham (3.4%) series and have similar organic matter contents to each other and to the Crediton (3.6%) series topsoil (Table 3.5), which is in agreement with the literature values (Table 3.6). The Greinton series was under arable management and therefore expected to have less organic matter relative to the other soils, although this was not observed (Table 3.5). Field soils of the Greinton, Frilsham and Crediton series are of similar textures; consequently, similar bulk densities and porosities were achieved (Table 3.5).

The Denbigh series has the highest pH and is classified as slightly acidic (pH 6.1) (FitzPatrick, 1986), and has the greatest organic matter content (6.8%). The highest organic matter content is in agreement with literature data (4.4% OC $\approx$ 7.7% OM), but the pH is lower (pH 5.6). This silty clay loam should have the greatest clay content (Table 3.6), but this was not observed by the procedure due to experimental error. The greater proportion of finer particles in the Denbigh series is reflected by the lower bulk density and elevated porosity after re-packing (Table 3.5).

The textures determined are reported in Table 3.5, but considered inaccurate. Table 3.6 gives values cited in literature. However, these values are also only an indication as soil is

highly heterogeneous in nature and the same soil type shows considerable variation from one point in the same field to another. A more quantitative and accurate technique than the hydrometer method is that of particle size distribution using a Laser Diffraction Analyser.

Table 3.5. Experimental result of soil classification, and the bulk density and porosity after re-packing.

Soil Type	% Clay (<0.002 mm)	% Silt (0.002 - 0.02 mm)	% Sand (0.02 - 2 mm)	pH	Organic Matter (%) [1]	Bulk Density (g cm^{-3})	Porosity (%)
Crediton Topsoil	8	14	78	4.9	3.6	1.18	56
Crediton Subsoil	7	14	80	5.5	1.9	1.30	51
Greinton Series	5	12	83	5.9	3.7	1.36	56
Frilsham Series	8	15	77	5.8	3.4	1.17	56
Denbigh Series	6	18	77	6.1	6.8	1.18	63

[1] Organic matter = loss-on-ignition

Table 3.6. Relative soil texture, pH and organic matter content according to the soil survey of England and Wales for a typical corresponding horizon of each of the four soil series.

Soil Type	% Clay (<0.002 mm)	% Silt (0.002 - 0.02 mm)	% Sand (0.02 - 2 mm)	pH [2]	Organic Matter (%)	Ref
Crediton Topsoil	16	43	42	5.8	1.7	[a]
Crediton Subsoil	12	33	55	6.3	0.3	[a]
Greinton Series	12	49	39	-	4.0 [1]	[b*]
Frilsham Series	20	46	34	8.3	1.8	[c]
Denbigh Series	23	57	20	5.6	4.4	[d]

[1] Organic matter = loss-on-ignition; [2] pH in water (1:2:5)

[a] Findlay *et al.* (1984); [c] Jarvis *et al.* (1984); [d] Rudeforth *et al.* (1984).

[b*] Donaldson (pers. comm.), experimental values not Soil Survey data.

3.4. Soil structure characterisation

3.4.1. Introduction

This section describes techniques used to characterise changes in soil structure formation and stability. Results are presented for the Crediton series topsoil and subsoil from Column Experiments 1 and 2. Measurements include soil structural stability to water and mechanical forces; visual observations of changes in soil structure; a novel oxygen diffusion technique as an indication of soil porosity, and permeability to water and gasses.

3.4.2. Soil structural stability to water

3.4.2.1. Introduction

Matkin and Smart (1987) compared six tests of soil structural stability to water and suggested that the Williams and Cooke Instability Test was most applicable to less stable soils. The simple method developed by Williams and Cooke (1961) was used to determine the stability of aggregates when saturated with water. The method is able to identify soils with unstable structures that will deteriorate in wet weather. Structural instability is determined from the percentage loss in pore space after repeated wetting and draining of the aggregates. The smaller the percentage, the greater the stability, and is reported as the Instability Factor.

3.4.2.2. Sample preparation

Vegetation was removed, and the soil cores were split into three sections: top (0-5 cm), middle (5-9.5 cm) and bottom (9.5-14 cm). Each subsample was separated by hand in a moist state and aggregates were allowed to air-dry naturally for 72 hours. Care was taken to minimise disruption of soil structure by the remoulding of wet samples. Aggregates of 4-6 mm were sieved and placed in labelled plastic bags.

3.4.2.3. Treatments

Four treatments (grass and clover grown in topsoil and subsoil) from three depths (top (0-5 cm), middle (5-9.5 cm) and bottom (9.5-14 cm)) gave a total of twelve subsamples. Measurements were replicated four times, giving a total sample set of 48.

3.4.2.4. Procedure

The apparatus used is shown in Figure 3.6. Air-dried aggregates (4-6 mm, 20 g) were accurately weighed into tubes 21 mm diameter x 111 mm high (A). The tubes were gently tapped to pack the aggregates and the height of the soil column was measured. Distilled water was admitted from a reservoir to the base of the soil column (B) via plastic pipe (C) until there was 10 mm of water above the soil (D). Care was taken to avoid trapping air between the aggregates. After 10 min the column was allowed to drain, the wetting and draining was repeated and the final height of the soil column measured (E). Williams and Cooke (1961) found that the height of the column was constant after two cycles of saturation and drainage.

The tubes (A) were calibrated to give the volumes of soil equivalent to the heights measured (E). The absolute volume of the solids excluding pore space was calculated from the absolute density, which is assumed to be approximately 2.5 g cm^{-3} (Williams and Cooke, 1961). The 'Instability Factor' was calculated from the decrease in volume and expressed as a percentage of the total possible decrease in volume when pore space is zero (Equation 3.15).

$$\text{Instability Factor (\%)} = \frac{(z-y)100}{z-x}$$

Equation 3.15.

where: z = initial volume of soil column, y = final volume of soil column and x = absolute volume of soil column with zero pore space.
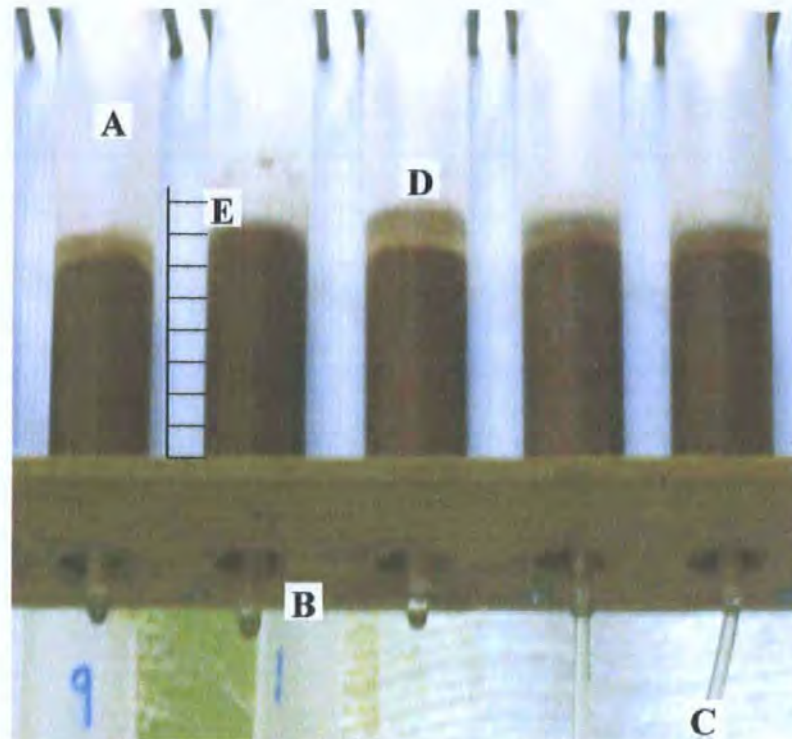
Figure 3.6. Apparatus used to measure Williams and Cooke Instability Factors of aggregates when saturated with water: (A) tubes containing soil; (B) base of tube where water is admitted and removed; (C) plastic pipe connected to reservoir; (D) point to which water is added; and (E) height of soil column.

3.4.2.5. Results

Mean instability factors of the four treatments at three different depths of the soil core are presented. The lower the value, the greater the structural stability to the action of water. Table 3.7 shows that aggregate stability is enhanced under clover treatments compared to grass treatments, and that grass treatments showed a greater variability. These data are represented graphically in Figure 3.7, and illustrate differences between the range (i.e. minimum and maximum) of samples for the grass treatments. The grass treatments also show variability in mean values, whereas the clover treatments are similar (except the bottom sample from the clover subsoil core).

Table 3.7. Mean instability factors (%), range and standard deviation of each treatment at 3 different depths in soil cores of Column Experiment 1. (n=4).

		Mean	Range			Standard Deviation
Grass - Topsoil	Top	7.0	4.2	-	12.3	4.6
	Middle	11.3	7.3	-	19.5	5.7
	Bottom	16.4	13.1	-	19.0	2.9
Grass - Subsoil	Top	16.5	12.1	-	21.4	5.0
	Middle	13.1	7.8	-	17.7	4.4
	Bottom	23.0	17.8	-	25.8	3.5
Clover - Topsoil	Top	4.2	4.1	-	4.3	0.1
	Middle	4.0	3.8	-	4.1	0.1
	Bottom	4.0	3.8	-	4.1	0.1
Clover - Subsoil	Top	4.3	4.2	-	4.3	0.1
	Middle	4.3	4.1	-	4.4	0.2
	Bottom	6.0	4.2	-	7.8	2.0
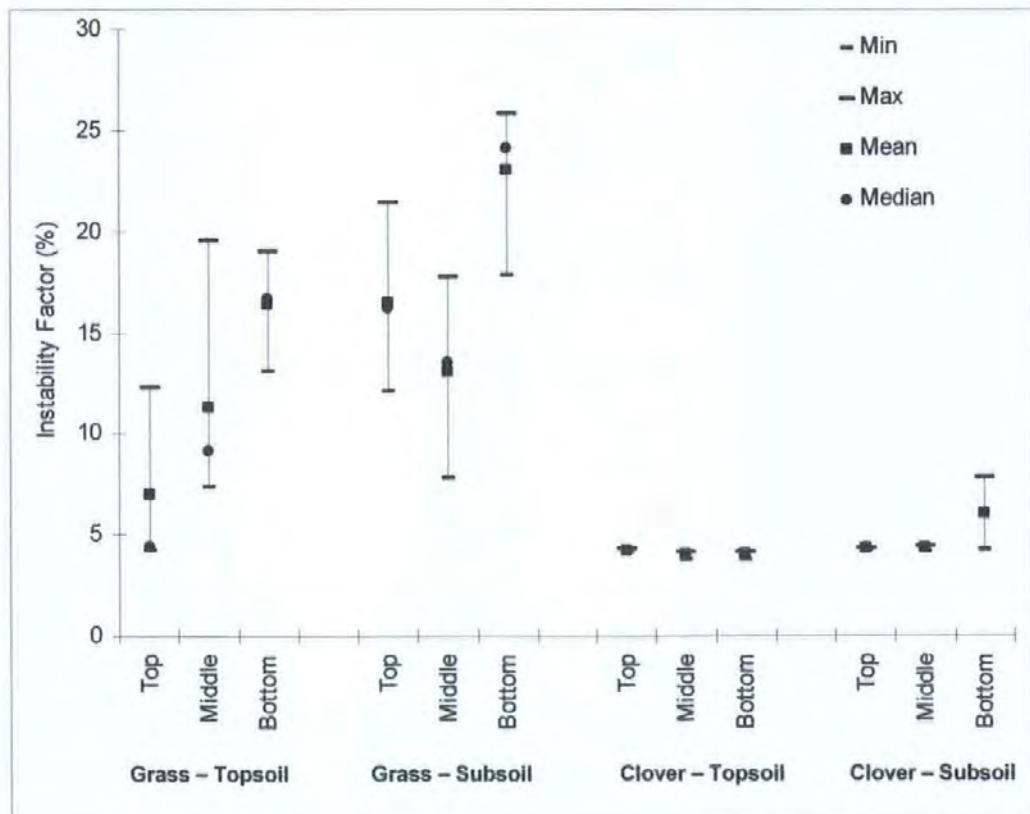
Figure 3.7. Minimum, maximum, mean and median instability factor (%) of 4 treatments at 3 different depths in soil cores of Column Experiment 1. (n=4).

Plant treatment effects, differences between topsoil and subsoil, and depth in soil core with respect to % instability factors were tested by analysis of variance (ANOVA), and comparisons among means were made using the least significant difference (LSD) multiple range test, calculated at the 95% confidence level (p<0.05). Three separate tests were performed: two soil types (topsoil and subsoil), two planting regimes (white clover and ryegrass) and twelve treatments (2 planting regimes x 2 soil types x 3 depths).

Figure 3.7 shows five homogeneous groups within which there are no statistically significant differences. Increased soil stability under clover was not related to the depth of the original field soil (i.e. topsoil vs. subsoil) and did not significantly change with depth in the soil core. The clover samples were all significantly different from other samples, with the exception of the top of the grass-topsoil core. In soils under grass, mean instability varied with the depth of the original field soil. There is also statistical evidence to suggest that aggregate stability varied with the depth of the core under grass although no clear trend was observed. Aggregate stability was poorest at the bottom of the grass-subsoil core.
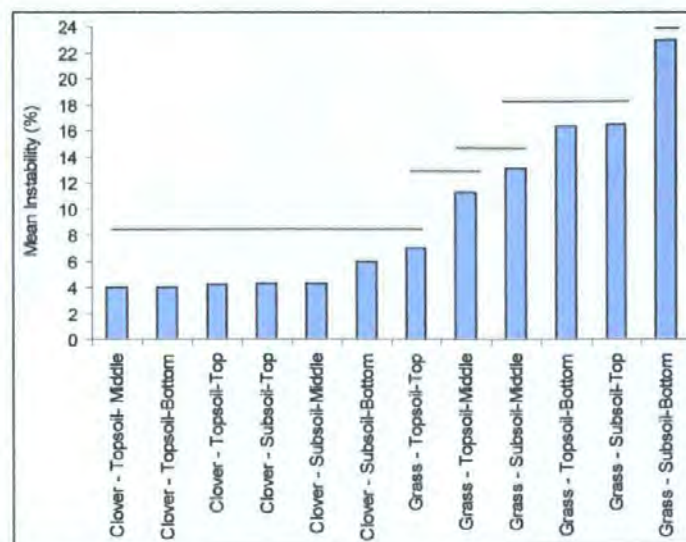
Figure 3.8. Mean instability factor (%) of 4 treatments at 3 depths in soil cores from Column Experiment 1. Bars under a horizontal line represent a homogeneous group within which there are no statistically significant differences (p>0.05). (n=4).

3.4.2.6. Discussion

The preliminary test of soil structural stability using the Williams and Cooke method showed that white clover increased aggregate stability compared to ryegrass. This increased stability was not related to the depth of the original field soil, which contained differential carbon levels at the start of the experiment (3.6% topsoil and 1.9% subsoil). Neither did the stability significantly change with depth in the soil core. The stability of soils under ryegrass did not show any clear trends with depth.

The results contradict other studies, which suggested ryegrass is more efficient than white clover in improving soil stability. Tidsall and Oades (1979) used the wet sieving method for aggregates <10 mm. They concluded that ryegrass was more efficient than white clover in stabilising aggregates. They attributed this to the greater lengths of fungal hyphae per unit mass present in stable aggregates under ryegrass compared to white clover. Gülser (2006) determined aggregate stability using the wet sieving method, and reported a slight difference for perennial ryegrass (72.15%) compared to subterranean clover (76.29%), and suggested that differences can also due to the differences in root type and density.

The study by Haynes and Beare (1997) showed that both Italian ryegrass and white clover had a similar positive influence on soil structure stability. The authors attributed this to the increasing levels of soil organic C, microbial biomass, carbohydrates and fungal hyphae associated with fine roots. The modified soil-water relationships under different plants will also have an effect (Tidsall and Oades, 1982; Angers, 1998).

Reid and Goss (1981, 1982) determined the stability of aggregates <2 mm by the turbidimetry method. They concluded that air-drying soil caused the restabilisation of aggregates due to the adsorption of polysaccharides onto soil surfaces. They suggest that the stability of freshly sampled aggregates should also be assessed. However, Zhang &

Horn (2001) regarded dry soil as the most sensitive indicator of variability of aggregate stability, and Dexter (1988) states that the stability of drier soil provides information on the soil's workability and its ability to withstand force applied.

The soil structural stability needs further investigation. Fresh and air-dried results should be compared. Useful information would be obtained by periodically repeating the determination to monitor temporal changes; such assessment would assist with assessing crop management practices (Gülser, 2006). A comparison should also be made between different methods, such as the wet-sieving technique (Kemper and Rosenau, 1986; Jastrow and Miller, 1991).

Generally, aggregate stability depends on soil properties such as organic matter, clay and oxide contents (Zhang & Horn, 2001). These properties should be accurately determined to investigate any correlation as a possible mechanism for increased stability in soils beneath white clover. Traore *et al.* (2000) reported that the production of mucilage by plant roots increased aggregate stability. This should be investigated for the soils in this study, and also the effect of the enhanced polysaccharide production in the presence of *rhizobium* beneath white clover. However, Haynes and Beare (1997) reported that the HCl-extractable and labile fraction of carbohydrates and microbial biomass C was higher under Italian ryegrass than under the white clover.

The implications of the results are that the possible enhanced structural stability in soil beneath white clover will render the soil more resistant to degradation and erosion (Gülser, 2006). Papadopoulos *et al.* (2006) reported that the enhanced macroporosity beneath red clover and red clover/ryegrass swards was not retained after cereal cropping (< 3 years). Further research is required to determine the mechanisms of enhanced structural stability to water in soils beneath white clover. It is also important to assess whether the effects are transient, temporary or persistent.

3.4.3. Structural stability to mechanical forces

3.4.3.1. Penetrometer Introduction

Soil penetrability is a measure of the soil's resistance to vertical penetration, and is determined using a penetrometer (Davidson, 1965; Bradford, 1986). Such measurements provide an indication of the resistance of soils to structural degradation, such as compaction, crusting and erosion (Gülser, 2006). Such resistance is largely controlled by water stable macroaggregates (Angers, 1998; Gülser, 2006).

Soil compaction is a worldwide concern, and crop productivity and soil structural qualities deteriorate under such conditions (Ball *et al.*, 1997). Compaction by the passage of wheels will result in loss of macropores and poorer aeration. The soils workability is most affected under enhanced rainfall, as is the drainable porosity (Ball *et al.*, 1997). As a consequence, the main environmental concerns for grassland soils is the enhanced potential for pollution through denitrification, nitrous oxide production and surface runoff (Ball *et al.*, 1997).

Another important consideration of soil strength is that physical stresses will restrict root growth, and such mechanical impedance occurs when the soil has become strong due to compaction or drying (Whalley *et al.*, 2004). In turn, crops can also influence the soil's physical properties due to improvements in soil structure, such as the enmeshment by roots, plant and microbial exudates, and modified soil-water relationships (Tisdall and Oades, 1982; Angers, 1998; Gülser, 2006). It is known that grasses and perennial forages act as a cover crop and can improve or maintain soil structure (Tisdall and Oades, 1982; Gülser, 2006), as discussed in Chapter One (Section 1.7.3 and 1.7.4).

3.4.3.2. Theory

The drop-cone or fall-cone device is widely used as a rapid measurement of shear strength of clays and as a standard determination of the liquid limit of soils (Towner, 1973). The liquid limit, and the plastic limit, are regarded as the moisture contents at which soil has two fixed strengths (Towner, 1973). The shear strength is the maximum shear resistance, which is a force generated in a soil to an external force applied (Sallberg, 1965) and a higher strength indicates more resilience to degradation. The shear strength of soils in agriculture is used as an indication of soils to support farm/field vehicles (i.e. trafficability) (Sallberg, 1965). It has been shown by semi-empirical analysis that the shear strength (τ) is related to the depth of penetration and the weight of the falling cone (Equation 3.16).

$$\tau = K \frac{Q}{h^2}$$

Equation 3.16.

where, h is the depth of penetration in mm, Q is the weight of the falling cone expressed in g and K is a factor of proportionality, which varies with soil texture, as given in Table 3.8. The soils were assigned a textural class from Table 3.2, according to the Soil Survey of England and Wales, rather than using the experimental classification, which are considered to be inaccurate.

Table 3.8. Experimentally determined values of K for seven soil textures, as given by Towner (1973).

Texture	K
Clay	7.8×10^3
Clay loam	5.4×10^3
Silty clay loam	7.4×10^3
Silt loam	1.0×10^4
Loam	6.9×10^3
Sandy loam	1.6×10^4
Loamy fine sand	1.2×10^4

3.4.3.3. Sample preparation

Selected soils from Column Experiment 2, representing different textural classes, were determined after 6 months of plant growth. The suction in the soil water will impose a compressive stress (Towner, 1973), and so soils were equilibrated to a water content of 25% prior to analysis. This was achieved by saturating the cores for 48 hours; they were allowed to drain and successively weighed until the gravimetrically determined water content was equal to 25%.

3.4.3.4. Procedure

Penetrometer resistance was measured using a standard drop-cone penetrometer with a stainless steel conical probe of 30°, 3.8 mm in length and a specific weight of 80g (Stanhope-Seta, Surrey, UK). The probe was placed with its point just touching the soil surface, released and allowed to free fall for 5 seconds. The penetration depth was recorded from the dial gauge. The cone was wiped clean between each measurement. The drop-cone penetrometer apparatus is shown in Figure 3.9. The mean of the cone penetrations are reported for five replicates of each treatment.

Figure 3.9. Drop-cone penetrometer to determine the stability of aggregates when exposed to external mechanical stresses, and resistance to forces that cause compaction.

3.4.3.5. Results

The shear strength data are represented graphically in Figure 3.10, and illustrate differences between the range (i.e. minimum and maximum) of the samples. The topsoil of the Crediton series under white clover and the mixed species had the greatest variability; the mean values for these treatments (2.18 and 1.51 x 10^3 N m^{-2}, respectively) was similar to that of white clover grown in the Frisham series (0.77 x 10^3 N m^{-2}), and the unplanted control of the Denbigh series (0.86 x 10^3 N m^{-2}). With the exception of this unplanted soil, the control soils of the other series gave lower values than their equivalent planted soils. The Denbigh soil planted with grass, was similar to white clover, and also gave an exception to the trend of all grass soils having low shear strength. There were other statistically significant trends detected in shear strength between white clover compared to ryegrass and the unplanted soils.
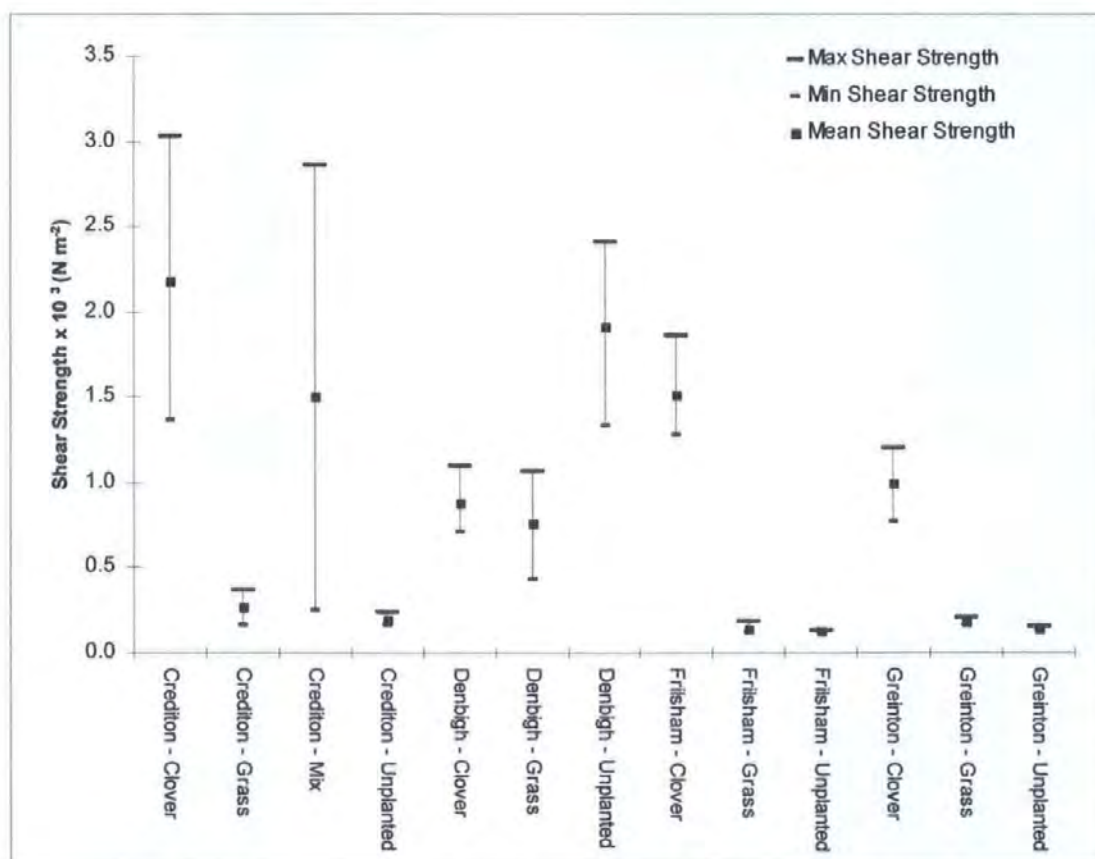
Figure 3.10. Minimum, maximum and mean shear strength of four topsoils under different plant regimes from Column Experiment 2. (n=5).

3.4.3.6. Discussion

Although the results suggest that white clover increased the shear strength of the soil compared to soil beneath ryegrass and the unplanted controls (Figure 3.10), this was only true for the Crediton, Frilsham and Greinton series. Soil of the Denbigh series beneath white clover and ryegrass gave similar results, both of which had consistently lower values than the equivalent unplanted soil.

Shear strength is influenced by the type of soil, and by the soil conditions, such as the soil structure, bulk density and water content (Sallberg, 1965). The water contents were equilibrated, but there were differences in the bulk densities of the soil (0.91–1.30 g cm^{-3}). The shear strengths measured in soils of the Denbigh series requires further investigation. The result may be a function of soil texture and bulk density, as this series is expected to have the greatest clay content (~23%), the least amount of sand (~20%) and the lowest bulk density (0.91 g cm^{-3}). However, this does not account for the exceptionally higher values for the unplanted Denbigh soil.

The significant differences in the white clover treatments also warrant further investigation, to ascertain if the findings are a function of enhanced structural stability. The results suggest that soil beneath white clover may withstand greater forces in the field to trafficability and the trampling effects of cattle. This also lends support for the idea that white clover has amelioration potential for compacted and degraded soils, or those highly worked.

The findings are in agreement with the structural stability test to the action of water (Section 3.4.2), which also showed evidence for enhance structural stability in soils beneath white clover relative to those beneath ryegrass. A recent study by Gülser (2006) reported a significant difference in penetrometer resistance and aggregate stability in

unplanted soils compared to those under perennial ryegrass and subterranean clover. The penetrometer resistance decreased (clover < grass < control) and the aggregate stability increased (clover > grass > control). Gülser (2006) concluded that the crops helped the development of aggregation and other soil structural parameters in a clay soil, with lower effects obtained with the ryegrass cropping and control soils.

3.4.4. Visual observations

3.4.4.1. Introduction

To accurately characterise the soil structural change, the pores and solids must be quantified in terms of size, shape, continuity and distribution (Holden, 2001). Various techniques have been discussed as a measure of soil structure (Chapter One, Section 1.6.5). Due to the extensiveness and complexity of setting-up the experiments, maintaining the growth of the plants, performing and analysising the breakthrough experiments, plus the water retention experiments and model simulations involved in this project, it was not possible within the time and resource constraints to carry out sophisticated soil structure investigation by methods such as thin sectioning and image analysis, or X-ray computed tomography (Chapter One, Section 1.6.5.2).

Photographs of soil structure were taken using a Ricoh RDC-4200 digital camera at 1280 x 960 pixels. They were used for qualitative comparison only, and were not captured under the specialised optical conditions necessary for image analysis (Morris and Mooney, 2004).

3.4.4.2. Results

The original images of white clover induced aggregation from Mytton *et al.* (1993) are given below in Figure 3.11. A Similar image was given in Figure 1.1 (Chapter One).

Figure 3.11. Soil under white clover after 12 weeks of growth, showing enhanced soil aggregation compared to perennial ryegrass (Mytton *et al.*, 1993).

Figure 3.12 to Figure 3.19 gives the images of the Credition Series topsoil beneath white clover and ryegrass after 8, 10, 12 and 14 weeks of growth (core diameter is 10.3 cm). Some interesting changes have occurred in the initial uniform soil structure under white clover compared to the ryegrass. The photographs show the movement of soil particles beneath white clover, particularly around the base of the plant, creating an undulating soil surface. Areas of improved aggregation in soil beneath white clover are evident from these pictures. Although the images suggest some soil aggregation induced by white clover, there is the need for more sophisticated techniques to quantify structural differentiation.

It was difficult to visually assess the soil structure under the pure ryegrass treatments due to the high density of the roots occupying the outside of the soil core, which increased with time. Figure 3.20 and Figure 3.21 give the images of soil beneath the mixed treatment of white clover and ryegrass (3:7) after 12 weeks of growth. It was difficult to visually assess the soil structure beneath the mixed species, although the root density was not as great as the mono-grass.

Figure 3.12. Core sown with ryegrass after 8 weeks of growth.

Figure 3.13. Core sown with white clover after 8 weeks of growth.

Figure 3.14. Core sown with ryegrass after 10 weeks of growth.

Figure 3.15. Core sown with white clover after 10 weeks of growth.

Figure 3.16. Core sown with ryegrass after 12 weeks of growth.

Figure 3.17. Core sown with white clover after 12 weeks of growth.

Figure 3.18. Core sown with ryegrass after 14 weeks of growth.

Figure 3.19. Core sown with white clover after 14 weeks of growth.

Figure 3.20. Core sown with white clover and ryegrass (3:7) after 12 weeks of growth.

Figure 3.21. Core sown with white clover and ryegrass (3:7) after 12 weeks of growth.

3.4.4.3. Discussion

The effects of white clover on soil aggregation have not been as pronounced as those previously observed by Mytton *et al.*, 1993 (Figure 1.1 (Chapter One) and Figure 3.11). There are two possible reasons for this. The first is that the soil used by Mytton *et al.* (1993) was a clay/silt loam of the Denbigh series, which would contain a greater proportion of finer particles (clay and silt) compared to the sandy loam of the Crediton series. Furthermore, the soil illustrated in Figure 1.1 (Chapter One) is a clay soil and would therefore contain an even greater proportion of fine particles (clay). The relationship between soil texture and degree of structural differentiation was addressed in Column Experiment 2 with the inclusion of different soil types. However, images of soil structure were not captured. Secondly, Mytton *et al.* (1993) used undisturbed soil, in which the effects of white clover may be enhanced because of its existing structure and greater microbial population. The degree of structural differentiation in re-packed and undisturbed cores requires further investigation. Notwithstanding this, Mytton *et al.* (1993) also used re-packed potting compost and determined enhanced soil structure beneath clover.

3.4.5. Oxygen Diffusion

3.4.5.1. Introduction

Soil porosity was measured using a non-destructive technique recently developed at IGER (Witty, 1998). This simple, direct method is based upon electrochemical measurement of decreasing O_2 concentration in the headspace above an open-ended soil core. The decreasing O_2 concentration is the sum of outward diffusion and respiratory consumption. The two processes can be mathematically separated and diffusive loss can be quantified. Soil permeability is related to soil porosity.

3.4.5.2. Theory

The decrease in headspace O_2 concentration with time can be expressed analytically by assuming the first-order relationship (Equation 3.17).

$$C_t = (C_0 - C_\infty)e^{-kt} + C_\infty$$

<div align="right">**Equation 3.17.**</div>

where t = time; C_t = headspace O_2 concentration at time t; C_0 = concentration at time zero; C_∞ = concentration at time infinity and k is a constant. The values of C_0, C_∞ and k can be determined for an individual sample by fitting the equation to measured data for headspace O_2 (Figure 3.22).

The rate at which O_2 diffuses through the core (ml s^{-1}) is used to indicate the porosity of the soil and can be calculated from the headspace volume (V) and the slope of the decay curve (k) (Equation 3.18).

$$O_2 \text{ Diffusion} = V \times k$$

<div align="right">**Equation 3.18.**</div>

where the headspace volume (V) is calculated from the volume of O_2 injected and from the O_2 concentration at time zero (C_0) (Equation 3.19).

$$V = \frac{O_2 \text{ added} \times (100 - \Omega)}{(C_0 - \Omega)}$$

<div align="right">**Equation 3.19.**</div>

where Ω = % relative atmospheric O_2 concentration (i.e. 20.9 %).

For Equation 3.17 - Equation 3.19, concentrations are expressed as % v/v, volumes in ml and time in s.
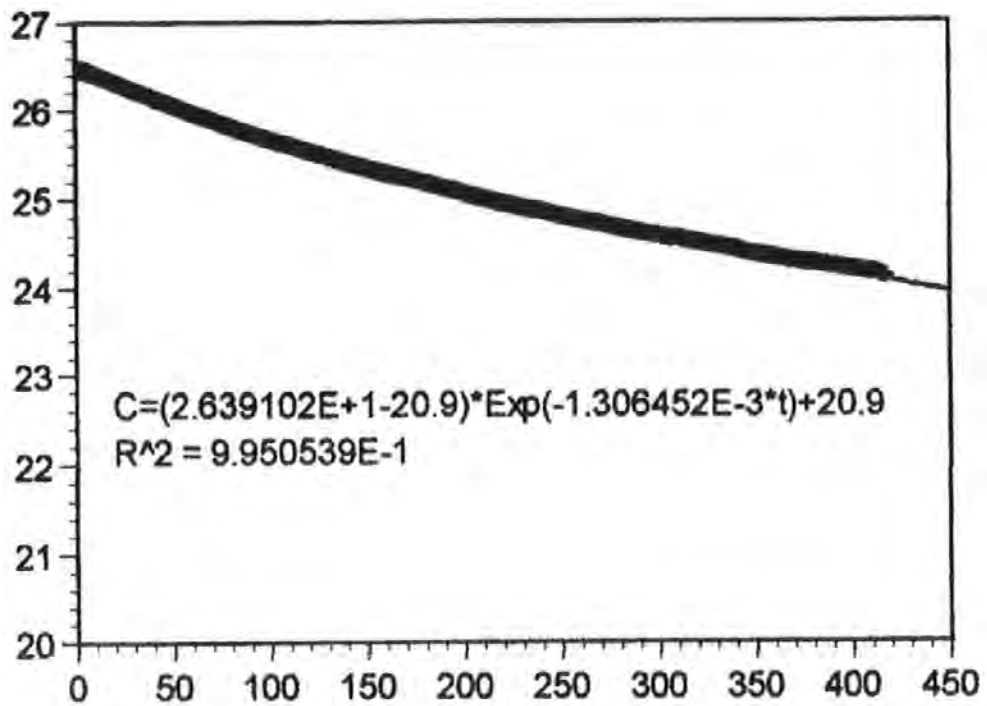
Figure 3.22. Example of an O_2 decay curve (headspace O_2 concentration, % vs. time, s), the fitted first-order decay (Equation 3.16) and the regression coefficient.

The graph shows:

$C=(2.639102E+1-20.9)*Exp(-1.306452E-3*t)+20.9$

$R^2 = 9.950539E-1$

3.4.5.3. Sample preparation

Selected soils from Column Experiment 1 were determined after 3½ months of plant growth. Soil permeability and porosity are strongly related to water content, and so soils were equilibrated to a water content of 15% prior to analysis. This was achieved by saturating the cores for 48 hours; they were allowed to drain and successively weighed until the gravimetrically determined water content was equal to 15%. The O_2 diffusion rate for various soils from Column Experiment 2 was determined after the soils were re-packed and allowed to settle prior to plant growth.

3.4.5.4. Procedure

Figure 3.23 illustrates the sensor assembly and Figure 3.24 shows the mounted samples. A machined plastic cap was used to seal the base of the intact soil core. The sample container rested on a porous spacing ring so that a small headspace remained. The cap was fitted with two injection ports and an electrochemical O_2 sensor linked to a data acquisition package.

10 ml of O_2 was introduced into the headspace via one of the injection ports to increase the ambient O_2 concentration by approximately 25%. Both injection ports were closed and after 200 seconds the O_2 concentration in the headspace was recorded at 10 second intervals. The diffusivity was calculated as above, and can indicate permeability and porosity.

Figure 3.23. The equipment turned upside-down: machined plastic cap, with oxygen sensor (shown unscrewed from the plastic cap) and oxygen injection ports.
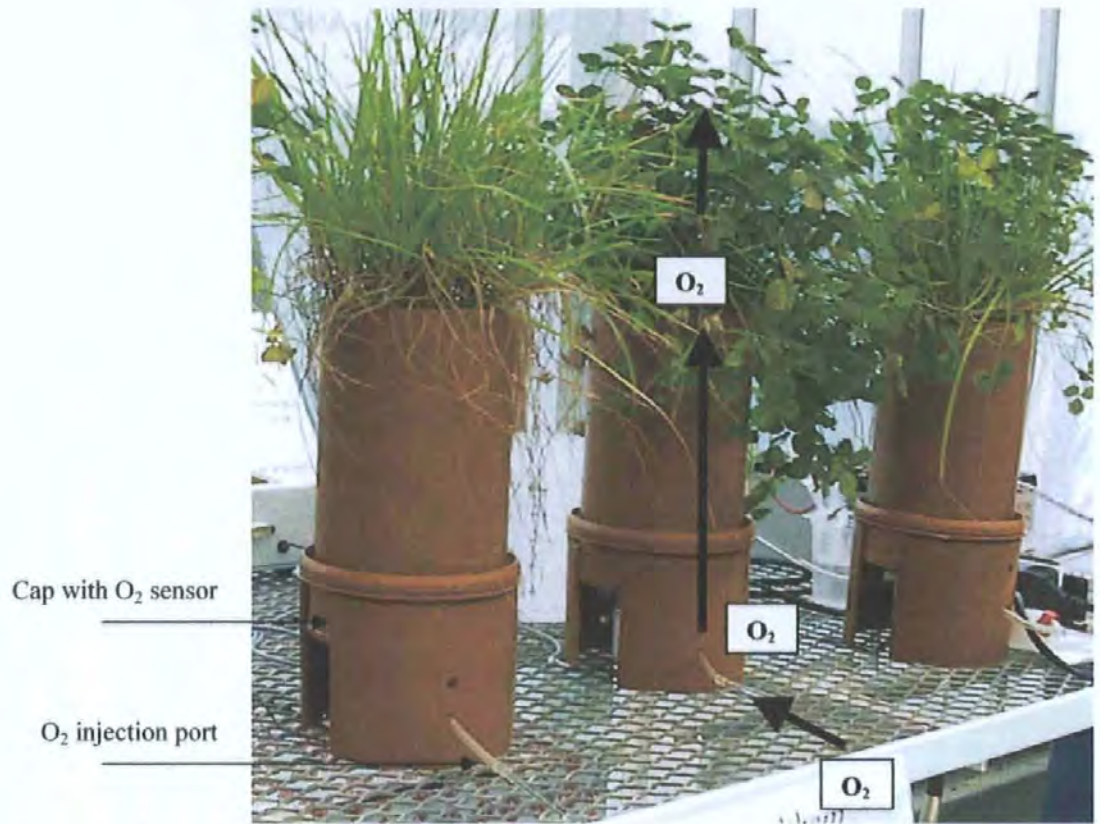
Figure 3.24. The sample pots mounted onto the sensor assembly as given in Figure 3.23, with additional supports to raise the assembly off the bench. The trajectory of oxygen is shown.

3.4.5.5. Results

The O_2 diffusion rate for each soil from Column Experiment 1 was determined after 3½ months of plant growth. This was a similar time period of enhanced structural differentiation reported by Mytton *el al*. (1993). Figure 3.25 illustrates the differences in the range (i.e. minimum and maximum values) of O_2 diffusion rates between treatments and indicates a similar mean and median value within plant treatments (i.e. topsoil vs. subsoil). The greater O_2 diffusion rate in both topsoils and subsoils containing white clover suggests a greater porosity compared to the pure grass and the unplanted control soils.
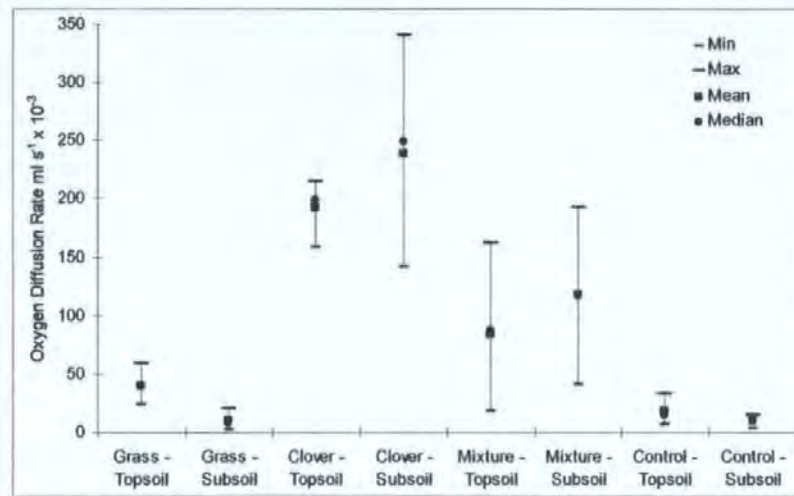
Figure 3.25. The O_2 diffusion rate for each treatment from Column Experiment 1 showing the range (minimum and maximum), mean and median of each replicate (planted treatment, n=7; unplanted controls, n=3).

Plant treatment effects, and differences between topsoil and subsoil, with respect to O_2 diffusion rates were tested by analysis of variance (ANOVA), and comparisons among means were made using the least significant difference (LSD) multiple range test, calculated at the 95% confidence level ($p<0.05$). Three separate tests were performed: two soil types (topsoil and subsoil), four planting regimes (white clover, ryegrass, mixed species and unplanted controls) and eight treatments (4 planting regimes x 2 soil types).

Of the eight treatments, the mean O_2 diffusion rate was greatest for clover grown in subsoil (Figure 3.25). This was significantly higher than the topsoil, and both were significantly greater than all other treatments. There were no significant differences between the grass and unplanted controls for both plant and soil types, and all four of these treatments were significantly different from the others, with the exception of the grass and mixed species in topsoil. However, the mixed species showed no significant difference with soil type. To summarise the effects of both plant and soil types on O_2 diffusion, the treatments that showed a statistically significant difference are illustrated in Figure 3.26 and Figure 3.27.

Figure 3.26. Treatments that show a statistically significant difference in O_2 diffusion from Column Experiment 1 are denoted by * (p<0.05). (For example, there is a statistically significant difference between clover and grass in topsoil, but no significant difference between grass in topsoil and subsoil).

Figure 3.27. Plant treatments that show a statistically significant difference in O_2 diffusion from Column Experiment 1 are denoted by * (p<0.05). (i.e. only grass and unplanted controls showed no significant difference).

When considering soil type (topsoil and subsoil), the depth of the original field soil had no significant effect on the mean O_2 diffusion rate. The planting regime did have an effect on O_2 diffusion: although there was no significant difference between the grass and unplanted treatments, both treatments were significantly lower than clover and the mixed species (Figure 3.27 and Figure 3.28).
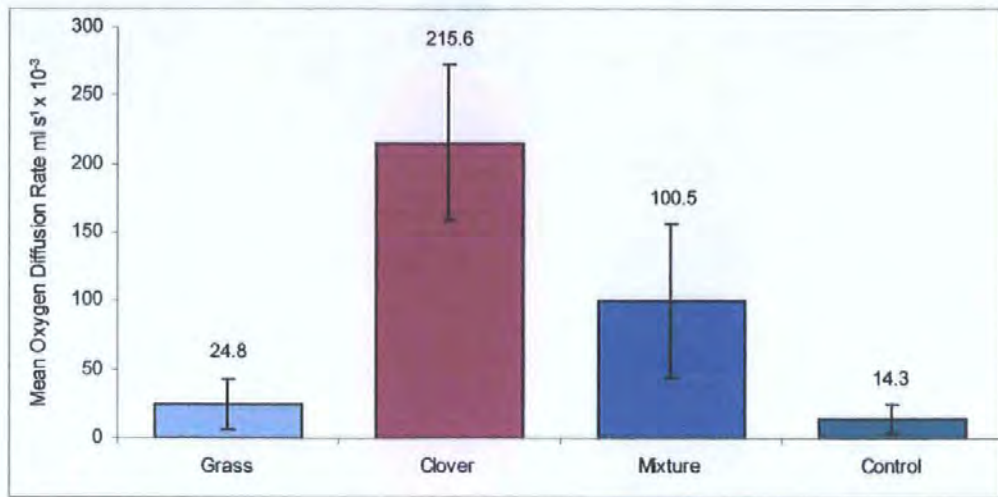
Figure 3.28. Mean O₂ diffusion rate for each planting regime from Column Experiment 1 (planted treatment, n=14; unplanted controls, n=6). (Error bars indicate the standard deviation).

The O_2 diffusion rate for five replicates of each soil from Column Experiment 2 was determined after the soils were re-packed and allowed to settle prior to plant growth. The O_2 diffusion rate is shown in Figure 3.29. There were no significant differences in mean O_2 diffusion rate, but the variation for each replicate is large. As expected, the oxygen diffusion rate increased with increasing soil porosity and decreasing bulk density. These relationships are shown in Figure 3.30. Values for both porosity and bulk density are given in Table 3.4.
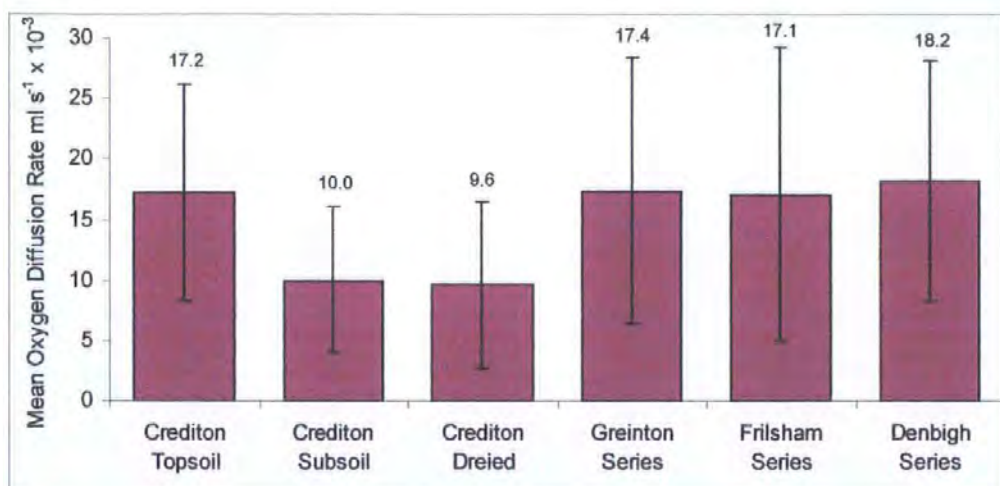
Figure 3.29. Mean oxygen diffusion rate for each soil of Column Experiment 2. (Error bars indicate the standard deviation, which ranges from 6.0 to 12.2). (n = 5).
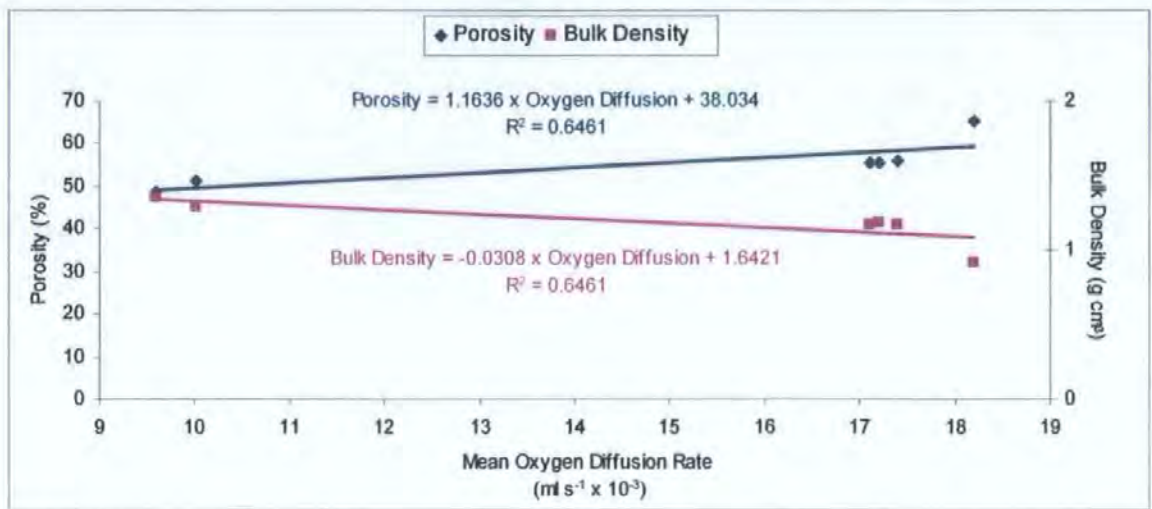
Figure 3.30. Mean oxygen diffusion rate for six soils of Column Experiment 2 correlated against both porosity and bulk density. (Porosity was mathematically derived from bulk density). (n = 5).

3.4.5.6. Discussion

The mean O_2 diffusion rate determined for treatments of Column Experiment 1 showed that diffusion was greatest for soils beneath white clover (215.6×10^{-3} ml s^{-1}). This diffusion rate was nearly nine times greater than that of soils beneath ryegrass (24.8×10^{-3} ml s^{-1}) and 15 times greater than the unplanted control soils (14.3×10^{-3} ml s^{-1}). The mixed species showed intermediate values in O_2 diffusion (100.5×10^{-3} ml s^{-1}), being half that of mono-white clover, four times greater than mono-ryegrass and seven times greater than the unplanted control soils. Similar results were also found in the parallel study by Scholefield *et al.* (2005) after six months of growth. Due to the novelty of this electrochemical technique of measuring O_2 diffusion through an open-ended soil core, no other similar experiments are reported in the literature.

The original study by Mytton *et al.* (1993) found significant differences in soil macroporosity with sward treatment, from 23.6% in grass, 45.3% in clover and 36.4% in the mixed species, after they were grown in undisturbed soil cores. Macroporosity

(diameter > 0.06 mm) was determined from the soil moisture characteristic curve at 50 cm water tension. A recent study by Papadopoulos *et al.* (2006) demonstrated enhanced soil macroporosity beneath red clover and red clover/ryegrass swards, 8.0% and 11.7%, respectively, at a 2 cm depth in field soils using image analysis. They also reported that the effect was not lasting (<3 years) following uniform cereal cropping, decreasing to 2.5% and 1.6%, respectively. High macroporosity is likely to have a significant impact on permeability of gases in and out of the soil, and also properties such as hydraulic conductivity, and potentially on factors like nutrient leaching.

The implications of the results are that white clover has improved soil permeability and altered soil porosity. The results suggest support for the hypothesis that white clover will have enhanced soil structure relative to soils beneath ryegrass and unplanted soils, and for the hypothesis that this will give rise to greater permeability of gases and freer drainage to water. In addition, the enhanced porosity in soils beneath white clover, will give rise to the potential for preferential flow of solutes (as discussed in Chapter One, Sections 1.6.6 and 1.6.8). Thus, soil beneath white clover has a greater potential for environmental pollution of surface waters, ground water and the atmosphere.

The results are not conclusive and only suggest a change in soil structure due to the link between diffusion, permeability and porosity. Furthermore, although pore space is an important feature of soil structure, information on porosity alone is not very useful (Dexter, 1998). For a more accurate indication of soil structure, the pores and solids must be quantified in terms of size, shape, continuity and distribution (Holden, 2001), using impregnated thin sections and image analysis techniques as Discussed in Chapter One (Section 1.6.5.2).

3.5. Conclusions

The soils of the Crediton, Greinton, Frilsham and Denbigh series were characterised as acidic soils, and had variable organic matter contents. The repacked soils of the Crediton, Greinton and Frilsham series had similar bulk densities and porosities, as a result of their coarser textures. Soil of the Denbigh series had a lower bulk density and elevated porosity after re-packing; this is a reflection of this soil having the highest clay and silt content. Particle size analysis by the hydrometer method was considered inaccurate. The Soil Survey textural classes were used, as handling the soil and observations deemed these classifications to be more realistic than the experimental data.

The structural stability to water showed that white clover increased aggregate stability compared to ryegrass. This increased stability was not related to the depth of the original field soil or depth in the core. The stability of soils under ryegrass showed evidence of decreasing stability with both depth of the original field soil and depth within the soil core.

White clover increased the shear strength of the soil compared to soil beneath ryegrass and the unplanted controls. However, this was only true for the Crediton, Frilsham and Greinton series. Soil of the Denbigh series beneath white clover and ryegrass gave similar results, both of which had consistently lower values than the equivalent unplanted soil.

The images of soil beneath white clover showed the movement of soil particles around the base of the plant and areas of enhanced aggregation. The images of soil beneath ryegrass and the mixed species were difficult to the visually assess due to the high density of roots.

O_2 diffusion rate was greatest for soils beneath white clover, the mixed species showed intermediate values and ryegrass was only slightly greater than the unplanted control soils. The mean O_2 diffusion rate was greater for subsoil than topsoil for both the white clover and mixed treatments.

CHAPTER FOUR

4. Modelling soil water retention

4.1. Overview of chapter and objectives

This chapter presents the routine method for the determination of soil water retention, and a 3-dimensional network model used to simulate void structure and hydraulic conductivity.

The objectives were:

1. to obtain water retention data as an indication of soil structure

2. to model the water retention data to simulate void structure

3. to use the model to simulate soil hydraulic conductivity

4.2. Introduction

4.2.1. Soil water

Soil holds water in its matrix by adsorption onto particles and by capillarity in the pores (Marshall *et al.*, 1996). Soil water will contain energy; its potential energy, and more specifically the pressure potential, is most important as it characterizes its physicochemical condition and movement. The pressure potential is considered to be negative as the water pressure is sub-atmospheric. It is often known as matric potential, tension or suction (Hillel, 1980). Soil-water potential is expressed in terms of energy per unit mass or volume (Table 4.1).

Water in unsaturated soil is constrained by the capillary and adsorptive forces and so energy is required to remove it from the soil. Finer pores exert greater force per unit cross-section area of soil water meniscus than larger pores and so at a given tension soils with smaller pores will retain more water (Klocke and Hergert, 1996). The relationship between soil water content and soil water tension is presented graphically and termed the soil-moisture characteristic curve or water retention curve. In saturated soil at equilibrium with

atmospheric pressure, the tension is zero. As the water content decreases, the tension used to hold water increases. Soil structure will affect the shape of the curve, as at low tensions (0-100 kPa) the amount of water retained is a function of capillarity and therefore pore-size distribution. At high tensions, water is retained due to adsorption and so texture is more influential (Hillel, 1980).

Table 4.1. Matric potential per unit mass, volume and weight in SI units showing its magnitude over a broad range of soil conditions (adapted from Marshall *et al.*, 1996).

Condition at quoted potential	Per unit volume		Per unit mass	
	kPa	m H_2O	bar	J kg^{-1}
Saturated or nearly so	10^{-1}	10^{-2}	10^{-3}	10^{-1}
Near-field capacity	10	1	10^{-1}	10
Near-permanent wilting point	1.5×10^3	1.5×10^2	1.5×10	1.5×10^3

Soil water can be classified into three categories: (1) gravitational water, which drains readily by gravitational force, (2) available water, which is retained by capillary forces and is available for extraction by plants, and (3) unavailable water, which is held by adsorptive forces and is unavailable for plant uptake (Klocke & Hergert, 1996). Field capacity refers to the water content at the upper limit of the available water range. This can be defined as the amount of water retained in a soil after it has been saturated and allowed to drain for 24 hours (Klocke & Hergert, 1996) and corresponds to 5 kPa suction under British conditions and in sandy soils (Hall *et al.*, 1977). The water content at 1500 kPa is an approximation of the permanent wilting point; this lower limit of the available water range is the point where plants have extracted all available water and will wilt and die. The available water capacity is a measure of the amount of water held between field capacity and wilting point, and varies with soil texture. Soil water content (θ) is often expressed as a percentage by mass (θ_m) or volume (θ_v).

4.2.2. Context of water retention measurements

Unsaturated hydraulic conductivity is the primary measure of the ease of transport of water and dissolved or suspended chemicals through the vadose region. Mualem (1976) has shown that unsaturated hydraulic conductivity can be approximately calculated from a soil's water retention characteristic. Water retention characteristics are difficult and time-consuming to measure, but are nevertheless easier to measure than unsaturated hydraulic conductivities over a full range of saturations. Therefore, water retention characteristics tend to be crucial in estimating hydraulic conductivity, and hence water and chemical transport. To provide more global estimates of water retention, the property is often related to the more readily measured properties of texture, density and organic carbon content using multiple regression functions known as pedo-transfer functions. Pedo-transfer functions have been used for a wide range of uncultivated soils, amongst others US soils (Pachepsky *et al.*, 2005), Danish soils (Borgesen and Schaap, 2005) and English and Welsh soils (Mayr and Jarvis, 1999). Pedo-transfer functions are also used more generally to relate a wider range of hydraulic properties, including run-off, infiltration and meteorological heat balance due to soil moisture (Pachepsky *et al.*, 2005). Despite their usefulness, pedo-transfer functions have weaknesses which are well known. These include their tendency to be based on laboratory measurements; water retention in the field situation tends to be lower (Pachepsky and Rawls, 2003).

In this work, we set out to model subtle structural changes in soil due to the action of roots of white clover. As soon as one attempts this, not only do pedo-transfer functions become inadequate, as might be expected, but also the experimental and theoretical frameworks on which they are based. We improve on some of the main theoretical approximations by use of a void network model. The experimental problems remain, however, and we describe how experimental procedures should be improved for further investigations.

4.2.3. Critique of current approaches to interpretation

There exist a series of major problems associated with the study of the void structure of soil, and here we need to make brief description of five of them. The first, (i), arises from the fact that there is an implicit assumption within much of soil physics that all voids within soil are fully accessible to the exterior of the sample with respect to fluid for flow, imbibition or drainage. Such accessibility can be thought of in terms of a bundle of capillary tubes which open to the surface. Each tube is implicitly assumed to be of a constant size, and not connected with others of a different size. Under these circumstances, it is possible to assume that the void size distribution can be directly derived from the first derivative (i.e. slope) of the water retention curve. On this basis, Mualem (1976) calculated unsaturated hydraulic conductivity from water retention, and Dexter (2004) derived the S-factor for measuring soil health. The assumption of complete accessibility is also implicit in fractal approaches, including the pore-solid fractal (Bird and Perrier, 2003) most recently used by Huang and Zhang (2005).

In practice, however, voids generated by geophysical processes rather than soil macro fauna are often surrounded by smaller connecting 'throats', a phenomenon often referred to as the 'shielding' or 'shadowing' of the voids. In the case of porous rocks, the extent of this shielding can be discovered by filling a sample with low-melting Woods metal, and dissolving away the rock (Wardlaw *et al.*, 1987). But Wood's metal destroys the structure of soil, and resin or carbowax leaves a structure from which the soil cannot easily be dissolved away. Neither do thin sections give an unambiguous determinant of the extent of shielding, because in two dimensions it is impossible reliably to differentiate between pores and throats. So one has to guess the extent of this phenomenon on the basis of the known water retention characteristics and the overall porosity of the soil. Guesswork is unsatisfactory, but is nevertheless better than disregarding the shielding. Furthermore, the

reliability of the guesswork can be estimated by carrying out a series of stochastic realisations of the model.

Another disadvantage of using the first derivative of the water retention curve, rather than the shape of the whole curve, is that it induces a lack of experimental rigour. This is most easily appreciated by viewing a schematic diagram. Figure 4.1 shows three water retention curves. One is complete (■); at the lowest experimental tension, the water retention is equal to that measured independently, for example gravimetrically on a portion of similar sample, and at the highest tension the water retention curve tends to zero. In practice, many water retention curves are incomplete (▲), because the sample drains by gravity at the lowest tension or the investigator has not measured water retention at the lowest tension, as shown in Figure 4.1. Often, as shown, the highest tension is not enough to remove water from e.g. clays. Another problem is that during water retention measurement, the sample can expand or shrink. If such volume change is not compensated for when calculating the total sample water retention capacity gravimetrically, illogical results may be derived, for example that the amount of water removed from the sample is greater than the total amount it can contain. This is also illustrated in Figure 4.1 (●).
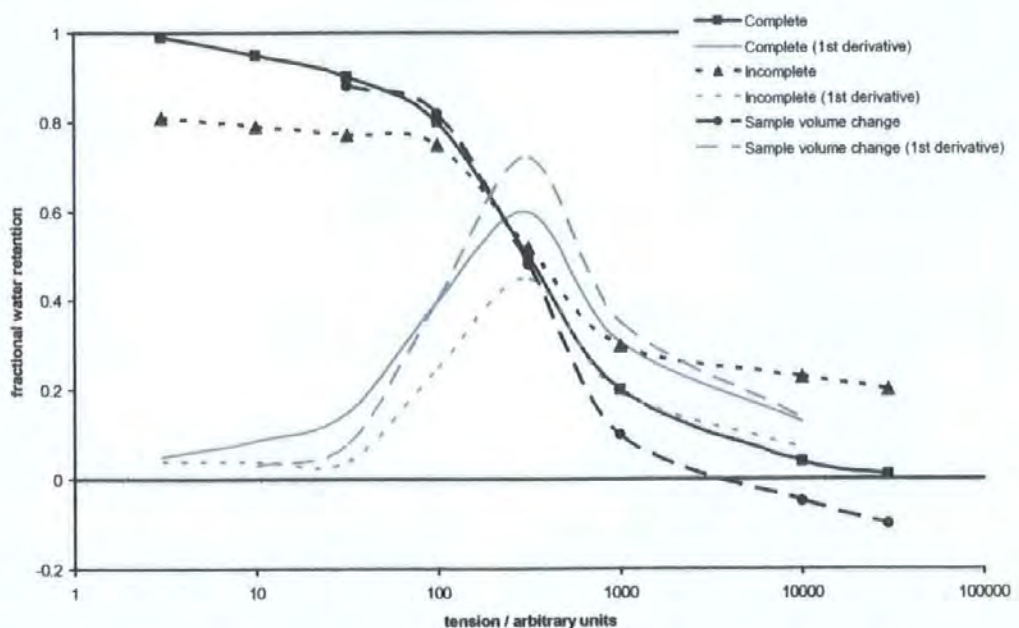
Figure 4.1. Schematic diagram of complete, incomplete and erroneous water retention curves.

Of the three water retention curves shown in Figure 4.1, only the complete one is fully modellable. Yet as shown, all three give similar (negative) first derivative curves which suggest, according to the capillary bundle approximation, a broad size distribution centred around the tension of 300 arbitrary units. So within the traditional approximation framework, all three experimental curves are acceptable.

In practice, complete curves are almost impossible to obtain, so we have to model incomplete curves. We then have to decide whether the modelled porosity should be that picked up from the observed water retention curve, or the total porosity measured gravimetrically from the total water retention capacity. In the present study, we took the former approach, equivalent to equating the modelled porosity to the fractional water retention range of 0.81 to 0.20 (v/v) of the incomplete curve in Figure 4.1. This approach avoids the danger of modelling immobile water, but opens us to the danger of not modelling large, gravity drained pores. The water release measurements are made over the range of 0.2 to 2500 μm, and converted to air-intrusion values (Peat *et al.*, 2000; Johnson *et al.*, 2003a). Thus, the modelled void network and therefore modelled porosity must include only the voids within this size range.

Problem (iii) is the intractability of the shapes of the water retention characteristic curves. The curves vary monotonically from maximum water retention at low tensions to minimum at high tensions, and usually, but not always, exhibit a point of inflection and position of maximum slope at an intermediate tension. Such behaviour is not much on which to base a mathematical fitting function. However, the necessity of parameterising water retention curves for input to pedo-transfer functions has spawned a host of fitting functions, such as the van Genuchten function (1980), Brooks-Corey function (Ma *et al.*, 1999), and modified Brooks-Corey function (Mayr and Jarvis, 1999). Although very useful for input to pedo-transfer functions, and convenient for applying to other soil

characteristics (Zhu *et al.*, 2004), the straight-jackets of the assumed functionalities of these fitting functions tend to mask subtle effects such as those caused by roots. The arbitrariness of the functions also tends to result in different predictions of water retention by pedo-transfer functions based on different fitting curves. McBratney (2002) suggests that this problem can be overcome by using Monte Carlo methods to choose the results from the pedo-transfer function which gives the least variance.

To avoid the problem of intrusion curve shape in the present study, the void network model performs a point by point fit to the experimental water retention curves. This procedure then exposes two further problems, (iv) and (v), which are both theoretical and practical. Problem (iv) is that the standard protocol for measurement of water retention curves is to measure around five points (ISO 11274:1998); although investigators tend to measure a minimum of eight points. Even this can take many weeks. Allowing for the fact that the minimum and maximum tend to be fixed within the fitting procedure, one is left with fitting three variable points using a fitting function with two or three parameters. There are therefore a minimal or zero number of statistical degrees of freedom. Coupled with this is that the fitting parameters of the Van Genuchten and Brooks-Corey functions are not mathematically orthogonal, so a range of fits are possible, which in practice are constrained to some narrower band thought appropriate to the samples.

The Pore-Cor void network model used in the present work uses four fitting parameters, so even though it is carrying out a point by point fit, it too is short of statistical degrees of freedom. So our procedure is to fit all the water retention curves allowing the model's fitting parameters to have unrestrained variation between stochastic realisations. The curves are then re-fitted, constraining the fitting parameters to a common range of variation for each parameter which does not include outliers. Again, this procedure is only partially satisfactory, but is better than the ignoring of the problem which occurs when fitting van Genuchten or Brooks-Corey functions.

Problem (v), also uncovered by the use of the point-by-point fit, is the absence of water retention data at low or zero applied tensions. Saturated soil samples mounted on water retention tables drain by gravity initially, and this initial drainage is usually ignored. However, this gravity drainage occurs through the largest voids within the sample, which have the greatest hydraulic conductivity. The functionality of the van Genuchten and Brooks-Corey functions overlooks this absence, by assuming that the gravity drainage can be inferred from the shape of the rest of the drainage curve. However, this inference is based on the mathematical functionality of the fitting function, and has no relation to the structure of the soil. A previous attempt has been made to address this problem by use of a 'matching point' for pedo-transfer functions at a tension of 1 kPa (Jarvis *et al.*, 2002). In the present study, the point-by-point fitting algorithm within the void network model sees no data in this region, and therefore allows itself to vary as much as it wishes to fit the data at the other points which are known. There are therefore wide variations in the gravity drainage region between stochastic realisations, and hence wide variations in the model's prediction of saturated hydraulic conductivity.

4.2.4. The void network model

The void network model has been described in detail in previous publications (Peat *et al.*, 2000; Johnson *et al.*, 2003a). An example of a Pore-Cor void structure is shown Figure 4.2. The void structure is arbitrarily split into larger voids, referred to as 'pores', connected by smaller inter-connecting 'throats'. The geometry of the pores is simplified to cubes of variable size, and of the throats to variably sized cylinders emerging from the centres of the faces of the pores in the directions of the three Cartesian axes *x*, *y* and *z*. The throats are of variable size, up to the size of the largest pore, or entirely absent. The geometry is further simplified by spacing the features equally in each of *x*, *y* and *z* directions. Each unit cell of the structure comprises 1000 pores in a 10 x 10 x 10 array, connected by up to 3000

throats. The unit cells connect to each other in each direction, thus generating a periodic boundary condition. A Boltzmann-annealed simplex (Johnson *et al.*, 2003a) is used to adjust four parameters so that the mercury intrusion curve of the simulated structure closely matches that of the experimental sample.

The four parameters are:

i. connectivity, defined as the average number of connected throats per pore, up to a maximum of six (one connected to every face of the cubic pore);

ii. throat skew, defined as the percentage of throats of the smallest size in a distribution of 100 sizes which is linear when plotted on a logarithmic size axis;

iii. pore skew, a scaling factor which bulks up the sizes of the pores to achieve the experimental porosity;

iv. correlation level, which sets the level of local size-autocorrelation of the features, in the present case giving rise to vertical banding within each unit cell.

The simplex takes into account three Boolean parameters, namely whether the network can be drawn with no overlapping features, whether it can be adjusted to the experimental porosity and whether the network is unfragmented.

Figure 4.2 shows 15 pores, i.e. 1.5 units cells, in the x and y directions, and one unit cell thickness (10 pores) in the z direction. Many of the throats are invisibly small in the figure (shown in purple). Fluids, such as air (shown in yellow) as it displaces water (shown in blue), are intruded from the top face of the unit cell in the $-z$ direction (downwards in Figure 4.2). The periodic boundary condition causes the system into which the fluid intrudes to be a sheet of infinite width and breadth (in the x and y directions), and with thickness the same as one unit cell in the z direction. This is a working approximation to the accessibility to fluids of the body of an experimental sample.
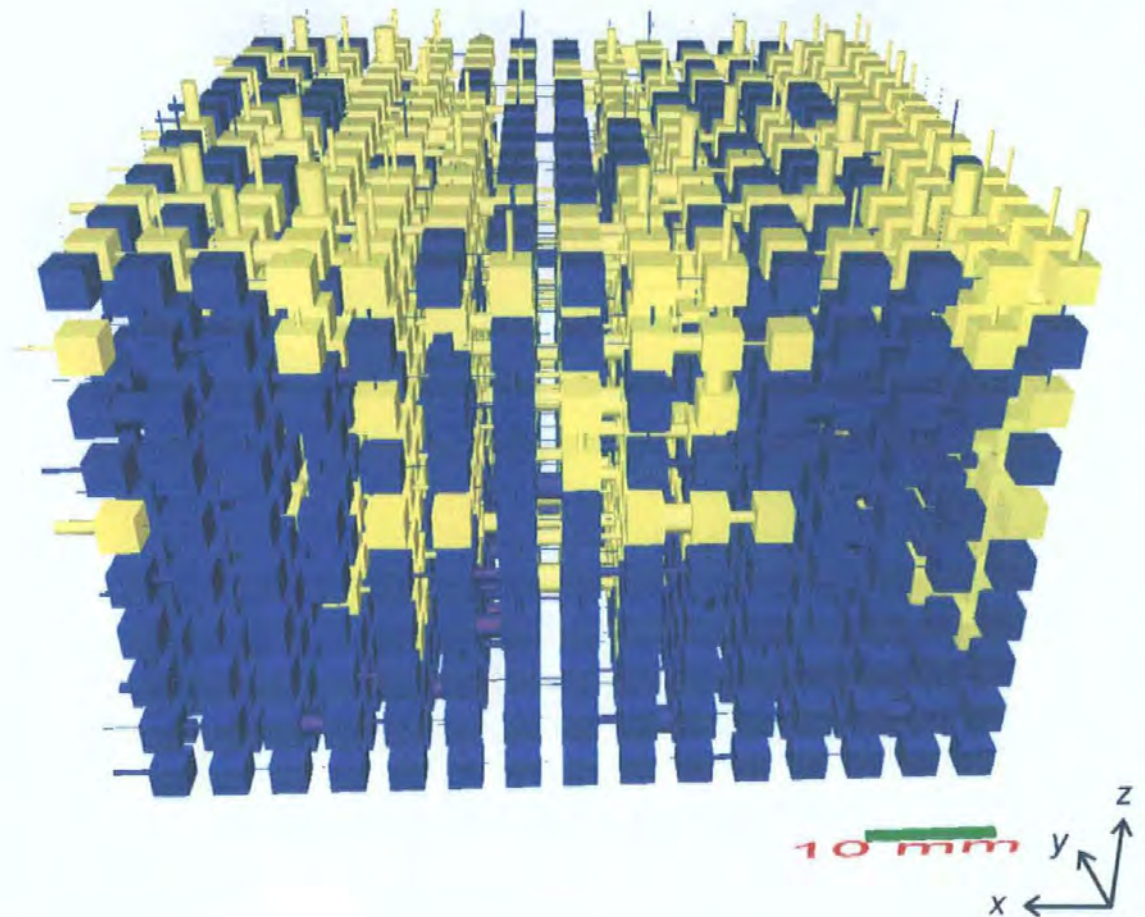
Figure 4.2. Void network model for soil structured by clover, showing air (yellow) displacing water (blue) at a tension of 1.15 kPa.

4.3. Experimental

4.3.1. Treatments

Samples were selected from Column Experiment 1. The soil type was re-packed subsoil of the Crediton series, which was either unplanted or had been sown to pure ryegrass or white clover. Undisturbed field cores were also taken from the sub-surface horizon. Triplicate samples were taken from each of these four treatments. The use of subsoil was in accordance with other water retention measurements of various soil types used to parameterize Pore-Cor (Peat *et al.*, 2000; Johnson *et al.*, 2003a).

4.3.2. Sampling and storage

The re-packed cores were removed from their pots and the top 40 mm of soil was removed in order to eliminate interference from roots. Metal sleeve corers (750 mm diameter x 50 mm tall) were hammered carefully into the exposed soil surface; soil was removed from the outside of the corer with a trowel and the base roughly trimmed with a knife. In the field, undisturbed cores were collected from a depth of 250 mm (B-Horizon/subsoil). Cores were double-wrapped in plastic bags to prevent drying and refrigerated at 2°C to reduce evaporation and biological activity.

4.3.3. Moisture release measurements

Water retention curves were measured by the National Soil Resources Institute (NSRI), University of Cranfield, UK, according to a standard protocol (ISO 11274:1998). Samples were saturated by standing on a piece of saturated sponge in a water bath. After wetting to a constant weight, each sample was successively equilibrated at four low tensions (1, 5, 10 and 40 kPa) on sand suction tables (Figure 4.3) and two high tensions (200 and 1500 kPa) in pressure membrane cells (Figure 4.4). The laboratory temperature was maintained at 20°C to prevent changes in the temperature and the viscosity of the soil water; this would otherwise alter the water release characteristics.

Samples were weighed frequently and considered to have reached equilibrium when the weight of the core remained constant at each tension on the sand suction tables and when water leaving the pressure membrane system ceased. When the water content had equilibrated, the tension was increased. At the end of the experiment, equilibrated samples were removed from the pressure cells, weighed, oven-dried and weighed again to determine moisture content. The volume of water retained and moisture content at each tension was calculated (Equation 4.1 and Equation 4.2). Tension was converted to pore diameter using the Laplace equation (Equation 4.3).

The moisture release measurements involve drying a soil from saturation to air-dryness, when re-wetting a different curve is traced. The drying soil has a higher water content than the wetting soil at the same tension. Such phenomenon is well documented and know as hysteresis (Marshall *et al.*, 1996).
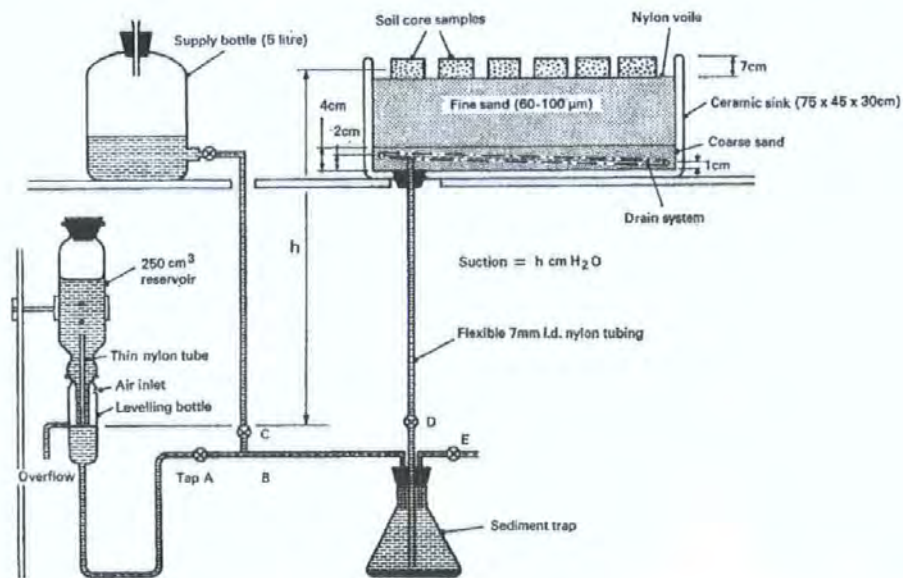
Figure 4.3. An example of a sand suction table used to equilibrate samples and determine the moisture content at four low tensions (Hall *et al.*, 1977).
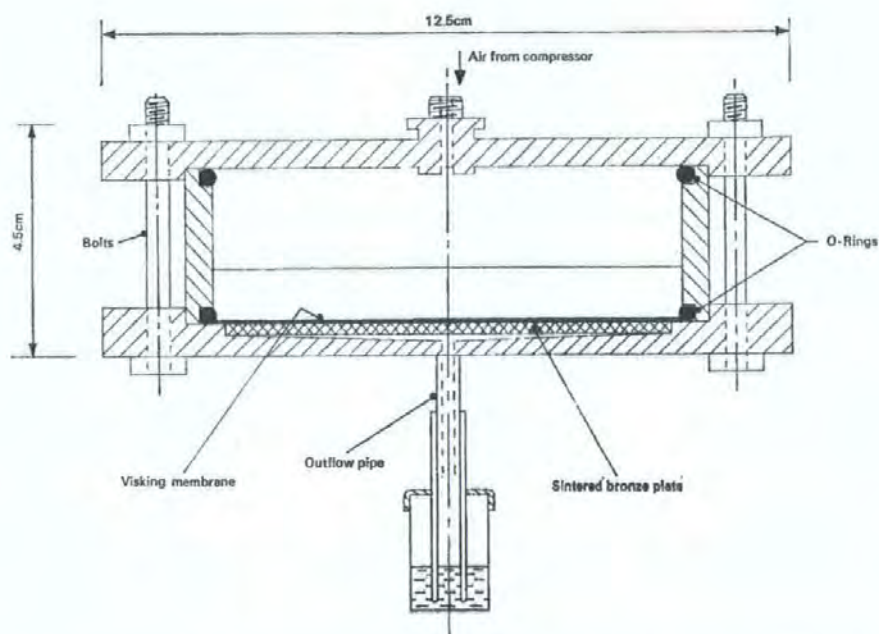
Figure 4.4. An example of a pressure membrane cell used to equilibrate samples and determine the moisture content at two high tensions (Hall *et al.*, 1977). Samples are subjected to pressure of air to release water.

$$\text{water content at } x \text{ tension (\% mass)} = \frac{\text{mass of water at } x \text{ tension} - \text{oven-dried mass}}{\text{oven-dried mass}} \times 100$$

<div align="right">**Equation 4.1.**</div>

$$\text{water content at } x \text{ tension (\% volume)} = \frac{\text{mass of water at } x \text{ tension} - \text{oven-dried mass}}{\text{density of water}} \times \frac{1}{\text{volume}} \times 100$$

<div align="right">**Equation 4.2.**</div>

$$r_i = -\frac{4\gamma_i \cos\theta_i}{P}$$

<div align="right">**Equation 4.3.**</div>

where r_i the pore radius of the i th pore, γ is the interfacial tension between air and water, θ is the contact angle where the water meniscus touches the solid surface and P is the pressure. Various approximations are implicit in the use of this equation. The contact angle and interfacial tension are assumed to have constant values (taken to be 0 degrees and 0.075 Nm^{-1} respectively), i.e. $\theta_i = \theta$ and $\gamma_i = \gamma$ for all i.

4.4. Results

4.4.1. Water retention

The results of the water retention experiments are shown in Figure 4.5 The total water retention capacities of the samples, determined gravimetrically, are shown as zero tension measurements. Measurements between 0-10 hPa were not determined, however this is an important range for gravity drainage, and it is unknown if the water release follows the line of the graph in this range. In calculating the relative volumetric retentions from the measurements of the relative masses of soil and water, no allowance was made for the density of roots in the clover and grass soils relative to the repacked soil. However, assuming there are 10g of roots in one of the 300g samples, the change in calculated water retention would be 1% in absolute terms – which is negligible compared with the standard deviation and differences between the samples.
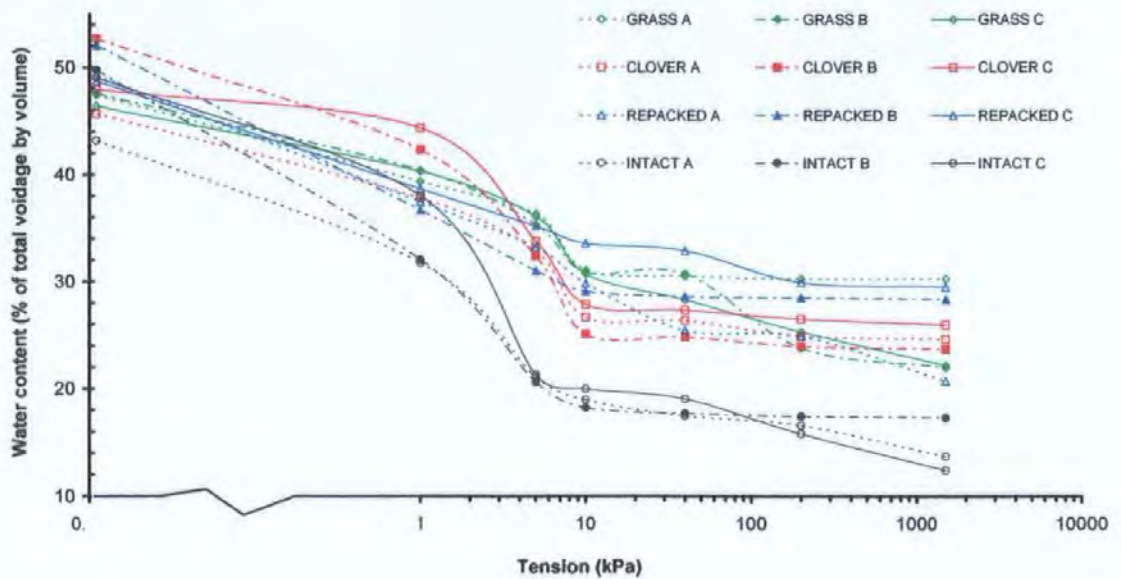
Figure 4.5. Water retention curves for the three replicates of each of the four samples (the 're-packed' and 'intact' treatments were unplanted)..

The water retention curves highlight differences in soil structure between the treatments (Figure 4.5) and suggest that the least amount of water is held in the intact soil due to its greater proportion of larger pores. As expected, the soil-moisture characteristics are different for the unplanted re-packed and intact soils; this is a function of pore-size distribution and hydraulic conductivity.

The re-packed and ryegrass soils are capable of holding the most water as they have smaller pores. The mean water content of soils previously growing white clover is lower than the unplanted re-packed and ryegrass soils. This is a function of pore-size distribution and supports the hypothesis that white clover will alter the structure of the soil compared to ryegrass and unplanted soils.

Figure 4.5 shows that there is major overlap between the samples, which is sufficient to mask the subtle structural differences. Months of effort were expended initially to model all the raw water retention curves, and then to average the modelled results. However, it was found that the trends were impossible to separate from the differences between different stochastic realisations of the model. Therefore, a single water retention curve was

produced for each sample type. This was the average of the three replicates, but ignoring anomalous results such as outliers and successive measurements that showed identical water retention at different tensions. The resulting modelled curves are shown in Figure 4.6. In order to make the error bars clearly visible, the tensions of each group of measurements have been offset from each other – the lowest tension in each group is the experimental one. The scale bars show one standard deviation of the experimental results, i.e. $\pm \sigma_{n-1}$
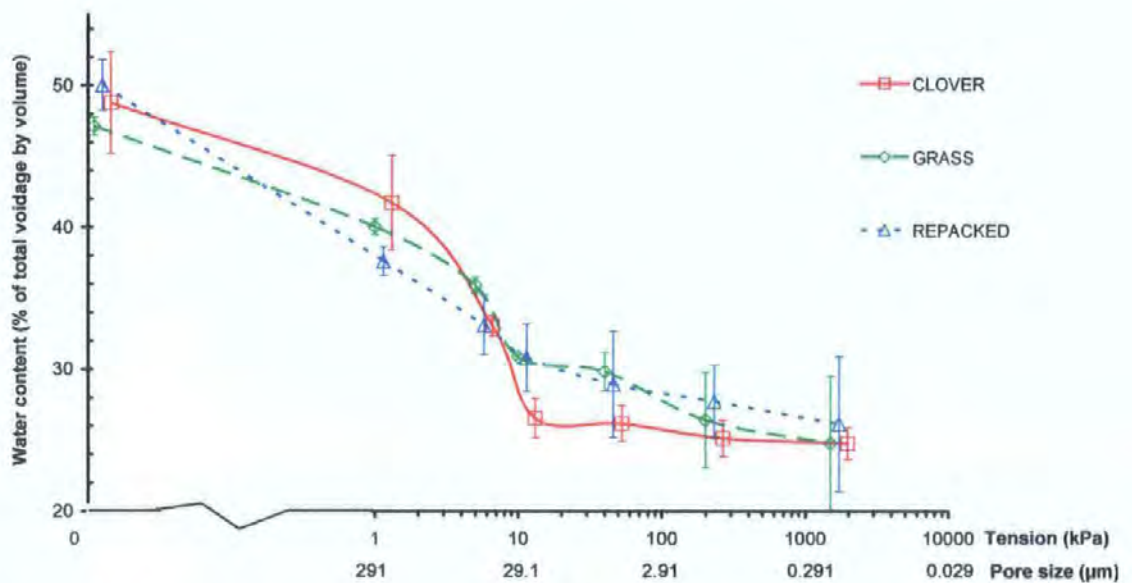
Figure 4.6. Mean water retention characteristics of each sample type, with error bars showing $\pm \sigma_{n-1}$ (All soils were re-packed prior to growth, the 're-packed' treatments were unplanted).

Available water is an estimate of the soil's water storage capacity and the amount of soil water available to plants. It is calculated from the water retained between 5 kPa (approximately field capacity) and 1500 kPa (permanent wilting point). Figure 4.7 and Table 4.2 indicate a greater proportion of available water in soil previously planted with white clover; the amount is nearly twice that of the re-packed unplanted soil. Available water is related to soil texture and organic carbon content. In subsoils over 50% of the variation in available water is attributed to the bulk density and the proportion of particles 2-100 μm (Hall *et al.*, 1977).

The water retention curves (Figure 4.5) suggest possible differential soil structure between the treatments. White clover increased the number of large pores in soil compared to the ryegrass and the initial unplanted re-packed soil. Re-packing a soil will alter the soil structure, the soil-moisture characteristics and pollutant transport (Mullins and Fraser, 1980; Bergström, 1990).

The original study by Mytton *et al.* (1993) also reported differences in the water retention characteristics of soil beneath white clover compared to ryegrass. The differences in the moisture characteristics were much more pronounced than in this study. They calculated the total porosity at the saturated weight, and the macropore space (pores >60 µm diameter) from the water retention curve at 50 cm tension (5 kPa).
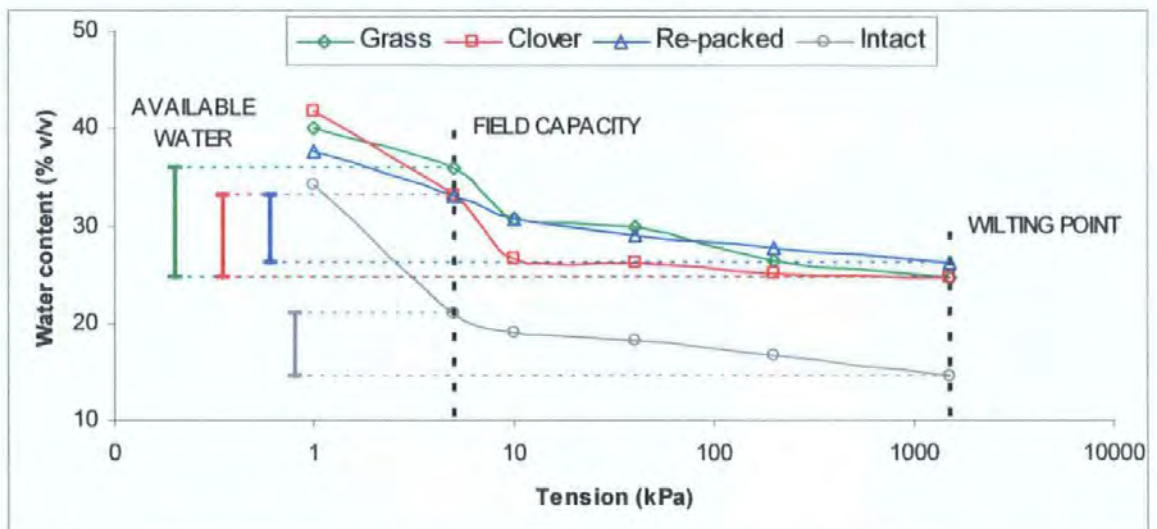
Figure 4.7. Water retention curves indicating the available water for each treatment (the re-packed and intact treatments were unplanted).

Table 4.2. Available water (i.e. the water retained between 5 kPa (approximately field capacity) and 1500 kPa (permanent wilting point).

Treatment	Available water (%)
Grass	11.1
Clover	8.3
Unplanted Re-packed	7.0
Unplanted Intact	6.5

4.4.2. Modelling

It can be seen in Figure 4.6 that the only tension at which all curves do not overlap is 10 kPa. There is a wide variation in the clover retention characteristics at the lowest tension measured on the sand tables, namely 1 kPa. So that this variation did not distort the modelling, the only case modelled was that for which the retentions at 1 kPa were equal for each sample. Ten stochastic generations were fitted for each sample type. A summary of the results is shown in Table 4.3.

Table 4.3. Values of modelling parameters for the first stochastic generation for each sample type, and the mean and standard deviation of the first ten stochastic generations.

Stochastic generation	Throat skew	Pore skew	Connectivity	Correlation level	Saturated hydraulic conductivity (10^{-14} m^2)
Clover					
1	0.43	1.93	3.26	0.16	3.23
2	0.35	1.13	3.22	0.26	90.58
3	0.22	1.33	2.99	0.07	3.58
4	1.05	737.84	4.55	0.34	24.66
5	0.75	111.74	4.26	0.20	16.71
6	1.31	60.31	5.00	0.40	39.88
7	1.26	31.90	4.50	0.38	45.69
8	0.52	1645.00	3.87	0.15	107.57
9	0.44	668.11	3.33	0.36	60.89
10	0.34	6.20	3.02	0.16	1.09
mean:	0.67	326.55	3.80	0.25	18.83*
σ_{n-1}	0.40	542.39	0.73	0.12	
Grass					
1	0.96	135.07	3.84	0.47	75.21
2	1.02	11.10	3.41	0.39	1.40
3	0.99	4.22	2.98	0.48	0.29
4	1.27	401.18	4.89	0.49	44.06
5	1.06	16.92	3.06	0.41	0.22
6	1.20	158.10	3.95	0.43	71.06
7	1.20	225.10	4.30	0.38	11.97
8	0.72	2646.40	3.60	0.36	55.12
9	1.28	1709.20	4.61	0.43	18.37
10	1.24	72.75	3.89	0.40	12.89
mean:	1.09	538.00	3.85	0.43	8.93*
σ_{n-1}	0.18	900.06	0.63	0.05	

* = geometric mean

As can be seen, the only two parameters which differ between clover and grass by more than their standard deviation are the throat skew and correlation level. The differences in the parameters can be revealed by plotting hydraulic conductivity against these parameters for ten stochastic generations. Figure 4.8 shows that the modelled throat skew varies in the range 0.22 to 1.31 for clover, but only from 0.72 to 1.28 for grass. Because of the stochastic nature of the modelling, statistical analysis is difficult. Cluster analysis, for example, would hide trends, whereas there are not enough degrees of freedom for reliable curve fitting. Therefore, all the data was fitted to a simple smoothing curve (Equation 4.4).

$$\log_{10} \text{(saturated hydraulic conductivity)} = a + b x^{\nu}$$

Equation 4.4.

where a and b are fitting coefficients, ν is an integer in the range -3 to +3, and x is the property being fitted. For each parameter, the entire set of modelled results, for both grass and clover for all stochastic generations, was fitted to curves with $-3 <= \nu <= 3$, and the value of ν chosen for which the correlation coefficient r^2_{n-1} was a maximum. The clover and grass data were then fitted individually to curves with identical values of ν. The results tabulated in Table 4.4, and shown in Figures 4.8 – 4.11 over the ranges of the stochastic generations, which are also shown in the table.

Table 4.4. Values of parameters of Eqn. 4.3 used to highlight the trends in the modelled data.

	Parameter	Throat skew	Correlation level	Pore skew	Connectivity
Clover	a	2.1194	2.8008	1.9011	3.3290
	b	0.24947	-0.09825	0.10124	-13.76400
	ν	3	-1	2	-2
	range minimum	0.222	0.068	1.129	2.990
	range maximum	1.310	0.400	1645.0	5.0
Grass	a	1.47395	2.19460	1.05165	4.34380
	b	0.34167	-0.10256	0.17874	32.97200
	ν	3	-1	2	-2
	range minimum	0.717	0.362	4.217	2.983
	range maximum	1.276	0.495	2646.4	4.9

Figure 4.8 shows that the saturated hydraulic conductivity is around a factor of 4 greater for clover than grass, for any particular value of throat skew.

Figure 4.9 shows the same exercise carried out for correlation level. The figure confirms the higher range of correlation level for grass, showing a higher local size correlation between the sizes of pores and throats.

Throat skew corresponds to the percentage of throats of minimum size, so soil beneath grass contains fewer small throats than clover. The correlation level is a measure of the local structuring of the soil. In this respect, clover is more randomly structured, with more large pores surrounded by smaller throats.

Figures 4.10 and 4.11 show that there were no clear trends in the other two parameters, connectivity and pore skew, relative to the scatter between stochastic generations of the model.

The 5th stochastic generation for clover and the 10th for grass are ones for which all the fitting parameters are close to the mean values for the whole group for that sample. These, therefore, are used for illustration purposes. The clover structure was shown in Figure 4.2, and the grass structure is shown in Figure 4.13.

Figure 4.2 shows air (light grey) displacing water (dark grey) at 1.15 kPa (11.7 cm H_2O). At this tension, assuming a soil/air/water interfacial tension of 0.0728 N m^{-1} and that the water is fully wetting, the Laplace relation predicts that cylindrical void features in the soil of 2.53 μm of larger will drain. For the present structure, the remaining water taking up 62.7% of the void volume.

152

saturated hydraulic conductivity / 10^{-12} m^2
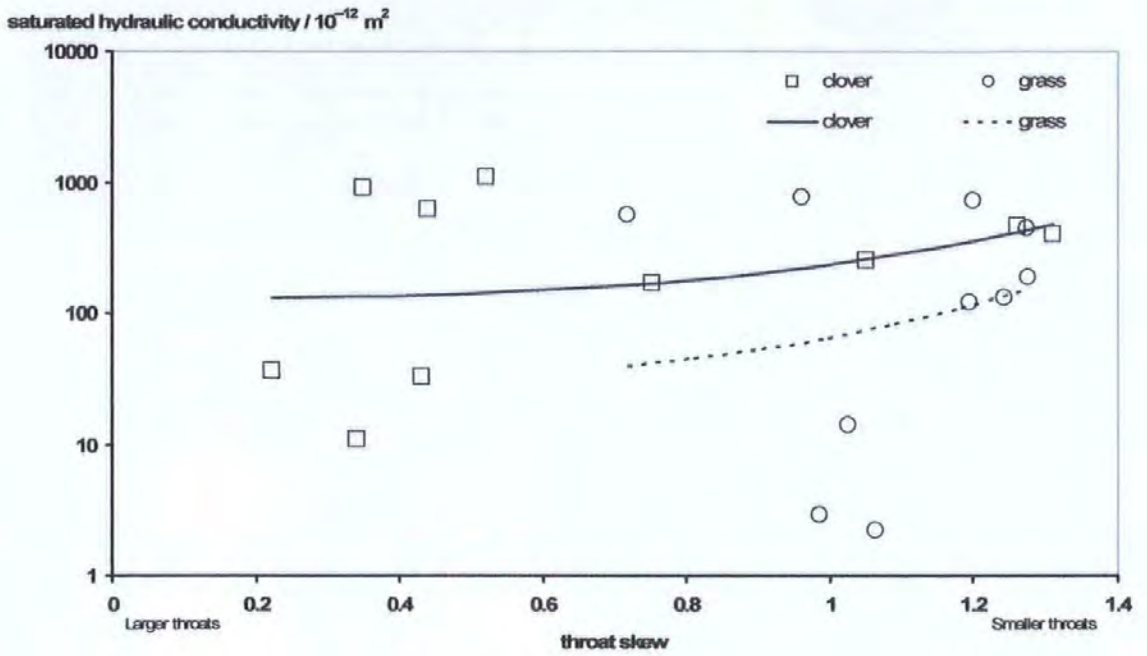
Figure 4.8. Variation of simulated saturated hydraulic conductivity with throat skew for soil beneath clover and grass

saturated hydraulic conductivity / 10^{-12} m^2
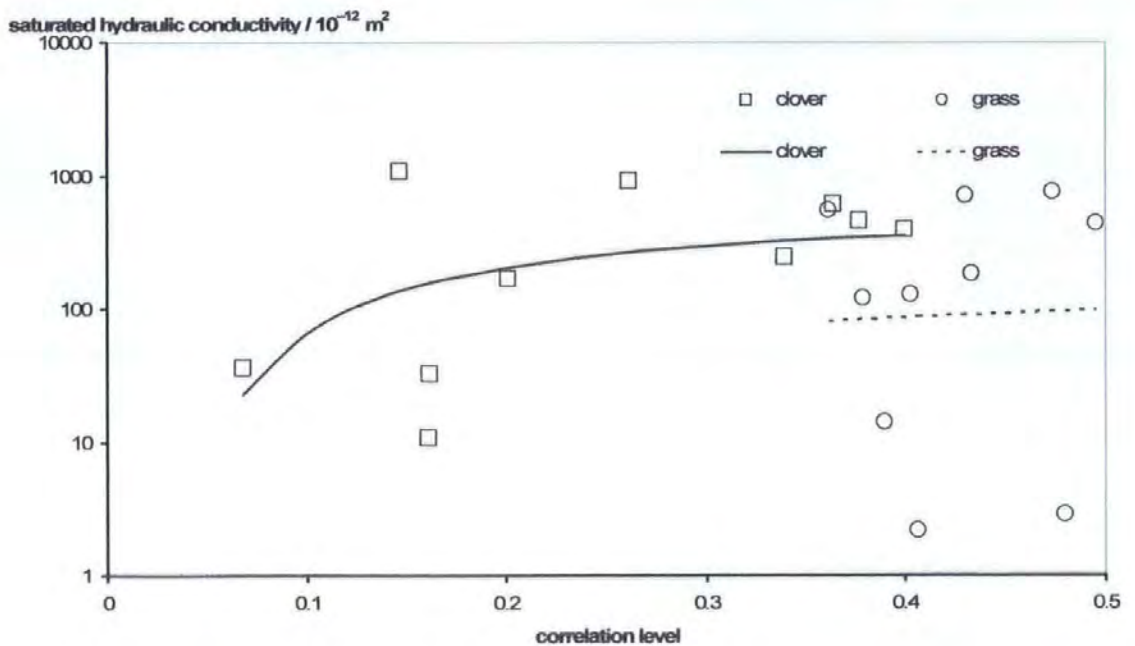
Figure 4.9. Variation of simulated saturated hydraulic conductivity with correlation level for soil beneath clover and grass.

153

saturated hydraulic conductivity / 10^{-12} m^2
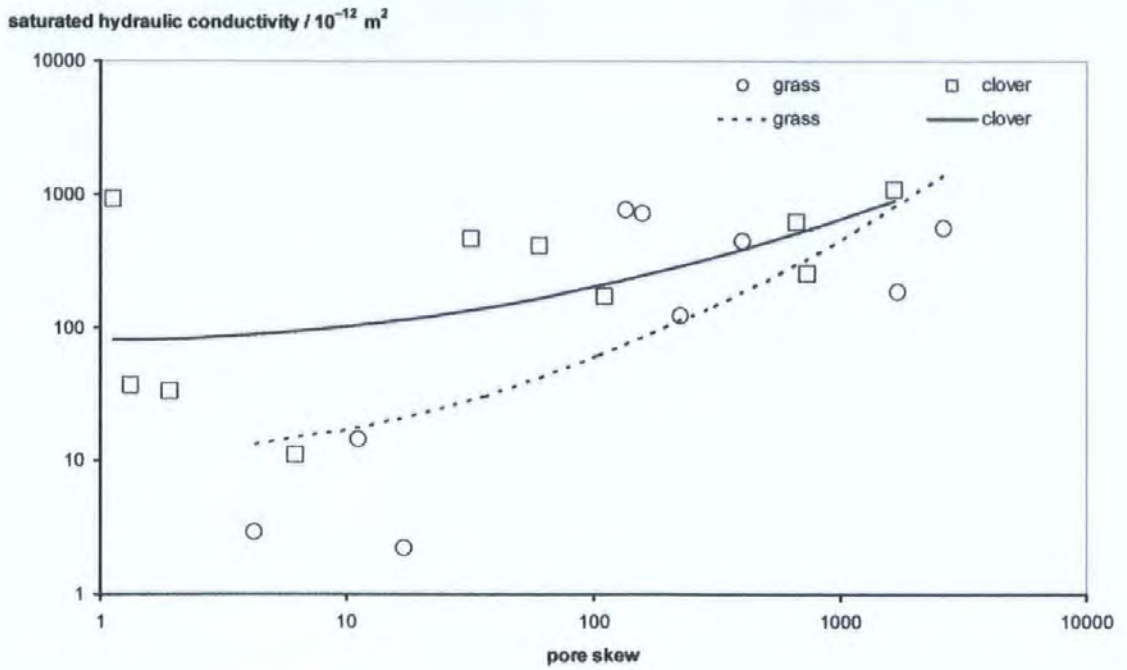
Figure 4.10. Variation of simulated saturated hydraulic conductivity with pore skew for soil beneath clover and grass.

saturated hydraulic conductivity / 10^{-12} m^2
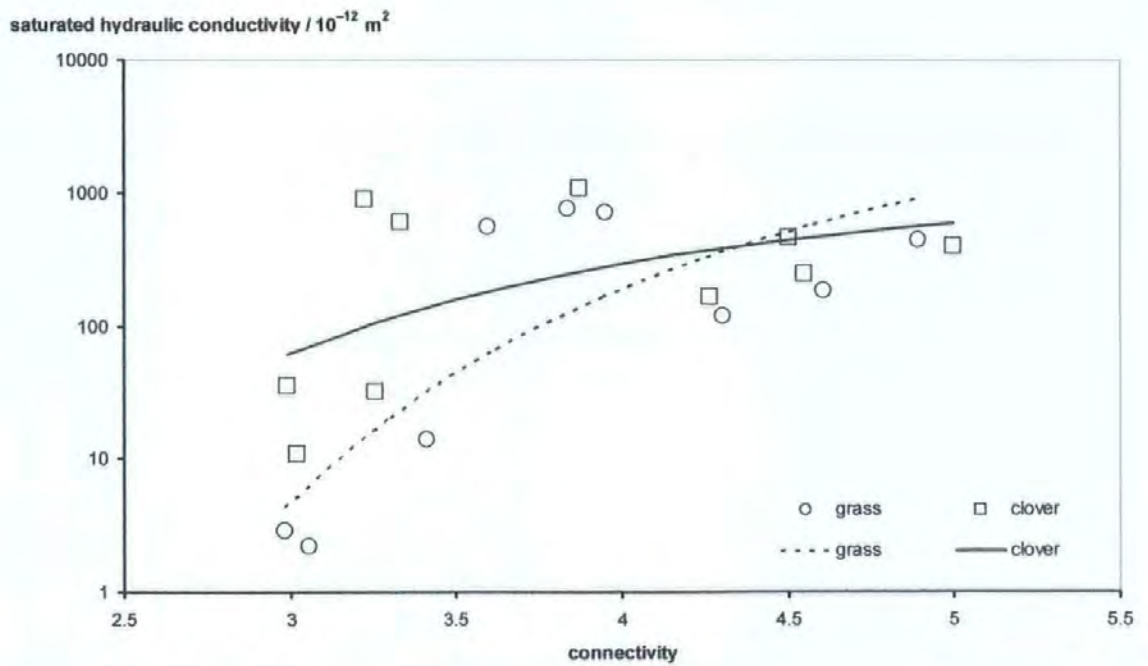
Figure 4.11. Variation of simulated saturated hydraulic conductivity with connectivity for soil beneath clover and grass.
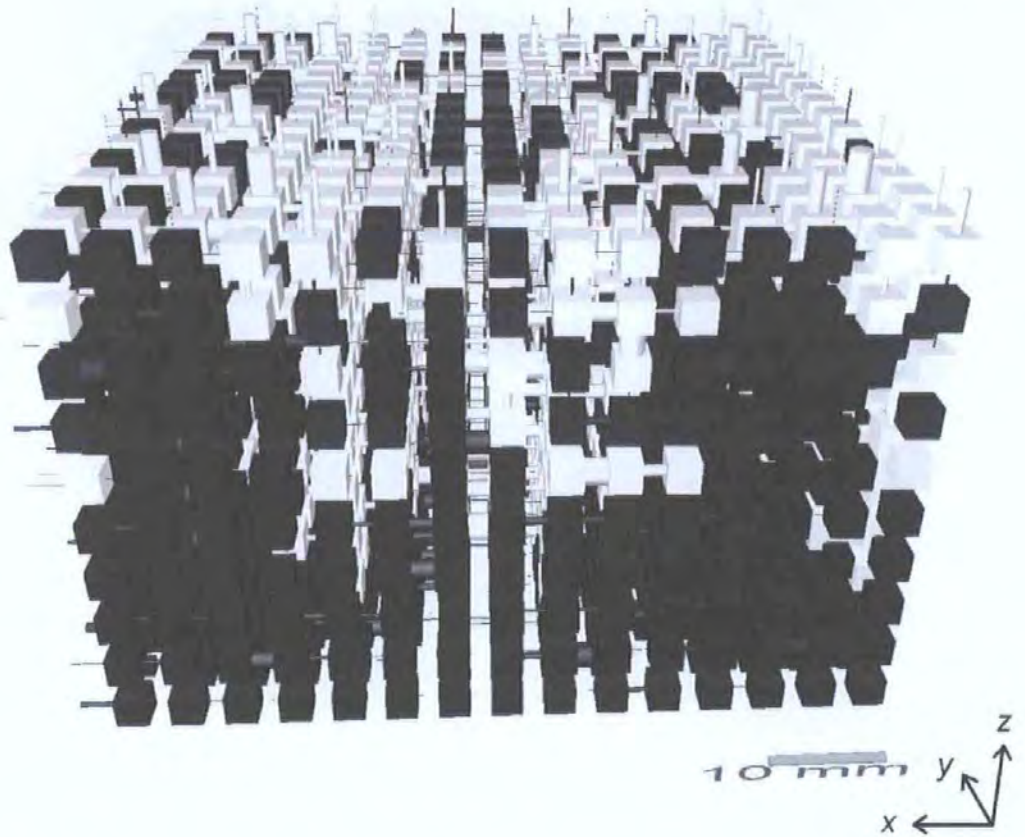
Figure 4.12. Void network model for soil structured by clover, showing air (light grey) displacing water (dark grey).
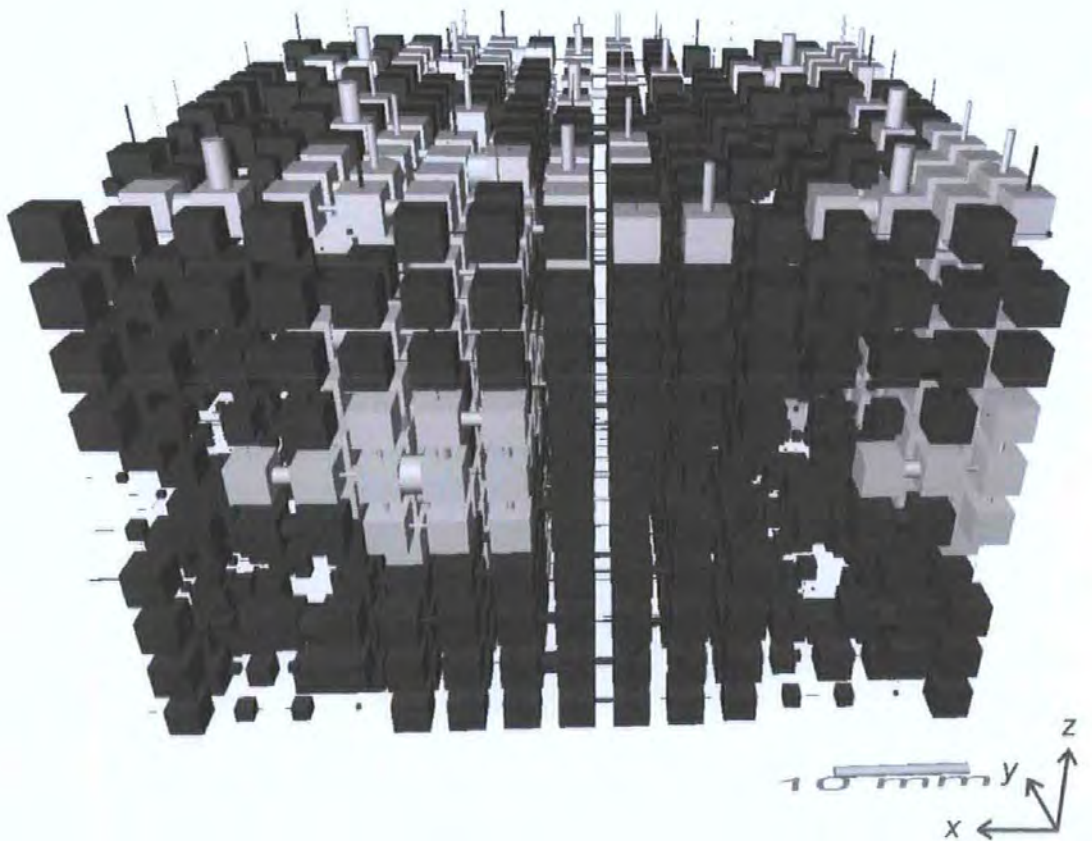
Figure 4.13. Void network model for soil structured by grass, showing air (light grey) displacing water (dark grey).

155

4.5. Conclusions

Water retention measurements highlighted differences in soil structure between the treatments, and suggested that white clover will hold less water at specific tensions and therefore has a greater number of larger pores than the grass and unplanted re-packed soil. This is in accordance with the findings of Chapter Three, which suggested enhanced soil structure beneath white clover.

This research demonstrated that very subtle differences in water release due to differences in pore size between the same soil structured by the roots of clover and of grass could be determined by the water retention curves, and can be simulated with a void space network model.

However, the exercise proved equally much a lesson in the need for better experimental data and protocol. Currently, the standard protocol (ISO 11274:1998) does not yield enough data for a model which takes the entire water retention curve shape into account, without any pre-supposition as to the mathematical analytical form of the water retention curve.

CHAPTER FIVE

5. Nutrient and tracer transport

5.1. Overview of chapter and objectives

This chapter presents methods and results of nutrient leaching and tracer transport studies on both re-packed soil cores and intact soil monoliths, by both manual and automated procedures and effective one- and two-dimensional flow.

The objectives were:

1. to develop suitable experimental protocols for the simulation and collection of nutrient and tracer transport studies.

2. to perform suitable analytical techniques to analyse aqueous leachate samples for the determination of nitrate, phosphate and bromide transport.

3. to assess the impact of enhanced structuring in soils beneath white clover on nutrient leaching (nitrate and phosphate), relative to a grass, unplanted control and a mixture of the two species as found in a typical pasture.

4. to compare the transport of nitrate and phosphate to the conservative tracer bromide.

5. to ascertain whether the impacts of enhanced soil structuring and the transport of nutrients were manifested at the scale of the whole soil profile, rather than simply within the rhizosphere.

6. to conduct leaching experiments at two scales (re-packed soil core and intact monolith).

7. to conduct experiments to reveal information about the effect of site of the pulse prior to leaching.

5.2. Experimental design and scales

Instrumented soil cores and blocks have been widely used to characterise preferential water and solute movement through soils (Lewis, 1990; Isensee, 1992; Schoen, 1999; Tindall, 1992). A rainfall simulator was used for measuring 2-dimensional flow through a half-metre soil block. Pot-scale experiments were performed using soil cores, measuring

vertical flow and not the lateral movement. For a discussion on water and solute transport in soil, see Chapter One (Section 1.6.6).

5.3. Nutrient and tracer solutions

The nutrient solutions applied were nitrate and phosphate; these species were chosen for their contrasting behaviour in the soil matrix and for their agricultural importance. A bromide tracer was also applied. The bromide anion (Br⁻), though observed to have some anionic repulsion, has been used successfully as a tracer of water and nitrate movement in soil (Stutter *et al.*, 2003). Bromide behaves similarly to nitrate in soils and was preferred over the use of chloride as a tracer; the use of 15N was not feasible due to the analysis time of the large number of leachates generated. Bromide and nitrate are non-reactive, conservative tracers due to their low level of interaction with the soil mineralogy (Ammann *et al.*, 2003). Phosphate is a reactive, non-conservative tracer, due to its tendency to bind and interact with the soil components particularly by adsorption onto clay particles. In addition, the three nutrients/tracers used in this study were selected because they have low toxicity, the potential for their decay is small, they have high water solubility and they are relatively easy to measure. For further reference to tracer studies, see Chapter One (Section 1.6.7).

5.4. Column Experiment 1 – Nitrate transport

Seven nitrate leaching experiments were conducted on samples from Column Experiment 1 and are referred to as Leaching Experiments (#1-7). Figure 5.1 gives a representation of the experimental design of *all* column experiments; in each instance the soil core was levelled. For Leaching Experiments (#1-7), the initial and boundary conditions were different (i.e. treatment, flow rate, initial water content, pulse application, duration). The conditions of each experiment are given where results are reported.

158

Potassium nitrate was always used as the source of nitrate. Rainfall was simulated with ultra pure water, deionised water and tap water to assess the effect of the water's ionic strength. The ionic strength was also increased by adding gypsum (calcium sulfate $CaSO_4$); this was done to see if coagulation of clay particles was responsible for reduced infiltration and ponding of water observed on the soil surface.
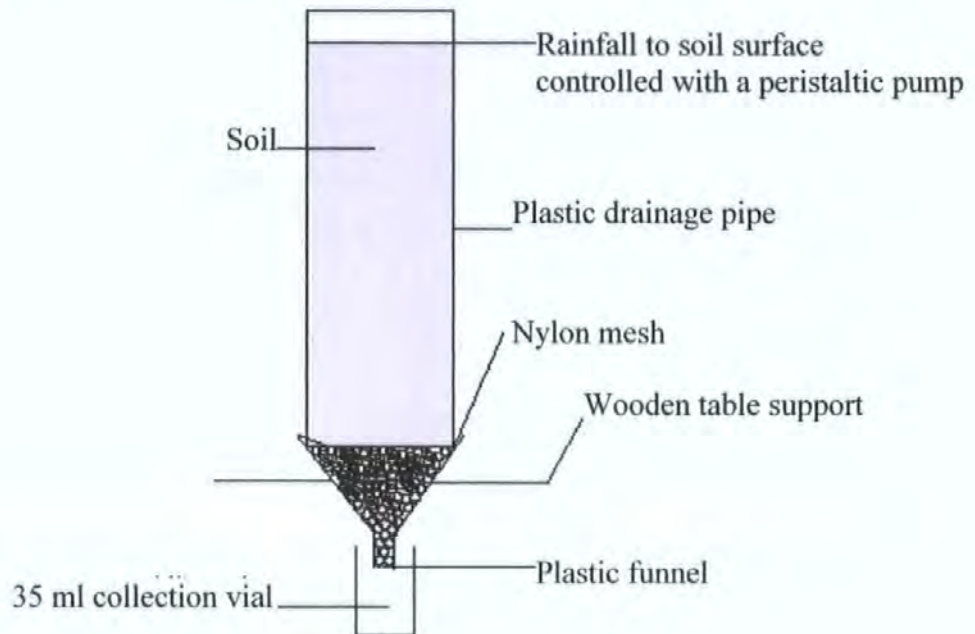
Figure 5.1. Diagrammatic representation of column lysimeter design.

5.5. Column Experiment 2 – Nitrate, phosphate and bromide transport

For Leaching Experiments (#8-11), the initial and boundary conditions were different (i.e. treatment, flow rate, initial water content, pulse application, duration). The conditions of each experiment are given where result are reported. For the main study of Column Experiment 2 (#12-14), rainfall was simulated using deionised water supplied via a multi-channel peristaltic pump at a constant rate of 0.33 ml min^{-1}, which is equivalent to a typical light rainfall rate in the UK of 2.4 mm h^{-1}. The infiltrating solution was delivered to the soil surface (Figure 5.2) in fine droplets via a circular array of 10 evenly spaced 25G

syringe needles (I.D. 0.318 mm, Richards, Leicester, UK) (which can be seen in Figure 5.4), thus ensuring even distribution and minimizing the kinetic energy of water dropping on the soil of the pots. The leachates passed through a funnel and into a collection vial for analysis. Collection vials were changed at hourly intervals for 48 h. Grass and unplanted treatments were prone to ponding, when this occurred, the supply of simulated rainfall was temporary stopped to avoid a large head of water accumulating on the soil surface.
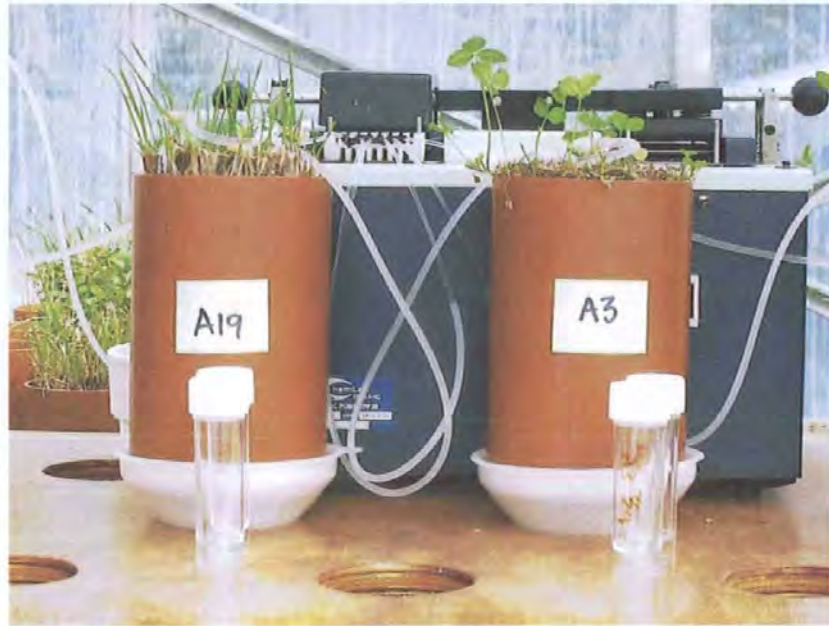
Figure 5.2. Peristaltic pump used to simulate constant rainfall at 0.33 mm min^{-1} to the surface of the soil cores. Leachates passed through a funnel and were collected in sample vials for analysis.

5.5.1. Experimental protocol

All samples were stood in 5 cm of water for 24 h and allowed to drain for 24 h, so that the samples were equilibrated and the initial starting conditions were near field capacity. The biomass was cut to a 50 mm height above the base of the plant. Three different experimental protocols were then used for the application of the tracer solution (Table 5.1 and Table 5.2). Firstly, (Type A) rainfall was simulated for 24 h to allow two pore volumes of water to percolate through the soil, so that saturation of the samples and steady state flow conditions was achieved before the application of the mixed tracer solution via the

peristaltic pump for 100 minutes (Table 5.2). Secondly, (Type B) a 6 ml aliquot of the

mixed tracer solution was applied to the samples at near field capacity and was allowed to

diffuse into the soils for 48 h before rainfall was simulated. Finally, (Type C) a single 6 ml

aliquot of the mixed tracer solution was applied to the samples under steady state flow

conditions. The aim was to investigate the effect of the site of the tracer prior to leaching

and to simulate different field scenarios (Table 5.1).

Table 5.1. Experimental protocol for the application of tracer solution and conditions simulated.

	Type A	Type B	Type C
Method of application:	Tracer applied via pump at rate of rainfall for 100 minutes.	Tracer applied as single aliquot and allowed to diffuse into soil prior to rainfall.	Tracer applied as single aliquot during steady state flow.
Simulated conditions:	Classical approach to demonstrate transport of pulse with incoming water.	Field scenario of homogeneous distributed N in soil after summer and prior to autumn rainfall.	Field scenario of a fertiliser application followed by heavy rainfall.

The concentrations and rainfall rates (Table 5.2) were selected to mimic realistic field

conditions in terms of natural rainfall and average fertiliser application rates. The

simulated rainfall rate (mm hour^{-1}) and equivalent fertiliser rate (kg ha^{-1}) were the same for

the column experiments and the monoliths (Table 5.2).

For the Type A experiment, approximately 2560 samples were generated in four

experiments over a two-month period (i.e. 40 hourly collections x 16 treatments (5 soils vs.

3 plants + 1 plant) x 4 replicates). Not all treatments and replicates could be run in one

single experiment. To eliminate differences a factorial design was selected, in which one

replicate of each treatment was included in each experiment. Samples were immediately

weighed after collection to determine drainage rate and subsequently analysed. For the

Type B experiment, approximately 640 samples were collected from four experiments over one month (i.e. 40 hourly collections x 4 treatments (1 soil vs. 4 plants) x 4 replicates). In the Type C experiment, 640 samples were collected (i.e. 40 hourly collections x 4 treatments (1 soil vs. 4 plants) x 4 replicates) over three days.

Table 5.2. Details of soil core leaching experiments in comparison with soil monolith lysimeter conditions.

Parameter	Units	Species	Column (Type A)	Column (Type B and C)	Monoliths
Volume of pulse	ml		35	6	995
Input time (Rainfall and Pulse)	ml		106	106 *	90
Input rate (Rainfall and Pulse)	ml min^{-1}		0.3	0.3 *	11
Input rate (Rainfall and Pulse)	mm hour^{-1}		2.4	2.4 *	2.4
Surface area	cm^2		83	83	2704
N stock solution	g L^{-1}	KNO$_3$	1.8	11	2.2
Br stock solution	g L^{-1}	KBr	0.1	0.4	0.1
P stock solution	g L^{-1}	KH$_2$PO$_4$	0.2	1.1	0.2
N tracer concentration	mg L^{-1}	NO$_3$-N	250	1500	300
Br tracer concentration	mg L^{-1}	Br	40	240	47
P tracer concentration	mg L^{-1}	PO$_4$-P	40	240	47
N tracer amount	mg	NO$_3$-N	8.7	9.0	298
Br tracer amount	mg	Br	1.4	1.4	47
P tracer amount	mg	PO$_4$-P	1.4	1.4	47
N application rate	Kg ha^{-1}	N	11	11	11
Br application rate	Kg ha^{-1}	Br	1.7	1.7	1.7
P application rate	Kg ha^{-1}	P	1.7	1.7	1.7

* Rainfall rate only (pulse as single aliquot)

5.6. Half-meter lysimeter

5.6.1. Experimental protocol

An apparatus was used for measuring high-resolution 2-dimensional flow through a half-metre soil block (Johnson *et al.*, 2003b). Previous experiments using soil cores, measured

vertical flow but not lateral movement. The half-metre cube allowed suitable lateral migration, and the scale is applicable for studying upscaling properties for pollutant transport.

Rainfall was simulated to the soil surface using a peristaltic pump, leachates were collected at the base of the soil block using a precision-machined collection plate. The automated, precision lysimeter provided a superior temporal and spatial analysis of leachates from the intact soil blocks under controlled laboratory conditions. Time domain reflectometry probes (TDR) were used for non-destructive in-situ measurement of volumetric water content (Section 5.6.5).

As described by Johnson *et al.* (2003b), the lysimeter was constructed of three towers of square section steel tubing; the soil block is located in the centre of the central tower with the rainfall simulator directly above and collection palettes below (Figure 5.3). Sample palettes, which contained empty sample vials, were positioned in the left tower, and those containing soil leachates were stored in the right tower. Automation was achieved using a series of computer controlled motors and drive chains.
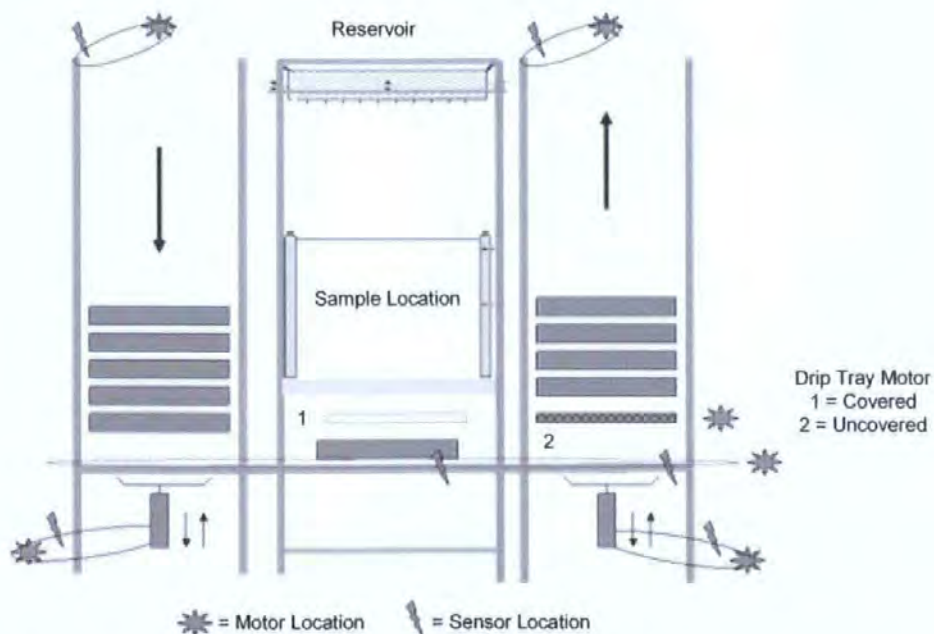
Figure 5.3. Schematic diagram of automated lysimeter (Johnson *et al.*, 2003b).

5.6.2. Rainfall simulation

Rainfall was simulated above the soil surface using a twenty channel peristaltic pump (rather than the fitted rainfall simulator (Appendix II)). Each outlet tube was attached to a network of ten needles, so that fine droplets of water were evenly dispersed over the soil surface (Figure 5.4) at a rate of 11.0 ml min^{-1} or 2.4 mm h^{-1}. This was the same rate as that applied to cores in Column Experiment 2. The volume, rates, and concentrations applied are listed in Table 5.2. As mentioned (Section 5.5), the rainfall rate and field fertiliser rate were up-scaled and set the conditions for the monolith lysimeter studies.

Figure 5.4. Simulation of rainfall and application of tracer solution to the surface of the soil block using a peristaltic pump attached to tubing and an array of 10 needles for fine delivery.

5.6.3. Eluent Collection

The soil blocks were mounted above a collection plate that was precision-machined from anodised aluminium by Computer Numerate Control. 100 square funnels (38 mm x 38 mm) were machined in a 10 x 10 array, separated by well-defined boundaries (Figure 5.5). This gave an active sample collection central zone of 380 mm x 380 mm. Around each edge was an isolated drainage channel (63 mm wide) to prevent sample bias from edge effects (Johnson *et al.*, 2003). Solution entering these four drainage channels was removed as waste and collectively analysed.

The soil leachates passed through the collection plate into cylindrical glass vials (35 ml volume, 70 mm height x 25 mm diameter) (BDH Chemicals, UK). The centre of each vial was aligned with a funnel that protruded from the base of the collection plate. Each square funnel was filled with glass wool to prevent movement of soil particles into the vials. The vials were housed in a precision-machined sample collection palette, made from a stout PVC tray. The surface of each collection palette was drilled with a 10 x 10 grid of holes. Attached to the corners of the palette was machined plate steel to grip to the drive chains. Figure 5.6 shows a sample collection palette aligned beneath the sample collection plate. Located between the collection palette and collection plate was a movable drip tray, which was used to prevent cross contamination of samples by automatically separating the funnels and vials during palette changeover. Figure 5.3 shows the two positions of the drip tray (1) covering and (2) uncovering the collection palette.
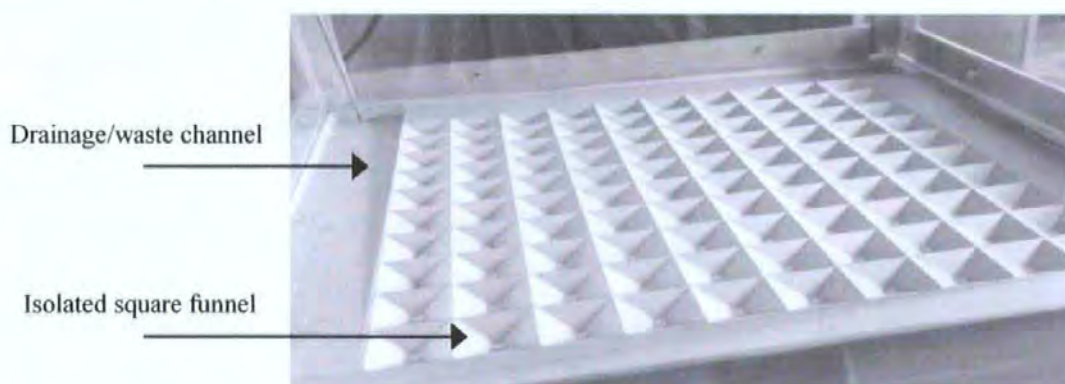
Figure 5.5. Top view of the precision-machined sample collection plate located at the base of the soil block, showing the 100 isolated square funnels and surrounding waste channels.

Figure 5.6. Precision-machined collection palette aligned with the sample collection plate.

5.6.4. Automation of the lysimeter

Automated sample collection was achieved using 6 electric motors (220V DC and 24V AC, Parvalux, Brighton, UK) which controlled a series of chain belts into which the collection palettes were mounted. Figure 5.3 illustrates the location of the motors and the arrows indicate the movement path of the collection palettes. The empty palettes underwent a downward movement from the left tower, lateral movement under the collection plate in the central tower, and after a set time (usually 4 hours) the lateral and upward movement of the samples and palettes to the right storage tower. Precise positioning of the palettes was achieved using six infrared sensors (Figure 5.7).
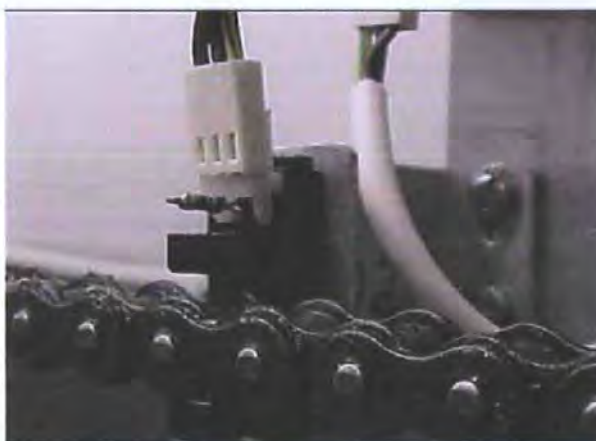
Figure 5.7. Example of one of the six infrared sensors, which precisely controlled the positioning of the collection palettes.

The high voltage circuitry that allows computer control of the apparatus is given schematic and pictorially in Appendix II. Signals that control the sensors and motors' activation or deactivation are processed by a digital input / output card *DIO24 TTL* (National Instruments, UK). The signals feed to specifically written virtual console software *LabVIEW*^{TM} (National Instruments, UK). The software is used to manually or automatically control the moving parts of the lysimeter. An important safety feature is that the computer interface is booted up before power is supplied to the lysimeter, and that an emergency stop button is fitted.

5.6.5. Time Domain Reflectometry

Determination of soil moisture content is crucial in any solute transport study. Time Domain Reflectometry (TDR) was used for non-destructive in-situ measurement of volumetric water content. TDR was originally proposed by Davis and Chudobiak, (1975) and has become a popular and recognised method of measuring the water content of soil (Davis and Annan, 1977; Topp *et al.*, 1980).

The principle of TDR is based on the measurement of a high frequency electromagnetic pulse as a guided wave along a transmission line. Part of the pulse is reflected back through the soil and the time interval between the incident and reflected pulses is measured (Smith and Mullins, 1991). A comprehensive review of its development is given by (Gardner *et al.*, 1991). The pulse velocity is used to calculate the dielectric constant of soil, which is dominated by the contribution from soil water (Johnson, 2004). Free water has a dielectric constant about 20 times greater than that of mineral matter, and so the effect of the mineral matter on the pulse velocity is small (Whalley, 1993). Topp *et al.* (1980) determined a third order polynomial relationship between dielectric constant, ε_c, and volumetric water content θ, for which they gave an error estimate of 0.013 for θ (Equation 5.1).

$$\theta = - 5.3 \times 10^{-2} + 2.92 \times 10^{-2}\varepsilon_c - 5.5 \times 10^{-4}\varepsilon_c^{2} + 4.3 \times 10^{-6}\varepsilon_c^{3}$$

Equation 5.1.

TDR tridents i.e. three stainless steel welding rods spaced 20 mm apart (300 mm long and 3 mm diameter) (Rightons, Plymouth, Devon, UK) were inserted at depths shown schematically in Figure 5.8 and pictorially in Figure 5.9. The TDR probes were connected to a Tektronix 1502C cable tester and a reading was recorded for each TDR probe at the time of eluent collection.

167
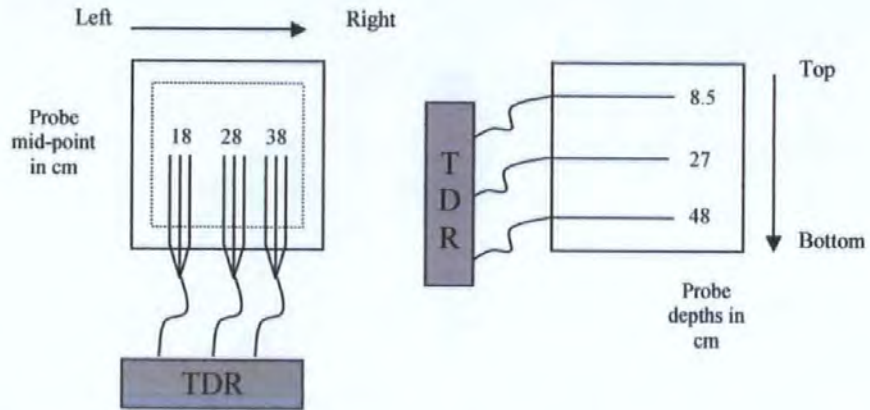
Figure 5.8. Location of the three TDR tridents in each soil block used to monitor moisture content.

Figure 5.9. A mounted sample with three-inserted TDR trident probes as shown schematically in Figure 5.8.

5.6.6. Experimental protocol

5.6.6.1. Pre-treatment

The extraction of the half-meter soil blocks is described in Chapter Two (Section 2.4.2). The soil blocks were mounted onto the collection plate using a hydraulic jack. The biomass was cut to 50 mm above the base of the plant. Soil blocks were equilibrated so that the initial water content was near field capacity by simulating rainfall was for 2-4 days. Rainfall (and solute application) was continuous throughout the duration of the experiment at a rate of 11.0 ml min^{-1} or 2.4 mm h^{-1} equivalent. The TDR probes revealed when a

consistent saturation level had been reached so that steady state flow conditions were achieved before the application of the mixed nutrient and tracer solution.

5.6.6.2. Water velocity and volume

The drainage water velocity and volume was determined by collecting soil leachate every 4 h using the automated sample collection procedure described above (Section 5.6.4). All vials were weighed at room temperature before and immediately after sample collection to determine the drainage rate. In the case of white clover, enhanced flow was observed; therefore, leachates from some channels were collected in 2 L bottles via plastic tubing attached to funnels at the base of the collection plate. Solution entering the four drainage channels was collected in separate 2 L plastic bottles, sub-samples were transferred to glass vials for storage before analysis. The leachates were subsequently analysed for bromide, nitrite/nitrate and orthophosphate.

5.6.6.3. Nutrient and tracer transport

A mixed nutrient and tracer solution containing bromide, nitrate and phosphate was prepared (Table 5.2). The nutrients and tracer were applied in 995 ml of deionised water delivered to the soil surface via the peristaltic pump for 90 mins. To obtain elution profiles and breakthrough curves, the leachates were subsequently analysed for bromide, nitrite/nitrate and orthophosphate using an air segmented flow analyser (Skalar SAN$^{Plus®}$, Skalar Analytical B.V., Breda, Netherlands), as detailed in Section 5.8.

5.7. Analytical instrumentation for nutrient/tracers studies

Ion chromatography was attempted as an alternative to segmented flow analysis for the determination of bromide, nitrate and phosphate in soil leachates. Instrumentation was a Dionex system (Dionex UK, Surrey, UK). The Instrument details are not discussed further

as the results are not reported (although comparable with segmented flow analysis). This analytical method was time-consuming, with analysis times as high as 45 min per sample, and not suitable for the large number of samples generated during leaching and transport experiments. Other applicable techniques are described in Chapter One (Section 1.7.11).

5.8. Segmented flow analysis

5.8.1. Theory of segmented flow analysis

Segmented flow analysis (SFA) was used for simultaneous detection of bromide, nitrate and phosphate in soil leachates generated during leaching and transport experiments. Also referred to as air segmented continuous flow analysis (ASCFA), this technique been used for a wide range of applications (Gardolinski *et al.*, 2001; Estela and Cerdà, 2005). Segmented flow analysis is a continuous flow technique of wet chemistry, in which a fluid stream of analytes and reagents are segmented with air bubbles are pumped through a manifold and towards a spectrophotometric detector recording absorbency at a given wavelength. A simplified schematic illustration of segmented flow analysis is given in Figure 5.10.
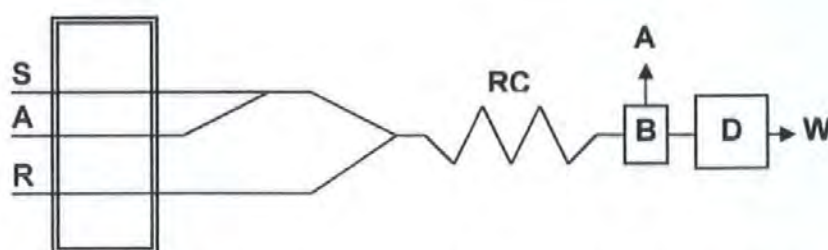
Figure 5.10. Simplified schematic illustration of segmented flow analysis (SFA). S, sample; A, air; R, reagent; PP, peristaltic pump; RC, reaction coil; B, debubbler; D, detector; W, waste.

5.8.2. Skalar SAN^Plus® analyzers and samples analyzed

Two segmented flow analysers were used; both were Skalar SAN$^{Plus®}$ (Skalar Analytical B.V., Breda, Netherlands). Both instruments are fundamentally the same and consist of an

autosampler, a chemistry unit, a water circulation bath, a matrix photometer and a digital interface, which transfers data to a computer (Figure 5.11). The difference between the two Skalar SAN^{Plus} systems lies with the autosampler, the chemistry unit and the analytes determined. The methods are interchangeable between instruments, providing the correct components and manifolds are available for the chemistry unit.
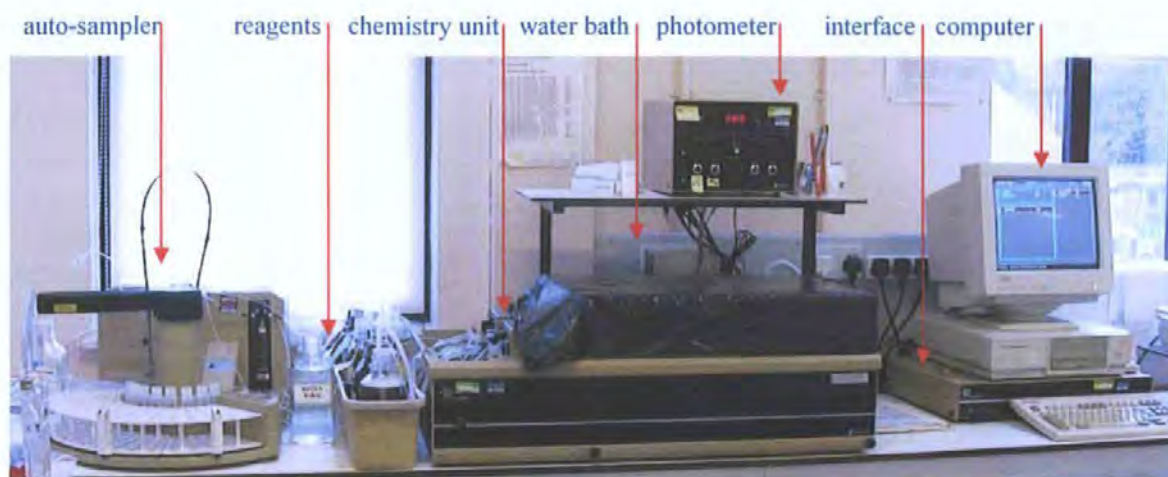
Figure 5.11. IGER's Skalar SAN^{Plus} segmented flow analyser showing the sub-units: autosampler (SA 1050d), chemistry unit (SA 4000), water circulation bath, reference photometer (SA 6250), digital interface (SA 8502), computer and printer.

Soil leachates collected from Column Experiment 1 were determined at IGER using a Skalar SAN^{Plus} analyser configured for two ranges of ammonium and one range of nitrate. Samples collected from Column Experiment 2 and the block lysimeter were analysed at the University of Plymouth using a Skalar SAN^{Plus} analyser configured for two ranges of both bromide and nitrite/nitrate and one range of orthophosphate. The analytical range and limit of detection for each analyte on both Skalar SAN^{Plus} systems is given in Table 5.4.

The autosampler (SA 1050d) at IGER was fitted with an automatic dilution chamber, which is not present on the autosampler at the University of Plymouth. The manifold for nitrate analysis at IGER is shown in Figure 5.12 compared to Figure 5.13 used for nitrite/nitrate at the University of Plymouth. The manifolds were different due to the chemistry used prior to detection (Section 5.8.9).

The automated lysimeter sample collection and automated segmented flow analysis provided a large data set of soil leachate concentrations and water velocity. The lysimeter experiments generated 2500 samples and Column Experiment 2 (Type A-C) generated approximately 3840 samples. Therefore, the rapidity and robustness of the analytical technique was paramount. The segmented flow analyser was regularly calibrated and high quality control was maintained (Section 5.8.7). The automated data processing allowed the data to be rapidly processed with confidence.

Figure 5.12. Skalar SANS^{PLUS} chemistry unit. The manifold used for nitrate segmented flow analysis at IGER is below the red line.
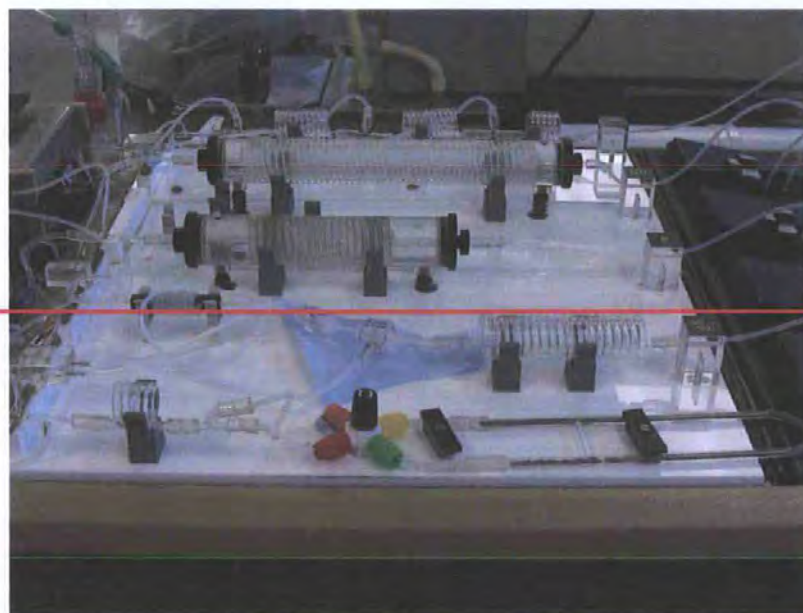
Figure 5.13. Skalar SANS^{PLUS} chemistry unit. The manifold used for nitrite/nitrate segmented flow analysis at the University of Plymouth is below the red line. The cadmium reduction column is shown on the bottom right.

5.8.3. Skalar SAN$^{Plus®}$ analyzer – instrument details

Automated data acquisition and control of the Skalar SAN^{Plus} system is achieved using the Skalar *FlowAccess*® software and the SA 8502 digital interface. The interface is connected to the sampler, analogue detectors and a computer. Messages sent from the *FlowAccess*® software on the computer are transferred to the sampler and detectors. In return, signals from sampler and detectors are transferred to the computer software.

The SA 1050 random access autosampler has a capacity of 140 samples (3.5 or 10 ml), 11 positions for calibration and control standards and 9 positions for working standards. The sample needle is returned to a rinsing vessel washed by a rinsing pump after each sample injection. Samples are pumped from the autosampler to the chemistry unit (SA 4000).

The chemistry unit consists of two 16-channel peristaltic pumps (to draw, proportion and propel the fluid stream), an air bubble injector and compressor (to segment the fluid stream with air bubbles), four independent chemistry manifolds (containing the components for the required reactions and colour development), inline heaters, waste receptacles and optical detection heads (flow-cells with single-channel beam colorimetric detectors).

The SA 6250 photometer is a detector that allows for optical matrix correction and consists of an optical detection section and a separate electronics section. The optical detection section for each manifold contains a lamp that emits light on to a focusing lens and passes a flow-cell where part of the light is absorbed. A mirror divides the light beam in two portions, the transmitted light passes an interference filter at two different wavelengths and a photocell. The signals produced by the photocell are sent to the electronics section. The detector is given schematically and pictorially in Appendix II.

The electronics section of the photometer treats signals according to the principle of colorimetry in which the transmission of sample colour is measured relative to absorption of light according to Beer-Lambert law, where the absorbance is proportional to the concentration of analyte and the path length of the light in the sample (Equation 5.2). (Li *et al.*, 2005, Zhang, 2000).

$$A = \alpha \, \ell \, c$$

<div align="right">**Equation 5.2.**</div>

where A = absorbance, α = absorption coefficient, ℓ = path length and c = concentration of absorbing species.

The selected colour wavelength at the maximum absorbance is used to measure the analyte and the wavelength at the minimum absorbance is used as the correction wavelength (Figure 5.14). Both signals are compared and subtracted from each other for optical matrix correction to eliminate the refractive index effect of other ions or molecules that absorb light while passing through the flow-cell, thus greatly increasing the accuracy and reliability of results.
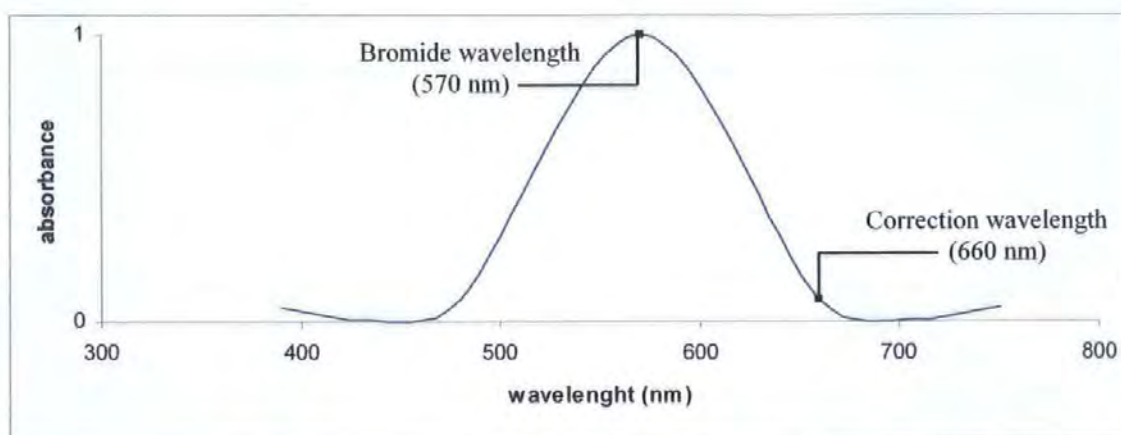
Figure 5.14. Optical matrix correction automatically compensates for the effect of the refractive index by subtracting the absorbance at a correction wavelength from the absorbance at the analyte wavelength.

The SA 8502 digital interface transferred analogue data from the detectors to the data handling *FlowAccess*® software. The software displays real time analysis peaks and allows baseline and sensitivity drift correction by analysing a known standard after every 10 samples. *FlowAccess*® also contains two other programs *QAccess*® for quality control and *FlowReport*® for extended reports.

Soil leachates were analysed simultaneously for bromide, nitrite/nitrate and orthophosphate by splitting the sample stream from the autosampler into the three separate manifolds on the chemistry unit. The instrument settings are given in Table 5.3. The analytical methods and chemical reactions of each analyte are given in Sections 5.8.8 to 5.8.11.

In addition to the hardware specified above, the bromide channel is fitted with SA 5521 reactor connected to a control unit used for high accuracy temperature regulation. The reactions for bromide and orthophosphate are temperature-controlled using a water bath and circulator. The bromide chemistry includes dialysis and nitrite/nitrate involves ion reduction through activated cadmium.

Table 5.3. Instrument settings for the Skalar SAN^{Plus} segmented flow analyser for the detection of bromide, nitrite/nitrate and orthophosphate.

Instrument specification	Setting		
Lamp	10 W Halogen		
Sample injection time	60 s		
Wash time	120 s		
Air injection	30 bubbles per min		
Sample through-put	20 samples per h		
Instrument specification	**Bromide**	**Nitrite/nitrate**	**Orthophosphate**
Absorbance at correction wavelength (nm)	660	620	1010
Absorbance at analyte wavelength (nm)	570	540	880
Flow-cell optical path length (mm)	10	10	50
Retention time in manifold (min)	1281	387	333

5.8.4. Analytical range and limit of detection

The analytical range and limit of detection for each analyte on both Skalar SAN^{Plus} systems is given in Table 5.4. The analytical range is based on a linear relationship between absorbance and concentration. Above the upper limit of the linear range, the absorbance was lower than predicted from the linear relationship. The limit of detection (LOD) is the lowest concentration of the target analyte that can be detected. LOD is calculated as the analyte concentration giving a signal equal to the blank plus three standard deviations of the slope (Miller and Miller, 1992).

Table 5.4. Analytical range for the determination of bromide, nitrate, orthophosphate and ammonium using Skalar SAN^{Plus} at the University of Plymouth (UoP) and IGER.

Analyte	Linear range	Limit of detection	Skalar SAN^{Plus} analyser
Bromide	1 – 50 mg L^{-1}	0.5 mg L^{-1}	UoP
Bromide	1 – 10 mg L^{-1}	0.3 mg L^{-1}	UoP
Orthophosphate	2 – 200 µg L^{-1}	2.0 µg L^{-1}	UoP
Nitrite/Nitrate	0.1 – 5 mg L^{-1}	0.3 mg L^{-1}	UoP
Nitrite/Nitrate	2 – 100 µg L^{-1}	2.5 µg L^{-1}	UoP
Nitrate	0.1 – 5 mg L^{-1}		IGER
Ammonium	0.1 – 5 mg L^{-1}		IGER
Ammonium	2 – 100 µg L^{-1}		IGER

5.8.5. Calibration and data acquisition

Concentrations of the analytes in the samples were automatically calculated from the linear regression, obtained from the standard curve in which the concentrations of known calibration standards are entered as the independent variable, and their corresponding peak heights are the dependent variable. The collection and analysis of data was simultaneously controlled using *FlowAccess*® software (an example is given in Appendix II).

5.8.6. Dilution procedures

For nitrite/nitrate and bromide, two analytical ranges were used. Some nitrite/nitrate and orthophosphate samples were diluted into range. This was achieved by pipetting aliquots of sample into 3.5 ml or 21 ml vials and diluting with ultra-pure water. The vials were capped and the contents mixed by inversion. Known standards were also diluted to ensure quality control.

5.8.7. Instrument performance, quality control and maintenance

The high precision in segmented flow analysis is attributed to air segmentation. However, segmentation bubbles are often the source of error (Zhang, 1997). A super-clean flow system was essential in establishing a regular bubble pattern and minimizing bubble breaking. The Brij-35 and FFD6 detergents used in reagents is effective for keeping low surface tension between quartz and sample mixture (Zhang, 2000), and therefore a smooth flow was achieved with low baseline noise was achieved.

A sample time of 60 s was found to be sufficient for reaching a maximum absorbance output and providing regular and symmetrical sample peaks. A wash time of 120 s eliminated 'carry-over' of the sample. This was regularly checked by analysing a high standard followed by two blanks as suggested by Zhang (1997).

High precision and accuracy was maintained by regular analysis of known standards, which were monitored using the QAccess® software for quality control. Within-run and between-run calibrations and quality control samples were monitored. A known standard was analysed after every 10 samples and the FlowAccess® software corrected for a drift in the baseline and sensitivity. The chemical integrity of the samples was assessed by regular analysis of known standards prepared at the time of sample collection.

After each set of analyses, the system was rinsed for at least 30 mins with ultra-pure water, and 0.5 M sodium hydroxide solution or 0.5 M HCl after prolonged use. The duration of each set of analyses was up to 36 h. Increasing the sample time (and sample concentration) might cause a build up of the analytes in the system. Such an error would cause a drift in the baseline, but was overcome by analysing a known standard after every 10 samples and automatic *FlowAccess*® baseline drift correction.

The shadow or coating effect is a well-known drawback of the molybdenum blue method for phosphate analysis (Zhang *et al.*, 1999). A blue complex coating is formed in the flow-cell and tubing from a colloidal product that is readily adsorbed onto the solid surfaces. The degree of coating was readily apparent in the shape of the sample peak; coating caused the distortion of peaks to asymmetric with excessive tailing at the end, but the peaks were symmetrical when there was no carryover. This coating effect was also monitored by running a high standard followed by two low standards, and by repeated sample-wash cycles.

The sensitivity of system to ambient temperature and reagent degradation was readily apparent from the baseline and photometer absorbance readings. Reagents were appropriately stored and equilibrated to room temperature before use to prevent changes in the baseline. The pump tube was replaced at least once a month and the pump deck greased as required to ensure the correct flow rate and prevent imbalanced reactions.

The bromide dialyser membrane was subject to a build up of colloidal material on the surface, which affected the baseline. This was prevented by rinsing or replacing the membrane. The efficiency of the nitrate reduction copperised-cadmium column was checked periodically by analyzing a nitrate standard and a nitrite solution of the same N concentration.

5.8.8. Determination of Bromide using segmented flow analysis

5.8.8.1. Theory

The automated procedure for the determination of bromide is based on the oxidation of bromide to bromate, reduction to bromine and the formation of tetrabromorosaniline. The method was introduced by Hunter & Goldspink (1956), and is not subject to interferences from other halides.

The sample is acidified with hydrochloric acid solution to produce Br^- anions and dialysed against a sodium orthophosphate solution buffer solution (pH 6.3) to remove interfering colloids in the sample. Br^- anions were diffused through a semi-permeable membrane (<2 μm) into the buffer stream. A hypochlorite solution was added as a chlorine donor and heated to 90°C to liberate the chlorine, which is a powerful oxidising agent that reacted with bromide to form bromate (Equation 5.3). A sodium formate solution was added to remove the excess chloride ions, and cooled to 60°C.

$$Br^- + 3ClO^- \longrightarrow BrO_3^- + 3Cl^-$$

bromide $\qquad\qquad\qquad$ bromate
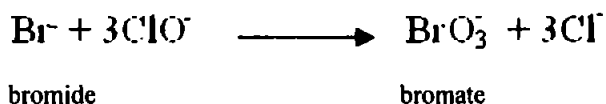
Equation 5.3.

After re-sampling, the colour reagent fuchsin (acidified rosaniline), propan-2-ol and H_2SO_4 were added. In this strong acidic alcoholic medium, the reduced bromine Equation 5.4 combined with rosaniline to produce a red-purple coloured complex tetrabromorosaniline. The absorption is measured at 570 nm and is in relation to the concentration of the bromide.

$$BrO_3^- + 5Br^- + 6H^+ \longrightarrow 3Br_2 + 3H_2O$$

bromate $\quad$ bromide $\qquad\qquad\qquad$ bromine

Equation 5.4.

The reagents and chemicals required for the determination of nitrate, and the manifold configuration flow diagram are given in Appendix II.

5.8.9. Determination of nitrite/nitrate using segmented flow analysis

5.8.9.1. Theory

The automated determination of nitrite/nitrate is based on the popular technique using copper-cadmium to reduce the nitrate to nitrite. The nitrite (plus reduced nitrate) is determined by a diazotization reaction to form a pink-coloured azo dye. This is known as the Griess reaction (Bendschneider and Robinson, 1952; Wetzel and Likens, 1991; Moorcroft et al., 2001; Ferree and Shannon, 2001) and is subject to interferences from silica.

Samples were passed through a copper-coated cadmium reduction column. Nitrate was reduced to nitrite in imidazole ammonium chloride buffer solution (pH 8.2) (Equation 5.5). The total nitrite was diazotized with sulphanilamide to form a diazonium salt. Under acidic conditions, this diazo compound coupled with N-(1-naphthyl)ethylenediamine dihydrochloride to form a pink azo dye (Equation 5.6). The absorbance was measured at 540 nm to quantify the total concentration of nitrite/nitrate in the samples (the sum of the nitrite present in the original sample and the nitrite derived from the reduction of nitrate).

Nitrite concentrations can be determined separately using the same method without the cadmium reduction procedure. Nitrate concentrations are obtained by subtracting nitrite from the total nitrite. However, this procedure was not necessary, as samples tested negative for the presence of nitrite using a reflectometer and paper test strips (Scholefield and Titchen, 1995).

$$NO_3^- + Cd + 2H^+ \longrightarrow NO_2^- + Cd^{2+} + H_2O$$

nitrate $\qquad\qquad\qquad\qquad\qquad$ nitrite

Equation 5.5.

sulfanilamide　　　　　　　　　　　　diazonium salt　　　　　α-naphthylehylenediamine

azo dye
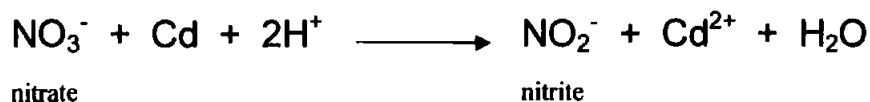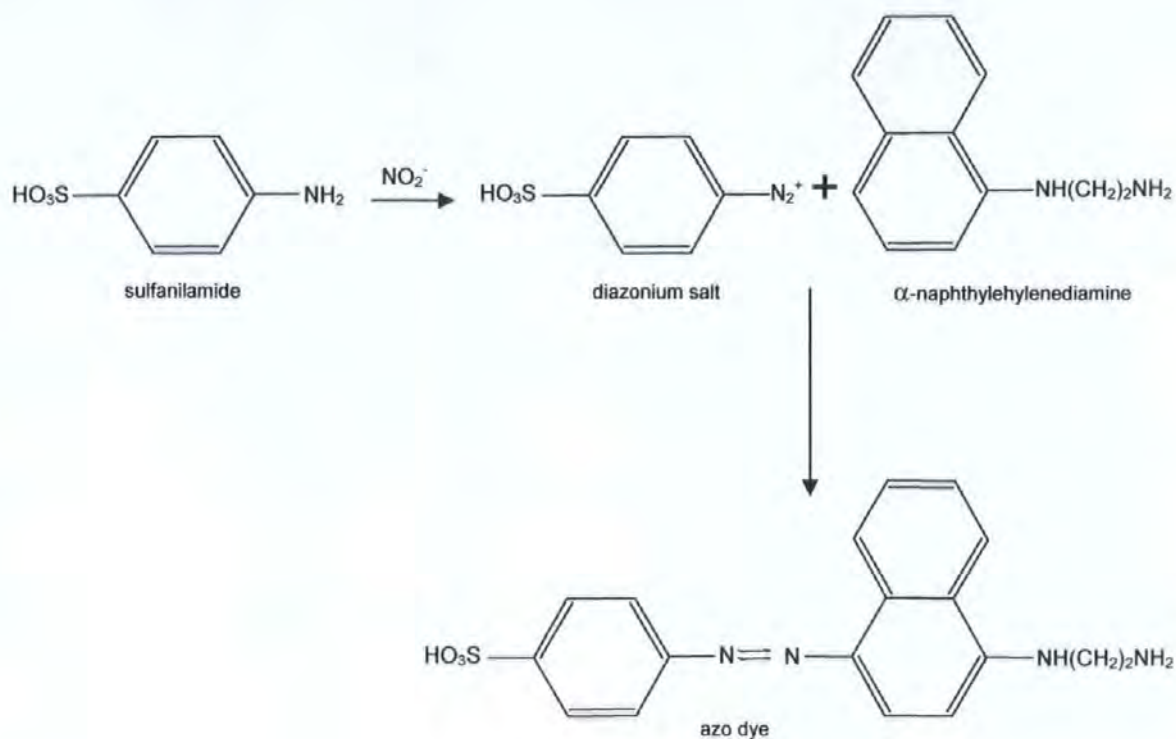
Equation 5.6.

The determination of nitrate using the Skalar SANS^{Plus} at IGER varied slightly to that described above used at the University of Plymouth. The difference lies in the manifold configuration and the absence of the cadmium column as nitrate was reduced to nitrite by hydrazine sulphate. The detection chemistry given in Equation 5.6 was then applied. In addition, sodium pyrophosphate was added to prevent interference from magnesium and calcium in soil extracts.

The reagents and chemicals required for the determination of bromide, and the manifold configuration flow diagram are given in Appendix II. Before connecting the cadmium column to the analytical manifold, a 5 mg L^{-1} N nitrite solution was pumped through the manifold and the absorbance signal was recorded. The column was then connected and a 5 mg L^{-1} N nitrate solution was pumped through the manifold. The absorbance increased with time and reached a steady state in 30 min. The reduction efficiency of the column was calculated from the ratio of the absorbance of the nitrate solution to that of the nitrite

solution of the same N concentration. The reduction efficiency of the cadmium column was checked periodically; a new column was attached if the efficiency was < 90 %.

5.8.10. Determination of Phosphate using segmented flow analysis

5.8.10.1. Theory

The automated procedure for the determination of phosphate is based on the phosphomolybdenum blue method (PMB), which lies in the reaction between orthophosphate ions with molybdate to form 12-molybdophosphoric heteropolyacid. The product is reduced by ascorbic acid in the presence of antimony tartrate serving as a catalyst. Detection is undertaken on the resulting phosphomolybdenum blue complex. The complex is very stable and obeys Beer's law up to a phosphate concentration of at least 2 mg L^{-1}. The technique is widely accepted as a routine methodology due to its high sensitivity and is an EPA certified method for phosphorus analysis in water (Method according to ISO/CD 15681). This method was originally presented by Murphy and Riley (1962), to which there are many modifications (Drummond and Maher, 1995; Zhang et al., 1997).

An acidified solution of ammonium molybdate and potassium antimony tartrate reacts rapidly with phosphate to yield an antimony-phospho-molybdate complex phosphomolybdate hetropolyacid (Equation 5.7). This heteropolyacid is reduced by ascorbic acid to phosphomolybdenum blue in a coil at 60 °C. (Equation 5.8) Ascorbic acid acts as a 2-electron reductant (Worsfold et al., 2005). Antimony as a catalyst increases the rate of reduction of the complex. The yielding intensely coloured blue-purple compound contains antimony and phosphorus in a 1:1 atomic ratio. The absorbance of the phosphomolybdenum blue complex was measured at 880 nm.

$$PO_4^{3-} + 12MoO_4^{2-} + 27H^+ \longrightarrow H_3PO_4(MoO_3)_{12} + 12H_2O$$

phosphomolybdate hetropolyacid

<div align="right">Equation 5.7.</div>

ascorbic acid

$$H_3PO_4(MoO_3)_{12} + 12H_2O \xrightarrow{C_6H_8O_6} \text{phosphomolybdenum blue} [Mo(VI) \rightarrow Mo(V)]$$
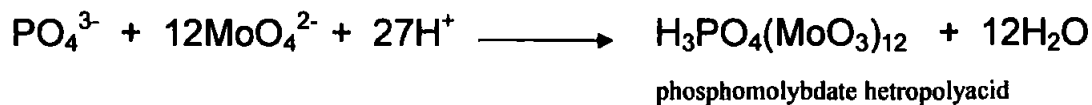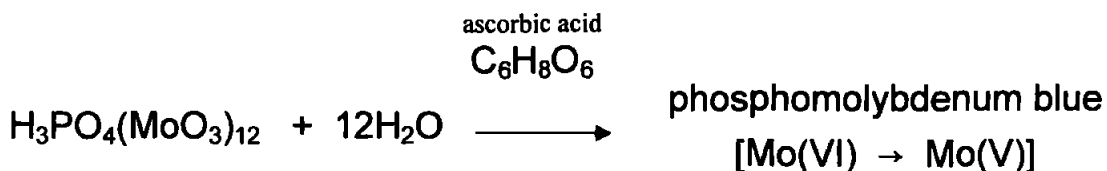
<div align="right">Equation 5.8.</div>

The reagents and chemicals required for the determination of phosphate, and the manifold configuration flow diagram are given in Appendix II.

5.8.11. Determination of Ammonium using segmented flow analysis

5.8.11.1. Theory

The automated procedure for the determination of ammonium is based on the modified Berthelot reaction. Ammonia is chlorinated with sodium dichlororisocyanurate to monochloramine, which reacts with salicylate to form the second intermediate, 5-aminosalicylate. Oxidation and oxidative coupling of 5-aminosalicylate with salicylate forms a green coloured indophenol dye. The absorption of the complex is measured at 660 nm. Nitroprusside stabilises the monochloramine intermediate and promotes the final oxidative coupling stage.

The reagents and chemicals required for the determination of ammonium, and the manifold configuration flow diagram are given in Appendix II.

5.9. Results - Column Experiment 1 – Leaching Experiments #1-7

The experiments were designed to assess the differences in nutrients leaching beneath ryegrass and white clover and to infer differences in soil structure. The amount of nitrate applied was not always realistic of agricultural systems.

The first protocol involved the application of inorganic N to the soil prior to leaching. It is hypothesised that nutrients that reside within inter-aggregate micropores will be relatively conserved by soil structural development. In the second approach, inorganic N is applied as a pulse in the irrigation water. It is hypothesised that the nutrients that enter the soil in incoming water will be leached more readily. In both instances, it is hypothesised that enhanced soil structure under white clover will give rise to preferential flow. A series of elution profiles and breakthrough curves were produced to give information on both levels of nutrient leaching and soil structure. These preliminary experiments led to improvements for subsequent studies.

5.9.1. Leaching Experiment 1

- Three replicates of two treatments (ryegrass and white clover grown in topsoil).
- A pulse of NO_3^- solution was applied to the soil surface (equivalent to 50 Kg N ha^{-1}).
- Rainfall was simulated at a rate of 0.6 ml min^{-1} for 3 hours.
- Drainage rate was highly variable.
- Results were rejected and method improved.

5.9.2. Leaching Experiment 2

- Three replicates of two treatments (ryegrass and white clover grown in topsoil).
- Soil was saturated and allowed to drain for 24 hours (i.e. field capacity).
- A pulse of NO_3^- solution was applied to the soil surface (equivalent to 5 kg N ha^{-1}) and left to diffuse into the aggregates for 48 hours.
- Using a peristaltic pump, rainfall was simulated at a rate of 0.6 ml min^{-1} for 3 days

Low nitrate-N concentrations were detected in the leachate (i.e. <1ppm). It is presumed that this mineral-N was taken up by plants and micro-organisms to satisfy their N needs in the low N system. The drainage rate was consistent within treatments; the mean drainage rate for the grass and clover treatments was 0.3 ml min^{-1} and 0.5 ml min^{-1} respectively.

5.9.3.   Leaching Experiment 3

- Three replicates of two treatments (ryegrass and white clover grown in topsoil).
- Soil was saturated and allowed to drain for 24 hours.
- A solution containing 90 mg N L^{-1} (400 mg NO$_3$ L^{-1}) was applied to the surface at a rate of 0.6 ml min^{-1} (equivalent to 4 mm h^{-1} i.e. enhanced rainfall and 93 kg N ha^{-1} d^{-1})
- After 11 days, deionised water was applied at the same rate but instead of nitrate solution.
- After 3, 4 and 5 days, the input rate exceeded the infiltration rate for the grass treatments, and water remained on the soil surface.

Drainage was inconsistent between treatments and within the grass treatments (Table 5.5). The mean drainage rate for the clover treatments was 0.5 ml min^{-1}. Mean drainage rate for the grass treatments was initially similar to the clover but then varied as ponding occurred (i.e. input rate > infiltration rate). Ponding caused a problem as the leachate volume and nitrate-N concentration rapidly declined for the grass treatments (Figure 5.15). However, this may illustrate differential soil structure and improved permeability under clover (both treatments were initially re-packed to the same bulk density and uniform structure). The mechanisms of ponding require further investigation. The drainage holes were checked for blockages. The problem may have been poor surface permeability due to the high density of grass roots; flocculation or translocation of clay particles resulting in blockages.

Table 5.5. Input volume when ponding occurred and drainage volume for each grass replicate compared with the total input volume and mean drainage volume for the clover treatments. The standard deviation of the clover drainage volume is given in parentheses.

Treatment	Input Volume (L)	Drainage Volume (L)
Grass 1	2.1	1.7
Grass 2	3.0	2.5
Grass 3	4.4	3.9
Clover mean	9.6	8.0 (0.40)
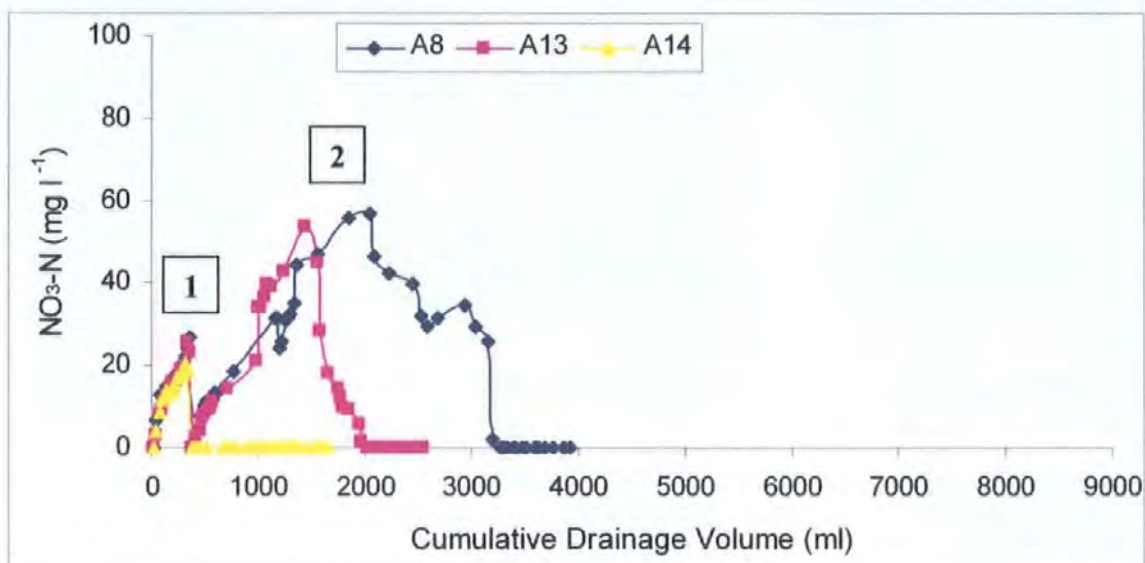
Figure 5.15. Experiment 3. Elution Profile: Ryegrass: Nitrate-N concentration with drainage volume. 1 = initial increase in concentration and decline when the supply of nitrate solution was stopped; 2 = second decline in concentration and drainage volume due to input rate exceeding infiltration rate. (A8, 13, 14 = ryegrass replicated ID).

The drainage volume and nitrate-N concentration within clover treatments were similar; elution profiles show a similar trend (Figure 5.16) with a sharp initial increase in concentration. The concentration in the leachate oscillated before it reached the concentration of the incoming solution (90 mg L^{-1}). When the concentration reached its maximum, deionised water was applied instead of nitrate solution, and the concentration readily declined. The mean elution profiles (Figure 5.17) are not very comparable due to the problem of ponding. The start of the profiles indicates a greater initial increase in nitrate leaching beneath grass. This may suggest a difference in soil structure. The

186

oscillation of nitrate-N concentration in Figure 5.18 illustrates a trend of increasing concentration with increasing light and temperature, and may be associated with biological activity.
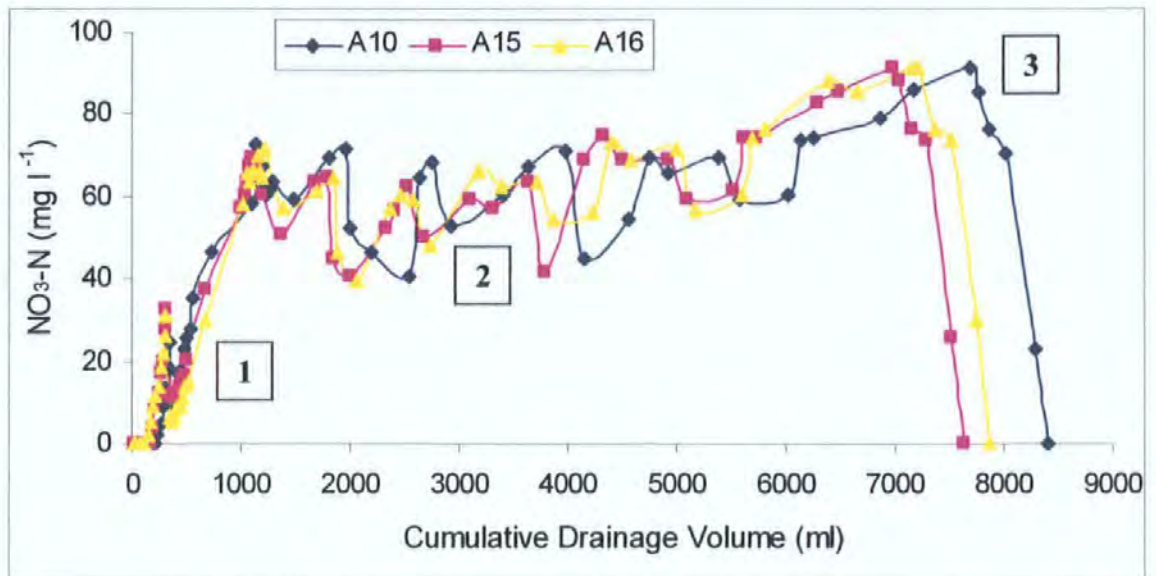
Figure 5.16. Experiment 3. Elution Profile: White Clover: Nitrate-N concentration with drainage volume. 1 = initial increase in concentration and decline when the supply of nitrate-N solution was stopped; 2 = oscillation in concentration; 3 = leachate concentration reached that of the incoming solution and declined when deionised water was applied. (A10, 15, 16 = white clover replicate ID)
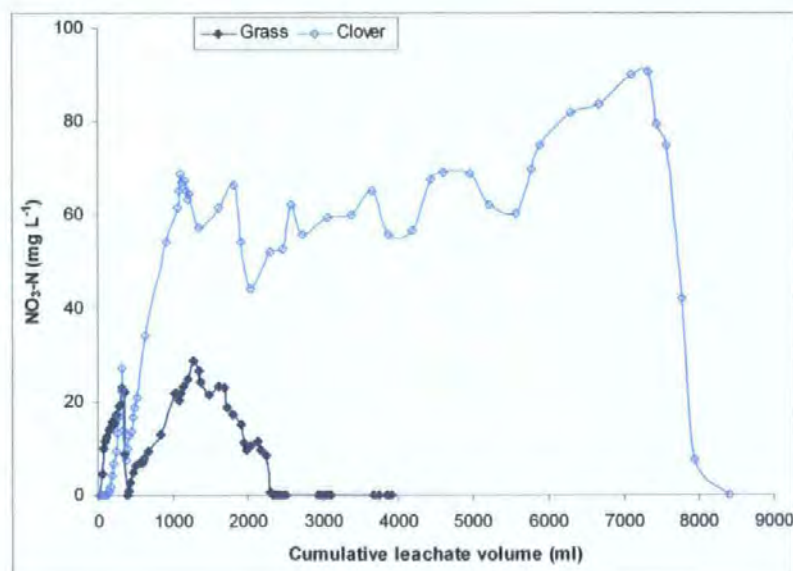
Figure 5.17. Experiment 3. Elution Profile: Mean nitrate-N concentrations with mean cumulative drainage volume for both treatments. Difference in leachate volume is due to poor permeability of the grass treatments. Comparison of elution profiles is difficult due to the initial decrease in concentration when water supply was removed and due to ponding of grass treatments. (n = 3).
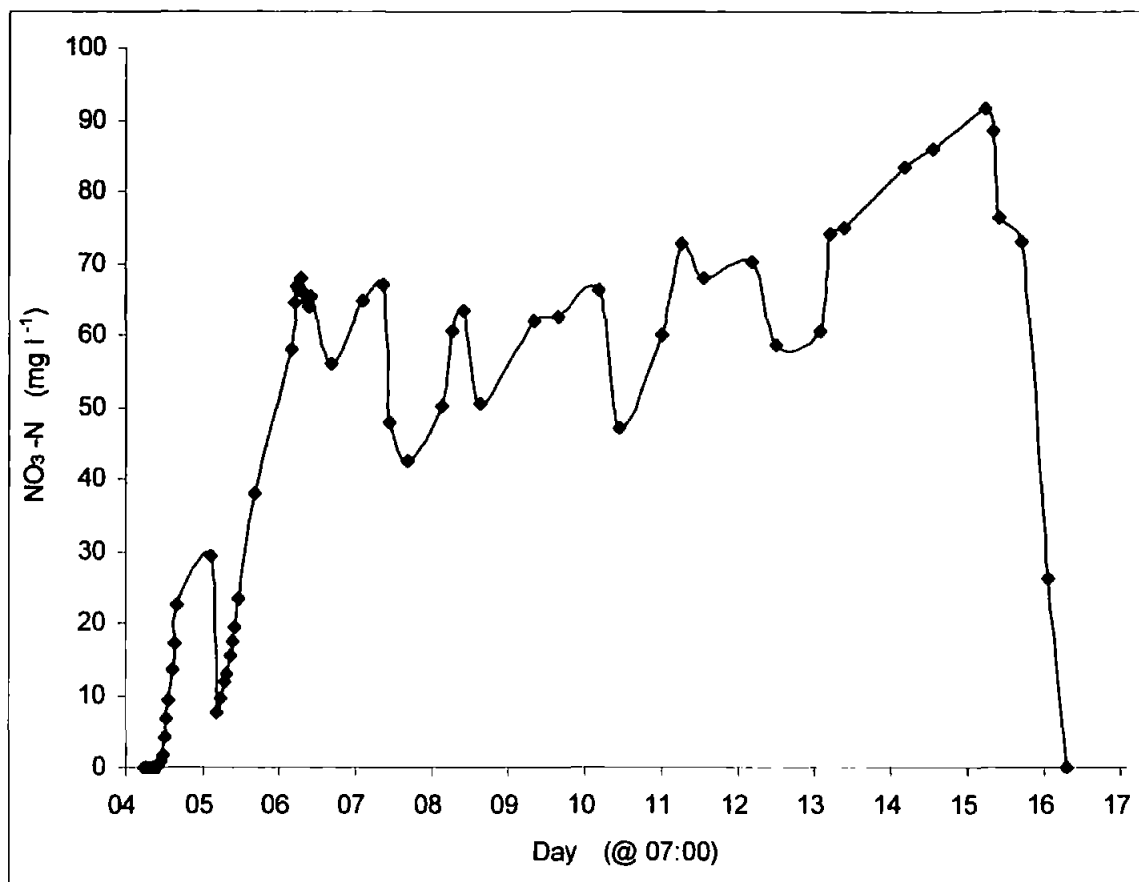
Figure 5.18. Experiment 3. Oscillation in mean nitrate-N concentration with time for the clover treatments. The vertical lines represent 12-hour periods between 07:00 and 19:00 for 13 days during March 2002. A possible trend appears where the concentration peaks in the morning, decreases during the afternoon/evening, increases throughout the night and again continues to rise until the afternoon.

The experiment also highlighted differences between the concentrations of ammonium-N in the leachate. Figure 5.19 shows that the clover treatments leached significantly more ammonium-N than the grass. This needs further investigation to highlight differences due to soil structure and microbial activity. Micro-organisms produce ammonium-N from organic-N during mineralization and from atmospheric N_2 during fixation. The activity of micro-organisms increases by a factor of 3 for each 10°C. The mean ammonium-N concentration with time is illustrated in Figure 5.20. There does not appear to be a clear trend. The concentrations in Figure 5.19 were detected before ponding occurred. However, anaerobic conditions would decrease the activity of micro-organisms and reduce the supply of ammonium-N.
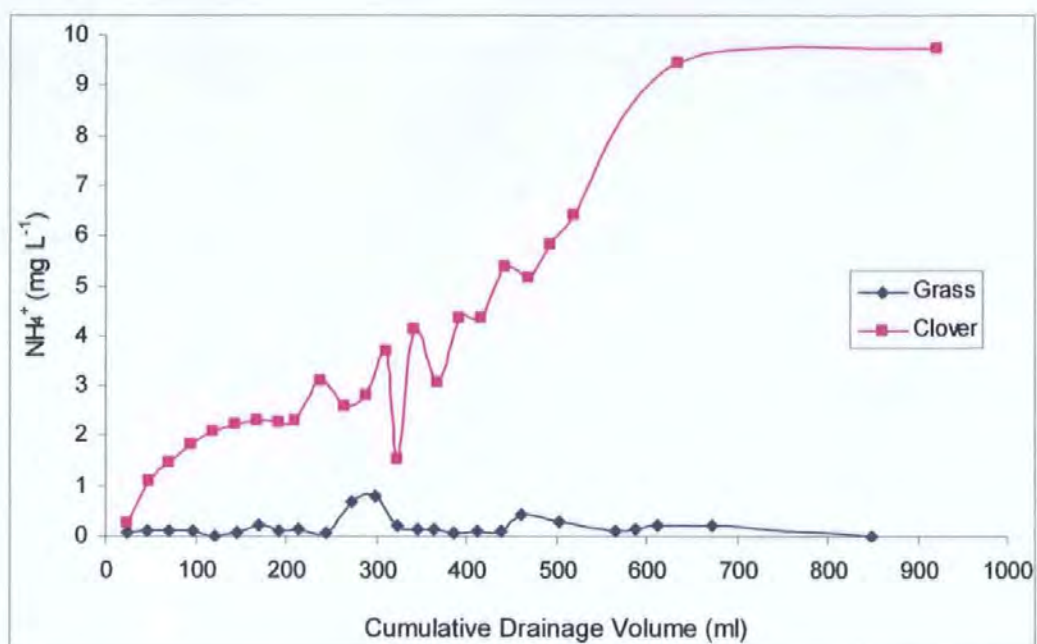
Figure 5.19. Experiment 3. Elution Profile: Mean ammonium-N concentrations with mean cumulative drainage volume for both treatments.
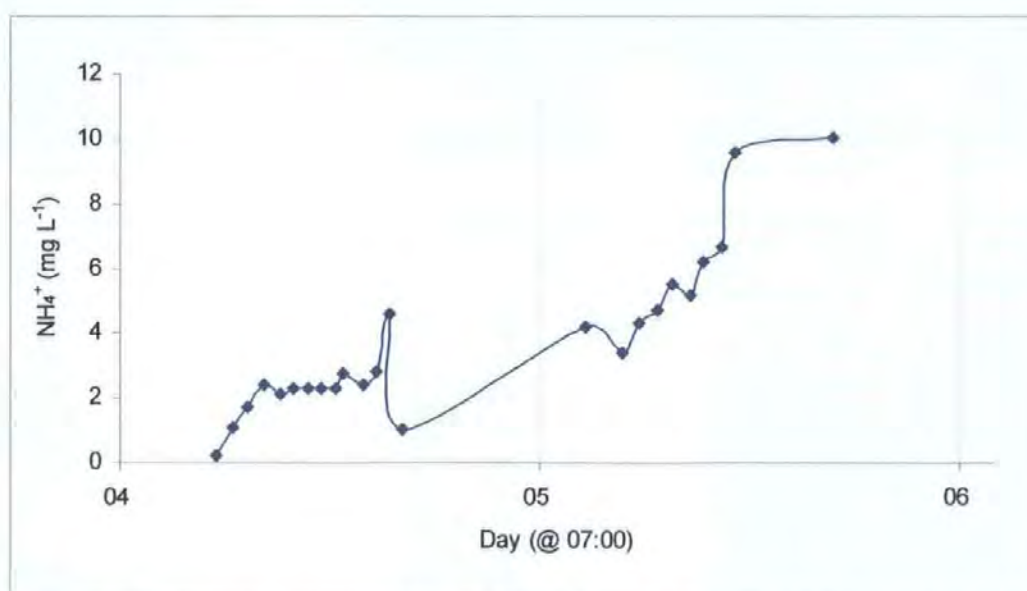
Figure 5.20. Experiment 3. Elution Profile: Mean ammonium-N concentration with time for the clover treatments. The vertical lines represent 12-hour periods between 07:00 and 21:00 for days during March 2001. No clear trend appears, except an increase with time.

Further observations were that water draining from soil beneath clover was discoloured and had a strong unpleasant smell (likened to cabbage). This was in contrast to the leachate from the grass treatments, which was clear and odourless. The leachate from the clover treatments also contained a hydrophobic substance, a sample of which was sent for analysis, but inconclusive results were obtained, and so this needs further investigation.

5.9.4. Leaching Experiment 4

- Three replicates of two treatments (ryegrass and white clover grown in topsoil).
- Soil was saturated and allowed to drain for 24 hours (i.e. field capacity).
- A solution containing 68 mg N L^{-1} (300 mg NO_3 L^{-1}) was applied to the soil surface at a rate of 0.6 ml min^{-1} (equivalent to 4 mm h^{-1} i.e. enhanced rainfall).
- After 18 days of applying nitrate solution, tap water was applied for 2 days.

This experiment provided valuable information on drainage. Figure 5.21 highlights difference in drainage between treatments that was consistent within treatments. Figure 5.22 suggest a diurnal change in drainage volume and therefore rate. A trend exists where the drainage volume increased during the day, reached a peak at 18:00 hours and then decreased throughout the night. This may be the effect of temperature and change in water viscosity. Experiment 3 showed peak concentration in the morning, therefore further work would be useful.
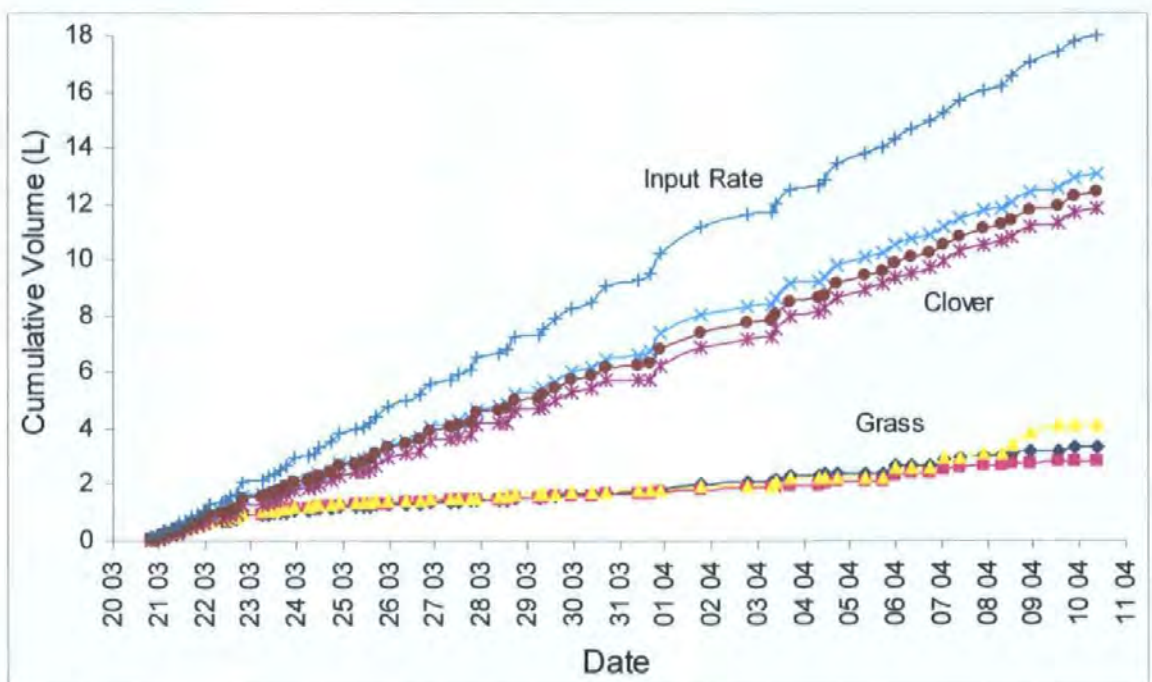
Figure 5.21. Experiment 4. Irrigation input rate compared to drainage volume beneath grass and clover.
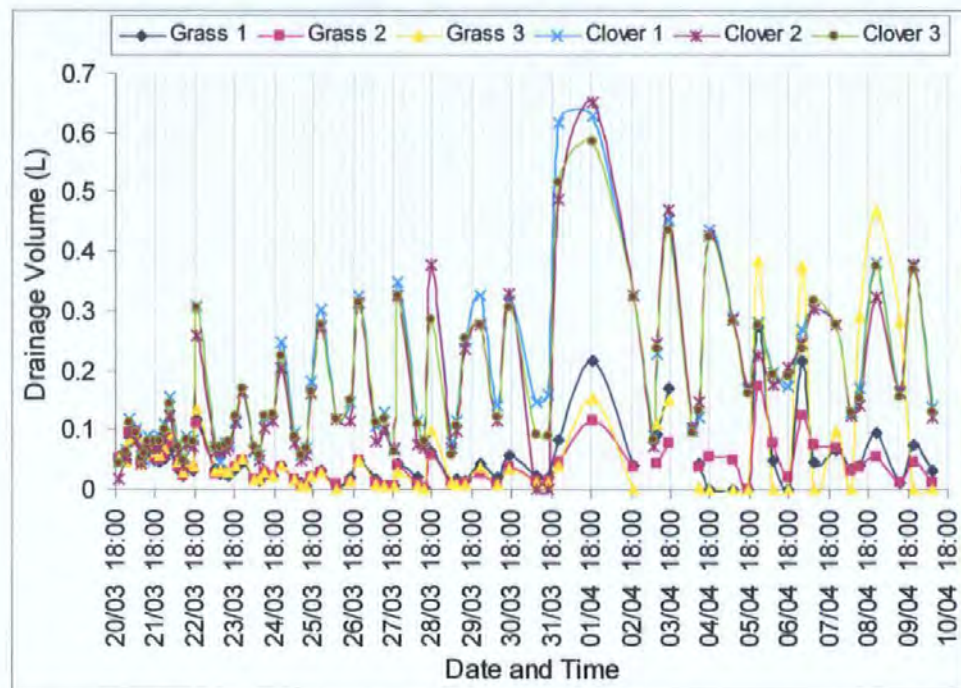
Figure 5.22. Experiment 4. Drainage volume with time for both treatments. The vertical lines represent 6-hour periods at 18:00, 00:00, 06:00 and 12:00 for 20 days. Peaks occur around 18:00 hours.

5.9.5. Leaching Experiment 5

- Two replicates of three treatments (ryegrass, white clover and mixed species), only one replicate of the unplanted control, all grown in subsoil.
- Soil was saturated and allowed to drain for 24 hours (i.e. field capacity).
- A pulse of NO_3^- solution (20 ml, 2.3 mg N L^{-1}) was applied to the soil surface (total of 45 mg N, equivalent to 54 kg N ha^{-1}) and left for 24 hours to diffuse into the aggregates.
- Rainfall was simulated at a rate of 0.32 ml min^{-1} (equivalent to 2.4 mm h^{-1} i.e. light rainfall) for 2 days.

Figure 5.23 illustrates the differences in elution profiles. For the grass, the maximum concentration was lower and was reached in a smaller drainage volume than the clover. The values of the mixed species were intermediate to those of the grass and clover. Table 5.6 shows the greatest amount of nitrate was leached beneath the unplanted control. Nitrate readily leached from the fallow soil (Figure 5.23). This is open to further interpretation; if this were indicative of a poor soil structure, we would expect a similar profile for the grass

191

treatments. The nitrate that is being removed from the planted samples may account for the differences. The use of ^{15}N may provide evidence for this hypothesis.

Figure 5.23. Experiment 5. Elution Profile: Mean nitrate-N concentrations with mean cumulative drainage volume for four treatments. (n = 2, except control where n = 1; error bars = standard deviation).

Table 5.6 shows the greatest amount of nitrate-N leached from the unplanted control and the least amount from beneath the grass. This can not be attributed to differences in soil structure as we would expect little difference. The utilization of nitrate by the plant and the soil organisms needs further investigation.

Table 5.6. Experiment 5. Amounts of nitrate-N leached (n = 2, except control where n = 1).

	Grass	Clover	Mixture	Control
Mean total mg leached	1	14	6	18
% leached of 45 mg applied	3	30	13	40

The experiment also highlighted a difference between the concentrations of ammonium-N, although no clear trend appeared. Table 5.6 shows that the clover treatments leached significantly more ammonium-N than the grass. The unplanted control also leached greater amounts of ammonium-N. This effect was not investigated further, but warrants future study.

Figure 5.24. Experiment 5. Elution Profile: Mean ammonium-N concentrations with mean cumulative drainage volume for four treatments. (n = 2, except control where n = 1).

5.9.6. Leaching Experiment 6

- Three replicates of two treatments (ryegrass and white clover grown in topsoil).
- Using a peristaltic pump, rainfall was simulated at a rate of 0.32 ml min^{-1} for 24 h.
- Once an even drainage rate was achieved a pulse of NO_3^- solution (50 ml, 226 mg N L^{-1}) was applied to the soil surface (total of 11 mg N, equivalent to 14 kg N ha^{-1}).
- Simulated rainfall was constant for 2 days.

The elution profiles (Figure 5.25) show that the pulse of nitrate was transported differently through soil beneath ryegrass and white clover. The grass treatment leached a higher concentration in a lower drainage volume. The shape of the clover curve indicated diffusion of nitrate into micropores. The implication of this is that at low rainfall a greater quantity and concentration of nitrate will be lost from soils beneath ryegrass. Both treatments reached their maximum concentration at similar drainage volumes, although the concentration was lower beneath clover. This suggests that soil beneath white clover is retaining the nitrate by interaction with micropore water.

193

Figure 5.25. Experiment 6. Elution Profile: Mean nitrate-N concentrations with mean cumulative drainage volume for both treatments. (n = 3). (Clover = pink, grass = blue).

Table 5.7 shows that the total amount of nitrate leached beneath clover was greater than the grass. The difference between nitrate applied and that leached equates to 6 kg ha^{-1} (grass) and 2 kg ha^{-1} (clover); a deficit of this proportion is probably a result of plant-uptake and denitrification (each processes utilizing 2-3 kg ha^{-1} d^{-1}). Future experiments would benefit from a ^{15}N labelled nitrate solution.

Table 5.7. Experiment 6. Amounts of nitrate-N leached (n = 3).

	Grass	Clover
Mean total mg leached	6	9
Standard Deviation	1.4	0.7
% leached of 11 mg applied	59	80

5.9.7. Leaching Experiment 7

- Three replicates of two treatments (ryegrass and white clover grown in topsoil).
- Rainfall was simulated at a rate of 0.32 ml min^{-1} for 24 h and an even drainage rate achieved.
- NO$_3$ solution (226 mg N L^{-1}) was applied at a rate of 0.32 ml min^{-1} for 90 min (total of 7 mg N, equivalent to 8 kg N ha^{-1}).
- Rainfall was simulated at the same rate for 2 days.

suggests the leaching of additional soil-N. In order to differentiate between the N applied and the background levels in the soil, one could use a nitrate solution labelled with ^{15}N. The soil beneath grass leached only a third of that applied. The difference between nitrate applied and that leached from the grass equates to 2 kg ha^{-1} and is probably a result of plant-uptake and denitrification (each processes using 2-3 kg ha^{-1} d^{-1}).

Table 5.8. Experiment 6. Amounts of nitrate-N leached (n = 3).

	Grass	Clover
Mean total mg leached	2	7
Standard Deviation	0.3	1.2
% leached of 7 mg applied	33	100

5.10. Summary of results for Column Experiment 1 – Leaching #1-7

The results of the first seven leaching experiments highlighted some interesting differences in the transport of nitrate through soils beneath white clover and ryegrass. Each experiment showed that white clover leached a greater amount of nitrate-N. There is also evidence to indicate differential soil structure between the treatments. Scholefield *et al.* (1996) suggest that soil structural differentiation is a major control of both the proportion of accumulated nutrient that actually leaches and the concentration at which it enters water bodies.

Furthermore white clover had a greater capacity to transmit water than ryegrass, which showed ponding on the soil surface. Another important observation which was not further pursued was the bad smell and colour of clover leachates.

An important observation was the oscillation in nitrate-N concentration (Figure 5.30). The trend of increasing concentration with increasing light and temperature may be associated

with biological activity. A trend was also observed in which drainage volume increased during the day, reached a peak at 18:00 hours and then decreased throughout the night. This may be the due to the effect of temperature and change in water viscosity. However, a mathematical investigation showed that water viscosity was not a mechanism. There is no known reporting of such a trend in the literature. Although Scholefield *et al.* (2000b) reported a diurnal pattern in riverine nutrient concentrations (including nitrate and phosphate). For future publications, the data will be investigated further for this phenomenon.

Direct comparison of the results with nitrate leaching reported in literature is not possible; most findings are of long-term field experiments. Furthermore, the quantity of nitrate applied was not intended to be realistic of fertiliser application. A simplistic implication for organic systems of livestock production is that the presence of white clover may enhance the total amount of nitrate leached although concentration may or may not be reduced compared to ryegrass.

The experimental procedure was assessed and various modifications were made in the subsequent experiments. In order to differentiate between the N applied and the background levels in the soil, one could use a nitrate solution labelled with ^{15}N; this was not possible in the time frame of this study. Using the isotopes ^{15}N and ^{18}O will provide greater information on the interaction and transport of water and nitrate in the soils.

5.11. Results - Column Experiment 2 – Leaching Experiments #8-10

The following experiments are presented to show the differences in nitrate-N transport as influenced both by the plant treatment and by the method of tracer application prior to rainfall. As defined in Table 5.1, the tracer application methods are classified as Type A and C.

5.11.1. Leaching Experiment 8

- Four replicates of four treatments (ryegrass, white clover, mixed species and unplanted control grown in re-packed topsoil).
- Rainfall was simulated at a rate of 0.32 ml min^{-1} for 24 h.
- NO$_3$ solution (55.5 ml of 200 mg N L^{-1}) was applied at a rate of 0.32 ml min^{-1} for 2.5 h (total of 11 mg N, equivalent to 13 kg N ha^{-1}).
- Rainfall was continued for 3.5 days.
- Samples were collected every hour.

Leaching Experiment 8 is classified as Type A (Table 5.1), i.e. the tracer was applied at a constant rate via a peristaltic pump to saturated soil. The mean elution curves for each treatment are given in Figure 5.27. The mean elution curves for the clover and unplanted treatments peaked at a similar concentration and were of a similar shape. The grass and mixed species also gave similar elution profiles (Figure 5.27). The variation in nitrate-N transport within treatments is indicated by the error bars in Figure 5.27

Table 5.9 gives the mean amounts of nitrate-N leached from each treatment. Of the 11 mg applied, 36% was leached from both the grass and mixed species. The greatest amount of N was leached from beneath the unplanted control (73%), which was comparable to that leached beneath white clover (67%).
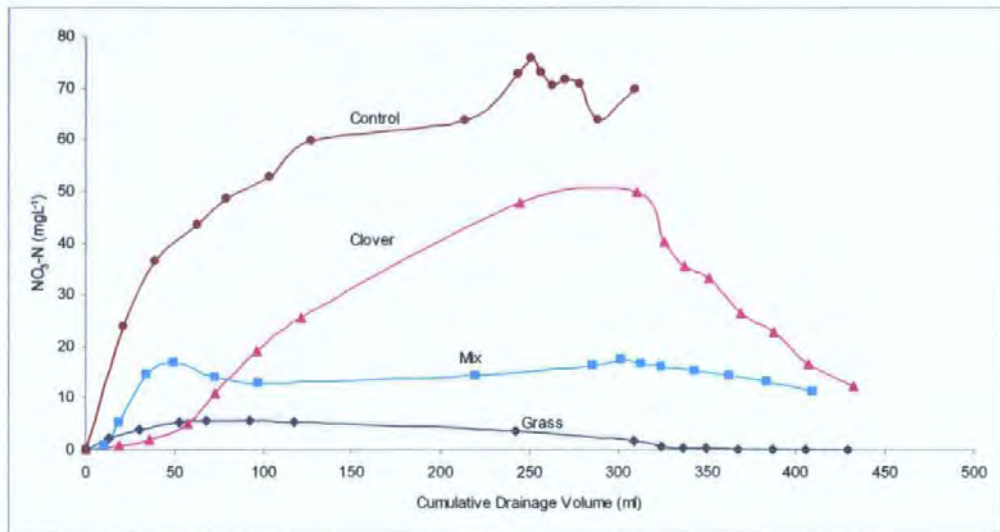
Figure 5.27. Experiment 8 – Type A. Elution Profile: Mean nitrate-N concentrations with mean cumulative drainage volume for four treatments. (n = 4; error bars = standard deviation).

Table 5.9. Experiment 8 – Type A. Mean nitrate-N leached. (n = 4).

	Clover	Grass	Mixture	Unplanted
Mean total mg recovered	7	4	4	8
% recovered of 11 mg applied	67	35	35	73
Mean total kg ha^{-1} recovered	9	5	5	10
kg ha^{-1} not recovered	4	8	8	3

5.11.2. Leaching Experiment 9

- Four replicates of four treatments (ryegrass, white clover, mixed species and unplanted control grown in topsoil).

- Soil was saturated and allowed to drain for 24 hours (i.e. approximate field capacity).

- A pulse of NO_3^- solution (35 ml, 1000 mg N L^{-1}) was applied to the entire soil surface (total of 35 mg N, equivalent to 42 kg N ha^{-1}) and left for 48 hours to diffuse into the micropores.

- Rainfall was simulated at a rate of 0.32 ml min^{-1} (equivalent to 4 mm h^{-1}) for 5 days.

- Samples were collected at 4 and 8 hour intervals.

Leaching Experiment 9 is classified as Type C (Table 5.1), i.e. the tracer was applied to unsaturated soil and allowed to diffuse and mix with the soil solution prior to simulated rainfall. The mean elution curves for each treatment are given in Figure 5.28. The mean elution curves for the clover and unplanted treatments were of a similar shape and concentration range. Nitrate-N leached beneath white clover peaked later and slightly higher than the unplanted control (Figure 5.28). The grass and mixed species gave similar elution profiles, with the grass yielding the least nitrate-N (Figure 5.28). The shape of the mean elution curve for white clover indicates that nitrate was moving rapidly through large pores, but delayed in small pores. There is more variation in nitrate-N transport within treatments for the unplanted control and white clover.

The shape of the elution profiles in Figure 5.28 reflect the method of applying the nitrate tracer, as well as the size, shape and continuity of the pores. As the tracer was applied 48 hours before simulated rainfall, the tracer solution will mix with the soil solution and become homogeneously distributed. This is in contrast to the elution profiles in Figure 5.27, where the curves showed that the tracer was less dispersed and peaked to a higher concentration.

Table 5.10 gives the mean amounts of nitrate-N leached from each treatment. Of the 35 mg applied, 9% and 18% was leached from the grass and mixed species, respectively. The greatest amount of N was leached from beneath the unplanted control (81%), which was similar to that leached beneath white clover (75%). A proportion of the nitrate may remain in the soil, whilst some will be lost through denitrification to the atmosphere and due to up-take by plants and micro-organisms. These processes were not quantified; the interest was with the amount of nitrate leaching.
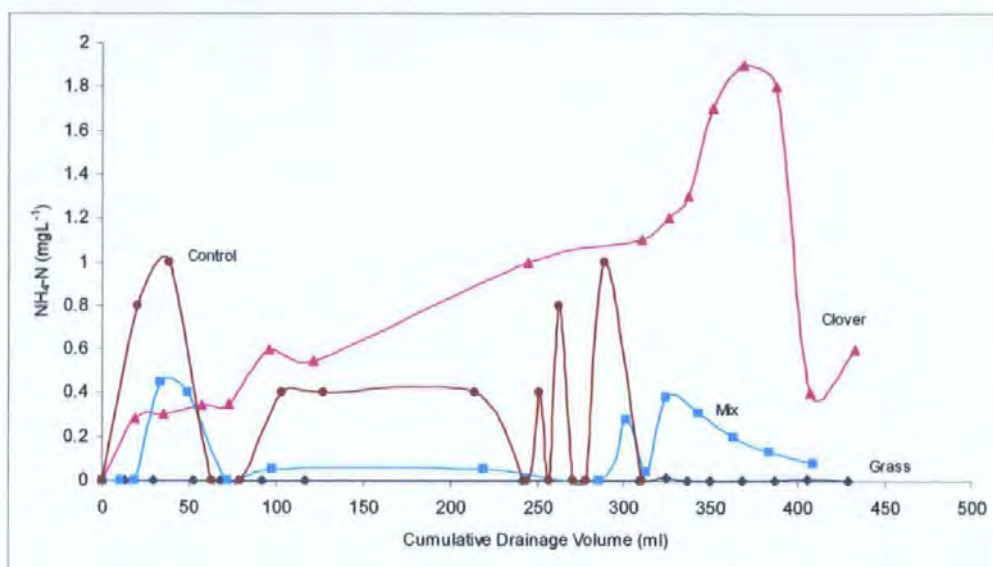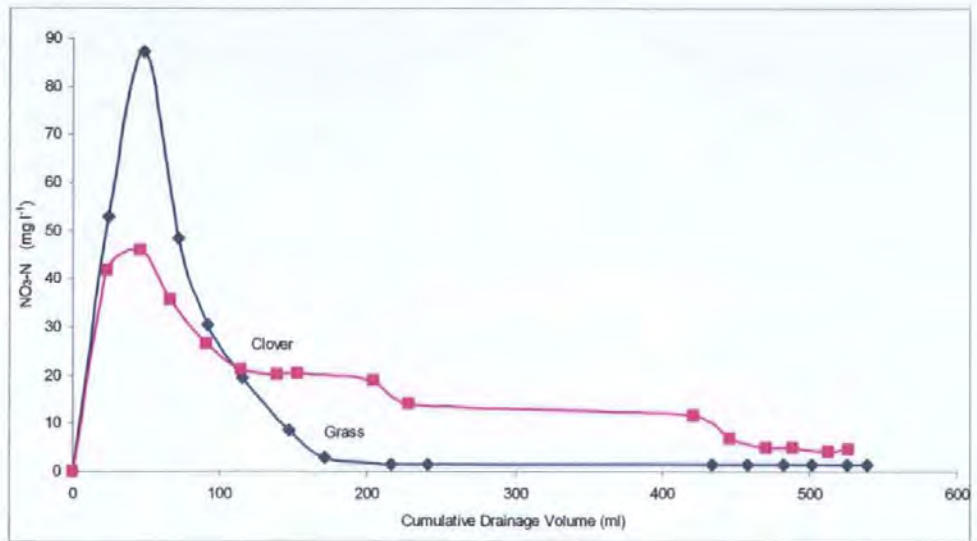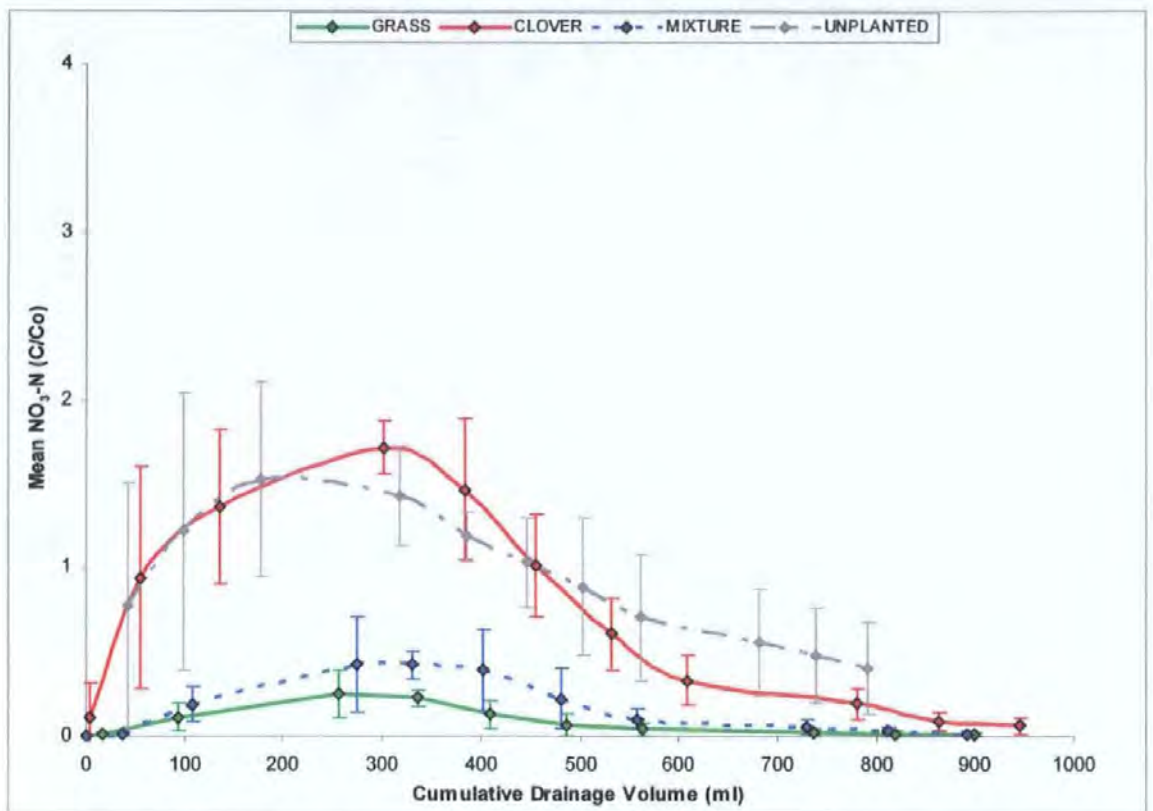
Figure 5.28. Experiment 9 – Type C. Elution Profile: Mean nitrate-N concentrations with mean cumulative drainage volume for four treatments. (n = 4; error bars = standard deviation).

Table 5.10. Experiment 9 – Type C. Mean nitrate-N leached. (n = 4).

	Clover	Grass	Mixture	Unplanted
Mean total mg recovered	26	3	6	28
% recovered of 35 mg applied	75	9	18	81
Mean total kg ha^{-1} recovered	32	4	7	34
kg ha^{-1} not recovered	10	38	35	8

5.11.3. Leaching Experiment 10

- Four replicates of four treatments (ryegrass, white clover, mixed species and unplanted control grown in topsoil).
- Soil was saturated and allowed to drain for 24 hours.
- Rainfall was simulated at a rate of 0.32 ml min^{-1} for 24 h.
- A nitrate solution containing 50 mg N L^{-1} (400 mg NO$_3$ L^{-1}) was applied to the soil surface at a rate of 0.32 ml min^{-1} (equivalent to 4 mm h^{-1} i.e. enhanced rainfall; total of 418 mg N, equivalent to 504 kg N ha^{-1}).

201

- After 14 days, deionised water was applied at the same rate for 2 days, followed by the nitrate solution for 12 hours.
- Samples were collected at hourly intervals at the start of the experiment and during changes in the irrigation/pulse solution. Samples were also collected at 4 and 8 hour intervals.

Leaching Experiment 10 is not classified in Table 5.1. The tracer was continuously applied to saturated soil for 14 days, followed by simulated rainfall for 2 days and subsequently reverted to nitrate solution for 12 hours. The mean elution curves for each treatment are given in Figure 5.29, which shows an initial increase in nitrate-N, a plateau followed by a decrease when water was applied, and a final rise in concentration when nitrate was re-applied. The variation in nitrate-N transport within treatments is indicated by the error bars in Figure 5.29.

The mean elution curves for the clover and unplanted treatments were of a similar shape, but not congruent as the unplanted soil leached the highest concentration (Figure 5.29). The concentration range for the mixed species was intermediate to the clover and grass treatments. The grass and mixed species gave similar shaped mean elution profiles with similar peaks and troughs (Figure 5.29).

Despite the application of the tracer for 14 days, the concentration in the leachate did not reach that of the incoming solution. The decrease in nitrate-N concentration with the addition of water was steeper than the initial increase in concentration, suggesting that water and nitrate are moving at different rates and that nitrate is more readily displaced by water than vice versa. This rapid decrease in concentration is more apparent for the clover and unplanted soils, coupled with the higher concentrations for both treatments, suggest that the transport process is dominated by preferential flow under these continuous conditions.

Table 5.11 gives the mean amounts of nitrate-N leached from each treatment. Of the 418 mg applied, the greatest amount was leached from beneath the unplanted control (59%), which was similar to that leached beneath white clover (53%). 10% and 25% was leached from the grass and mixed species, respectively. Table 5.11 also shows that a large proportion of the nitrate was not recovered.

The shape of the elution curves in Figure 5.29 are as expected for the method of applying the tracer solution. However, the curves do not show a smooth increase to and around the plateau, suggesting a possible diurnal fluctuation in concentration. This was not investigated further, neither was the amount of nitrate remaining in the soil nor the removal processes. Such studies may explain the differences in concentrations leaching from the clover and unplanted treatments compared to the ryegrass and mixed species.
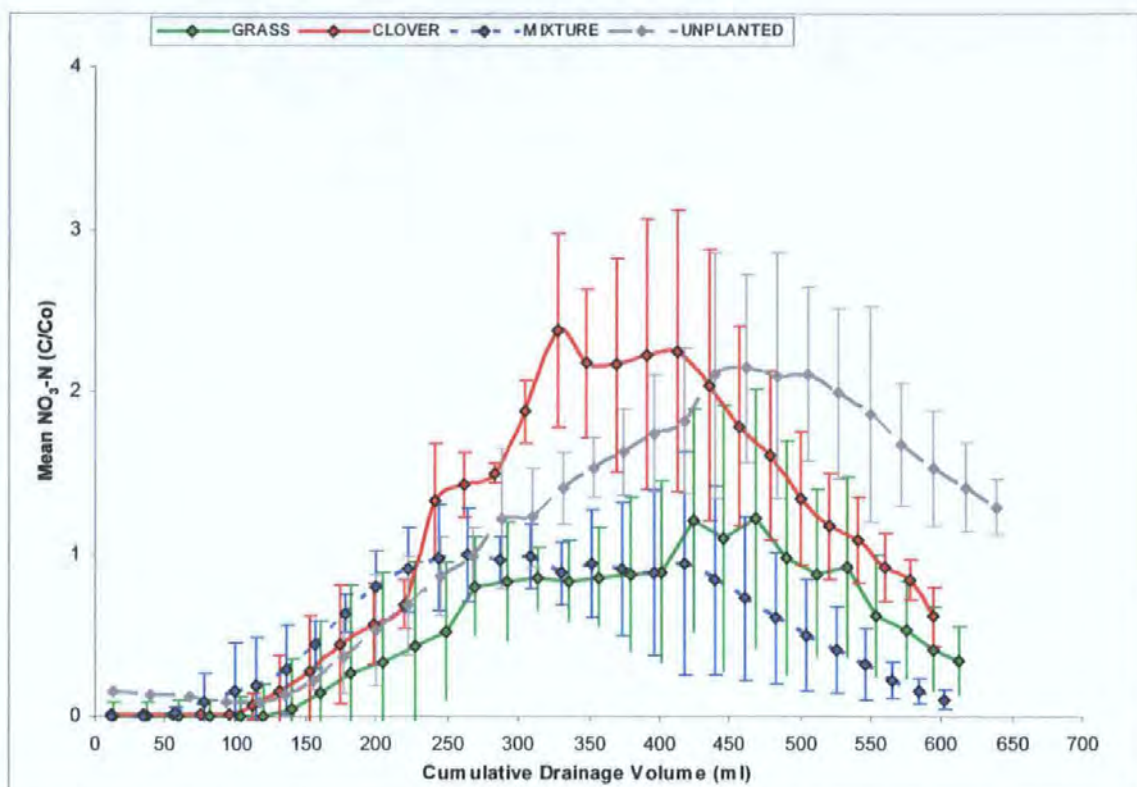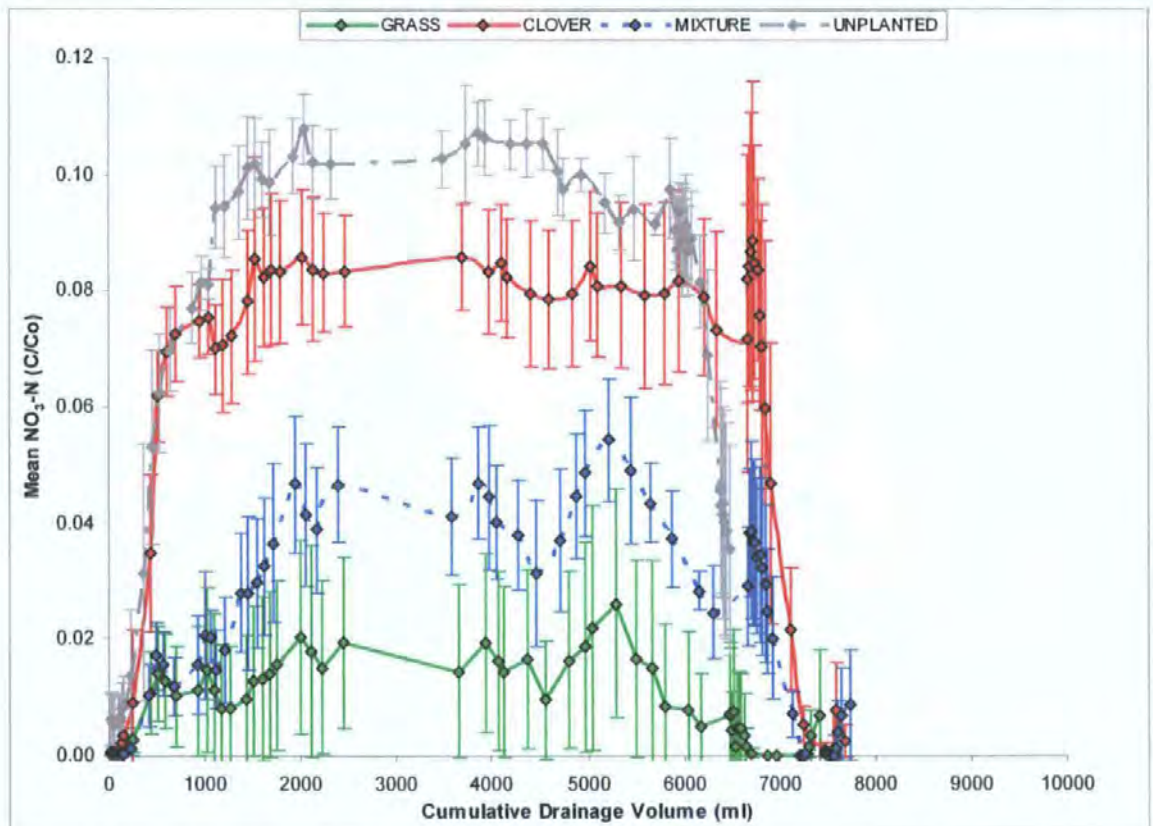

Figure 5.29. Experiment 10. Elution Profile: Mean nitrate-N concentrations with mean cumulative drainage volume for four treatments. (n = 4; error bars = standard deviation).

Table 5.11. Experiment 10. Mean nitrate-N leached. (n = 4).

	Clover	Grass	Mixture	Unplanted
Mean total mg recovered	223	40	103	246
% recovered of 418 mg applied	53	10	25	59
Mean total kg ha^{-1} recovered	268	49	124	296
kg ha^{-1} not recovered	236	455	380	208

5.12. Summary of results for Column Experiment 2 – Leaching #8-10

The differences in the shapes of the elution profiles in Figure 5.29 reflect the method of applying the nitrate tracer. The effect of the size, shape and continuity of the pores is less apparent. The pore volume of the soil is estimated at 600 cm^3, and as all elution profiles show an asymmetric peak in concentration prior to this volume, a degree of preferential flow is suggested beneath all treatments.

The three experiments (#8-10) consistently showed that the unplanted controls leached the greatest amount of nitrate-N, and were similar to the concentrations leached beneath white clover. The three experiments also showed similar elution profiles for ryegrass and the mixed species, ryegrass generally leached the lowest concentrations. If the concentration of the leached tracer was simply a function of soil structure, the unplanted soil would be expected to yield low concentrations as it is expected to have less structural development than the planted soils. Thus, there are other processes removing or retaining the nitrate that need further investigation and quantification. The significance of the experiments is that white clover will leach more nitrate than ryegrass regardless of the method of applying the nutrient.

These experiments have practical implications for the transport of nitrate in the field. Experiment 8 simulated the effect of a fertiliser application prior to rainfall. Experiment 9 simulated the homogeneous distribution of nitrate at equilibrium with the soil solution at

the end of the growing season prior to the onset of autumn/winter rain. Experiment 10 may be likened to a sustained period of acid rain. Thus, the findings suggest that nitrate will be more susceptible to enhanced leaching in soils beneath white clover. This potential problem would be accelerated if the supply of nitrate to the soil beneath white clover exceeded that to ryegrass. Such situation occurs due to fixation, and is enhanced under livestock production and particularly intensive dairy farming.

5.13. Results - Column Experiment 2 – Leaching Experiment #11

This section presents elution curves for nitrate-N leached beneath five different soils of Column Experiment 2. As in previous sections, topsoil and subsoil refer to re-packed soil of the Crediton series. Figure 5.30 presents the mean nitrate-N concentration of four replicates of each treatment to which a Type A nitrate pulse was applied. Figure 5.32 shows the same data but is plotted as separate profiles to show the differences in nitrate leaching as an effect of soil type as well as planting regime.

Figure 5.30 shows that the greatest concentrations were leached beneath soils planted with white clover. The earliest breakthrough of nitrate-N was observed beneath grass and unplanted soils, although both plant treatments also showed a later breakthrough than white clover for the Denbigh series, which has a greater pore-volume. The Crediton series topsoil planted with the mixed species showed a semi-symmetrical breakthrough curve with attenuation, which gave a concentration similar to both the grass and unplanted treatments and peaked before the estimated pore-volume of 600 cm^3.

Figure 5.32 (a) shows that for soils planted with white clover, the earliest breakthrough and peak concentration were observed from the Greinton series, followed by Crediton series topsoil and subsoil. The lowest and latest breakthrough and peak concentration was

observed from the Denbigh series. Figure 5.32 (b) shows that for soils planted with white clover, the earliest breakthrough and peak concentration were observed from the Crediton series topsoil and subsoil. The Denbigh series was again the lowest concentration and latest to breakthrough. Figure 5.32 (c) shows that for the unplanted soil, the highest concentrations were detected beneath the Denbigh series, which occurred with more drainage volume than the other unplanted soils. The Crediton series subsoil showed a fluctuating nitrate-N concentration and the Frilsham series hardly drained, both a result of poor infiltration.

Figure 5.30. Experiment 11 – Type A. Elution Profile: Nitrate-N concentrations for 16 treatments (4 planting regimes, 5 soil types). (n=4).

The mean elution curves are plotted separately in Figure 5.31 and together in Figure 5.32 to enable a classification of their leaching characteristics. Figure 5.31 shows that the shape of the elution curve and the nitrate-N concentration for each soil type changes with plant regime. In the case of the Crediton series topsoil, the breakthrough volume and the peak concentration decreased from the clover to the grass to the unplanted soils. This was also observed for the Greinton series, although the decrease in nitrate-N concentration between the grass and unplanted treatments were not as marked as for the clover treatment, and the

clover treatment gave a slight second peak. In accordance, the clover treatment of the Crediton series subsoil gave a higher peak concentration after a greater drainage volume compared to the grass treatment.

The treatments of both the Frilsham and Denbigh series did not show the same trend mentioned above. The nitrate leached beneath clover in these two soils is comparable to the other three soil types. However, the Frilsham grass treatment showed a slow initial increase in concentration, which rapidly declined to background levels, whilst the unplanted soil leached low nitrate-N concentrations due to a lower drainage volume and infiltration rate. The Denbigh unplanted soil leached more nitrate-N than the clover but at a similar concentration. The leaching profile of the Denbigh grass, like the Frilsham grass, was not characteristic of the grass in the other three soil types.
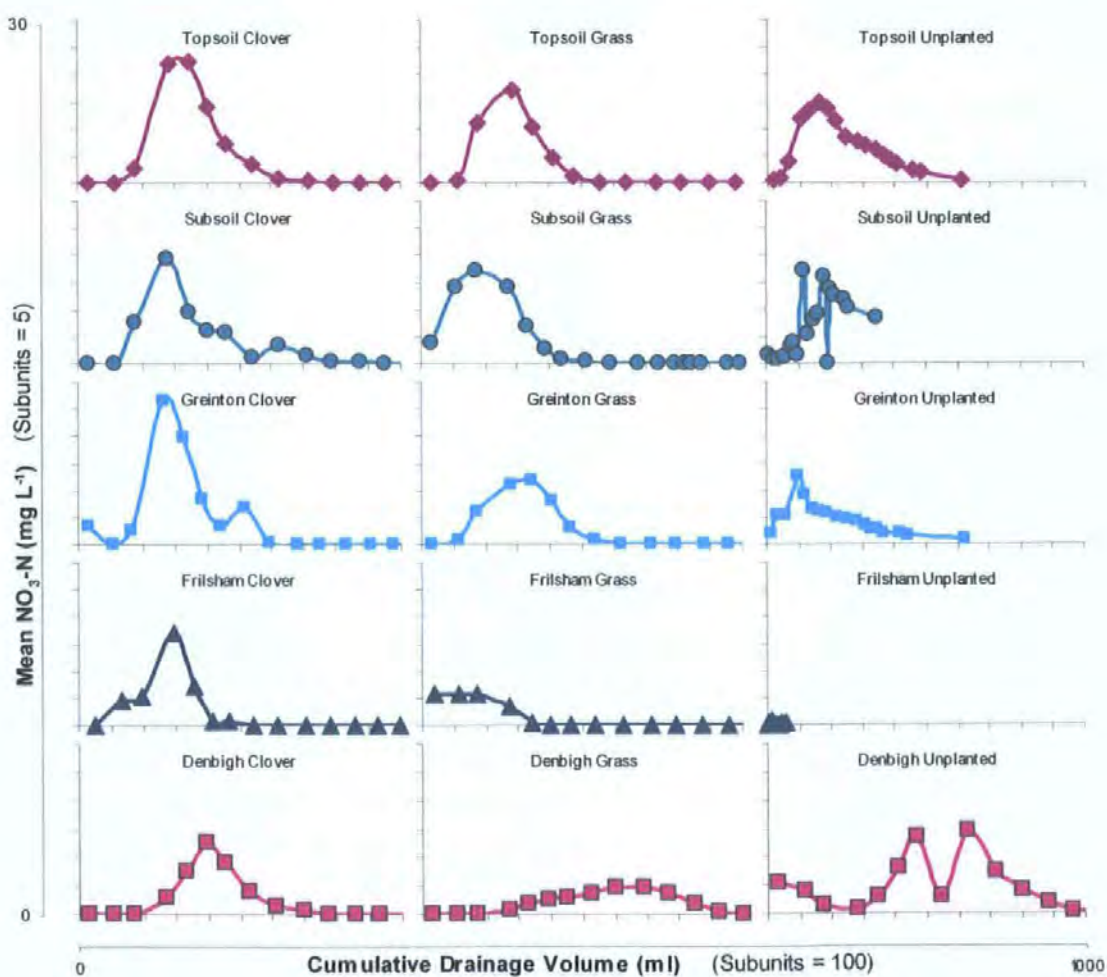
Figure 5.31. Experiment 11 – Type A. Elution Profiles: Mean nitrate-N concentrations for 15 treatments (3 planting regimes, 5 soil types).

207
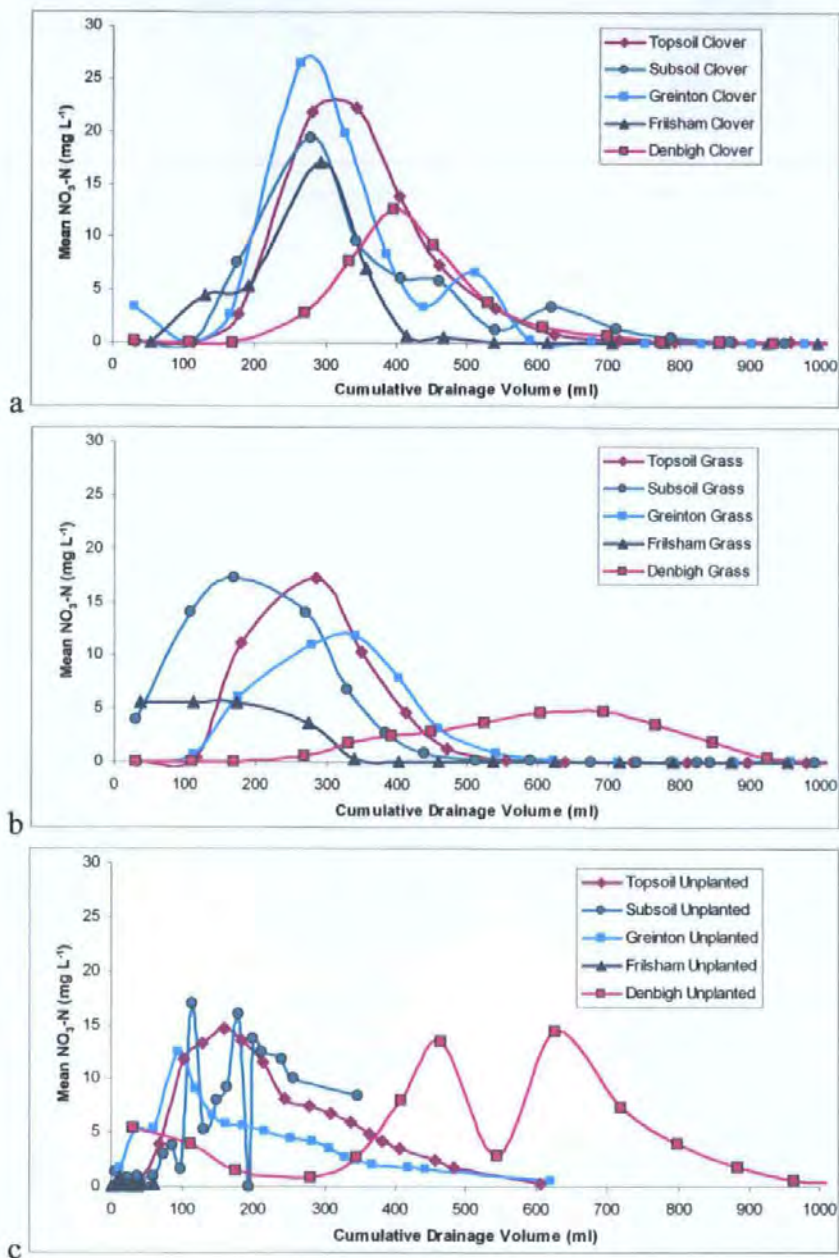
Figure 5.32. Experiment 11 – Type A. Elution Profile: Mean nitrate-N concentrations for five soil types of three plant treatments. (n=4).

5.14. Summary of results for Column Experiment 2 – Leaching #11

Clear trends in the elution profiles were seen. Clover leached the greatest concentration and amount of nitrate-N. These elution profiles need to be plotted as breakthrough curves showing the response as a function of pore-volume. This will provide additional information on soil structure. The mass recovered and the drainage characteristics need calculating.

5.15. Results - Column Experiment 2 – Leaching Experiments #12-14

A series of elution profiles are presented (Figure 5.33 to Figure 5.38), which compare the behaviour of three tracers under 16 treatments (combinations of five soils, four plants) when applied in three different ways (Type A, B, C). As explained in Table 5.1, an aim was to investigate the effect of the site of the tracer prior to leaching and to simulate different field scenarios. The protocol for these experiments was standardised and details are given in Section 5.5 and Table 5.2.

Figure 5.33 illustrates the transport of bromide applied under a Type A tracer scenario in five soils planted with white clover and ryegrass (Figure 5.33 (a) and (b), respectively), five unplanted control soils and topsoil of the Crediton series planted with a mixture of grass and clover (Figure 5.33 (c) and (d), respectively). Figure 5.33 (a) shows that all soils planted with white clover showed an initial peak in concentration followed by a secondary higher attenuated peak. The initial peak concentrations were similar for all soil types beneath white clover. The second peaks reached a greater maximum concentration for the Frilsham series and Crediton topsoil and subsoil compared to the Greinton and Denbigh series. There was also a difference in the drainage volume at which the second peaks occurred; the Frilsham series appeared first at ~200 ml.

Figure 5.33 (b) shows that all soils planted with ryegrass gave initial peak concentrations which were higher than the initial peaks beneath clover. This is also the case for three of the unplanted soils (Figure 5.33 (c)).The unplanted controls of the Frilsham series and Crediton topsoil did not drain as much as the other unplanted soils. The transport of bromide through Crediton topsoil planted with the mixed species shows a similar elution profiles to the mono-clover treatments (Figure 5.33 (d) and (a), respectively).

The shapes of the curves indicate that preferential flow is occurring in all soils, but largely beneath ryegrass and the unplanted soils. The elution profiles for white clover and the

mixed species showed an early initial peak and a second delayed peak; this was due to rapid movement of the tracer solution in larger pores, followed by a greater degree of dispersion and retardation in smaller pores.

Figure 5.34 illustrates the transport of nitrate applied under the Type A experiment as above. The relative nitrate-N concentration (Figure 5.34) is scaled at half that of bromide (Figure 5.33) as it will be lost in various soil processes. The elution profiles suggest similar transport behaviour for nitrate as bromide. However, nitrate-N leached beneath soils planted with white clover did not show an initial peak concentration as seen with bromide (Figure 5.34 (a) and Figure 5.33 (a), respectively). Furthermore, the grass and unplanted soils did not show well-defined peaks.

Figure 5.35 illustrates the transport of phosphate-P applied under the Type A experiment as above. The relative phosphate-P concentration (Figure 5.35) is scaled lower than both bromide (Figure 5.33) and nitrate (Figure 5.34) as it was detected in parts per billion rather than parts per million. Figure 5.35 shows that the concentration of phosphate-P fluctuates rather than peaks, unlike the transport of bromide and nitrate. This is expected due to the chemical processes of adsorption/desorption controlling the solution composition of phosphate.

Figure 5.35 (a) shows that all soils planted with white clover leached a similar concentration, which was comparable to the mixed species grown in Crediton series topsoil (Figure 5.35 (d)). These concentrations were lower than all soils planted with ryegrass and the unplanted controls (Figure 5.35 (b) and (c), respectively). The greatest amount and concentration of phosphate-P was leached beneath the unplanted control and grass treatment of the Greinton series. The Crediton series subsoil leached more phosphate-P from the unplanted control and the grass soils than the equivalent treatments in Crediton series topsoil.

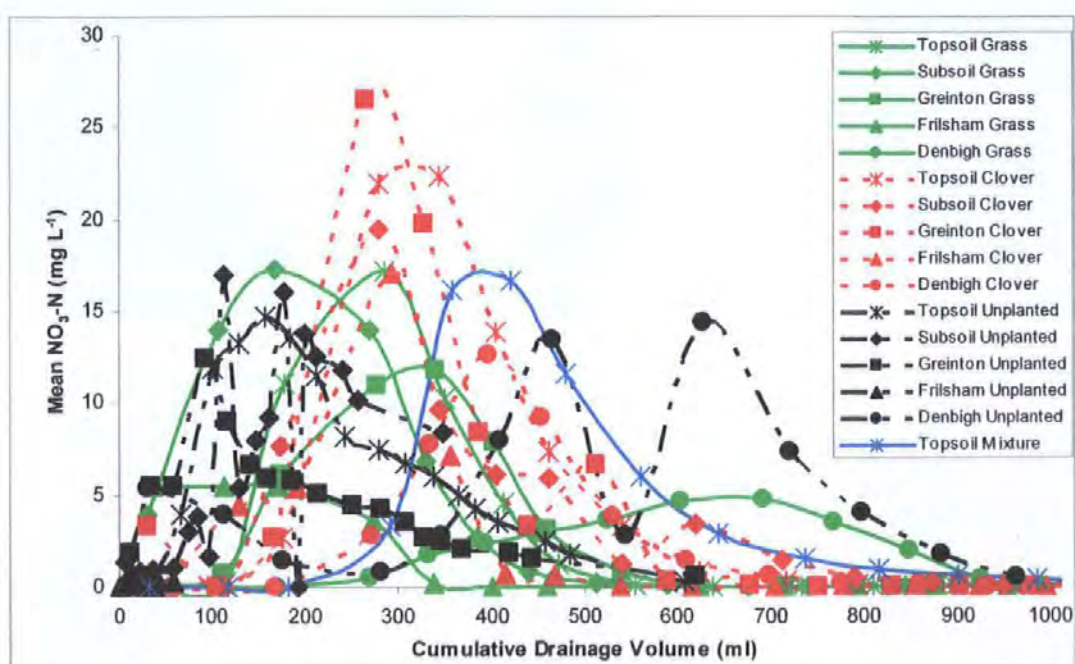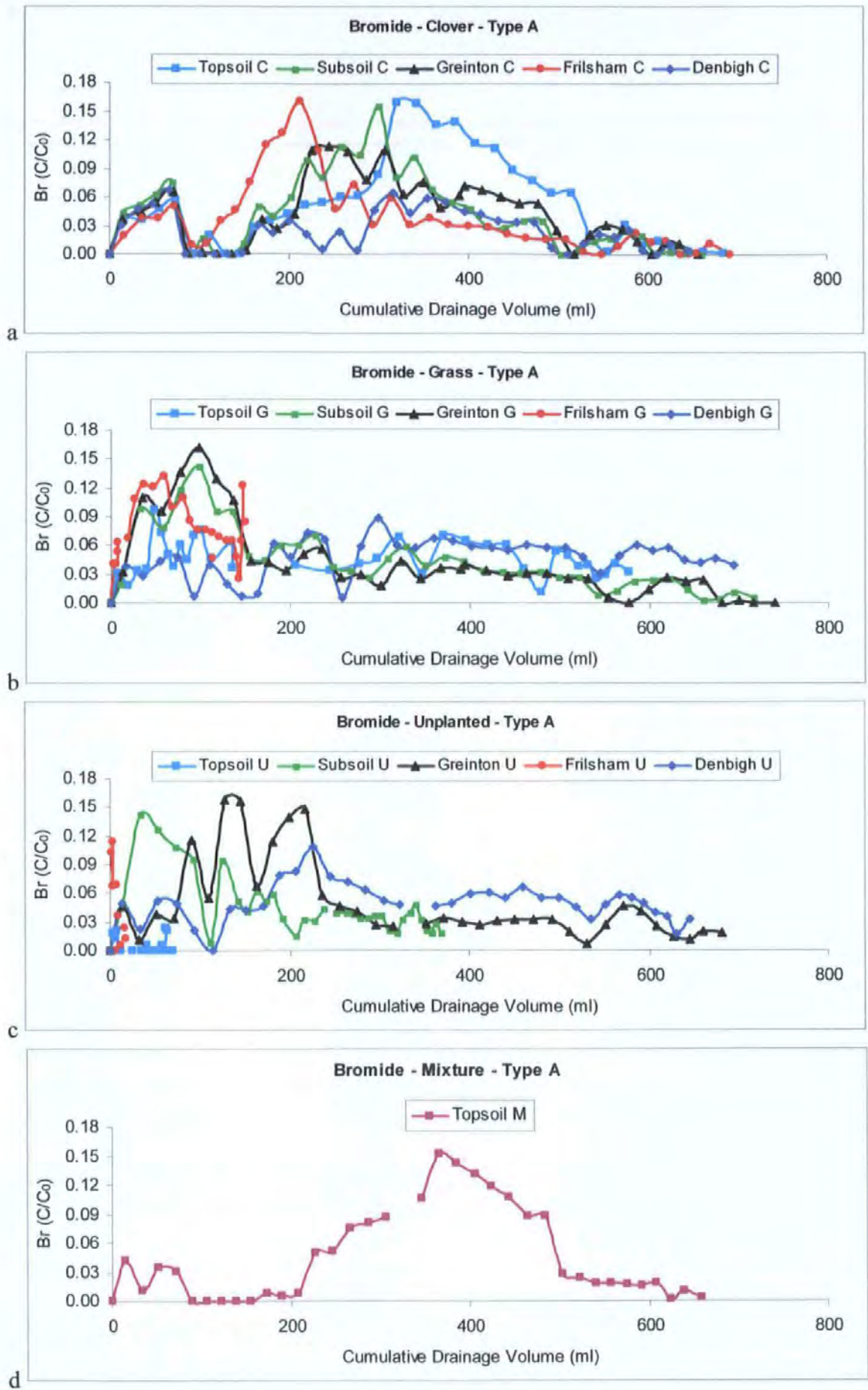**Figure 5.33. Experiment 12 - Type A. Elution Profiles: Bromide concentrations for 16 treatments (4 planting regimes, 5 soil types).**
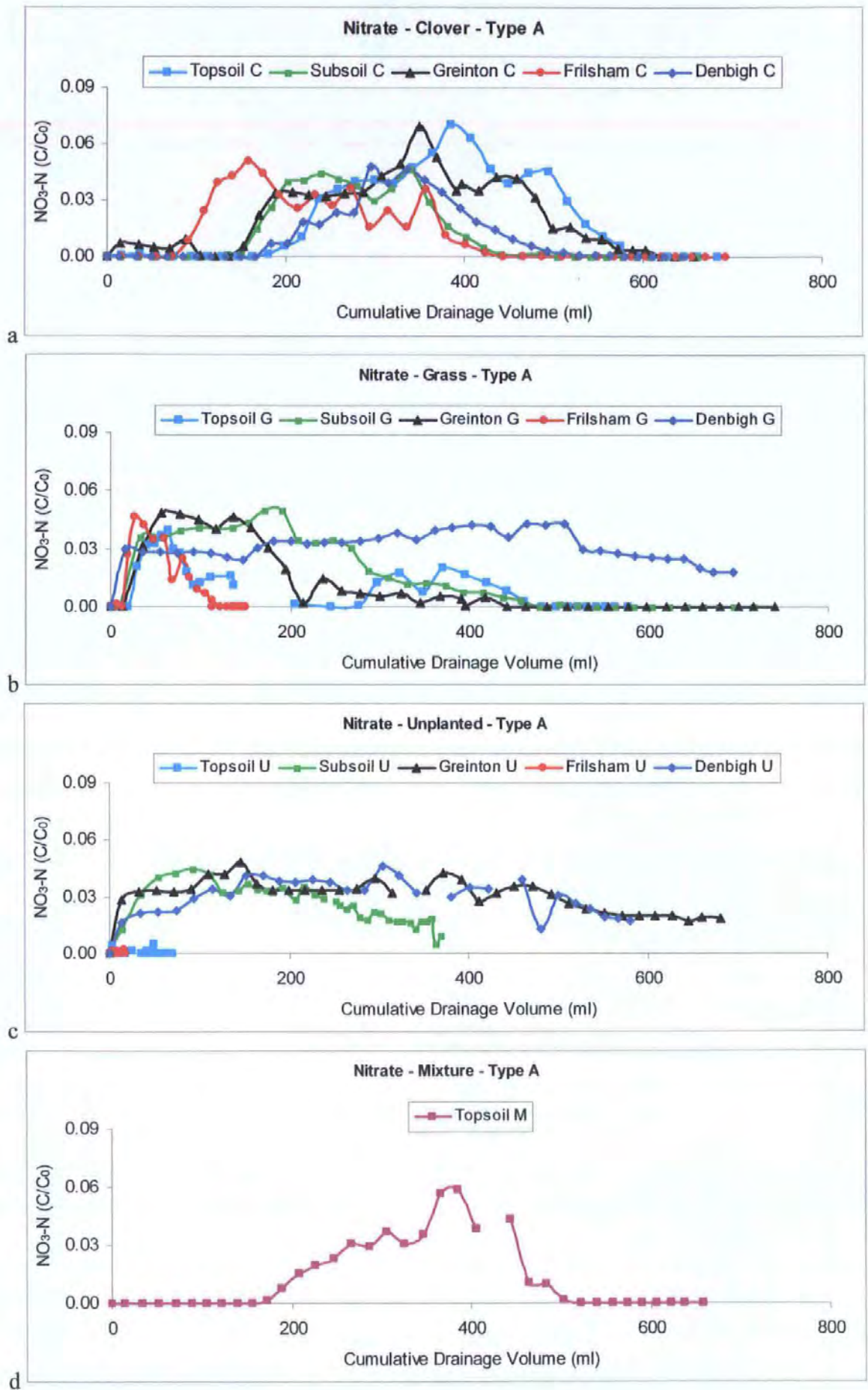
Figure 5.34. Experiment 12 - Type A. Elution Profiles: Nitrate-N concentrations for 16 treatments (4 planting regimes, 5 soil types).
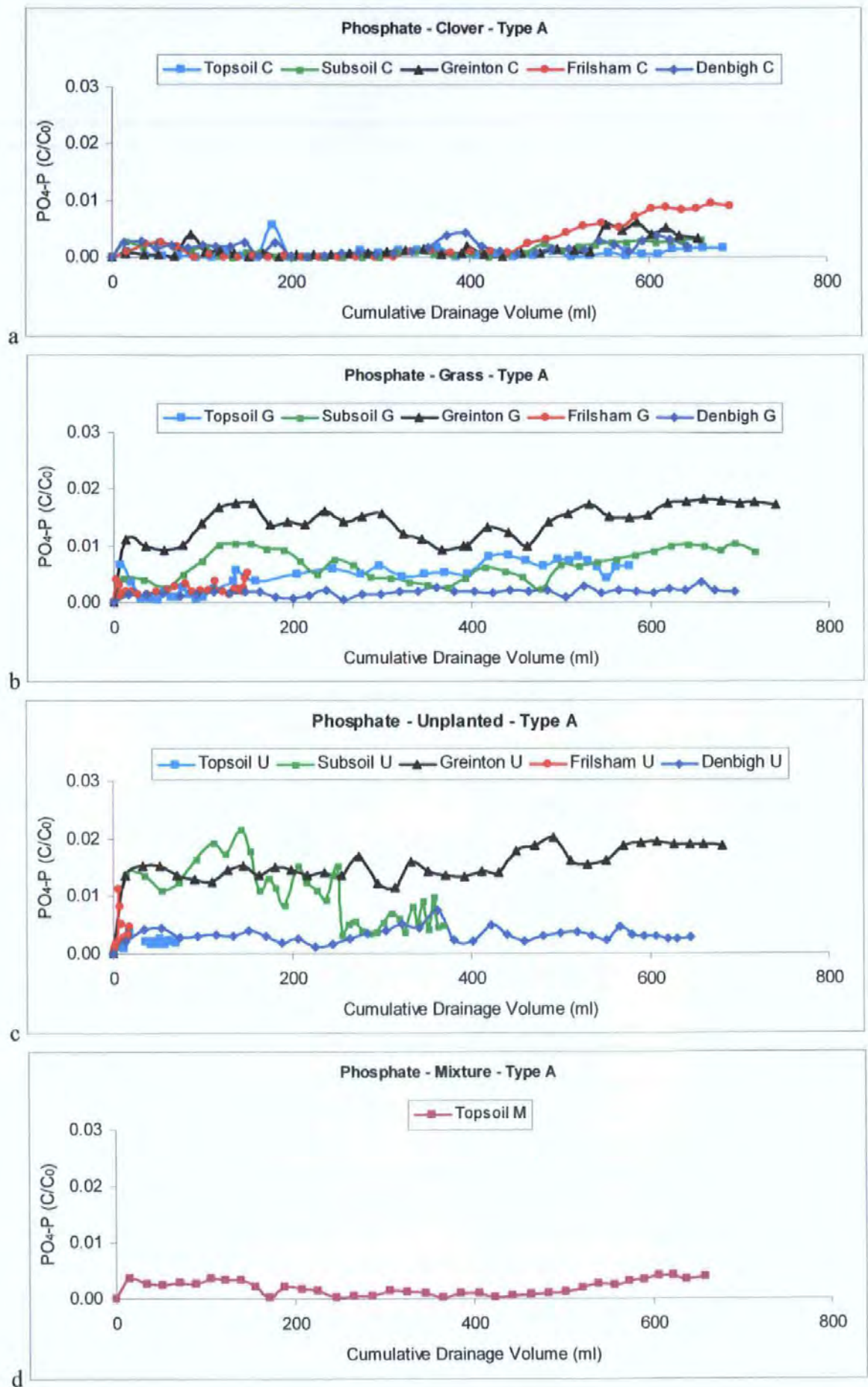
Figure 5.35. Experiment 12 - Type A. Elution Profiles: Phosphate-P concentrations for 16 treatments (4 planting regimes, 5 soil types).

Figure 5.36 (a) gives the same data for the Crediton series topsoil as presented in Figure 5.33. The data is repeated to show comparison between the tracer behaviour under Type A, B and C conditions (Type B and C experiments were only performed on the Crediton series topsoil). Figure 5.36 (b) gives the elution curves for bromide applied according to Type C conditions (i.e. the tracer solution is applied as a single aliquot under constant rain-fall). Figure 5.36 (c) gives the elution curves for bromide applied according to Type B conditions (i.e. the tracer solution is homogeneously distributed within unsaturated aggregates prior to rain-fall).

As previously discussed, the Type A elution profiles in Figure 5.36 (a) show that bromide quickly rose to an initial peak followed by a rapid decline and a rise to a higher secondary peak. This was observed for the planted treatments of the Crediton series topsoil, with the exception of ryegrass, where the initial peak was higher than the second. By comparison, Figure 5.36 (b) gives the elution profile of bromide when applied as a single aliquot of higher solution concentration (Type C conditions).

The breakthrough for white clover under Type C conditions (Figure 5.36 (b)) occurred at a much lower drainage volume and with a sharper peak than the Type A experiment (Figure 5.36 (a)). This was as expected: due to the higher concentration of the pulse solution applied over a much shorter period of time. However, the shape of the elution curve may also suggest a greater degree of preferential flow. The method of applying the pulse, showed no major difference in the elution of bromide from the mixed species, despite the differences in the initial water content of the soil and the concentration of the pulse solution (Figure 5.36 (a) and (b)).

The bromide leached beneath ryegrass showed different characteristics under Type C conditions (Figure 5.36 (b)) to those observed under Type A (Figure 5.36 (a)): the initial

214

peak was not as high and the secondary peak was higher. This elution curve for ryegrass showed a similar trend and concentration to that of the unplanted soil (Figure 5.36 (b)). Type A and C conditions cannot be compared for the unplanted controls because the drainage volume and concentration was low in the Type A experiment.

Figure 5.36 (c) gives the elution curves for bromide applied according to Type B conditions (i.e. the tracer solution is homogeneously distributed within the soil). Figure 5.36 (c) is scaled lower than Figure 5.36 (a) and (b), indicating the greater degree of dilution and diffusion into micropores due to the method of applying the pulse. Under such conditions, it is expected that the infiltrating water will move past the aggregates leaving the tracer behind. This was not observed in the elution of the unplanted control, which quickly peaked with the highest concentration and slowly declined to background levels (Figure 5.36 (c)). This suggests that the unplanted control had fewer micropores than the planted soils. When the pulse is held in micropore water, diffusion to the mobile water will take longer and so leaching will be delayed. A later breakthrough and lower concentrations was observed in the elution profiles of both white clover and the mixed species, compared to the unplanted control and ryegrass (Figure 5.36 (c)). This suggests that soils beneath white clover and the mixed species had more micropores.

Figure 5.37 (a), (b) and (c) gives the elution profiles for nitrate-N leached under Type A, C and B conditions, respectively. The elution profiles for nitrate under Type A and C experiments (Figure 5.37) parallel those observed for bromide (Figure 5.36): the relative concentrations for nitrate-N were lower than bromide, but the differences in the curves between treatments were of similar proportions for both tracers; the maximum peak concentrations also occurred at similar breakthrough volumes. Major differences were seen in the initial shape of the curves for the unplanted control, clover and the mixed species: the nitrate curves lacked the first peak observed for bromide. Furthermore, all nitrate curves declined to background levels more rapidly than the bromide curves.

The nitrate-N leached beneath the planted soils was low under Type B conditions compared to Type A and C (Figure 5.37). As suggested for bromide, this indicated the greater degree of dispersion and diffusion into micropores. The nitrate elution profile for the unplanted soil under Type B conditions (Figure 5.37) was analogous to that of bromide (Figure 5.36). The most notable was that both tracers were leached at the same relative concentrations. This supports the idea of the unplanted control having fewer micropores than the planted soils. If the unplanted nitrate elution curve was lower than bromide, the higher nitrate concentration of the unplanted control compared to the other soils would be a function of nitrate up-take in the planted soils.

Figure 5.38 (a), (b) and (c) gives the elution profiles for phosphate-P leached under Type A, C and B conditions, respectively. The relative phosphate-P concentration is scaled lower than both bromide (Figure 5.36) and nitrate (Figure 5.37). As previously discussed, the concentration of phosphate-P continuously fluctuates rather than peaks. Figure 5.38 (a) shows that the ryegrass leached the greatest amount and concentration of phosphate-P. The elution profiles for the white clover and the mixed species were fairly similar, although the mixed species gave a higher initial concentration (Figure 5.38 (a)).

The elution profiles for phosphate-P showed different characteristics under Type C conditions (Figure 5.38 (b)) to those observed under Type A (Figure 5.38 (a)). Under Type C the unplanted control leached the most phosphate-P, and the concentration of the grass and the mixed species was much lower than under Type A. the unplanted control under Type B conditions (Figure 5.38 (c)) leached the most phosphate-P, as also observed under Type B for both bromide (Figure 5.36 (c)) and nitrate (Figure 5.37 (c)).
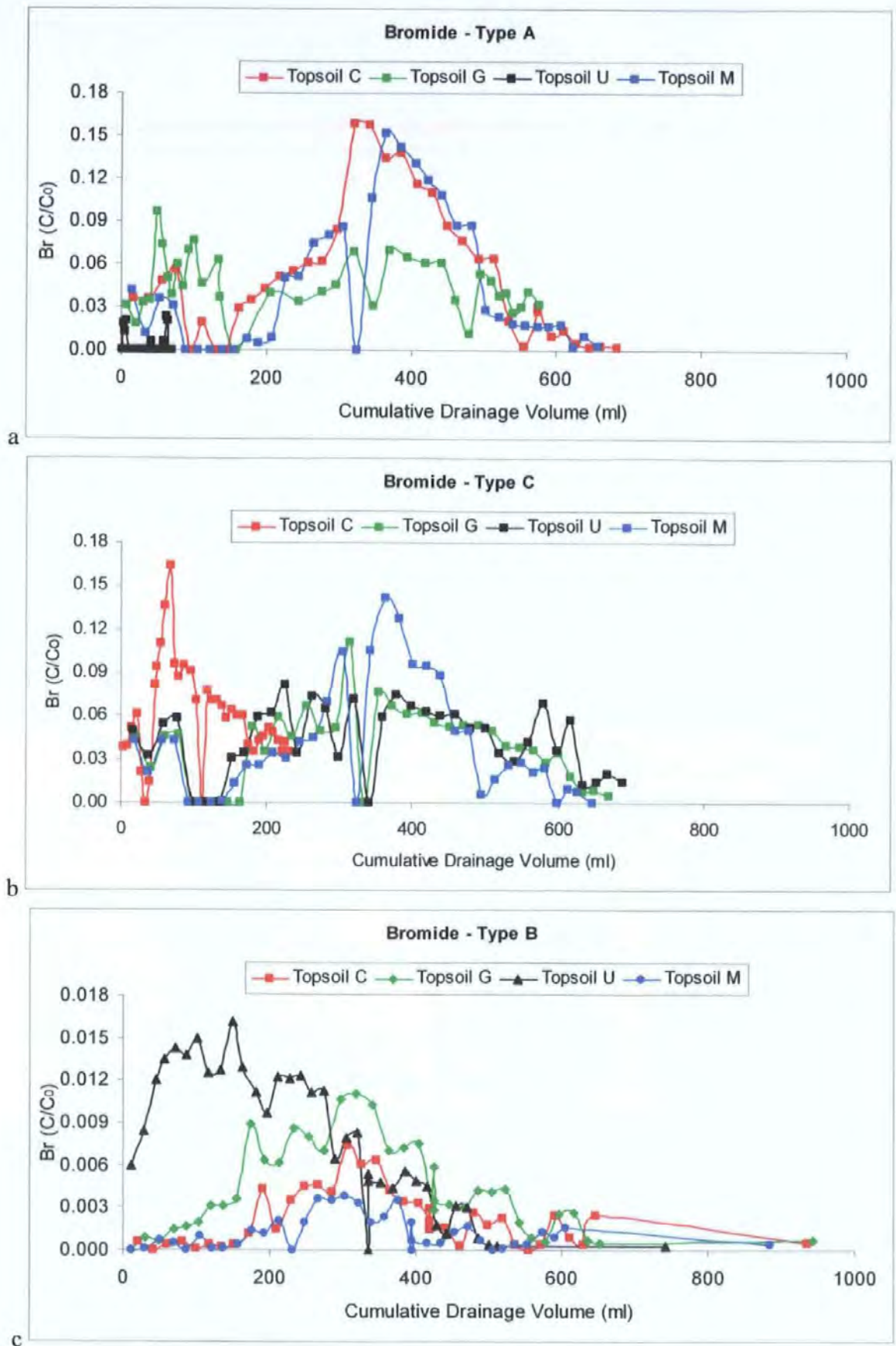
Figure 5.36. Experiments 12-14 - Type A, Type B and Type C. Elution Profiles: Mean bromide concentrations for 4 planting regimes under Crediton series re-packed topsoil. (C= clover, G = grass, M= mixed species, U= unplanted control).
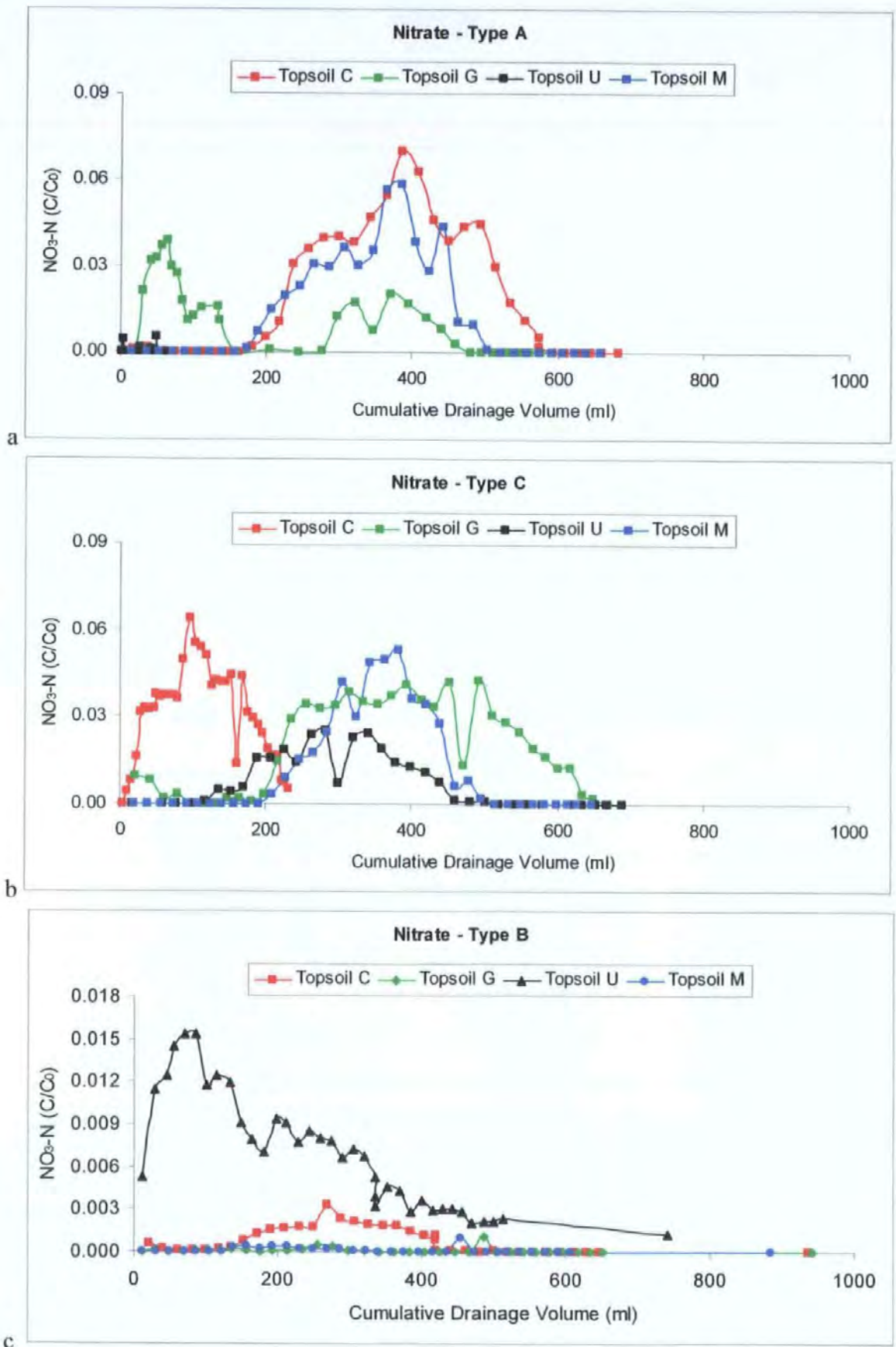
Figure 5.37. Experiments 12-14 - Type A, Type B and Type C. Elution Profiles: Mean nitrate-N concentrations for 4 planting regimes under Crediton series re-packed topsoil. (C= clover, G = grass, M= mixed species, U= unplanted control).
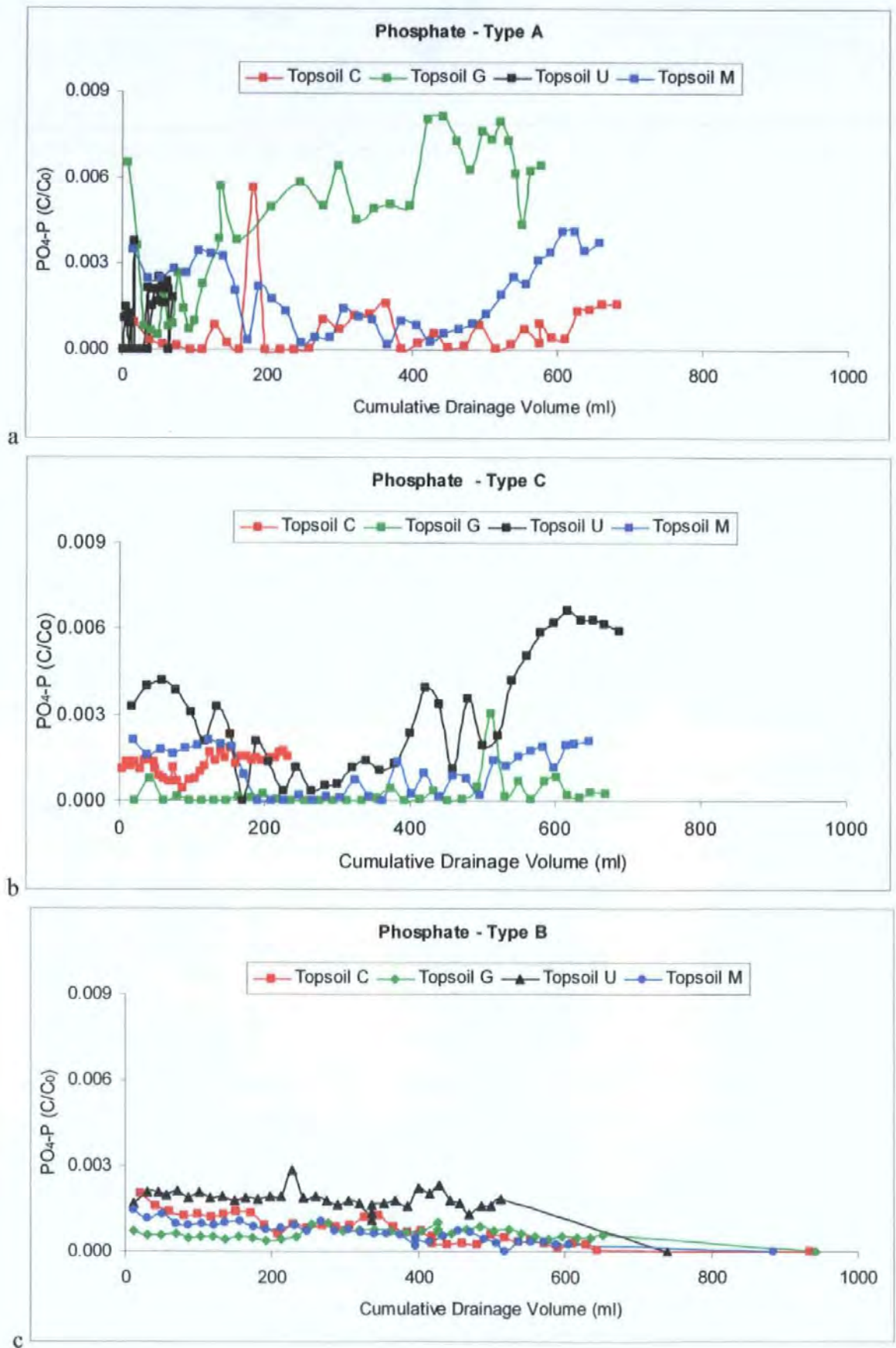
Figure 5.38. Experiments 12-14 - Type A, Type B and Type C. Elution Profiles: Mean phosphate-P concentrations for 4 planting regimes under Crediton series re-packed topsoil. (C= clover, G = grass, M= mixed species, U= unplanted control).

5.16. Summary of results for Column Experiment 2 – Leaching #12-14

To semi-quantify the series of elution profiles presented in Section 5.15 (Figure 5.33 to Figure 5.38), the curves were classified into three types as proposed by Holden *et al.* (1995b). These types are explained in Table 5.12 and characterised in Table 5.13 to Table 5.14. The elution profiles presented in this study were not all as well defined as those summarised by Holden *et al.* (1995b).

Table 5.12. Classification of breakthrough curves as proposed by Holden *et al.* (1995b).

Type I	Type II	Type III
Tracer quickly peaks with high concentration and then rapidly declines to near background level.	Tracer concentration slowly rises slightly above background and very slowly returns	Tracer quickly rises to an initial peak (but with lower concentration than Type I) followed by a rapid decline and a slow rise to a second peak

The mass and concentration leached from each of the Type A, Type B and Type C experiments are given in tables Table 5.13, Table 5.15 and Table 5.14, respectively. The greatest mass recovery was for bromide from white clover grown in Crediton series topsoil.

Table 5.13. Numerical values of mass and concentration leached from the Type A Experiments, including breakthrough curve (BTC) Type as proposed by Holden et al. (1995).

Tracer	Plant Type	Soil Type^	BTC Type[#]	Maximum Relative Concentration	% mg* recovered
Bromide	Clover	Topsoil	*III*	0.16	96.71
Bromide	Clover	Subsoil	*III*	0.15	83.67
Bromide	Clover	Greinton	*III*	0.11	82.28
Bromide	Clover	Frilsham	*III*	0.16	73.68
Bromide	Clover	Denbigh	*III*	0.07	47.62
Bromide	Grass	Topsoil	*III*	0.10	73.40
Bromide	Grass	Subsoil	*III*	0.14	90.92
Bromide	Grass	Greinton	*III*	0.16	88.57
Bromide	Grass	Frilsham	*I*	0.13	36.72
Bromide	Grass	Denbigh	**II**	0.09	95.52
Bromide	Unplanted	Topsoil	Low drainage	0.02	0.63
Bromide	Unplanted	Subsoil	**III**	0.14	57.79
Bromide	Unplanted	Greinton	*III*	0.16	93.63
Bromide	Unplanted	Frilsham	Low drainage	0.11	1.32
Bromide	Unplanted	Denbigh	*III*	0.11	91.19
Bromide	Mixture	Topsoil	**III**	0.15	86.55
Nitrate-N	Clover	Topsoil	**II**	0.07	41.26
Nitrate-N	Clover	Subsoil	**II**	0.05	23.79
Nitrate-N	Clover	Greinton	**II**	0.07	41.79
Nitrate-N	Clover	Frilsham	**II**	0.05	25.72
Nitrate-N	Clover	Denbigh	**II**	0.05	21.70
Nitrate-N	Grass	Topsoil	**II**	0.04	14.42
Nitrate-N	Grass	Subsoil	**II**	0.05	34.37
Nitrate-N	Grass	Greinton	**II**	0.05	24.11
Nitrate-N	Grass	Frilsham	*I*	0.05	6.97
Nitrate-N	Grass	Denbigh	**II**	0.04	63.46
Nitrate-N	Unplanted	Topsoil	Low drainage	0.01	0.12
Nitrate-N	Unplanted	Subsoil	*II*	0.05	30.24
Nitrate-N	Unplanted	Greinton	*II*	0.05	59.02
Nitrate-N	Unplanted	Frilsham	Low drainage	0.002	0.04
Nitrate-N	Unplanted	Denbigh	*II*	0.05	51.48
Nitrate-N	Mixture	Topsoil	**II**	0.06	26.84
Phosphate-P	Clover	Topsoil	*II* Low conc	0.006	1.33
Phosphate-P	Clover	Subsoil	*II* Low conc	0.003	2.36
Phosphate-P	Clover	Greinton	*II* Low conc	0.006	2.81
Phosphate-P	Clover	Frilsham	*II* Low conc	0.009	5.35
Phosphate-P	Clover	Denbigh	*II* Low conc	0.004	3.10
Phosphate-P	Grass	Topsoil	*II*	0.008	8.33
Phosphate-P	Grass	Subsoil	*II*	0.010	13.57
Phosphate-P	Grass	Greinton	*II*	0.018	30.29
Phosphate-P	Grass	Frilsham	Low drainage	0.005	0.97
Phosphate-P	Grass	Denbigh	*II*	0.004	3.55
Phosphate-P	Unplanted	Topsoil	Low drainage	0.004	0.30
Phosphate-P	Unplanted	Subsoil	*II*	0.022	12.12
Phosphate-P	Unplanted	Greinton	*II*	0.020	30.38
Phosphate-P	Unplanted	Frilsham	Low drainage	0.011	0.16
Phosphate-P	Unplanted	Denbigh	*II*	0.008	6.07
Phosphate-P	Mixture	Topsoil	*II* Low conc	0.004	3.57

^ Topsoil and subsoil refer to soils of the Crediton series

[#] Samples that showed the exact characteristics of BTC Type proposed by Holden et al. (1995) are highlighted in bold, whereas those that showed similar characteristics are in italics. Low refers to low concentrations or drainage volumes where specified.

* mg for bromide and nitrate-N, µg for phosphate-P

221

Table 5.14. Numerical values of mass and concentration leached from the Type B Experiments, including breakthrough curve (BTC) Type as proposed by Holden *et al.* (1995).

Tracer	Plant Type	Soil Type ^	BTC Type[#]	Maximum Relative Concentration	% mg* recovered
Bromide	Clover	Topsoil	**II**	0.01	27.20
Bromide	Grass	Topsoil	**II**	0.01	55.55
Bromide	Unplanted	Topsoil	*III*	0.02	74.13
Bromide	Mixture	Topsoil	**II**	0.004	15.06
Nitrate-N	Clover	Topsoil	**II**	0.003	8.76
Nitrate-N	Grass	Topsoil	*II* Low conc	0.001	0.94
Nitrate-N	Unplanted	Topsoil	**III**	0.02	69.19
Nitrate-N	Mixture	Topsoil	*II* Low conc	0.001	1.16
Phosphate-P	Clover	Topsoil	*II* Low conc	0.002	9.12
Phosphate-P	Grass	Topsoil	*II* Low conc	0.001	7.63
Phosphate-P	Unplanted	Topsoil	*II* Low conc	0.003	15.54
Phosphate-P	Mixture	Topsoil	*II* Low conc	0.001	7.63

^ Topsoil refers to soils of the Crediton series

[#] Samples that showed the exact characteristics of BTC Type proposed by Holden et al. (1995) are highlighted in bold, whereas those that showed similar characteristics are in italics. Low refers to low concentrations or drainage volumes where specified.

* mg for bromide and nitrate-N, µg for phosphate-P

Table 5.15. Numerical values of mass and concentration leached from the Type C Experiments, including breakthrough curve (BTC) Type as proposed by Holden *et al.* (1995).

Tracer	Plant Type	Soil Type ^	BTC Type[#]	Maximum Relative Concentration	% mg* recovered
Bromide	Clover	Topsoil	*I*	0.03	40.48
Bromide	Grass	Topsoil	*III*	0.02	75.44
Bromide	Unplanted	Topsoil	*III*	0.01	86.36
Bromide	Mixture	Topsoil	*III*	0.02	76.99
Nitrate-N	Clover	Topsoil	*I*	0.01	20.82
Nitrate-N	Grass	Topsoil	**II**	0.01	36.51
Nitrate-N	Unplanted	Topsoil	**II**	0.004	13.50
Nitrate-N	Mixture	Topsoil	**II**	0.01	21.84
Phosphate-P	Clover	Topsoil	Low conc	0.0003	0.84
Phosphate-P	Grass	Topsoil	Low conc	0.001	0.48
Phosphate-P	Unplanted	Topsoil		0.001	5.92
Phosphate-P	Mixture	Topsoil	Low conc	0.0004	1.91

^ Topsoil refers to soils of the Crediton series

[#] Samples that showed the exact characteristics of BTC Type proposed by Holden et al. (1995) are highlighted in bold, whereas those that showed similar characteristics are in italics. Low refers to low concentrations or drainage volumes where specified.

* mg for bromide and nitrate-N, µg for phosphate-P

5.17. Results – Intact 0.5 m monolith lysimeters

The results from the intact 0.5 m monolith lysimeters are presented in this section. The data are illustrated as elution profiles of relative tracer concentration (i.e. concentration in the effluent divided by concentration applied (C/C_0)) against both time (in hours) and cumulative drainage volume (in L) (Figure 5.39 to Figure 5.44). These figures show the transport behaviour of the tracers bromide, nitrate and phosphate through soil under white clover, ryegrass, a mixture of the two species, and an unplanted control.

Data are presented for the leaching characteristics within treatments, in the order of white clover, ryegrass, mixed species and the unplanted control, for the transport dynamics of each tracer, in the order of bromide, nitrate-N and phosphate-P. The data is then compared between treatments and tracers. Section 5.17.5 gives the drainage characteristics of each treatment in terms of flow rate (ml min^{-1}) and volume (L). This water release is then related to the tracer transportation for each treatment.

Experimental details are previously given (Section 5.6.6). Each graph is for an individual experiment. The data is not averaged as only one experiment was performed using only one replicate of each soil block. Each line on the graphs represents a single drainage channel at the base of the soil, separated by the 10 x 10 collection plate explained in Section 5.6.3.

5.17.1. Bromide leaching.

Figure 5.39 (a), (b), (c) & (d) illustrate the transport of Br beneath each treatment as a function of drainage volume. Figure 5.39 shows that white clover had a greater amount of bromide in the drainage water compared to ryegrass, the mixed species and the unplanted soil. Figure 5.39 also shows that a greater number of channels drained at the base of the soil under clover, and that the leaching of Br continued for longer than that beneath the

223

grass and mixture. The leaching of Br appears to be bi- or multi-modal as the concentration fluctuates during drainage. The maximum relative concentration drained beneath clover (0.17) was similar to the maximum from the mixed species (0.16); these maxima appeared at around 1 L and 50 ml of drainage water, for the clover and mixture, respectively. Although the clover reached its maximum at 1 L, several sharp peaks were observed in <500 ml.

The maximum relative leachate concentration beneath grass (0.10) was similar to the maximum from the unplanted control (0.11), both occurring in <150 ml of drainage water. Bromide draining beneath all treatments showed high concentrations at <500 ml, which peaked again between ~1-2 L of drainage water, but did not increase above those initial peaks. The clover and mixture showed a third peak between 2L and 3L, which then decreased towards the maxima drainage volume (~7.5L clover; ~6.5L mixed species). A channel draining beneath the unplanted soil eluted an above average Br concentration after 2L and again ~8L, with no drainage in between.

Figure 5.40 (a), (b), (c) & (d) illustrate the transport of bromide beneath each treatment as a function of time; the concentrations are the same as those presented in Figure 5.39. Figure 5.40 shows that all maxima peaks were before 50 hours of drainage. The highest concentrations were from clover and the mixture, both with initial peaks at 10 hours, and again at ~30-40 hours. Channels draining beneath clover continued to rise and fall between 70-150 hours. The Br leaching profile of ryegrass was similar to that of the unplanted control, the latter having slightly higher concentrations and more drainage channels.

By comparison of Figure 5.39 and Figure 5.40, the differences in the Br elution profiles as a function of time and drainage volume are apparent. In turn, this is a function of drainage rate and soil structure.

a)
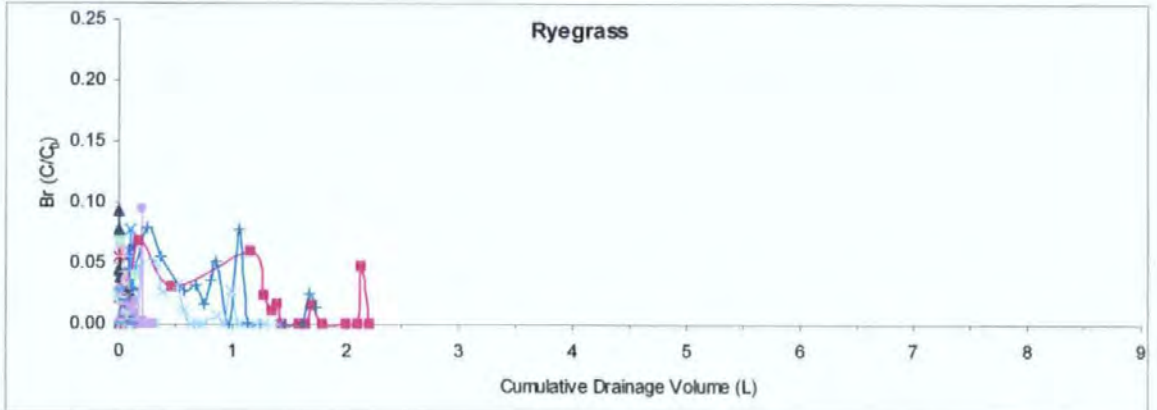
b)
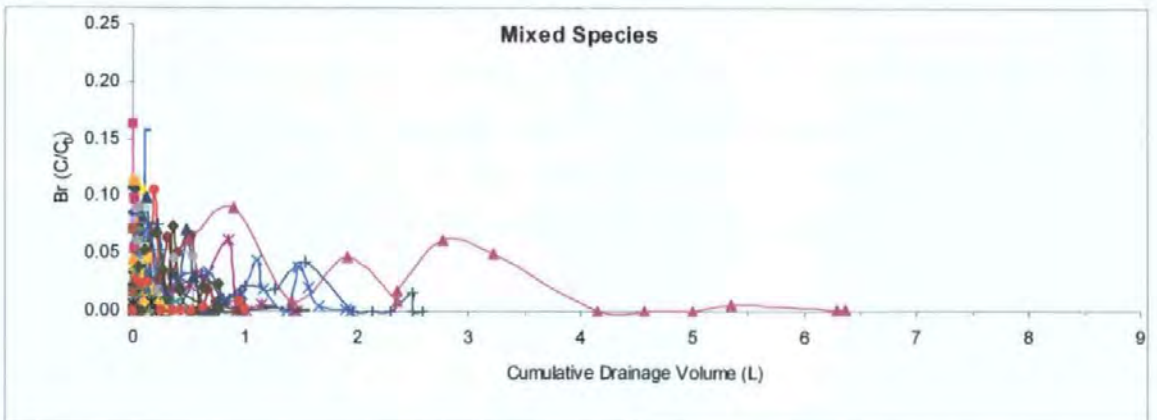
c)
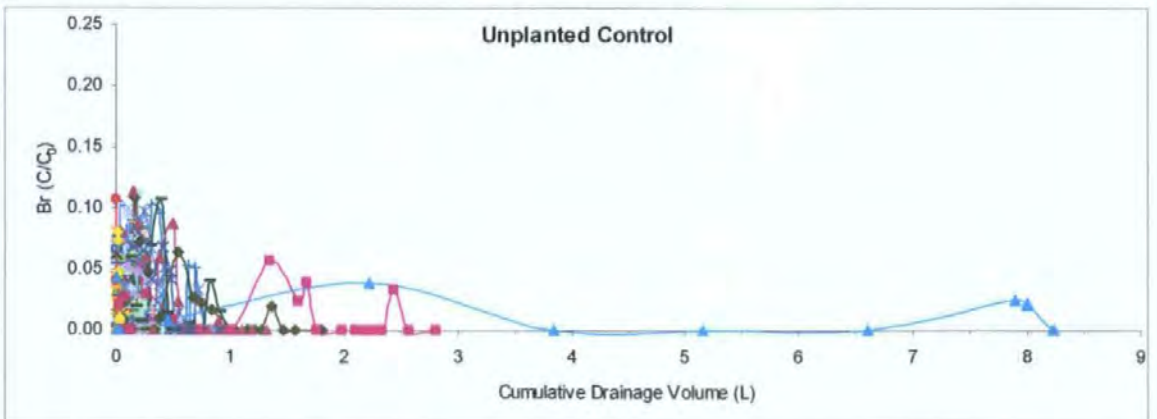
d)

Figure 5.39 Bromide elution profiles from the intact 0.5 m lysimeters as a function of drainage volume. Each line represents a drainage channel.
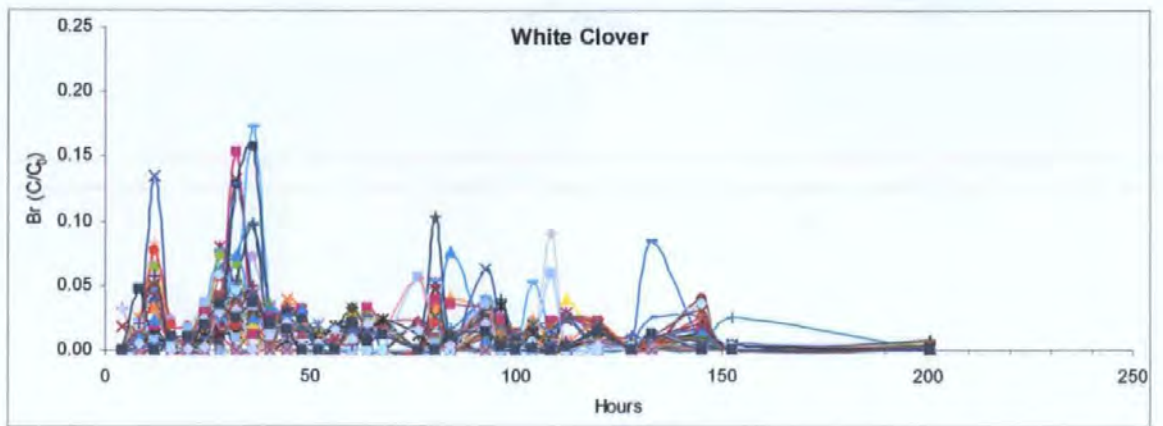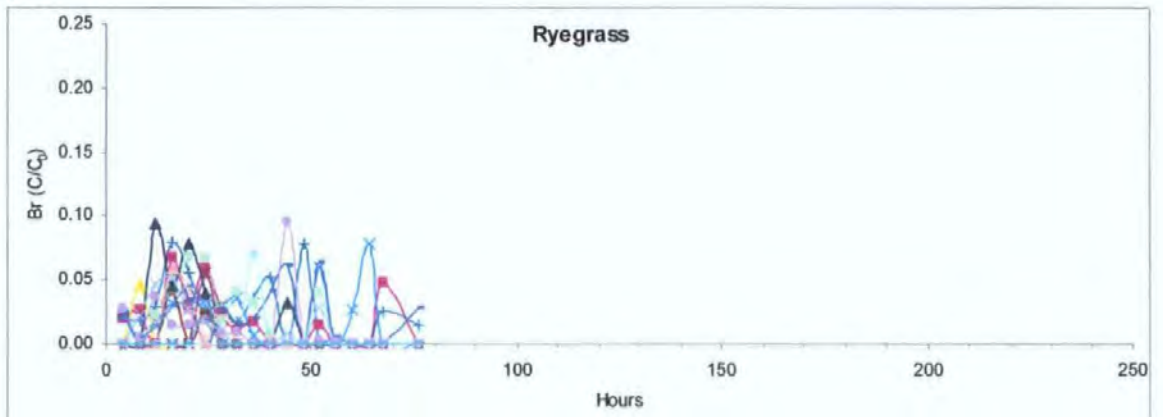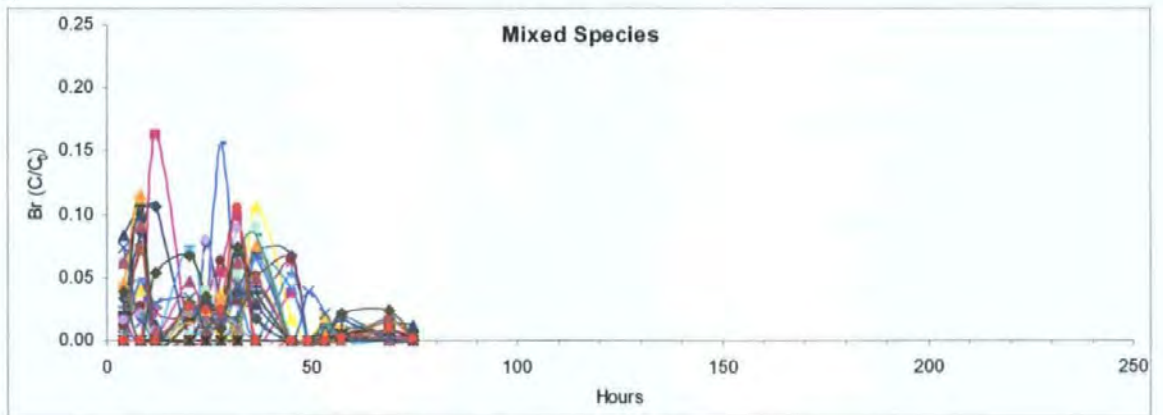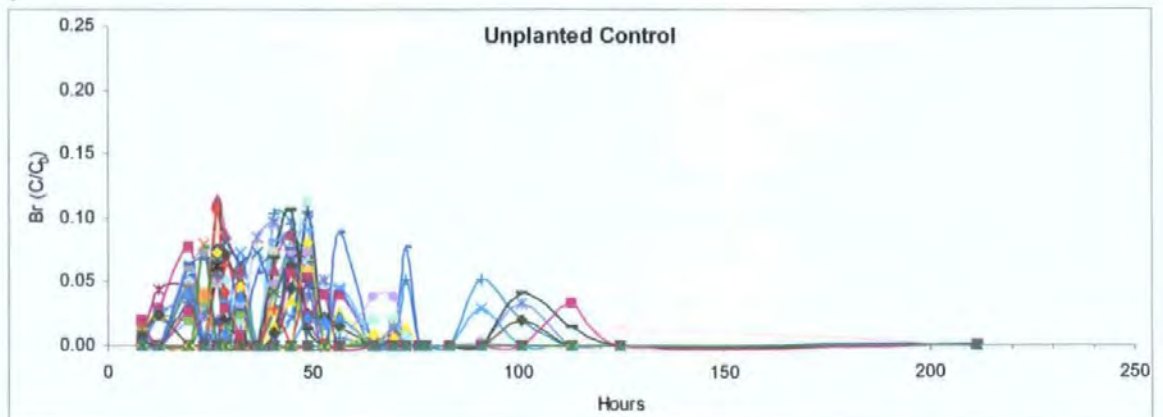
Figure 5.40. Bromide elution profiles from the intact 0.5 m lysimeters as a function of time. Each line represents a drainage channel.

5.17.2. Nitrate-N leaching.

Figure 5.41 (a), (b), (c) & (d) illustrate the transport of N beneath each treatment as a function of drainage volume. Figure 5.41 shows that clover had a much greater amount of nitrate-N leached than grass and unplanted soils. The maximum concentration from clover (0.21) occurred in the first 200 ml. This peak was greater than the maxima for both the grass (0.05) and unplanted control (0.01), but less than the mixed species (0.22), which occurred around 400 ml. A few channels draining below the mixed species had high initial peaks characteristic of the clover, and several channels with low drainage concentrations like the unplanted soil.

For the clover treatment, the elution profile of nitrate-N as a function of drainage volume (Figure 5.41) showed a similar trend to that of the equivalent bromide profile (Figure 5.39) The mean relative concentration of clover bromide (0.008), and clover nitrate-N (0.009) were similar, reflecting a similar dilution of the tracers in the soil. The nitrate-N concentrations for the unplanted control and ryegrass treatment were much lower than bromide.

Figure 5.42 (a), (b), (c) & (d) illustrate the transport of nitrate-N beneath each treatment as a function of time. Several channels beneath the clover and the mixture gave high sharp peaks at ~30 hours and 30-40 hours, respectively. At the scale shown in Figure 5.42 (and Figure 5.41) it is impossible to assess the behaviour of nitrate-N leaching from the grass treatment (and the unplanted soil). However, it is clear that the concentration was much lower than the clover and mixed species. For the unplanted control, the behaviour of the individual channels leaching nitrate-N is slightly clearer as a function of time (Figure 5.41) compared to volume (Figure 5.42).
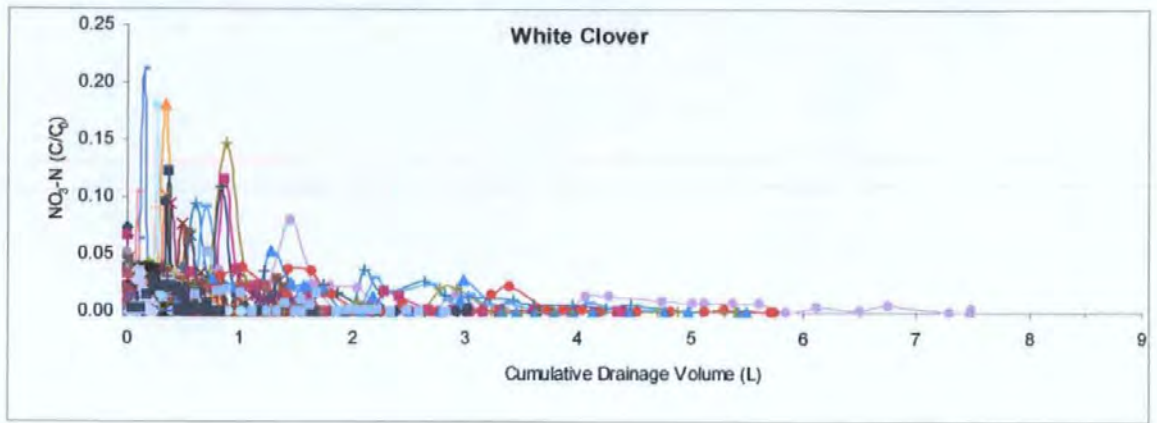
a)
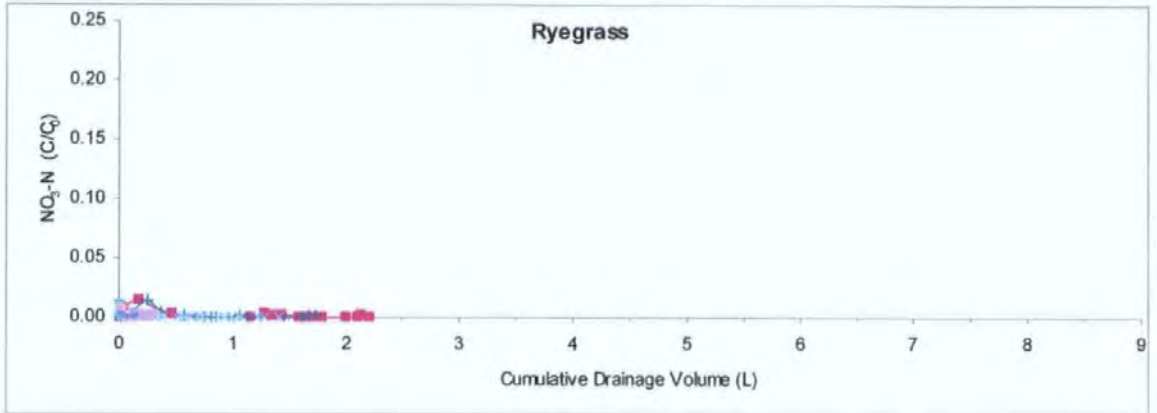
b)
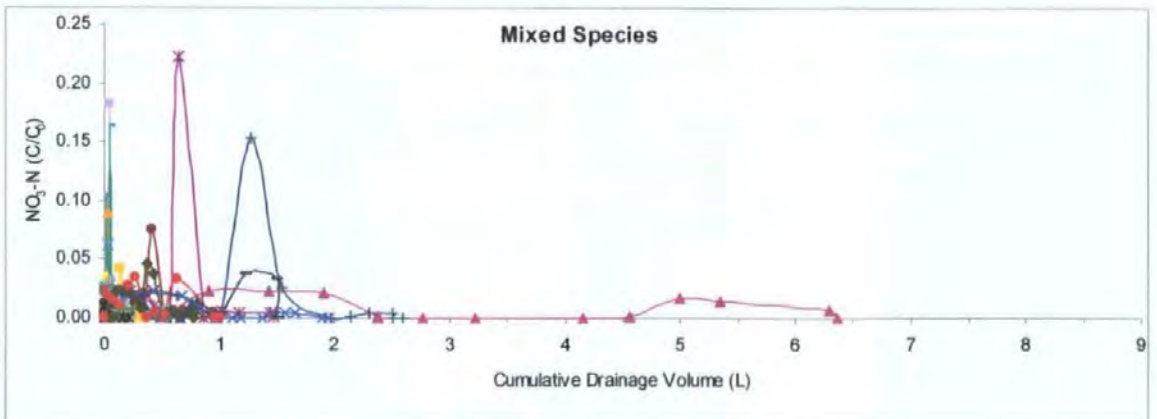
c)
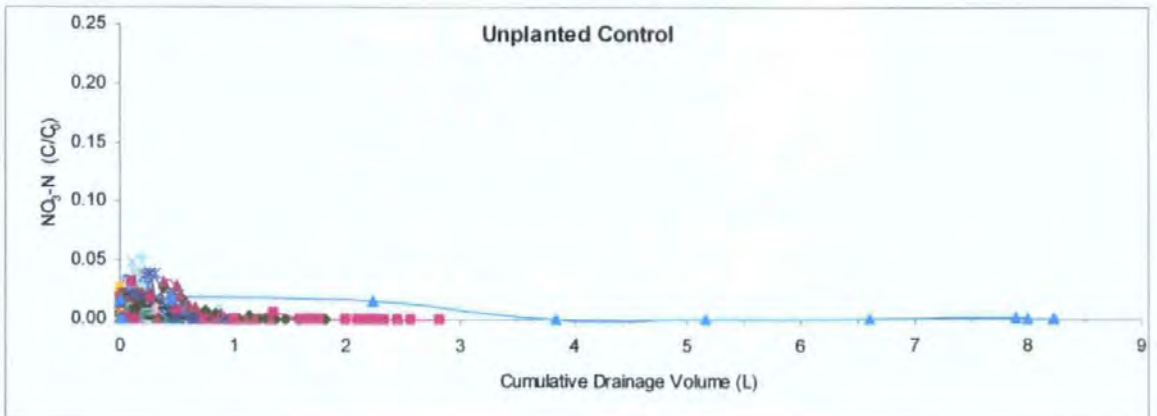
d)

Figure 5.41. Nitrate-N elution profiles from the intact 0.5 m lysimeters as a function of drainage volume. Each line represents a drainage channel.
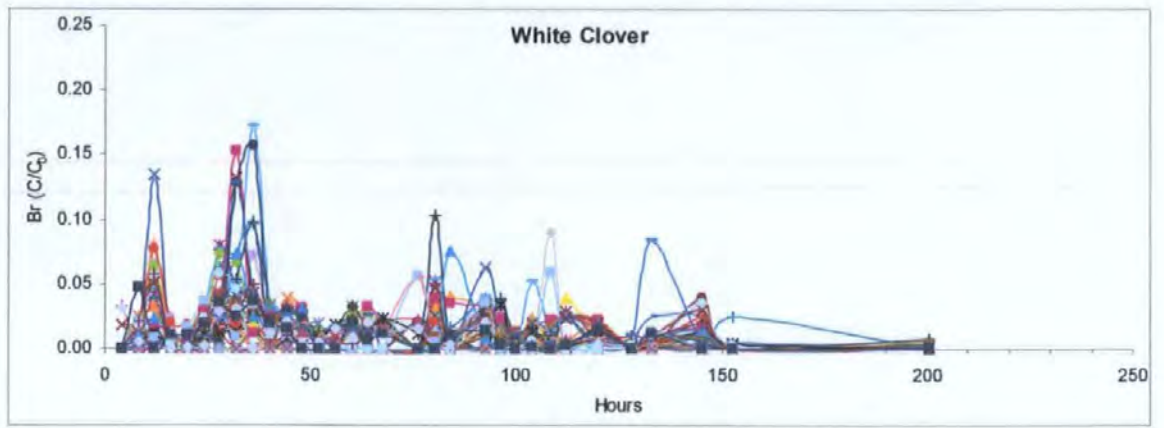
a)
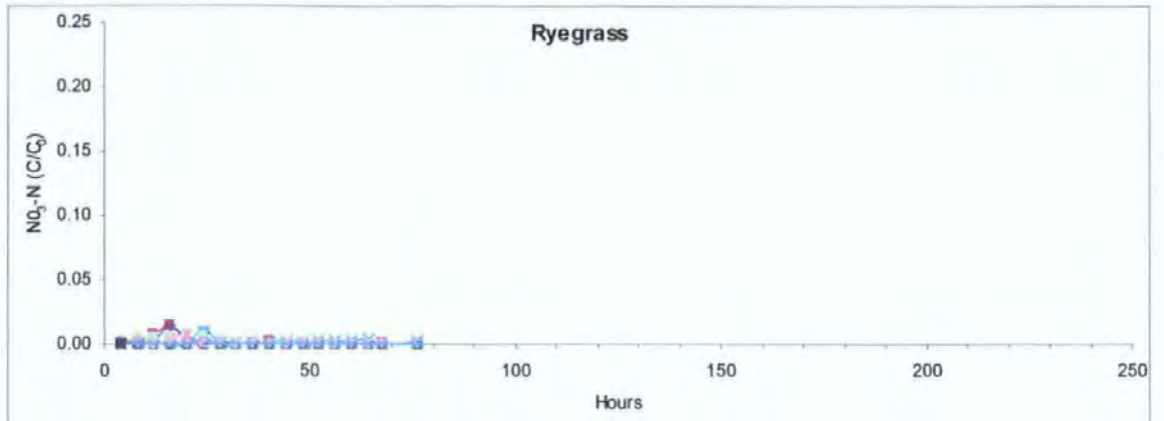
b)
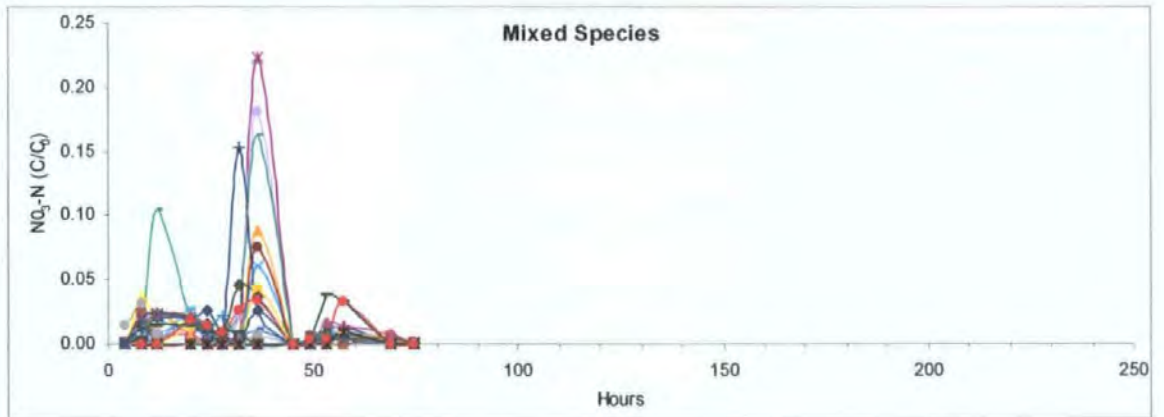
c)
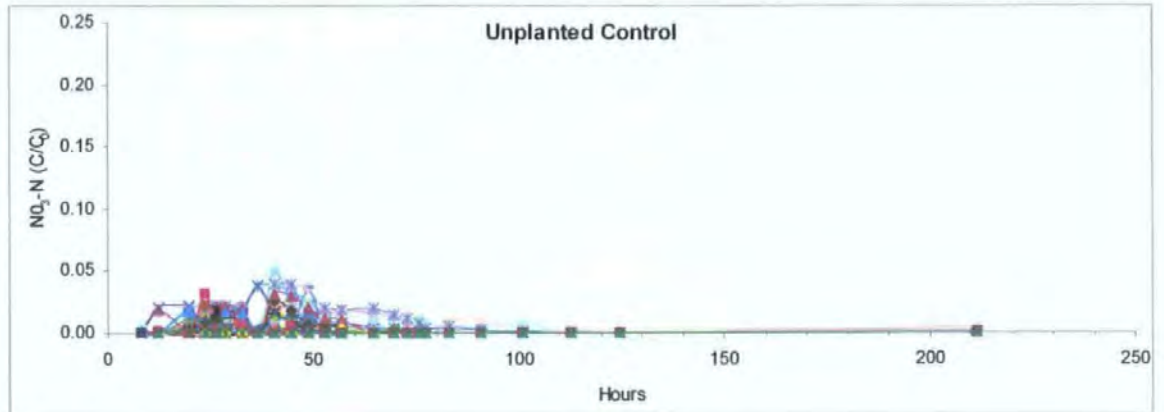
d)

Figure 5.42. Nitrate-N elution profiles from the intact 0.5 m lysimeters as a function of time. Each line represents a drainage channel.
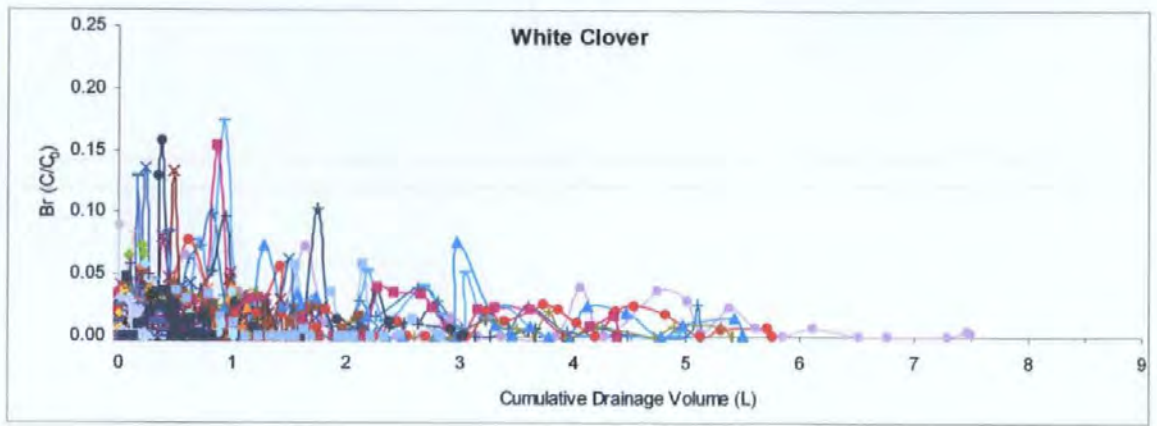
5.17.3. Phosphate-P leaching.

Figure 5.43 (a), (b), (c) & (d) illustrate the transport of phosphate-P beneath each treatment as a function of drainage volume. The scale is ten times lower than the bromide and nitrate-N graphs presented above, which shows that the relative concentrations of phosphate-P are much lower than both bromide and nitrate-N. This is a function of the reactive nature of phosphate-P, and the dominant chemical processes of adsorption/desorption which control the soil solution composition of phosphate-P. Figure 5.43 shows that the phosphate-P concentrations leached from both clover and the mixture do not rise and fall to same extent as bromide and nitrate-N. For all treatments, the maximum phosphate-P concentrations are in the first 1L of effluent. The unplanted control (Figure 5.43) shows that one of the drainage channels is behaving similar to that of bromide (Figure 5.39) with an elevated concentration at ~8L, the overall leaching pattern is also generally similar.

Figure 5.44 (a), (b), (c) & (d) illustrate the transport of phosphate-P beneath each treatment as a function of time. The scale is ten times lower than the bromide and nitrate-N graphs presented above. Figure 5.44 shows that the elution profile for phosphate-P is different to the previous elution characteristics shown for bromide and nitrate-N. For the leaching of bromide and nitrate-N, the concentrations from clover gave similar concentrations and characteristics to that of the mixed species. In the case of phosphate-P leaching, the clover is more liken to that of the unplanted soil. The mean relative phosphate-P concentrations leached from both clover and the unplanted control were the same (0.001). However, the maximum relative concentration was greater beneath the unplanted control (0.018) than the clover (0.010). The mixed species gave low relative concentrations like the grass at maxima of 0.004 and 0.005, respectively.
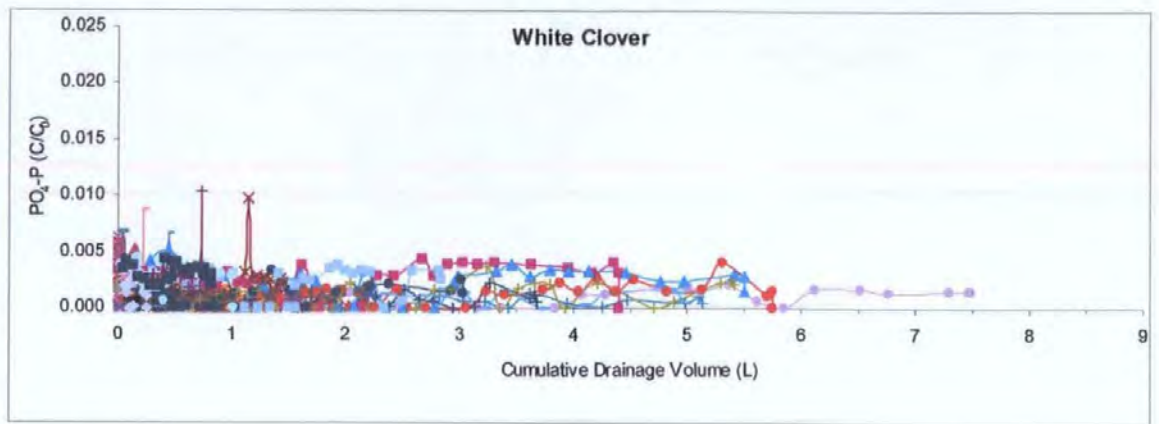
a)
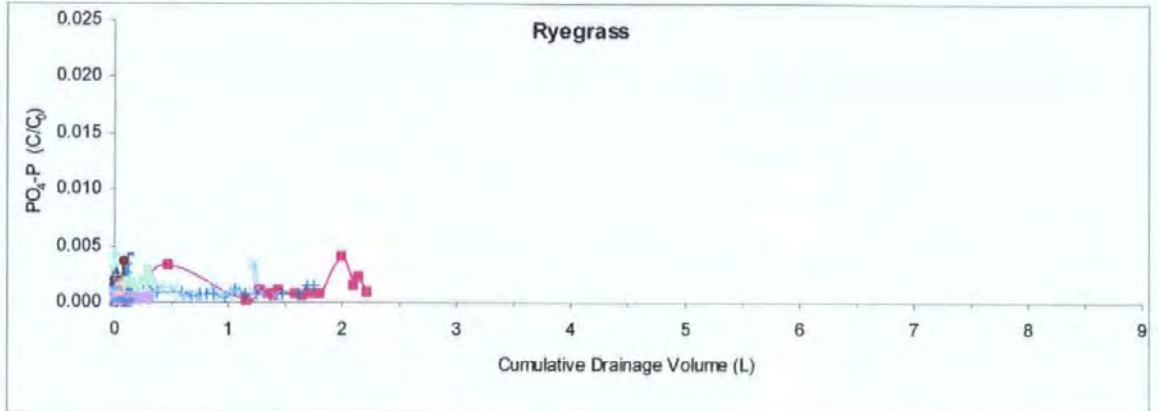
b)
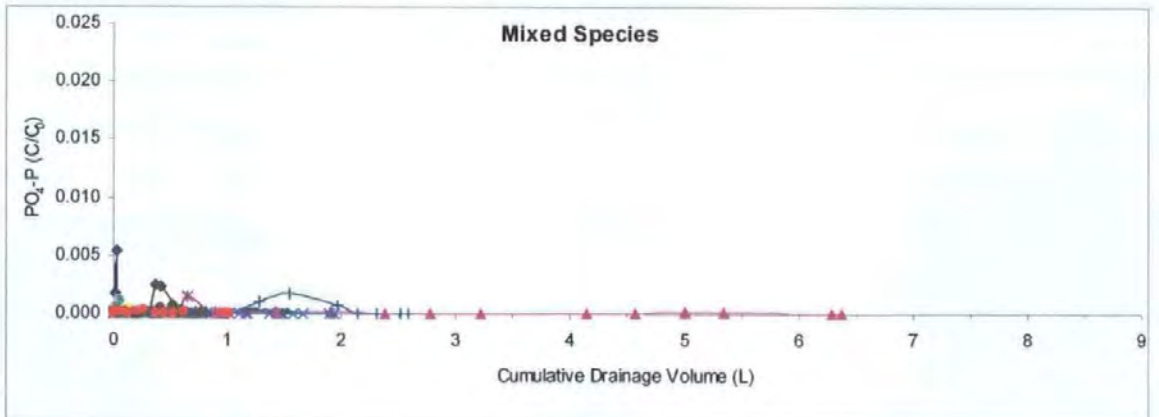
c)
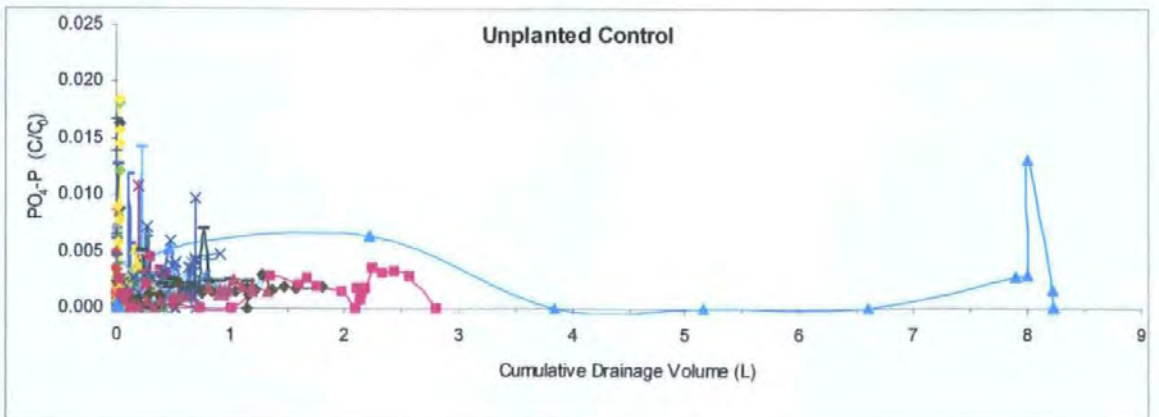
d)

Figure 5.43. Phosphate-P elution profiles from the intact 0.5 m lysimeters as a function of drainage volume. Each line represents a drainage channel. The relative concentration is shown at a scale ten times lower than pervious graphs for both bromide and nitrate-N.
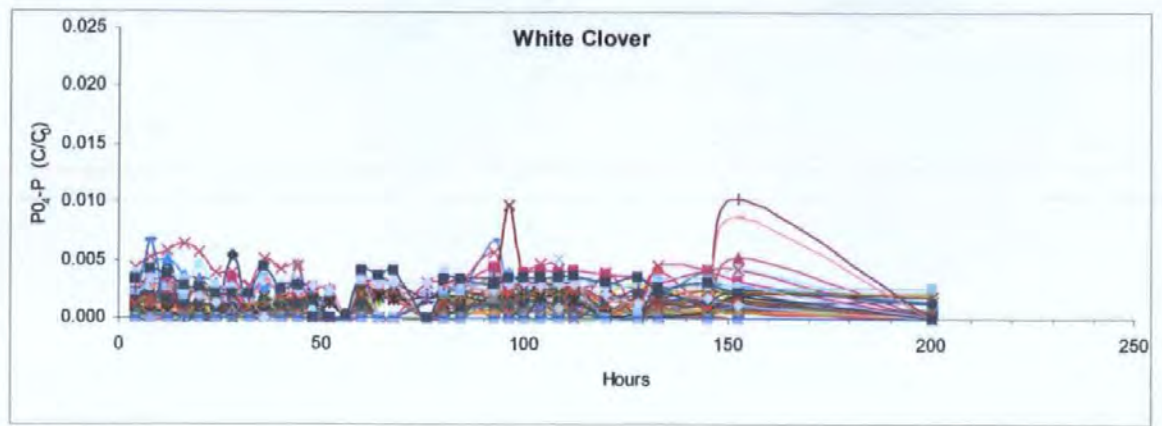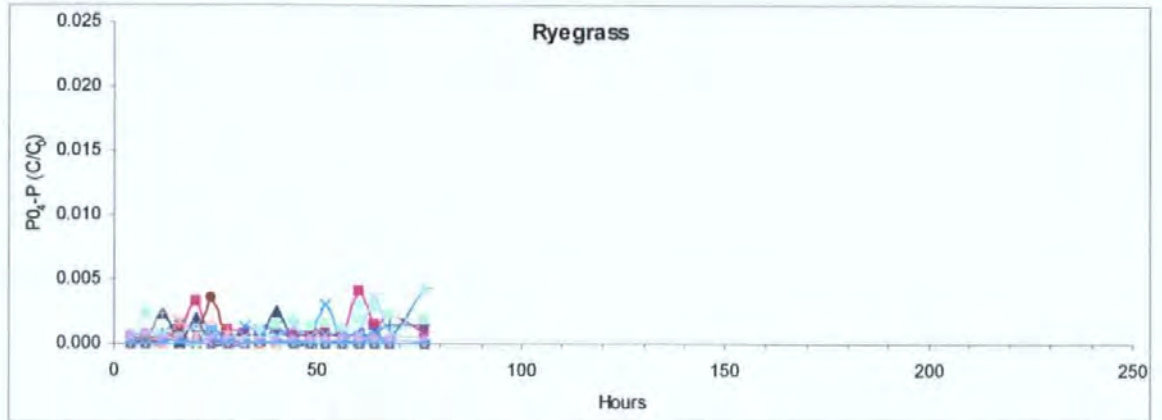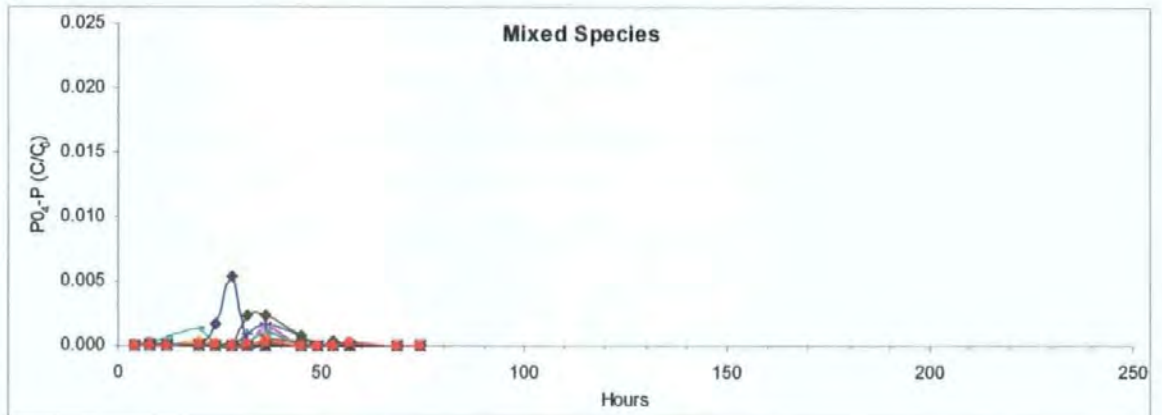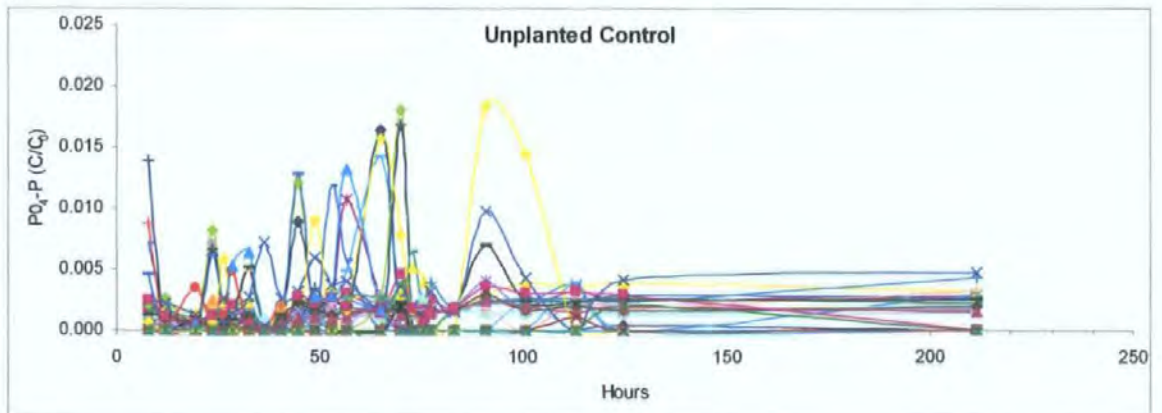
Figure 5.44. Phosphate-P elution profiles from the intact 0.5 m lysimeters as a function of time. Each line represents a drainage channel. The relative concentration is shown at a scale ten times lower than pervious graphs for both bromide and nitrate-N.

5.17.4. Bulk Elution profiles

The bulk elution profiles were calculated from the total mass and total drainage volume and each four-hourly collection and are given in Figure 5.45 (bromide), Figure 5.46 (nitrate-N) and Figure 5.47 (phosphate-P). These elution profiles show that the maximum relative concentrations for both bromide and nitrate-N were leached beneath white clover within 10-20 L; the maximum for the other plant treatments was leached in a lower drainage volume. An alternative way to present the data would be as relative concentration against time. This would be more representative of field studies.
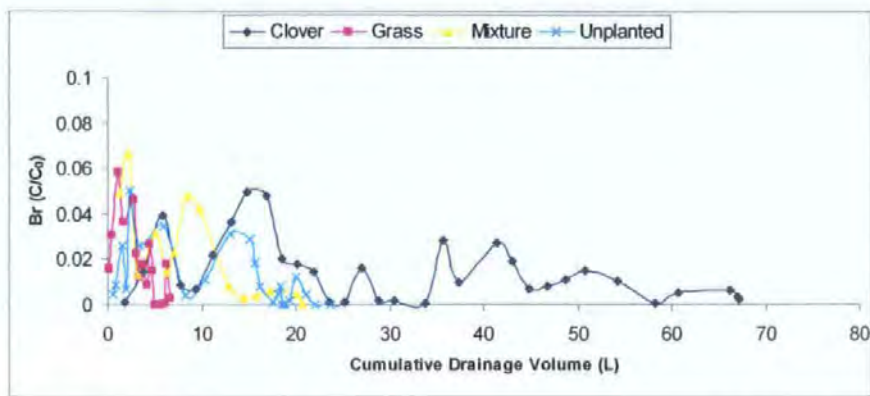
Figure 5.45. Bromide bulk elution profiles from the intact 0.5 m lysimeters for all treatments.
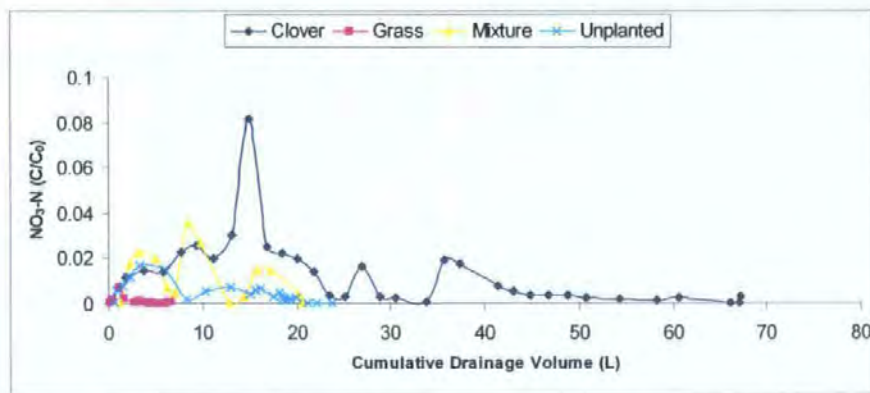
Figure 5.46. Nitrate-N bulk elution profiles from the intact 0.5 m lysimeters for all treatments.
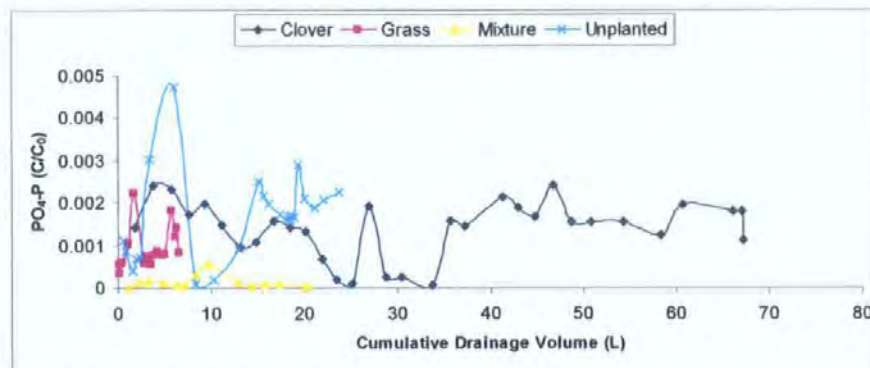
Figure 5.47. Phosphate-P bulk elution profiles from the intact 0.5 m lysimeters for all treatments.

5.17.5. Drainage characteristics.

The drainage characteristics given in Table 5.16 show that the total number of drainage channels and total drainage volume was the greatest for the white clover treatment and the lowest for the ryegrass. The maximum drainage volume for an individual channel at one collection was observed below the unplanted control (1769 ml), which gave the highest drainage rate per channel (7.37 ml min^{-1}). The mean drainage rate of all channels was greatest for the mixed species (0.19 ml min^{-1}) and lowest for the ryegrass (0.08 ml min^{-1}). Figure 5.48 to Figure 5.51 illustrate the channel ID number and position under the soil monoliths. These figures also show that the flow beneath ryegrass was confined to channels that were much more isolated, whereas the other treatments show a greater degree of connectivity between drainage channels.

Table 5.16. Drainage characteristics of the 0.5 m intact block lysimeters.

		White Clover	Ryegrass	Mixed Species	Control
Number of drainage channels		56	18	33	41
Total drainage volume of each block	L	67	6.6	21	24
Mean drainage volume of each block	ml	66	20	45	46
Maximum drainage volume in 4-hour collection time	ml	545	697	943	1769
Mean drainage rate of each block	ml min^{-1}	0.13	0.08	0.19	0.10
Maximum drainage rate in 4-hour collection time	ml min^{-1}	1.29	2.90	3.93	7.37

10	20	30	40	50	60	70	80	90	100
9	19	29	39	49	59	69	79	89	99
8	18	28	38	48	58	68	78	88	98
7	17	27	37	47	57	67	77	87	97
6	16	26	36	46	56	66	76	86	96
5	15	25	35	45	55	65	75	85	95
4	14	24	34	44	54	64	74	84	94
3	13	23	33	43	53	63	73	83	93
2	12	22	32	42	52	62	72	82	92
1	11	21	31	41	51	61	71	81	91

Figure 5.48. Drainage characteristics of 56 of the possible 100 drainage channels beneath white clover. Each channel is numbered 1-100. Dark grey represents channels that constantly drained, light grey represent channels that occasionally drained and white represents non-draining channels.

10	20	30	40	50	60	70	80	90	100
9	19	29	39	49	59	69	79	89	99
8	18	28	38	48	58	68	78	88	98
7	17	27	37	47	57	67	77	87	97
6	16	26	36	46	56	66	76	86	96
5	15	25	35	45	55	65	75	85	95
4	14	24	34	44	54	64	74	84	94
3	13	23	33	43	53	63	73	83	93
2	12	22	32	42	52	62	72	82	92
1	11	21	31	41	51	61	71	81	91

Figure 5.49. Drainage characteristics of 18 of the possible 100 drainage channels beneath ryegrass. Each channel is numbered 1-100. Dark grey represents channels that constantly drained, light grey represent channels that occasionally drained and white represents non-draining channels.

10	20	30	40	50	60	70	80	90	100
9	19	29	39	49	59	69	79	89	99
8	18	28	38	48	58	68	78	88	98
7	17	27	37	47	57	67	77	87	97
6	16	26	36	46	56	66	76	86	96
5	15	25	35	45	55	65	75	85	95
4	14	24	34	44	54	64	74	84	94
3	13	23	33	43	53	63	73	83	93
2	12	22	32	42	52	62	72	82	92
1	11	21	31	41	51	61	71	81	91

Figure 5.50. Drainage characteristics of 33 of the possible 100 drainage channels beneath the mixed species. Each channel is numbered 1-100. Dark grey represents channels that constantly drained, light grey represent channels that occasionally drained and white represents non-draining channels.

10	20	30	40	50	60	70	80	90	100
9	19	29	39	49	59	69	79	89	99
8	18	28	38	48	58	68	78	88	98
7	17	27	37	47	57	67	77	87	97
6	16	26	36	46	56	66	76	86	96
5	15	25	35	45	55	65	75	85	95
4	14	24	34	44	54	64	74	84	94
3	13	23	33	43	53	63	73	83	93
2	12	22	32	42	52	62	72	82	92
1	11	21	31	41	51	61	71	81	91

Figure 5.51. Drainage characteristics of 41 of the possible 100 drainage channels beneath the unplanted control. Each channel is numbered 1-100. Dark grey represents channels that constantly drained, light grey represent channels that occasionally drained and white represents non-draining channels.

Figure 5.52 illustrates the drainage characteristics of each draining channel at each four-hourly collection under white clover, ryegrass, a mixture of the two species, and an unplanted control. This is compared to the leaching of bromide, nitrate and phosphate: the absolute (Figure 5.53) and relative concentrations (Figure 5.54) of each tracer are given, as well as the mass recovered (Figure 5.55). Figure 5.52 to Figure 5.55 are scaled to maximum values, but are incremented evenly to allow comparison. Only the active drainage channels are represented in Figure 5.52 to Figure 5.55, so where a gap appears, this indicates zero drainage, or a very low value. Each line on these figures represents a single collection.

It can be seen that the flow characteristics are entirely different for all four treatments, with soil beneath white clover draining the most freely (Figure 5.52). This preferential flow beneath white clover resulted in a mean drainage volume of the order of three times higher than beneath ryegrass (Table 5.16), and over many more channels (Figure 5.52). The elution of bromide, nitrate and phosphate species occur in the same channels (Figure 5.53 and Figure 5.54), with the relative concentration of phosphate being an order of magnitude lower than the other solutes (Figure 5.54). The results therefore suggest that the preferential flow is dominated by hydraulic rather than chemical or adsorption effects.

In the unplanted control, there was high preferential flow in channel 94 (Figure 5.52). The flow was 2-3 times greater than the maximum recorded for the other treatments (Table 5.16), and the flow was so great that it depleted the concentration of both bromide and nitrate (Figure 5.53 and Figure 5.54) in this channel relative to the other channels. Nevertheless, the overall effect was that the total amount of all solutes leaching from the unplanted soil was greatest through this channel.

Table 5.17 shows that overall 93.75% of the bromide was recovered beneath white clover, but only 15.67% below ryegrass. The table confirms that the recovery of bromide beneath white clover, although greater than for ryegrass, was more evenly distributed between channels (max 1.99% relative to max 4.16% respectively). For nitrate, the recovery is high beneath white clover (total 73.62%, max 2.31%) and low beneath rye grass (total 0.81%, max 0.20%). Correspondingly for phosphate, where the recovery is 9.61% total (0.14% max) under white clover, relative to 0.67% total (0.10 % max) beneath ryegrass.
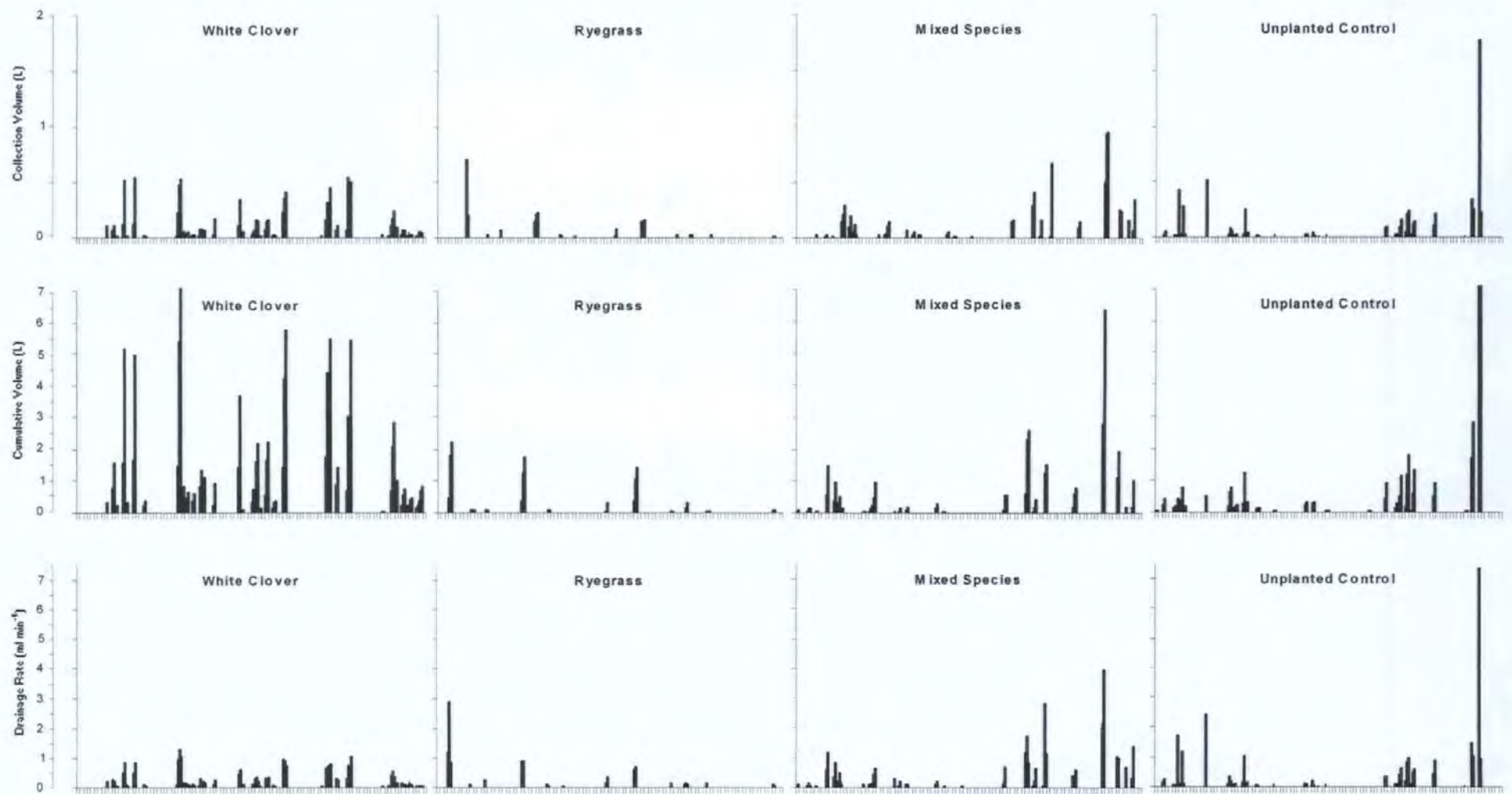
Figure 5.52. The drainage characteristics of each channel (shown on x axis from 1-100) at each four-hourly collections under white clover, ryegrass, a mixture of the two species, and an unplanted control. Drainage volume is presented for each individual collection, then as a cumulative volume for each channel.

239
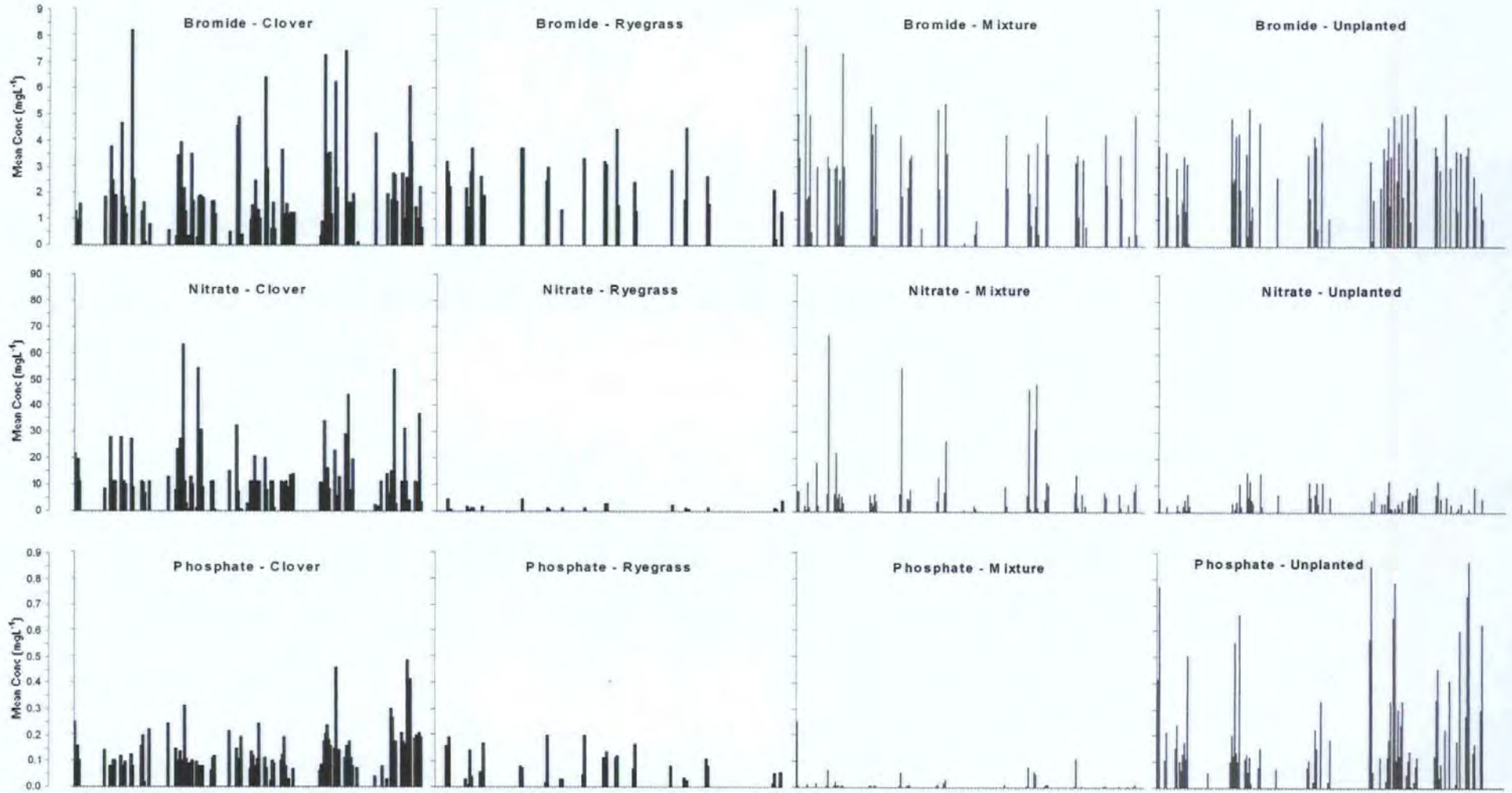
Figure 5.53. The absolute concentration of bromide, nitrate-N and phosphate-P of each channel (shown on x axis from 1-100) at each four-hourly collections under white clover, ryegrass, a mixture of the two species, and an unplanted control.
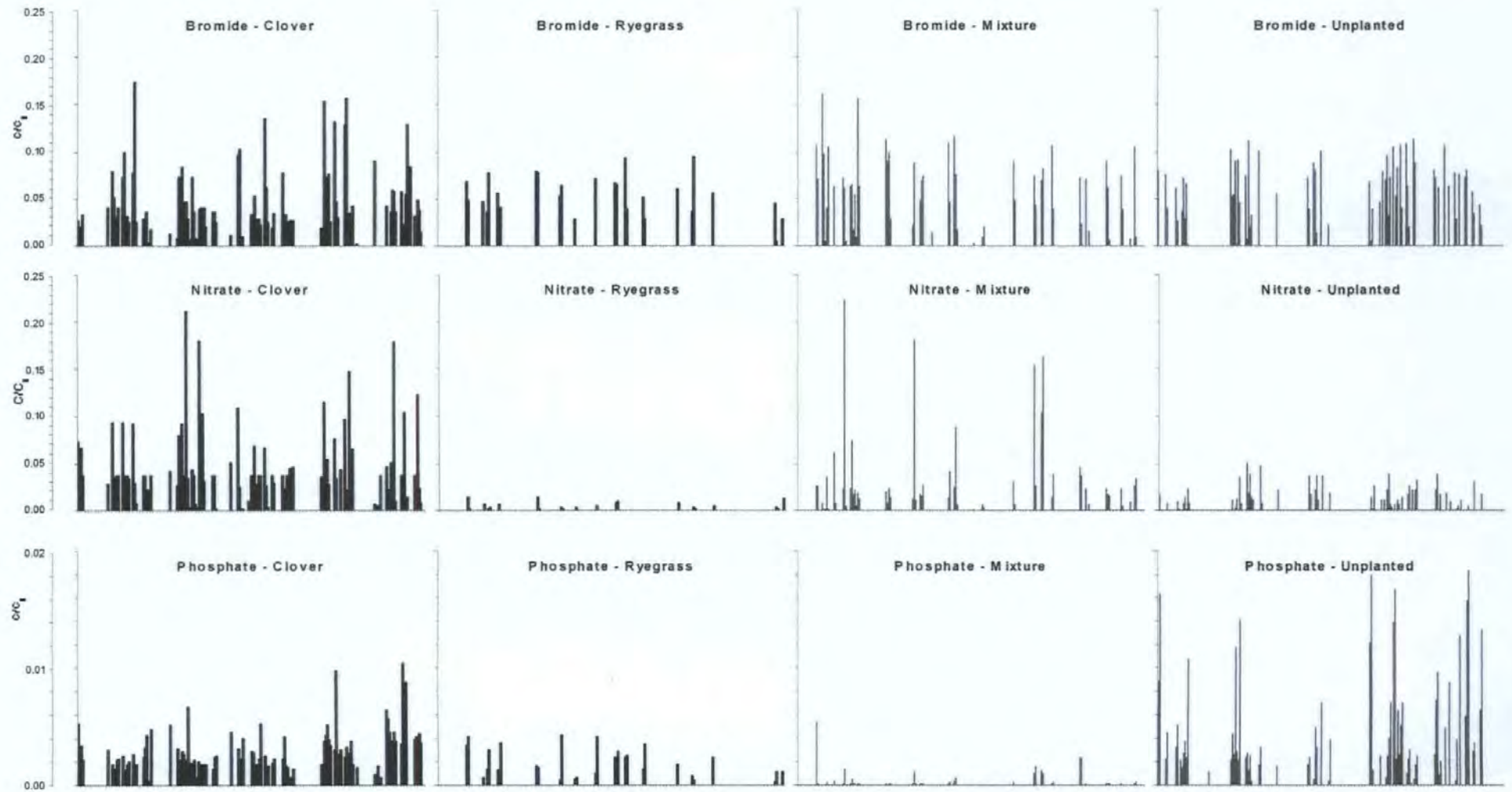
Figure 5.54. The relative concentration of bromide, nitrate-N and phosphate-P of each channel (shown on x axis from 1-100) at each four-hourly collections under white clover, ryegrass, a mixture of the two species, and an unplanted control.
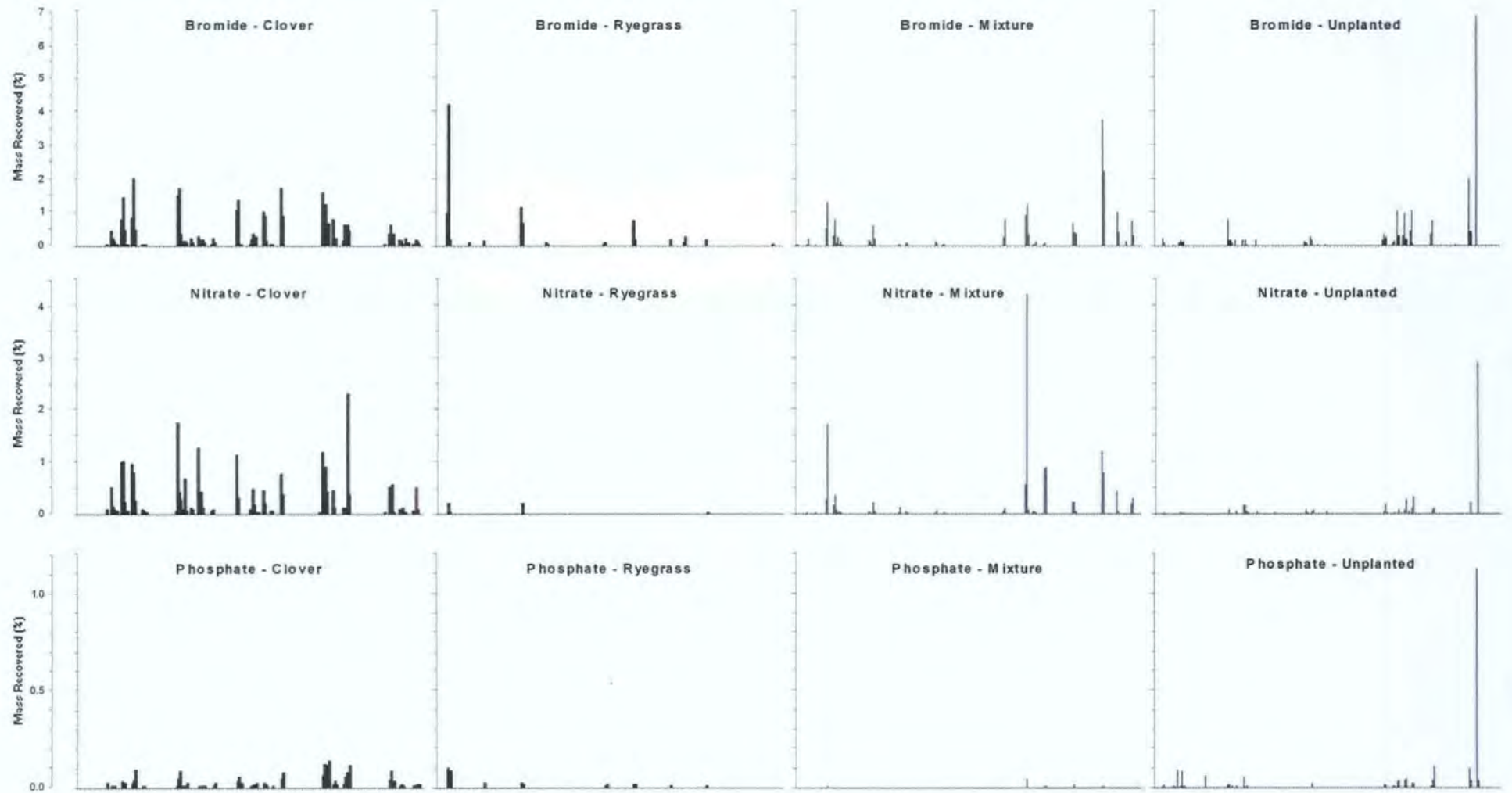
Figure 5.55. The mass recovered (%) of bromide, nitrate-N and phosphate-P of each channel (shown on x axis from 1-100) at each four-hourly collections under white clover, ryegrass, a mixture of the two species, and an unplanted control.

Table 5.17. Numerical values of mass and concentration leached from the 0.5 m lysimeters. (Total and mean of soil blocks. Maximum of a given drainage channel).

BROMIDE		White Clover	Ryegrass	Mixed Species	Control
Total mass recovered	mg	44.06	7.37	19.30	17.24
Mean mass recovered	mg	0.025	0.023	0.042	0.018
Maximum mass recovered	mg	0.93	1.95	1.75	3.20
Total relative mass recovered	%	93.75	15.67	41.07	36.69
Mean relative mass recovered	%	0.05	0.05	0.09	0.04
Maximum relative mass recovered	%	1.99	4.16	3.72	6.81
Mean relative concentration	C/C_0	0.008	0.010	0.015	0.010
Maximum relative concentration	C/C_0	0.173	0.095	0.162	0.114
Mean concentration	mg L^{-1}	0.4	0.5	0.7	0.5
Maximum concentration	mg L^{-1}	8.1	4.5	7.6	5.4

NITRATE-N		White Clover	Ryegrass	Mixed Species	Control
Total mass recovered	mg	220.86	2.43	69.09	39.09
Mean mass recovered	mg	0.12	0.01	0.15	0.04
Maximum mass recovered	mg	6.92	0.60	12.55	8.72
Total relative mass recovered	%	73.62	0.81	23.03	13.03
Mean relative mass recovered	%	0.041	0.003	0.050	0.013
Maximum relative mass recovered	%	2.31	0.20	4.18	2.91
Mean relative concentration	C/C_0	0.009	0.001	0.007	0.004
Maximum relative concentration	C/C_0	0.211	0.014	0.223	0.051
Mean concentration	mg L^{-1}	2.6	0.2	2.1	1.1
Maximum concentration	mg L^{-1}	63.4	4.3	67.0	15.3

PHOSPHATE-P		White Clover	Ryegrass	Mixed Species	Control
Total mass recovered	μg	4515	313	121	2003
Mean mass recovered	μg	2.52	0.97	0.26	2.04
Maximum mass recovered	μg	64.35	45.03	22.02	529.24
Total relative mass recovered	%	9.61	0.67	0.26	4.26
Mean relative mass recovered	%	0.005	0.002	0.001	0.004
Maximum relative mass recovered	%	0.14	0.10	0.05	1.13
Mean relative concentration	C/C_0	0.0009	0.0004	0.0001	0.0010
Maximum relative concentration	C/C_0	0.0103	0.0042	0.0054	0.0184
Mean concentration	μg L^{-1}	41.5	18.9	3.7	47.5
Maximum concentration	μg L^{-1}	486.2	196.9	253.8	864.5

5.18. Discussion

5.18.1. Re-packed soil columns

Fourteen column experiments were presented that involved various initial and boundary conditions. The wealth of convoluted information provided requires further investigation.

5.18.1.1. Tracers and treatments

The transport of bromide was similar to that of nitrate, but different to phosphate. This is as expected due to the conservative and non-conservative nature of the tracers. The recovery of bromide was greater than that of nitrate, which were both greater than phosphate. Again this is as expected. Bromide is a non-reactive tracer and not involved in any biological processes in the soil. Although bromide has some anionic repulsion it is successfully used as a tracer of water and nitrate movement in soil (Stutter *et al.*, 2003). Nitrate is very soluble and repelled from negatively charge clay surfaces (Marshall *et al.*, 1996), but subject to losses due to uptake by plants, mineralization and denitrification (Rowell, 1994), whereas phosphate is largely insoluble and generally adheres to soil particles preventing significant leaching (Rowell, 1994).

In general, the amount and concentration of nitrate leached beneath white clover exceeded that of ryegrass, with intermediate values for the mixed treatment. The elution profiles of bromide also showed the same trend, but at higher concentrations. The unplanted control soil occasionally gave higher nitrate concentrations, although this may be attributed to the lack of growing plants and lower microbial populations which would otherwise utilise nitrate, the phenomenon requires further explanation. This was attempted by studying the concomitant transport of bromide. However, the unplanted soils showed enhanced leaching of bromide in both the pulse and diffusion experiments. A possible explanation of enhanced concentrations in the diffusion experiment was the lack of micropores in the

244

absence of plants. However, this is only an idea and has not been further investigated. The opposite scenario is that the roots in the planted soils restrict water and solute flow.

The method of applying the tracer solution also has an effect on the amount and concentration of the solute leached. Applying the pulse as a single aliquot of a greater amount or concentration generally showed earlier and higher breakthrough than applying the solution at a greater volume over a longer time. The application of the tracers antecedent to leaching inevitably showed different elution characteristics due to diffusion and mixing with micropore water. In addition, the boundary condition of water content was also lower for the diffusion Type B experiment. Information on the displacement of water by nitrate and vice versa was gained by continuously applying the tracer solution. It was shown that nitrate is transported at a different rate to water.

It is well documented in the literature that numerous factors will alter the transport of solutes and thus the shape of an elution profile, such as soil water content, displacing water velocity, pore-water velocity, chemical charge of solute (anion/cation exclusion), mobile/immobile water inclusion/exclusion, adsorption/reactivity of solute, type of mixing (diffusion/dispersion), extent of mixing (intra-aggregate diffusion, hydrodynamic dispersion, piston flow/preferential flow), soil texture, soil structure, application method of pulse, background concentration of pulse, degradation rate of pulse, etc. (Hillel, 1980; Marshall, 1996).

A consideration omitted from this work is the information gained from the shape of a breakthrough curve as a function of pore-volume, which will provide additional information on the structure of the soils under investigation. In addition, field experiments are often plotted as a function of time. Most graphical representations of solute transport in this study are plotted as elution curves as a function of drainage volume. This offers

theoretical information on transport behaviour. Furthermore, as data points on each graph were collected at the same time, additional information is provided on the drainage rate and the pore-volume can also be judged.

It was also found that the plane of measurements had an effect on the ease of interpretation. Under low time resolution (readings every four hours), elution profiles of typical shapes are recorded. Whilst at higher time resolution (readings every hour), results are much more difficult to characterize due to their spiky nature and noise.

Further interpretation of the data obtained is required, with particular reference to the effect of soil type on leaching. For example, Quisenberry *et al.* (1993) showed that displacement of water decreases with increased clay content.

5.18.2. Intact soil monoliths

The figures and tables for the 0.5 m intact soil monoliths give a very detailed picture of the specific flow characteristics of individual channels beneath white clover, ryegrass and the unplanted control and were compared to relative concentrations and mass recoveries. It is clear that overall, clover allows much greater elution to take place, but there is relatively less preferential flow occurring. Nearly all the bromide was recovered, as expected from a conservative tracer. Around 75% of the total nitrate was recovered beneath white clover, but only around 1% beneath ryegrass. The phosphate recovery was smaller still, at ~10% and ~0.7% for white clover and ryegrass, respectively.

However, this study is limited, as due to financial and time constraints, only one replicate of each treatment was studied. Soil structural elements such as biopores (earthworm burrows, decayed plant root channels) or mechanical shrinkage patterns (cracks or fractures) were not examined. Nevertheless, the studied provided valuable information and

was of sufficient scale to show that these effects are likely to be of consequence in the field.

5.18.3. Water release

It was shown that white clover grown in both the re-packed columns and the intact monoliths gave rise to freer drainage of water, whereas the ryegrass and unplanted treatments were susceptible to ponding, when the input rate exceeded the infiltration rate. Both will have implications for field soils, soils beneath white clover will be able to accept more water, which is beneficial to the current changing climatic conditions. Whilst grass soils may enhance surface runoff and promote detrimental effects.

It was shown in Chapter Two, and in the parallel study by Scholefield *et al.* (1995), that white clover had a greater transpiration rate compared to ryegrass. This may have a negative effect on the soil-water balance during summer months. It has been presumed that the greater elution in soils beneath white clover is a result of enhanced soil structure. However, it may be that there is a greater degree of aggregate hydrophobicity due to the hydrogen gas liberated by the *rhizobia* during energy transfer.

5.18.4. Literature studies

There are no comparable studies in the literature for the leaching of bromide, nitrate and phosphate leaching beneath grass and clover. Most of the studies of nitrate leaching from beneath forage legumes involve white clover in combination with grasses under grazing management. A comparable study is that of Scholefield *et al.* (2001), who also reported enhanced nitrate leaching beneath white clover compared to ryegrass. The details of this, and numerous other studies are discussed in Chapter One. Also discussed in the introductory chapter are various studies on solute transport, of which the literature abounds.

247

This research offers support for the work of Scholefield *et al.* (1996, 1998) who suggest that in well-structured soils nitrate leaching can be reduced due to relative protection from nitrate leaching by inter- and intra-aggregate diffusion and retention in micropores, and thus the soil's capacity to buffer watercourses is enhanced. In turn this research is confirmed by an earlier study that found levels of nitrate leaching were determined by the factors that control accumulation and generation in the soil, and transport during the leaching process (Scholefield *et al.*, 1993).

The topic of nitrate leaching from agricultural land has been the focus of much research (Cuttle *et* al., 1998; Jarvis, 2000; Powlson, 2000; Schröder *et al.*, 2004). Of more recent concern is the movement of P through soil (Sharpley, 1995; Hawkins and Scholefield, 1996; Haygarth *et al.*, 2005), which has generally been considered insignificant because P is fixed firmly by soil colloids or organic matter. Previous research stressed the P losses through surface runoff, whereas relatively less is know about P losses through leaching. However, it has been shown that enriched P content and good drainage of soils can facilitate P losses by leaching (Turner and Haygarth, 2001), and that subsurface transport is enhanced by artificial drainage systems (Sharpley and Withers, 1994).

5.18.5. Implications of the research

N and P are indispensable inputs for the sustainability of agriculture. The use of both inputs has increased dramatically in recent decades and so has the nutrient losses Schröder *et al.* (2004). N and P losses can negatively affect the quality of soils, ground water, surface water, and the atmosphere. They may affect the functioning of ecosystems, including the earth as a whole (Schröder *et al.*, 2004). The losses also put drinking water quality and human health at risk, and the financial consequences are considerable. Agriculture has been found to be a major contributor to N and P losses to the environment and justifies the call for effective environmental policy. Thus, a better understanding of the

soil processes and properties that favour preferential water pathways is essential for developing integrated management and regulatory strategies to reduce the environmental impacts of non-point agricultural pollutants (Zehe and Flühler, 2001; Williams *et al.*, 2003).

5.19. Conclusions

Bromide leaching was similar to that of nitrate, whilst phosphate showed different elution profiles. At the column and block scale, white clover leached more bromide and nitrate compared to the other treatments. The elution of phosphate showed differences between treatments and scales. At the 0.5 m block scale, soil beneath white clover leached a greater amount and concentration of phosphate compared to the other treatments. At the column scale, soil beneath white clover leached a lower amount and concentration of phosphate than the grass treatments. There were also marked differences in water flux data and in the drainage pattern beneath the 0.5 m blocks.

The data show support for hypotheses that nitrate and phosphate losses through leaching are higher with improved aggregation. The mode of leaching (from micropores or from pulse) determined the relative effects of the plants, with the latter the greater permeability and pore continuity conferred by clover gave rise to higher leaching levels, but with greater contribution from slower pathways. Most importantly, it was shown that these effects were manifested at the soil profile scale and therefore likely to be of consequence in the field.

CHAPTER SIX

6. Summary, overview and future work

6.1. Aims of the chapter

As stated in Chapter One, the project aimed to test a series of hypotheses with respect to the structuring of soil beneath white clover and ryegrass, and the impact of such soil structuring on water and nutrient transport. This study also aimed to achieve a balanced insight into the sustainability and environmental consequences of manipulating soil structure in agricultural systems.

This final chapter aims to revisit the hypotheses in turn, and to summarise the findings of this research that disprove or support each hypothesis. The results reported in Chapters Three to Five are synthesised and integrated with the findings of other workers. The implications of this research are contextually discussed.

6.2. Hypotheses

i.   **White clover will enhance structural differentiation relative to perennial ryegrass.**

Images of soil beneath white clover and ryegrass after 8, 10, 12 and 14 weeks of controlled growth were presented in Chapter Three. Some interesting changes were observed in the initial uniform soil structure under white clover compared to the ryegrass, notably the movement of soil particles beneath white clover, particularly around the base of the plant, which created an undulating soil surface. Areas of improved aggregation in soil beneath white clover were also evident from the pictures.

It was difficult visually to assess the soil structure under the pure ryegrass and mixed treatments due to the high density of the roots occupying the outside of the soil core, which

increased with time. However, qualitative visual evidence supports hypothesis i, and further support is given in relation to the other hypotheses.

ii. This enhanced soil structuring will increase both the amount and concentration of nitrate and phosphate leaching below the root zone.

The results presented in Chapter Five generally supported this hypothesis that enhanced soil structuring will give rise to a greater amount and concentration of both nitrate and phosphate. However, there were very large variations that require further investigation, notably with the unplanted control soils.

At the 0.5 m block scale, soil beneath white clover leached a greater amount and concentration of both nitrate and phosphate (Figure 5.41 and Figure 5.43). At the column scale, soil beneath white clover leached a greater amount and concentration of nitrate (Figure 5.34) but less phosphate than the grass treatments (Figure 5.35).

iii. Nitrate, phosphate and bromide will have different transport behaviour and therefore elution profiles through the soil.

It was shown in Chapter Five that nitrate and bromide behave similarly, which is expected due to their conservative nature. However, phosphate eluted at much lower concentrations.

iv. The elution behaviour of nitrate, phosphate and bromide will depend on soil saturation conditions and the initial distribution of the eluting species prior to simulated rainfall.

The results in Section 5.1.5 strongly support this hypothesis. When the eluting species is diffused into the microporous matrix, much less elution results.

v. **Analysis of the leaching results can be carried out semi-quantitatively by characterising the elution profiles.**

Section 5.1.3 shows that under low time resolution (readings every four hours), breakthrough curves of tractable shapes are recorded. However, Section 5.1.5, shows that higher resolution (readings every hour) results are much more difficult to characterize.

vi. **Differences will be identified at the core scale compared to the monolith scale; thus a spectrum of useful information will be obtained by using a wider range of samples at the core scale and studying detail of some samples at the monolith scale.**

At the monolith scale we saw that the drainage channels were acting as if they were switching on and off, because of changing pathways. In Section 5.1.6, many different behaviours were observed in the same block. So the monolith experiments demonstrated that the column experiments show only a small segment of the real behaviour. So as suggested by the hypothesis, experiments at both scales are indeed useful and complementary.

vii. **Enhanced soil structuring under white clover will be detectable by changes in oxygen diffusion rates.**

As given in Chapter Three, O_2 diffusion was greatest for soils beneath white clover. This diffusion rate was nearly nine times greater than that of soils beneath ryegrass and 15 times greater than the unplanted control soils. The mixed species showed intermediate values in O_2 diffusion, being half that of mono-white clover, four times greater than mono-ryegrass and seven times greater than the unplanted control soils. So this hypothesis is strongly proven.

viii. Enhanced soil structuring under white clover will alter soil stability.

The preliminary test of soil structural stability using the Williams and Cooke method showed that white clover increased aggregate stability compared to ryegrass. This increased stability was not related to the depth of the original field soil, which contained differential organic matter contents at the start of the experiment (3.6% topsoil and 1.9% subsoil). Neither did the stability significantly change with depth in the soil core. The stability of soils under ryegrass showed some statistically significant differences in decreasing stability with both depth of the original field soil and depth within the soil core.

Although the results suggested that white clover increased the shear strength of the soil compared to soil beneath ryegrass and the unplanted controls, this was only true for the Crediton, Frilsham and Greinton series. Soil of the Denbigh series beneath white clover and ryegrass gave similar results, both of which had consistently lower values than the equivalent unplanted soil.

The soil structural stability and sheer strength test on soils with carefully equilibrated water contents supported the stability measurements. So hypothesis (viii) has been shown to hold for many, but not all, soils.

ix. Enhanced soil structuring under white clover will cause differences in water retention characteristics.

We showed in Chapter Four that the very subtle differences between the same soil structured by the roots of clover and of grass could be detected in the water retention curves. However, as previously stated, the exercise proved equally much a lesson in the need for better experimental data and protocol. Currently, the standard protocol (ISO 11274:1998) does not yield enough data for a model that considers the entire shape of the

water retention curve, without any pre-supposition as to the mathematical analytical form of the water retention curve.

x. The precise nature of soil structuring under white clover, in terms of the changes to the void network can be discovered by modelling water retention curves with the void network simulator Pore-Cor.

The modelling exercise proved remarkably difficult, mainly because of the problems with the data described above. After painstakingly removing the noise and artefacts from the experimental data, it was shown that soil beneath grass contains fewer small void throats than clover. It was also shown that soil beneath white clover is more randomly structured, with more large pores surrounded by smaller throats.

6.3. Integrating discussion

6.3.1. The influence of soil properties on soil structure and fluid dynamics

Experiments were carried out after growing white clover and ryegrass on carefully characterised acidic soils of the Crediton, Greinton, Frilsham and Denbigh series with variable organic matter content (Chapter Three). Soils of the Crediton and Greinton series had similar textures, classified according to the Soil Survey of England and Wales as sandy and silt loams and consequently the re-packed samples had similar bulk densities and porosities (Chapter Three, Table 3.5). Soil from the Denbigh series was the least acidic and had the most organic matter. After repacking, the clay loam of the Denbigh series had the lowest bulk density and therefore an elevated porosity, this was as expected due to the soil texture of this series. The Frilsham series is also classified as a clay loam, but had a similar bulk density and porosity to that of the Crediton and Greinton series.

Experimentally determined soil pH and organic matter content was similar to that reported by the Soil Survey of England and Wales (Chapter Three). The soil texture determination by the hydrometer method was considered inaccurate and therefore the soil textural classification of the Soil Survey of England and Wales was used (Chapter Three).

The soil properties of pH, organic matter content and texture were determined at the start of the experimentation on the initial re-packed soil, but were not determined after soil was planted with white clover and perennial ryegrass. The influence of such soil properties are considered below.

Many soil processes will influence the end pH of the soils studied. For example, the physiological constitution of white clover induces a net efflux of protons at the root–soil interface, as a result the exchangeable bases are displaced and the soil pH is lowered (Lesturgez *et al.*, 2006). Nitrate leaching is associated with removal of cations and will also acidify the soils (Lesturgez *et al.*, 2006). In turn, soil pH can influence the fertility of the soil and the nutrient availability to plants (Heilman & Norby, 1998), and so soil pH is often regulated to ensure the optimum conditions for plant utilization.

The organic matter (OM) in soils consists of residues and decomposition products of plants, animals and micro-organisms (FitzPatrick, 1983). The amount of organic matter depends on several factors and is the net result of the input of organic materials and the rate of breakdown (Davies *et al.*, 1993). As well as containing the soil's reserve of nutrients (Davies *et al.*, 1993), organic matter enhances the structure and stability of the soil (Chapter One, Section 1.6.3), and is capable of absorbing large quantities of water (FitzPatrick, 1983).

The Denbigh series had the greatest amount of organic matter and the highest soil pH. As organic matter induces acidity when present in large amounts but is neutralised by high

concentrations of basic cations (FitzPatrick, 1983), it is suggested that the Denbigh series has a greater proportion of calcium, magnesium, sodium and potassium, which tend to raise the pH (Chapter Three). Cations such as hydrogen, aluminium and iron produce acid soil solutions due to the hydrolysis of the cations (Fergusson, 1982), and are perhaps more concentrated in the soils of the Crediton, Greinton and Frilsham series, as these soils are more acidic but contain less organic matter than the Denbigh series (Chapter Three).

As noted by FitzPatrick (1983), soil texture is an important physical characteristic, which influences factors such as water retention (Chapter Four) and drainage (Chapter Five), and White (1997) states that these parameters determine a soil's agricultural potential. As expected, this research demonstrated that coarse textured soils, such as the sandy loams of the Crediton series, permit freer drainage (Chapter Five) although crops may be more susceptible to drought (FitzPatrick, 1983; White, 1997). Medium textured soils, such as the sandy silt loams of the Greinton series, are often preferred for their ability to hold water and nutrients (White, 1997); this is also demonstrated in Chapter Five. It is also known that clay loams will have poor infiltration rates and lower drainage volumes (FitzPatrick, 1983; White, 1997), as shown in soils of the Frilsham and Denbigh series (Chapter Five). The stone content of a soil may be just as important as the texture of the fine earth fraction (clay, silt and sand) (Hall *et al.*, 1977). For example, a stony sandy loam like the Crediton series will hold less water than a soil of the same textural class with fewer stones, such as the Greinton series.

The bulk density and porosity achieved when re-packing (Chapter Three) will influence water and nutrient transport (Chapter Five). The re-packed samples of the Crediton, Greinton and Frilsham series had similar bulk densities and porosities (Chapter Three). Soils of the Crediton and Greinton series often exhibited similar transport properties in terms of drainage volume and solute concentration (Chapter Five). However, the Frilsham

series is a finer textured clay loam and therefore consistently gave lower drainage volumes and rates, and often had a lower leaching potential than the Crediton and Greinton series (Chapter Five). The Denbigh series, which had lower bulk density and elevated porosity after re-packing is also a clay loam, but was generally comparable to the Crediton and Greinton series in terms of drainage, and showed some similarity in solute concentration (Chapter Five).

When sandy loams are more compacted, it is possible for an increase in the occurrence of preferential flow (Mooney and Nipattasuk, 2003). In agreement with this, the Crediton series subsoil had a higher bulk density and generally exhibited greater preferential flow than the topsoil (Chapter Five). It is known that preferential flow in clay loams is prevented by compaction (Mooney and Nipattasuk, 2003). This research showed that the clay loams of the Frilsham series had a similar texture, but higher bulk density than the Denbigh series, and as a result, the Frilsham series often exhibited greater preferential flow and reduced drainage volumes than the Denbigh series (Chapter Five).

The bulk density and porosity achieved for the initial re-packed soils also correlated with the oxygen diffusion measurements (Chapter Three), suggesting this technique is reliable and a suitable indicator of porosity and pore connectivity. The oxygen diffusion rate for the Crediton series soils after plant growth was much greater for the white clover treatments than that of soils beneath ryegrass and the unplanted controls, with intermediate values for the mixed species.

6.3.2. The influence of plant type on soil structuring and fluid dynamics

The influence of plant type was considered on soil structure, water flow and nutrient transport. There were clear differences in these parameters between white clover, perennial ryegrass, the mixture of the two species and the unplanted controls for all soil types. In

general, white clover had a greater influence on soil structure than ryegrass, demonstrated through oxygen diffusion measurements (Chapter Three) and the shape and magnitude of the elution profiles (Chapter Five). The mixed species were only planted in Crediton series soil, and intermediate results were reported

Soils beneath white clover generally had a greater water flux and gave elevated levels of nutrient leaching (Chapter Five). The transport of nitrate was enhanced in soils beneath white clover compared to those planted with ryegrass. This was observed at both the column and block scale and was attributed to the improved structural differentiation beneath white clover (Chapter Five). Such enhanced soil structuring and nitrate transport beneath white clover holds important implications for the organic/conventional farming debate and the transport qualities of soils. Such findings are also important when considering the management of Nitrate Vulnerable Zones (Chapter One).

The elution profiles for phosphate were less conclusive than those for nitrate. It was shown that greater amounts and concentrations of phosphate were leached from white clover than ryegrass at the block scale, whereas phosphate leaching was sometimes greater beneath ryegrass than white clover at the column scale (Chapter Five). This needs further investigation for the understanding of phosphate transport in the field, which has only recently been addressed in the literature (Chapter One).

This research was run in parallel with a study which aimed to assess such mechanisms of enhanced structural differentiation (Scholefield *et al.*, 2005). The parallel study also found enhanced soil structuring under white clover compared with ryegrass. They further demonstrated that this cannot be guaranteed and depends on clover variety, rhizobium strain (polysaccharide production), weather patterns (watering regime, light levels) and initial soil conditions. The study showed support for hypotheses that *rhizobial* gums bind

and stabilise aggregates, and that the two plants have differential effects on microbiological populations. However there was no evidence to suggest that clover roots generate the forces necessary to cause aggregation.

As with this research, Scholefield *et al.* (2005) also found that the mode of leaching (from micropores or from pulse) was determined by the relative effects of the plants, with the latter the greater permeability and pore continuity conferred by clover gave rise to higher leaching levels, they also found a greater contribution from slower pathways. They also showed that these effects were manifested at the soil profile scale and therefore have relevance in the field.

6.3.3. Scales of observation

Experimentation was conducted at a range of scales from the pore-scale (modelling), the aggregate (mechanical stability), the re-packed soil core (structural visualisation, nutrient leaching and modelling) to the monolith lysimeter (leaching through intact soil profiles). It was shown that the effects of enhanced soil structuring, water transport and nutrient leaching were manifested at the block scale, which is equivalent to the soil profile scale and therefore likely to be of consequence in the field. Water and nutrient transport at the column scale gave similar trends to the block scale. Furthermore, it is suggested that the results generated at the pore-scale by modelling would, if upscaled give results resembling those gained at the experimental scales.

The investigation across different scales provides valuable insight into the mechanisms and influential soil properties. Although there are many general studies of water and nutrient transport reported in the literature at both the column and block scale (Chapter One)., most studies of white clover and ryegrass are generally concerned with nitrate leaching at the field scale (MacDuff *et al.*, 1990; Mannetje and Jarvis, 1990; Parsons *et al.*, 1991; Tyson *et*

al., 1997; Cuttle *et al.*, 1998; Schils *et al.*, 2000; Loiseau *et al.*, 2001; Scholefield *et al.*, 2001; Eriksen *et al.*, 2001, 2004).

6.3.4. Soil structuring and stability

Evidence of enhanced soil structuring beneath white clover was demonstrated through visual assessment (Chapter Three), oxygen diffusion measurements (Chapter Three), water retention measurements (Chapter Four), and from water flow and nutrient leaching experiments (Chapter Five).

Evidence of increased structural stability beneath white clover was gained from tests to determine the instability to water and the shear strength of the soils (Chapter Three). These findings have important implications, and show that the resulting soil structure will be able to withstand forces in the field. However, it is also important to assess whether the effects are transient, temporary or persistent. As Tidsall and Oades (1979, 1982) suggest that different binding agents have different abilities to persist, monitoring the longevity of the enhanced soil structure may help to identify the driving mechanisms. Papadopoulos *et al.* (2006) demonstrated enhanced soil macroporosity beneath red clover (*Trifolium pretense*) and red clover/ryegrass swards, and reported that the effect was not lasting (< 3 years).

6.3.5. Water and nutrient transport

Water retention measurements (Chapter Four) give the quasi-static fluid properties of the soil. It was shown that soil structured by the roots of white clover had had a greater potential to release water due to greater macroporosity compared to the other plant treatments of the same soil series (Chapter Four). Although the differences in water release between the treatments were very subtle, this research demonstrated that these differences could be determined by the water retention curves, and could be simulated with the void space network model Pore-Cor.

260

The dynamic fluid properties and concomitant solute leaching were assessed in great detail (Chapter Five). It was shown that relative to ryegrass and the unplanted control soils, soil beneath white clover had a greater potential to allow the transport water and nutrients (Chapter Five). The literature lacks comparable studies of nitrate and phosphate leaching beneath white clover and ryegrass. Most studies concentrate on nitrate leaching from beneath white clover in combination with grasses under grazing management (Scholefield *et al.*, 2001). However, such studies are at the field scale, and so also suggest that this research can be upscaled and has implications at the field and even catchment scale.

Parsons *et al.* (1991) and Eriksen *et al.* (2001, 2004) found that nitrate leaching from grazed, unfertilised, mixed grass-white clover is generally much smaller than from highly fertilised grass. Thus, such research suggests that legume-based systems are environmentally benign. However, it is believed that the N loss is smaller because the level of production is lower in the grass-clover system than the pure grass (Scholefield *et al.*, 2001). Eriksen *et al.* (2001, 2004), attributed the higher leaching losses from fertilised grass than from unfertilised grass-clover systems to both a reduction in N_2-fixation in grass-clover over time, and a reduction in dry matter production in grass-clover over time lowering the grazing intensity and the recycling of grassland N via animal excreta.

Several studies are in accordance with this work and have shown that legume-based systems are not environmentally benign, and N from clover is just as likely to leach to the environment as fertiliser N, particularly under grazing (Mannetje and Jarvis, 1990). Tyson *et al.* (1997) and Cuttle *et al.* (1998) note that similar amounts of N and P are leached from beneath grass-clover swards as those leached from beneath fertilised grass operating at the same level of production. In some circumstances, clover rich swards can give rise to very high levels of nitrate leaching (MacDuff *et al.*, 1990; Loiseau *et al.*, 2001; Scholefield *et al.*, 2001).

The most comparable literature study is that of Scholefield *et al.* (2001), who report a large scale study of twelve sites across northern Europe over three years, which compared nitrate leaching beneath five forage legumes grown in pure strands and in combination with a companion grass as the basis for economically and environmentally sustainable systems of livestock production. Although nitrate leaching varied considerably with site, the greatest leaching potential was from beneath red clover (32 kg N ha^{-1}) and white clover (36 kg N ha^{-1}). The lowest potential was from grass without fertiliser N (17 kg N ha^{-1}), whilst fertilised grass receiving 200 kg N ha^{-1} had a leaching potential (29 kg N ha^{-1}) slightly below that of red and white clover.

Loiseau *et al.* (2001) reported leaching losses over six years from lysimeters sown with pure white clover as 28-140 kg N ha^{-1}, compared to 1-19 kg N ha^{-1} for grass-white clover. A three year study from a dairy farm in the Netherlands reported slightly higher nitrate leaching from grass-white clover systems (28 mg L^{-1}) compared to fertilised N grass systems (26 mg L^{-1}), and that the nitrate leaching was positively correlated with clover content in the sward (Schils *et al.*, 2000). By comparison, this research (Chapter Five) showed that white clover had a greater nitrate leaching potential than ryegrass (Table 5.9-5.11). However, in some experiments, the unplanted soils gave even higher values those beneath white clover.

6.4. Overall conclusions

6.4.1. Soil structure and stability

There is evidence of enhanced soil structuring beneath white clover relative to the other plant treatments. This was demonstrated through visual assessment, oxygen diffusion rates, water retention measurements, and water flow and nutrient leaching experiments. This enhanced structuring beneath white clover was consistent between soil types, shown by the size and shape of the elution profiles.

There was also evidence to suggest that enhanced structuring beneath white clover was accompanied by an increased in soil structural stability. The instability tests demonstrated the stability of soil structure to water, whilst shear strength measurements implied increased stability to mechanical forces which are likely to occur in the field.

6.4.2. Water release

The research focused heavily on dynamic fluid properties through concomitant solute leaching. It was shown that white clover grown in both the re-packed columns and intact monoliths gave rise to freer drainage of water, whereas the ryegrass and unplanted treatments were susceptible to ponding. This was attributed to improved soil structure beneath white clover. This finding has important implications for water transport in field soils. Soils beneath white clover may be able to accept more water, whereas soils beneath grass may enhance surface runoff and increase the potential for detrimental effects.

The determination of the quasi-static fluid property of water retention proved a lesson in the need for accurate measurements. Notwithstanding this, it was shown that white clover grown in the re-packed sandy soil of the Crediton series had a greater potential to release water due to its enhanced soil macroporosity relative to the other treatments. Furthermore, the water retention curves were successfully modelled at the pore-scale using Pore-Cor.

The simulated output parameter of saturated hydraulic conductivity showed similar trends to the findings of the experimental properties determined at both the re-packed column and intact block scale.

It has been suggested that the movement of water and leaching of solutes was enhanced in soils beneath white clover relative to ryegrass. In addition, some leaching characteristics observed at the column scale were replicated at the block scale. As this was an intact monolith of 0.5m depth, it gives an insight into properties and transport at the field scale, and therefore potentially the catchment scale. Thus, the Pore-Cor model was successful at predicting properties of soil as a geometric porous media that show relevance at both experimental scales and in turn the field.

6.4.3. Solute transport

The elution profiles for bromide were similar to those of nitrate, but different to phosphate. The recovery of bromide was greater than that of nitrate, and both were greater than phosphate. This was as expected due to the conservative and non-conservative nature of the tracers, and their interactions with the soil.

In general, the amount and concentration of both nitrate and bromide leached beneath white clover exceeded that of ryegrass, with intermediate values for the mixed treatment. This was attributed to enhanced structural differentiation beneath white clover relative to ryegrass. There was some evidence of enhanced phosphate leaching beneath white clover at the block scale, and reduced leaching at the column scale. However, the findings of this research for phosphate leaching are not as conclusive as nitrate leaching and so need further investigation. The unplanted control soil occasionally leached higher nitrate and bromide concentrations; although this may be attributed to pore-size, and to the absence of growing plants and lower microbial populations which would otherwise utilise nitrate, the phenomenon still requires further explanation.

Another important aspect of solute leaching highlighted in this research was the method of applying the tracer solution, which had an effect on the amount and concentration of the solute leached. Applying the pulse as a single aliquot of a greater amount or concentration generally showed earlier and higher breakthrough than applying the solution at a greater volume over a longer time. The application of the tracers antecedent to leaching inevitably showed different elution characteristics due to diffusion and mixing with micropore water. It was also found that the plane of measurements had an effect on the ease of interpretation. Under greater time resolution, elution profiles were much more difficult to characterize due to their spiky nature and the presence of noise.

This research demonstrated similarities in soil structuring and fluid dynamic properties across the scales of observation. For example, the pore-scale modelling gave results resembling those gained at the experimental column and block scales. Furthermore, the effects of soil structuring and fluid transport identified at the block scale are equivalent to the soil profile scale and therefore likely to have relevance in the field.

6.4.4. Significance of this research

N and P are indispensable inputs for the sustainability of agriculture, but losses can negatively affect the quality of soils, ground water, surface water, and the atmosphere. The losses also put drinking water quality and human health at risk, and the financial consequences can be considerable.

This research has important implications for soil quality and resilience, pollutant transport qualities of soil, water and solute transport mechanisms, water quality control and environmental management. It is in line with the increasing appreciation of the importance of soil quality in the grassland sector and the need to comply with water quality directives. The research is also highly relevant to grassland and extensive agricultural systems and the organic/conventional debate.

This study has wider implications and effects beyond the scope of the present work, for example: the impacts of a well developed and stable soil aggregate structure in relation to other soil functions, such as fertility; buffering watercourses from pollutants and pathogenic organisms; storing and transmitting water to offset risk of land flooding in the event of extreme climatic conditions; acting as a sink rather than source of biogenic greenhouse and pollutant gases; and, acting as a resilient bio-reactor and initiating biodiversity in the landscape. In addition, white clover has potential for use in soil structure remediation and mediation of soil processes.

6.5. Future work

There is a wealth of information that has come from this project, all of which invites further, more detailed study. Some specific suggestions, already mentioned in previous chapters, are summarised below.

6.5.1. Soil structuring

Although the photographic images suggested some soil aggregation induced by white clover, there is the need for more sophisticated image analysis techniques to quantify structural differentiation. Image analysis techniques would provide a quantitative comparison between soil structures under the different treatments. Useful information on porosity, and pore size, shape and connectivity would be obtained.

The study would have benefited from periodic determination of O_2 diffusion rate to monitor developments in the possible soil structural formation in planted treatments relative to the unplanted controls. The O_2 diffusion rate for each soil from Column Experiment 2 was determined after the soils were re-packed and allowed to settle prior to plant growth. The procedure should have been periodically repeated to indicate temporal changes in soil structural development. Such studies may greatly contribute to our

266

knowledge of soil structural dynamics and would provide information on the mechanisms of soil structural formation and provide the framework for further development of simulation models, and in turn management policies.

6.5.2. Soil stability

The shear strengths measured in soils of the Denbigh series require further investigation. The result may be a function of soil texture and bulk density, as this series is expected to have the greatest clay content (~23%), the least amount of sand (~20%) and the lowest bulk density (0.91 g cm^{-3}). However, this does not account for the exceptionally higher values for the unplanted Denbigh soil. The significant differences in the white clover treatments also warrant further investigation, to ascertain if the findings are a function of enhanced structural stability. The results suggest that soil beneath white clover may withstand greater forces in the field to trafficability and the trampling effects of cattle. This also lends support for the idea that white clover has amelioration for compacted and degraded soils, or those highly worked.

6.5.3. Soil modelling

The modelling part of the study requires better experimental data, and this will form part of a future project funded by the BBSRC.

6.5.4. Water and nutrient transport

It is intended to perform quantitative analysis on all elution curves using a multicompartmental model that has been proposed by Dhanoa *et al.* (1985) and has already been used by Càrdenas *et al.* (2003) to fit a mathematical model to experimental flux data.

In order to differentiate between the N applied and the background levels in the soil, one could use a nitrate solution labelled with ^{15}N; this was not possible in the time frame of this study. Using the isotopes ^{15}N and ^{18}O will provide greater information on the interaction and transport of water and nitrate in the soils.

Nitrate could be applied in a different chemical form – $NaNO_3$ rather than KNO_3 for example – which may cause different effects. It would also be interesting to determine the potassium in the tracer solution to gain insight into the behaviour of cations and the effect of cation exclusion on the shape of the elution profiles.

It is strongly recommended to repeat the experiments using a dye tracer, which will stain the active transport pathways, after subsequent de-structuring images could be captured that would provide further valuable information (Morris and Mooney, 2004).

A mass balance study of the tracers would also assist with the understanding of N and P transport and enable quantification of the losses.

Another important aspect is the transport of N in the gaseous phase, which also has important environmental implications (Càrdenas *et al.*, 2003).

The diurnal cycling of nitrate needs to be further investigated, as this is a novel observation in soils, but has been observed in riverine nutrients (Scholefield *et al.*, 2005).

Analysis of the soluble carbohydrates in the leachates is suggested as the leachates were often discoloured with a bad odour.

APPENDICES

APPENDIX I – SOIL CLASSIFICATION

AI.1. Soil pH of initial soil

Soil pH is an important soil property. Within the range of pH 3 to 9 the principal controlling factors are organic matter and the type and amount of cations (FitzPatrick, 1983). Organic matter induces acidity when present in large amounts but is neutralised by high concentrations of basic cations (FitzPatrick, 1983) such as calcium, magnesium, sodium and potassium, which tend to raise the pH (Equation A.1). Cations such as hydrogen, aluminium and iron produce acid soil solutions due to the hydrolysis of the cations (Equation A.2) (Fergusson, 1982). Soil pH can influence the fertility of the soil and the nutrient availability to plants (Heilman & Norby, 1998). So soil pH is often regulated to ensure the optimum conditions for plant utilization.

$$Clay–Na + H_2O \rightarrow Clay–H + Na^+ + OH^-$$

Equation A.1.

$$Clay–Al + 5H_2O \rightarrow Clay–H_3 + Al(OH)_4^- + H_3O^+$$

Equation A.2.

In this research, the pH of soils was determined before the soils were re-packed and prepared for plant growth. This was performed as routine soil classification. The pH was not determined after or during experimentation. However, many soil processes will influence the end pH of the soils studied. For example, the physiological constitution of legumes induces a net efflux of protons at the root–soil interface that is significantly higher than that observed under non-nitrogen fixing species (Lesturgez *et al.*, 2006). The addition of protons results in the displacement of exchangeable bases and subsequently lowers the soil pH. Acidification of soils is also controlled by the removal of cations associated with nitrate leaching (Lesturgez *et al.*, 2006).

AI.2. Organic matter content of initial soil

As discussed in Chapter One, different pools of soil organic matter (SOM), with varying stability and turnover rates, have been identified (Spaccini *et al.*, 2004). SOM is classified as inorganic carbon (carbonates) and organic carbon, which can consist of both labile and stable fractions (particulate organic matter (POM), carbohydrates, polyschacarides, phenols, lignin, lipids and humic substances). The organic matter (OM) in soils consists of residues and decomposition products of plants, animals and micro-organisms (FitzPatrick, 1983). The amount of organic matter depends on several factors and is the net result of the input of organic materials and the rate of breakdown (Davies *et al.*, 1993). The amount of organic matter in soils varies; upper soil horizons generally contain <15% and a large number contain <2% (FitzPatrick, 1983).

The majority of organic matter is derived from plants and their roots, and contains carbohydrates, proteins, lignins, waxes, oils and pigments. Humus or colloidal organic matter is often translocated within the soil and subsequently deposited; it can be dispersed or flocculated like clays (FitzPatrick, 1983). As well as containing the soil's reserve of nutrients (Davies *et al.*, 1993), the properties of organic matter determine the characteristics of many upper horizons. It enhances the structure and stability of the soil (Chapter One, Section 1.6.3), and is capable of absorbing large quantities of water (FitzPatrick, 1983).

AI.3. Soil texture of initial soil

Texture is an important physical characteristic, which influences factors such as water retention (Chapter Four) and drainage (FitzPatrick, 1983) and so determines a soil's agricultural potential (White, 1997). Coarse textured soils are better for drainage although crops may be more susceptible to drought, whilst medium textured soils are often preferred for their ability to hold water and nutrients (White, 1997). The stone content of a soil may be just as important as the texture of the fine earth fraction (clay, silt and sand). For example, a stony sandy loam like the Crediton series will hold less water than a soil of the same textural class with fewer stones, such as the Frilsham series.
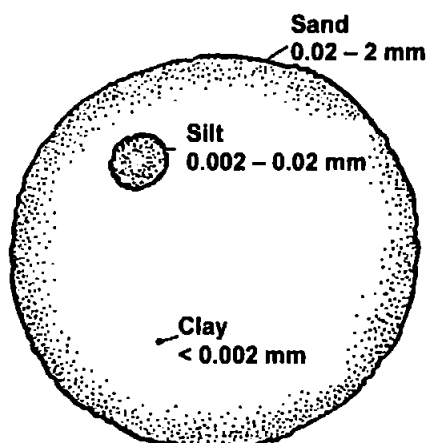
Figure A.1. The relative sizes of clay, silt and sand, based on the International Classification System. (adapted from Klocke & Hergert, 1996).

APPENDIX II – EXPERIMENTAL DESIGN

AII.1. 0.5 m lysimeter design

A square PVC reservoir (451 x 451 x 114 mm) was fitted with an adjustable constant-head device to supply the water. Rainfall can be simulated at a rate of 6.4 mm h^{-1} via an array of 100 25G syringe needles (I.D. 0.318 mm, Richards, Leicester, UK). The oscillating reservoir is powered by an electric motor that turned a vertical brass rod and cam mounted within a PVC ring attached to an edge of the rainfall reservoir. Mathews (1997) showed that the rainfall simulator had a relative standard deviation of 8.8%. However, the rainfall simulator was not used; rainfall was simulated with a peristaltic pump at a rate of 2.4 mm h^{-1} to achieve the same as that applied to the cores in Column Experiment 2 (Chapter Five).
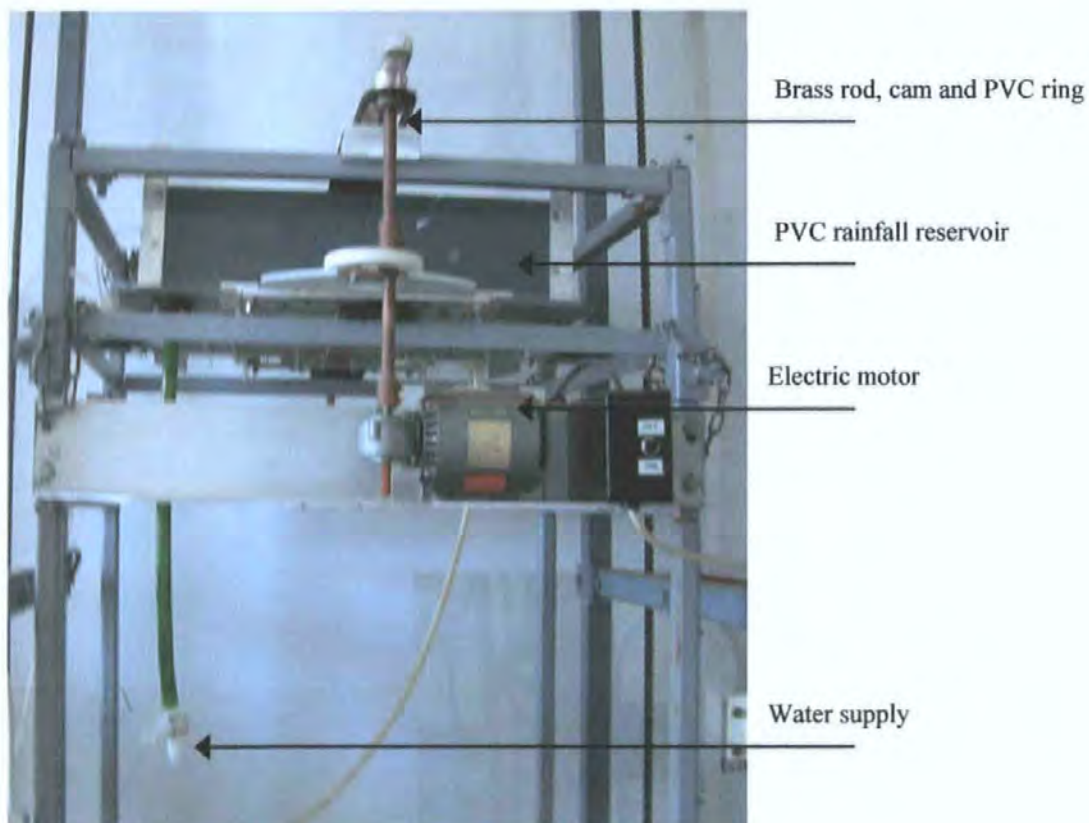
Figure A.2. Rainfall Simulator located in the central tower above the soil block (**Johnson** *et al.*, **2003b**).
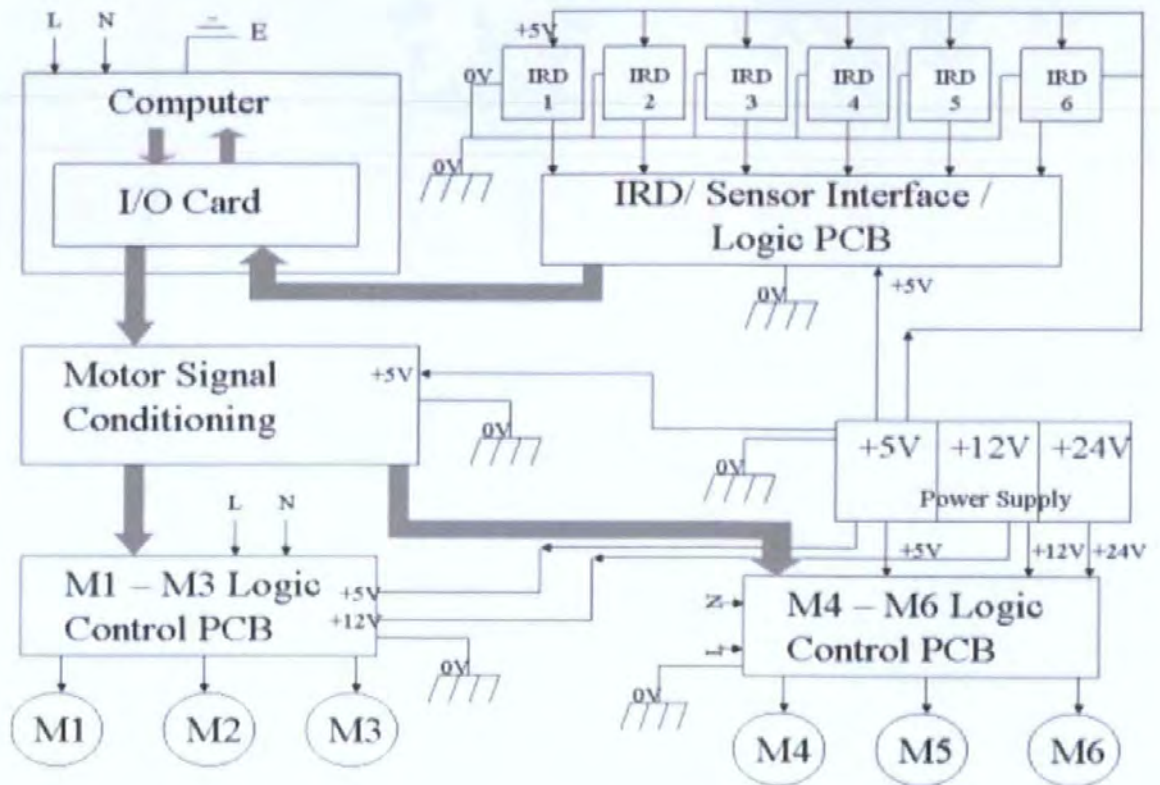
Figure A.3. A Schematic layout of the circuitry that allows automated computer control of the lysimeter. M1 - M6 denotes the six motors and IRD 1 - IRD 6 the infrared detectors(Johnson *et al.*, 2003b).
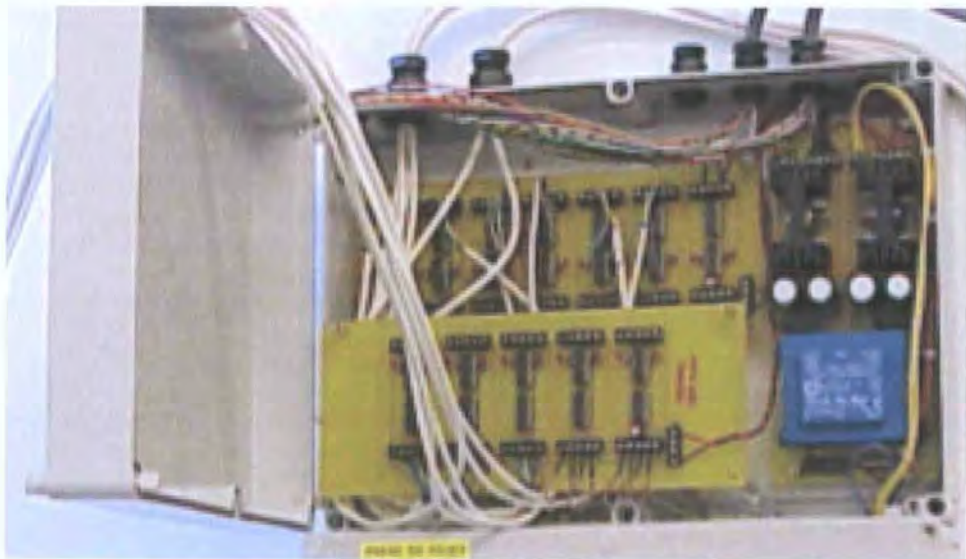
Figure A.4. Photograph of the circuitry that allows automated computer control of the lysimeter as given schematically in Figure A.3.

AII.2. Skalar SAN$^{Plus®}$ analyzer
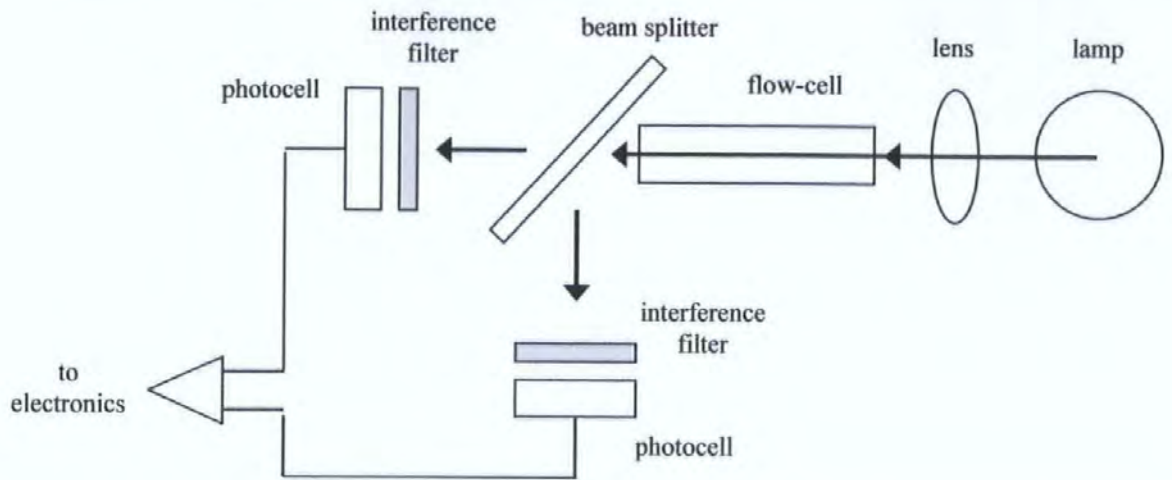
Figure A.5. Schematic representation of the SA 6250 photometer single channel detector with matrix correction as shown in Figure A.6.
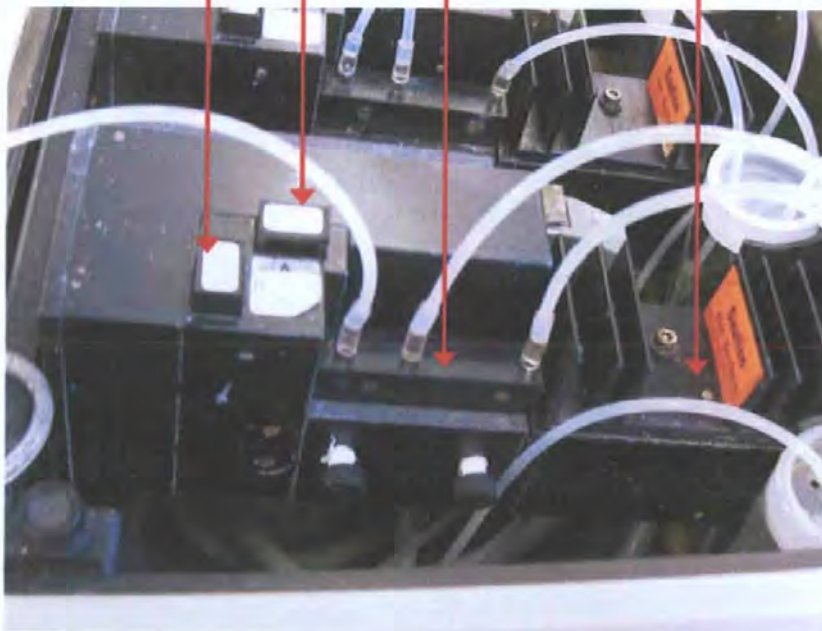
Figure A.6. The SA 6250 photometer single channel detector with matrix correction. This optical detection head is positioned in the chemistry unit and sends signals to a separate electronics section.
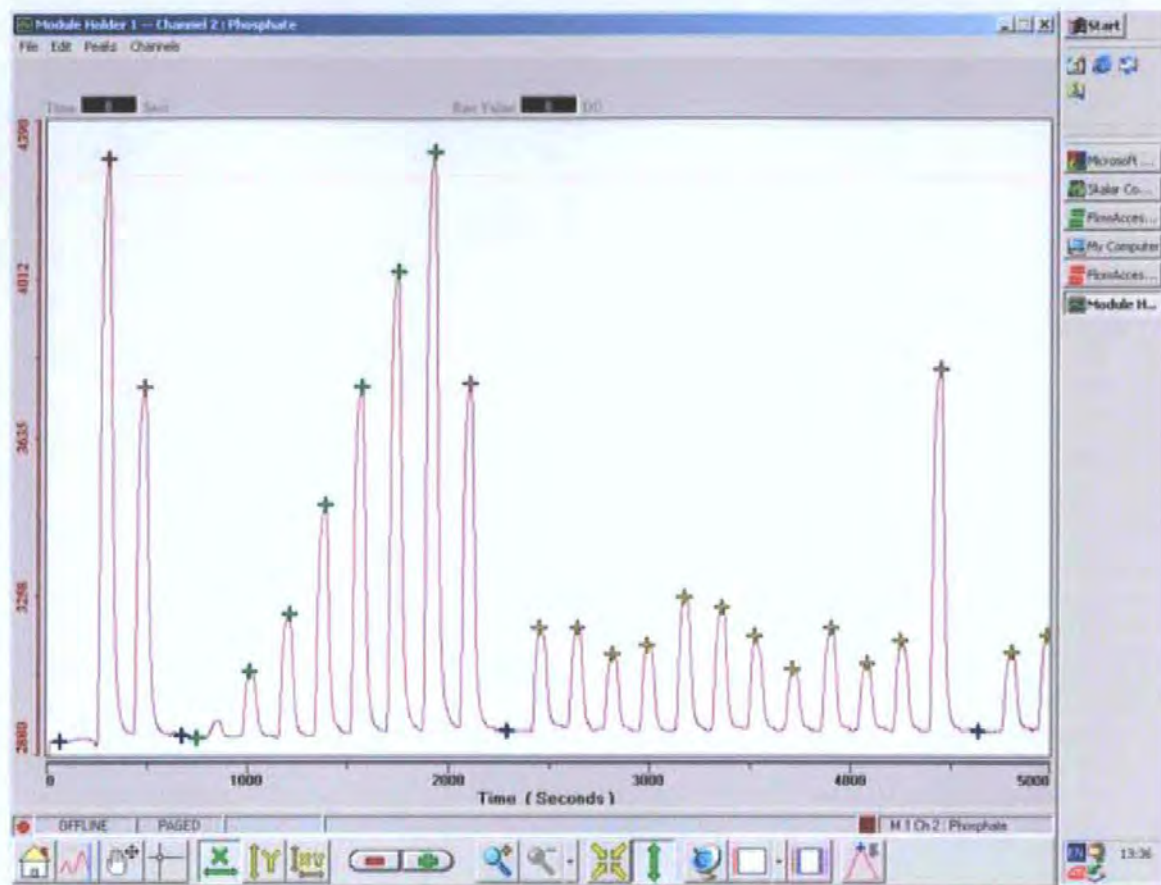
Figure A.7. *FlowAccess*® **software showing a typical output of signals for the calibration of 1– 5 mg L^{-1} nitrate analysis. Peaks represent standards (green crosses), samples (yellow crosses) and base line correction (red crosses). These peaks are shown in sections separated by washes (blue crosses) at the base line.**

AII.3. Skalar SAN$^{Plus®}$ - Bromide analysis

The manifold configuration and flow diagram shown in Figure A.8 illustrates how the reagents and sample are mixed for the desired reactions to occur. Figure A.9 gives a key to the manifold components and flow diagrams for all analyses. The reagents and chemicals required for the determination of bromide are listed in Table A.1.

Figure A.8. Skalar SANS^Plus manifold configuration and flow diagram for high range bromide analysis (1 - 50 mg L^-1 Br). For low range analysis (0.2 - 10 mg L^-1 Br), the pump tubing for the hydrochloric acid solution and the sample stream are changed to 0.42 ml min^-1 and 0.60 ml min^-1, respectively.

Figure A.9. Key to manifold components and flow diagrams for all analyses.

Table A.1. Reagents and requirements for bromide analysis. Reagent A. (hydrochloric acid solution) varies according to the analytical range (*high range*: 1 - 50 mg L^{-1} Br and *low range*: 0.2 - 10 mg L^{-1} Br).

Reagent	Required chemicals	Special requirements
A. Hydrochloric acid solution (0.5N) (*High range*: 1 - 50 mg L^{-1})	Hydrochloric acid HCl (32%) - 50 ml; Ultra-pure water - 930 ml; Stock solution 1000 ppm Br - 20 ml; Brij 35 (30%) - 3 ml.	Solution is stable for 1 week. Store the solution at 4°C when the solution is not used.
A. Hydrochloric acid solution (1N) (*Low range*: 0.2 - 10 mg L^{-1})	Hydrochloric acid HCl (32%) - 100 ml; Ultra-pure water - 860 ml; Stock solution 1000 ppm Br - 40 ml; Brij 35 (30%) - 3 ml.	Solution is stable for 1 week. Store the solution at 4°C when the solution is not used.
B. Buffer solution (pH 6.3)	Sodium dihydrogen o-phosphate NaH_2PO_4 - 200 g; Sodium hydroxide NaOH - 28 g; Ultra-pure water ~ 1000 ml; FFD6 - 3 ml.	Solution is stable for 1 week at 4°C. Check the pH of the solution daily.
C. Sodium hypochlorite solution	1N sodium hypochlorite solution in 0.1M sodium hydroxide solution	Use hypochlorite with low bromine concentration. Sensitive to light.
D. Sodium formate solution (50%)	Sodium formate HCO_2Na - 50 g; Ultra-pure water - 100 ml.	Solution is stable for one day.
E. Stock solution bromide molybdate	Potassium bromide KBr - 0.150 g; Ammonium molyddate $(NH_4)_6Mo_7O_{24}.4H_2O$ - 3 g; Ultra-pure water ~ 100 ml.	
F. Stock solution fuchsine	Fuchsine (basic) $C_{20}H_{20}ClN_3$ - 0.030 g; Sulfuric acid H_2SO_4 (97%) - 28 ml; Ultra-pure water - 472 ml.	Store in a dark coloured bottle.
G. Stock solution sulfuric acid (14N)	Sulfuric acid H_2SO_4 (97%) - 389 ml; Ultra-pure water - 611 ml.	
H. Colour reagent	Stock solution bromide molybdate (E) - 100 ml; Stock solution fuchsine (F) - 500 ml; Stock solution sulfuric acid (14N) (G) - 400 ml.	Stable for one day if stored in a dark coloured bottle.
I. 2-Propanol	2-Propanol C_3H_8O	
J. Sulfuric acid solution (7N)	Sulfuric acid H_2SO_4 (97%) - 195 ml; Ultra-pure water - 805 ml.	Solution is stable for 1 month.
K. Rinsing liquid	Ultra-pure water	Refresh daily.

FFD6 and Brij 35 are ionic and non-ionic surfactants, respectively.

AII.4. Bromide standards and reagents

A standard stock solution (1000 mg L^{-1} Br) was prepared by dissolving 1.149 g of potassium bromide (KBr) in ± 800 ml ultra-pure water, diluted to 1 L with ultra-pure water and mixed. The stock solution was stored at 4°C and remade after 1 month. A dilute standard solution (200 mg L^{-1} Br) was made daily by diluting 20 ml of standard stock solution (1000 mg L^{-1} Br) in 100 ml of ultra-pure water. Both solutions were diluted to prepare working standards for the high range (1 - 50 mg L^{-1} Br) and low range (0.2 - 10 mg L^{-1} Br) bromide analysis (Table A.2).

The analytical range was altered by reducing the ratio of the buffer to sample. This was achieved by reducing the concentration of the buffer solution (Table A.1) and by increasing the flow rate of the sample and decreasing that of the buffer solution (Figure A.8).

Table A.2. Concentration and preparation of bromide working standards for *high range* (1 - 50 mg L^{-1} Br) and *low range* (0.2 - 10 mg L^{-1} Br) analysis.

Concentration of working standards (mg L^{-1} Br)

High range: 1 - 50 mg L^{-1} (1000 mg L^{-1} stock solution)	Low range: 0.2 - 10 mg L^{-1} (200 mg L^{-1} stock solution)	Volume (ml) of stock solution to dilute to 100 ml
50	10	5
40	8	4
30	6	3
20	4	2
10	2	1

AII.5. Skalar SAN[Plus®] - Nitrite/nitrate analysis

The manifold configuration and flow diagram shown in Figure A.10 illustrates how the reagents and sample are mixed for the desired reactions to occur. The reagents and chemicals required for the determination of nitrite/nitrate are listed in Table A.3. By comparison, Table A.4 lists the reagents for the determination of nitrate with the Skalar manifold and detection chemistry deployed at IGER for soil leachates from Column Lysimeters 1.
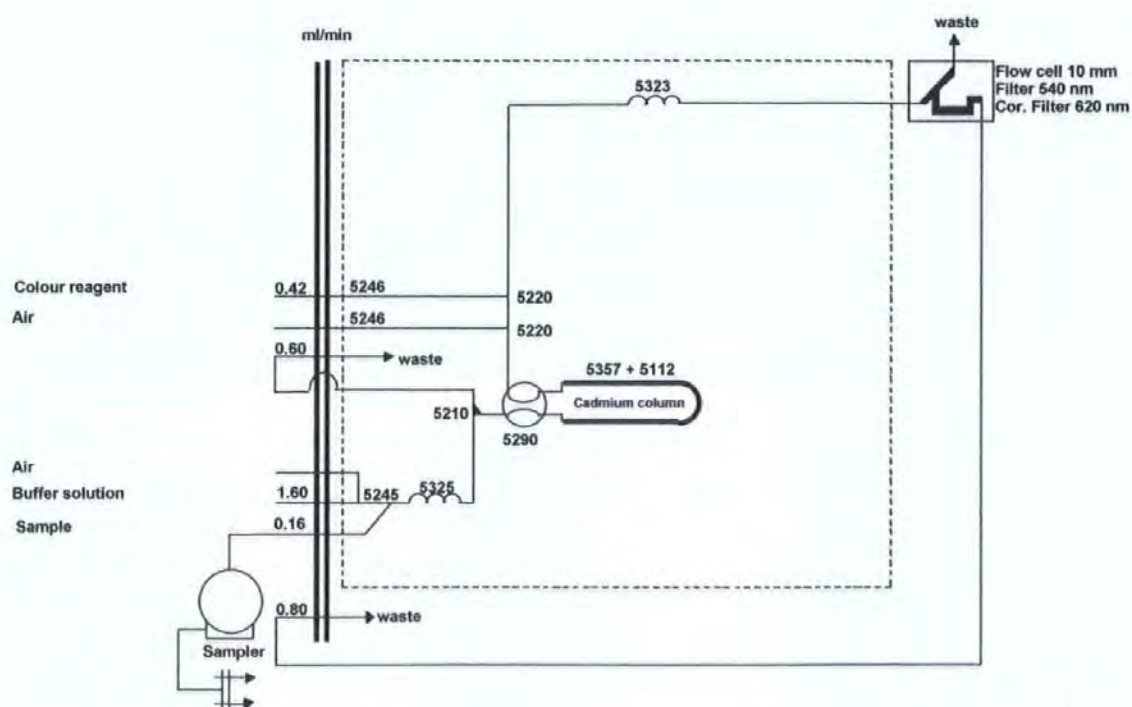

Figure A.10. Skalar SANS[Plus] manifold configuration and flow diagram for high range nitrite/nitrate analysis (0.1 - 5 mg L^{-1} N). For low range analysis (2 - 100 µg L^{-1} N), the tubing for the buffer solution and the sample stream are changed to 0.80 ml min^{-1} and 1.40 ml min^{-1}, respectively, their position of entry is also exchanged.

Table A.3. Reagents and requirements for nitrite/nitrate analysis. Reagent A. (Buffer solution) varies according to the analytical range (*high range*: 0.1 - 5 mg L^{-1} NO$_3$-N and *low range*: 2 - 100 µg L^{-1} NO$_3$-N).

Reagent	Required chemicals	Special requirements
A. Buffer solution (pH 8.2) (*High range*: 0.1 - 5 mg L^{-1})	Ammonium chloride NH$_4$Cl - 25 g; Ammonium hydroxide solution NH$_4$OH (25%) ~ 1ml; Ultra-pure water ~ 1000 ml; Brij 35 (30%) - 3 ml.	Degas the reagent before adding Brij 35. Adjust to pH 8.2. Solution is stable for 1 week. Store at 4°C when not in use.
A. Buffer solution (pH 8.2) (*Low range*: 2 - 100 µg L^{-1})	Ammonium chloride NH$_4$Cl - 50 g; Ammonium hydroxide solution NH$_4$OH (25%) ~ 1ml; Sodium hydroxide NaOH - 5g; Ultra-pure water ~ 1000 ml; Brij 35 (30%) - 3 ml.	Degas the reagent before adding Brij 35. Adjust to pH 8.2. Solution is stable for 1 week. Store at 4°C when not in use.
B. Colour reagent	o-Phosphoric acid H$_3$PO$_4$ (85%) - 150 ml; Sulfanilamide C$_6$H$_8$N$_2$O$_2$S - 10 g; N-(1-Naphthyl)ethylene diamine dihydrochloride C$_{12}$H$_{16}$Cl$_2$N$_2$ - 0.5 g; Ultra-pure water ~ 850 ml.	Solution is stable for 2 weeks. Store in a dark coloured bottle.
C. Rinsing liquid	Ultra-pure water	Refresh daily.

Table A.4. Reagents and requirements for nitrate analysis (0.1 - 5 mg L^{-1} NO$_3$-N) using the Skalar manifold and detection chemistry deployed at IGER for soil leachates from Column Lysimeters 1.

Reagent	Required chemicals	Special requirements
A. Buffer solution (pH 5.2)	Potassium sodium tartrate C$_4$H$_4$O$_6$KNa.4H$_2$O - 33 g. Sodium citrate C$_6$H$_5$O$_7$Na$_3$.2H$_2$O - 24 g; Ultra-pure water ~1000 ml; Brij 35 (15%) - 2 ml.	Degas the reagent before adding Brij 35. Check the pH and adjust if necessary with hydrochloric acid to 5.2 ± 0.1. Solution is stable for 1 week. Store at 4°C.
B. Sodium hydroxide / pyrophosphate solution	Sodium hydroxide NaOH - 6 g; tetra-sodium pyrophosphate Na$_4$P$_2$O$_7$.10H$_2$O - 22.303 g; Ultra-pure water ~1000 ml; Brij 35 (30%) - 1 ml.	Solution is stable for 1 week. Store in a dark coloured bottle.
C. Stock solution cupric sulfate	Cupric sulfate CuSO$_4$.5H$_2$O - 1.2 g; Ultra-pure water ~ 100 ml.	Solution is stable for 1 month. Store at 4°C.
D. Hydrazinium sulfate solution	Hydrazinium sulfate N$_2$H$_6$SO$_4$ - 5 g; Stock solution cupric sulfate (C) - 1.5 ml; Ultra-pure water ~1000 ml.	Solution is stable for 1 week. Store at 4°C.
E. Colour reagent	o-Phosphoric acid H$_3$PO$_4$ (85%) - 150 ml; Sulfanilamide C$_6$H$_8$N$_2$O$_2$S - 10 g; N-(1-Naphthyl)ethylene diamine dihydrochloride C$_{12}$H$_{16}$Cl$_2$N$_2$ - 0.5 g; Ultra-pure water ~ 850 ml.	Solution is stable for 2 weeks. Store in a dark coloured bottle. Filter before use.
F. Rinsing liquid	Ultra-pure water	Refresh daily.

AII.6. Nitrite/nitrate standards and reagents

A standard stock solution (1000 mg L^{-1} N) was prepared by dissolving 6.068 g of sodium nitrate ($NaNO_3$) in ± 800 ml ultra-pure water, diluted to 1 litre with ultra-pure water and mixed. The stock solution was stored at 4°C and remade after 1 month. Dilute standard solutions were made daily by diluting 10 ml of standard stock solution (1000 mg L^{-1} N) in 100 ml of ultra-pure water (100 mg L^{-1} N) or by diluting 2 ml of diluted stock solution (100 mg L^{-1} N) to 100 ml (2 mg L^{-1} N). These stock solutions were diluted to prepare working standards for the high range (0.1 - 5 mg L^{-1} N) and low range (2 - 100 µg L^{-1} N) nitrite/nitrate analysis (Table A.5).

The analytical range and sensitivity was altered by reducing the ratio of the buffer to sample. This was achieved by 1) reducing the concentration of the buffer solution (Table 5.8) because a smaller buffer capacity is required to accommodate the pH change brought about by the reduction of nitrate to nitrite (Zhang, 2000) and 2) by increasing the flow rate of the sample and decreasing that of the buffer solution (Figure A.10) as this will increase the width of the peak height plateau and thus the precision of analysis.

Table A.5. Concentration and preparation of nitrite/nitrate working standards for *high range* (0.1 - 5 mg L^{-1} NO_3-N) and *low range* (2 - 100 µg L^{-1} NO_3-N) analysis.

Concentration of working standards (mg L^{-1} NO_3-N and µg L^{-1} NO_3-N)

High range: 0.1 - 5 mg L^{-1} (100 mg L^{-1} stock solution)	Low range: 2 - 100 µg L^{-1} (2 mg L^{-1} stock solution)	Volume (ml) of stock solution to dilute to 100 ml
5	100	5
4	80	4
3	60	3
2	40	2
1	20	1

AII.7. Skalar SAN$^{Plus®}$ - Cadmium reduction column

Cadmium granules were sieved (0.3-1.0 mm) and washed twice with 30 ml of 4 M HCl and repeated with deionised water until acid free (pH > 7). 50 ml of 2% (w/v) $CuSO_4$ solution was added and swirled until brown flakes of colloidal copper appeared and the blue colour of the $CuSO_4$ solution faded. The solution was decanted and the procedure was repeated until the blue colour did not fade. The granules were repeatedly washed with deionised water until the blue colour disappeared and the supernatant was free of fine particles. The activated cadmium was submerged in ammonium chloride buffer solution to avoid exposure of any cadmium filings to the air before packing. Table A.6 lists the chemicals required for the preparation and activation of the reduction column.

A U-shaped glass tube (2 mm ID) was plugged at one end with plastic tubing; the other end was connected to a 10 ml pipette. The column was filled with buffer solution and activated cadmium was transferred in suspension through the pipette to the column. With gentle tapping, cadmium granules were packed tightly and uniformly in the column. Caution was exercised to avoid any entraining air bubbles during packing. When filled, the column was plugged with plastic tubing and flushed with buffer solution.

Table A.6. Reagents required the activation of copper-cadmium reduction column for nitrite/nitrate analysis.

Reagent	Required chemicals
D. Hydrochloric acid solution (4 M)	Hydrochloric acid HCl (32%) - 400 ml; Distilled water - 600 ml.
E. Copper(II) sulfate solution (2%)	Cupric sulfate $CuSO_4.5H_2O$ - 20 g; Distilled water - 1000 ml.
F. Cadmium	Cadmium granules - ± 4.5 g size 0.3-1.0 mm (sieved)
A. Ammonium chloride buffer solution (pH 8.2)	As in

AII.8. Skalar SAN^{Plus®} - Phosphate analysis

The manifold configuration and flow diagram shown in Figure A.11 illustrates how the reagents and sample are mixed for the desired reactions to occur. The reagents and chemicals required for the determination phosphate are listed in Table A.7.

Figure A.11. Skalar SANS^{Plus} manifold configuration and flow diagram for orthophosphate analysis (2 - 100 µg L^{-1} P).

Table A.7. Reagents and requirements for orthophosphate analysis (2 - 100 µg L^{-1} PO$_4$-P).

Reagent	Required chemicals	Special requirements
A. Ammonium molybdate solution	Potassium antimony tartrate K(SbO)C$_4$H$_4$O$_6$.0.5H$_2$O - 0.230 g; Sulfuric acid H$_2$SO$_4$ (97%) - 35 ml; Ammonium molybdate (NH$_4$)$_6$Mo$_7$O$_{24}$.4H$_2$O - 6 g; Ultra-pure water ~ 965 ml; FFD6 - 2 ml.	Do not use metal spoons for ammonium molybdate. The end pH must be < 1. Solution is stable for 1 week. Store at 4°C when not in use.
B. Ascorbic acid solution	Ascorbic acid C$_6$H$_8$O$_6$ - 11 g; Acetone C$_3$H$_6$O - 60 ml; Ultra-pure water ~ 940 ml; FFD6 - 2 ml.	Stable for 5-7 days. Store at 4°C when not in use. Sensitive to light.
C. Rinsing liquid	Ultra-pure water	Refresh daily.

AII.9. Phosphate standards and reagents

A standard stock solution (100 mg L^{-1} P) was prepared by dissolving 0.4394 g of potassium dihydrogen o-phosphate nitrate (KH_2PO_4) in ± 800 ml ultra-pure water, diluted to 1 litre with ultra-pure water and mixed. The stock solution was stored at 4°C and remade after 1 month. A dilute standard solution (2 mg L^{-1} P) was made daily by diluting 2 ml of standard stock solution (100 mg L^{-1} P) in 100 ml of ultra-pure water. Working standards (2 - 100 μg L^{-1} P) were prepared by serial dilution (Table A.8).

Table A.8. Concentration and preparation of working standards for orthophosphate analysis (2 - 100 μg L^{-1} PO$_4$-P).

Concentration of working standards (μg L^{-1} PO$_4$-P) 2 - 100 μg L^{-1} (2 mg L^{-1} stock solution)	Volume (ml) of stock solution to dilute to 100 ml
100	5
80	4
60	3
40	2
20	1

AII.10. Skalar SAN$^{Plus®}$ - ammonium analysis

The manifold configuration and flow diagram shown in Figure A.12 illustrates how the reagents and sample are mixed for the desired reactions to occur. The reagents and chemicals required for the determination of ammonium are listed in Table A.9.
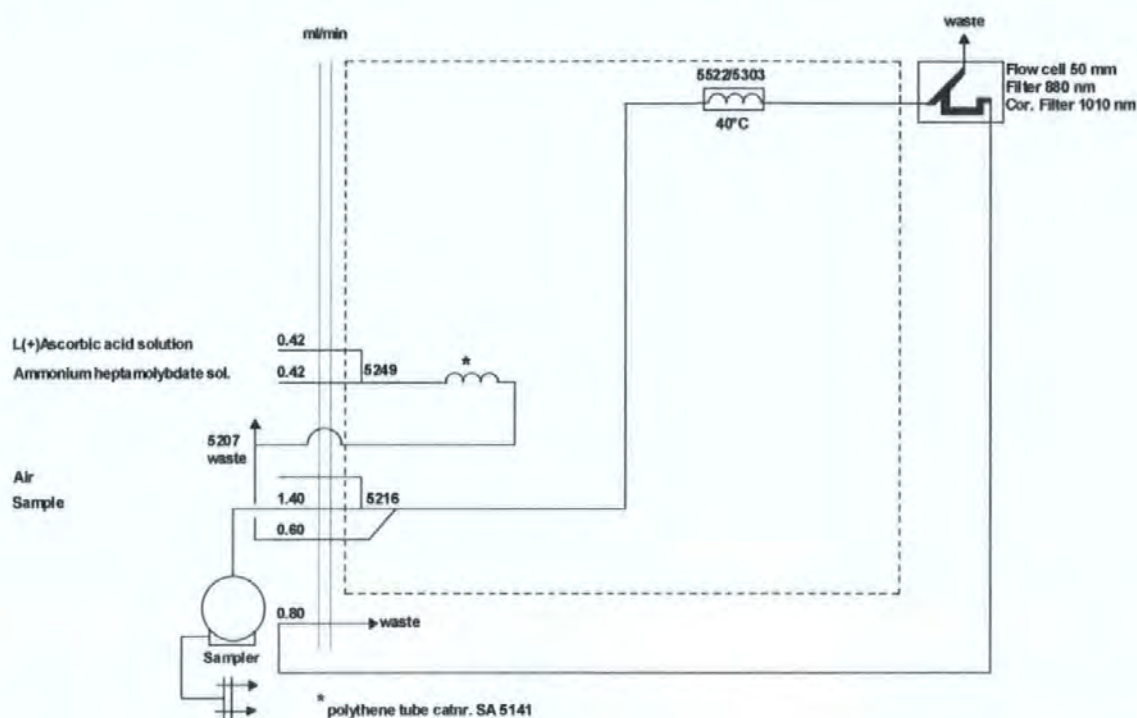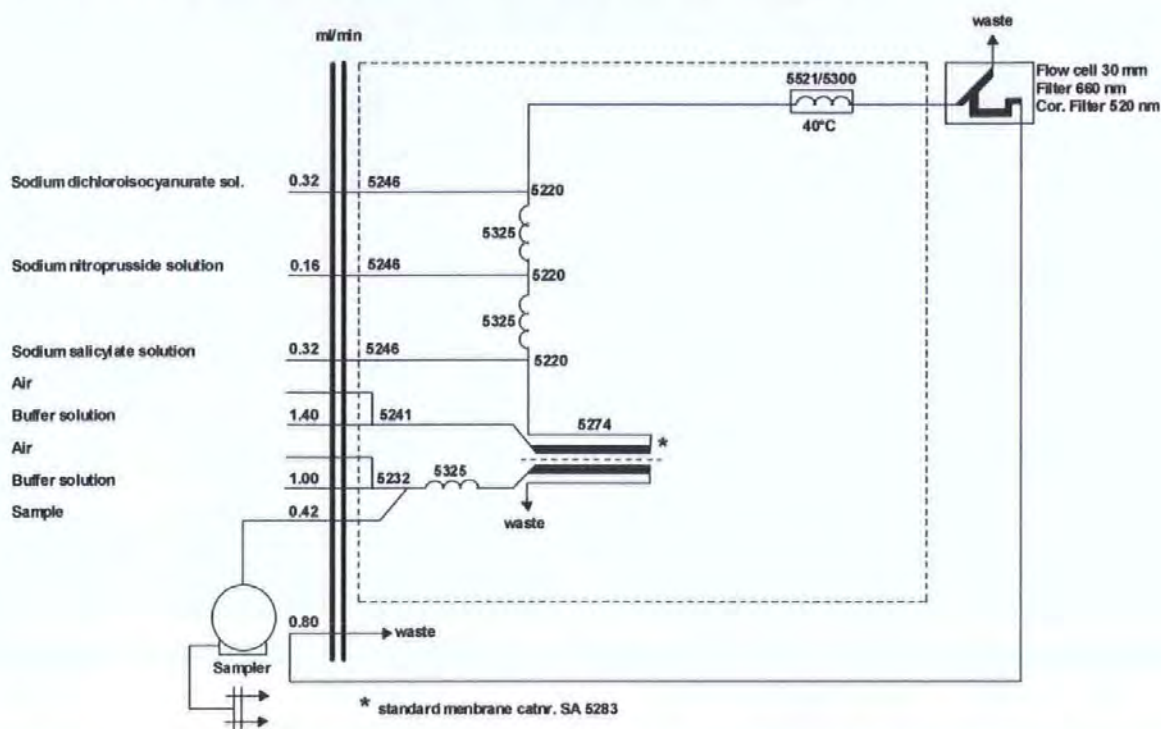

Figure A.12. Skalar SANS^{Plus} manifold configuration and flow diagram for ammonium analysis.

Table A.9. Reagents required for ammonium analysis (*high range*: 0.2 - 10 mg L^{-1} NH$_4$-N and *low range*: 0.1 - 1 mg L^{-1} NH$_4$-N).

Reagent	Required chemicals	Special requirements
A. Buffer solution (pH 5.2)	Potassium sodium tartrate C$_4$H$_4$O$_6$KNa.4H$_2$O- 33g Sodium citrate C$_6$H$_5$O$_7$Na$_3$.2H$_2$O - 24g; Ultra-pure water ~ 1000 ml; Brij 35 (15%) - 2 ml.	Check pH and adjust if with HCl to 5.2 ± 0.1. Solution is stable for 1 week. Store at 4°C.
B. Sodium salicylate solution	Sodium hydroxide NaOH - 25 g; Sodium salicylate C$_7$H$_5$NaO$_3$ - 80 g; Ultra-pure water ~ 1000 ml.	Solution is stable for 1 week. Store in a dark coloured bottle.
C. Sodium nitrusside solution	Sodium nitroprusside Na$_2$[Fe(CN)$_5$NO].2H$_2$O - 1 g Ultra-pure water ~ 1000 ml.	Solution is stable for 1 week. Store in a dark coloured bottle.
D. Sodium dichlororisocyanurate solution	Sodium dichloroiso-cyanurate C$_3$N$_3$O$_3$Cl$_2$Na.2H$_2$O - 2 g; Ultra-pure water ~ 1000 ml.	Solution is stable for 1 week.
E. Rinsing liquid	Ultra-pure water	Refresh daily.

AII.11. Ammonium standards and reagents

A standard stock solution (1000 mg L^{-1} N) was prepared by dissolving 3.819 g of ammonium chloride (NH$_4$Cl) in ± 800 ml ultra-pure water, diluted to 1 litre with ultra-pure water and mixed. The stock solution was stored at 4°C and remade after 1 month. A dilute standard solution (100 mg L^{-1} N) was made daily by diluting 10 ml of standard stock solution (1000 mg L^{-1} N) in 100 ml of ultra-pure water. The dilute standard solution (100 mg L^{-1} N) was diluted ten-fold for the lower range analysis standard solution (10 mg L^{-1} N). These stock solutions were diluted to prepare working standards for the high range (0.2 - 10 mg L^{-1} N) and low range (0.1 - 1 mg L^{-1} N) ammonium analysis (Table A.10).

Table A.10. Concentration and preparation of ammonium working standards for *high range* (0.2 - 10 mg L^{-1} NH$_4$-N) and *low range* (0.1 - 1 mg L^{-1} NH$_4$-N) analysis.

Concentration of ammonium working standards (mg L^{-1} NH$_4$-N)

High range: 0.2 - 10 mg L^{-1} (100 mg L^{-1} stock solution)	*Low range*: 0.1 – 1 mg L^{-1} (10 mg L^{-1} stock solution)	Volume (ml) of stock solution to dilute to 100 ml
10	1	10
8	0.8	8
6	0.6	6
4	0.4	4
2	0.2	2
1	0.1	1

REFERENCES

REFERENCES

Aeby, P., Forrer, J., Steinmeier, C. & Flühler, H. (1997) Image analysis for determination of dye tracer concentrations in sand columns. *Soil Science Society of America Journal* **61**, 33-35.

Agricultural Advisory Council (1970) *Modern Farming and the Soil*. HMSO.

Allaire-Leung, S.E., Gupta, S.C. & Moncrief, J.F. (2000) Water and solute movement in soil as influenced by macropore characteristics. 1. Macropore continuity. *Journal of Contaminant Hydrology* **41**, 283-301.

Allen, S.E., Gimshaw, H.M., Parkinson, J.A. & Quarmby, C. (1974) Chemical *Analysis of Ecological Materials*. Blackwell Science Publications.

Alter, S.R., Brusseau, M.L., Piatt, J.J., Ray-Maitra, A., Wang, J.-M. & Cain, R.B. (2003) Use of tracer tests to evaluate the impact of enhanced-solubilization flushing on in-situ biodegradation. *Journal of Contaminant Hydrology* **64**, 191-202.

Amarger, N. (2001) Rhizobia in the field. *Advances in Agronomy* **73**, 109-168.

Ammann, A.A., Hoehn, E. & Koch, S. (2003) Ground water pollution by root runoff infiltration evidenced with multi-tracer experiments. *Water Research* **37**, 1143-1153.

Anderson, T.-H. & Domsch, K.H. (1989) Ratios of microbial carbon to total organic carbon in arable soils. *Soil Biology & Biochemistry 21, 471-479.*

Angers, D.A. & Carter, M.R. (1996) Aggregation and organic matter storage in cool, humid agricultural soils. In: Carter, M.R. & Stewart, B.A. (Eds.) *Structure and Organic Matter Storage in Agricultural Soils*, pp. 193-211, CRC Press Inc., Boca Raton, Florida.

Angers, D.A. & Caron, J. (1998) Plant-induced changes in soil structure: processes and feedbacks. *Biogeochemistry* **42**, 55-72.

Aspiras, R.B., Allen, O.N., Harris, R.F. & Chesters, G. (1971) The role of micro-organisms in the stabilization of soil aggregates. *Soil Biology and Biochemistry* **3**, 347-353.

Baker, M.J. & Williams, W.M. (1987) *White Clover*. CAB International, Wallingford, UK.

Balabane, M. & Plante, A.F. (2004) Aggregation and carbon storage in silty soil using physical fractionation techniques. *European Journal of Soil Science* 55, 415-427.

Ball, B.C., Campbell, D.J. Douglas, J.T., Henshall, J.K. & O' Sullivan, M.F. (1997) Soil structural quality, compaction and land management. *European Journal of Soil Science* 48, 593-601.

Bartoli, F., Bird, N.R.A., Gomendy, V., Vivier, H. & Niquet, S. (1999) The relation between silty soil structures and their mercury porosimetry curve counter parts: fractals and percolation. *European Journal of Soil Science* 50, 9-22.

Baveye, P. (2005) Comment on 'Soil structure and management: A review' by C.J. Bronick & R. Lal. *Geoderma* 124, 1-2.

Beare, M.H., Hu, S., Coleman, D.C. & Hendrix, P.F. (1997) Influences of mycelial fungi on soil aggregation and organic matter storage in conventional and no-tillage soils. *Applied Soil Ecology* 5, 211-219.

Bendschneider, K. & Robinson, R.J. (1952) A new spectrophotometric method for the determination of nitrite in sea water. *Journal Marine Research* 11, 87-96.

Bergström, L. (1990) Use of lysimeters to estimate leaching of pesticides in agricultural soils. *Environmental Pollution* 67, 325-347.

Bird,N.R.A. & Perrier,E.M.A. (2003) The pore-solid fractal model of soil density scaling. *European Journal of Soil Science* 54, 467-476.

Boix-Fayos, C., Calvo-Cases, A. & Imeson, A.C. (2001) Influence of soil properties on the aggregation of some Mediterranean soils and the use of aggregate size and stability as land degradation indicators. *Catena* 44, 47-67.

Boller, B.C. & Nosberger, J. (1987) Symbiotically fixed nitrogen from field grown white and red clover with rye-grass at low levels of ^{15}N-fertilization. *Plant and Soil* 104, 219-226.

Borgesen, C.D. & Schaap, M.G. (2005) Point and parameter pedotransfer functions for water retention predictions for Danish soils. *Geoderma* 127, 154-167.

Bouma, J., Jongerius, A., Boersma, O., Jager, A. & Schoonderbeek, D. (1977) The function of different types of macropores during saturated flow through four swelling soil horizons. *Soil Science Society of America Journal* **41**, 945-950.

Bouma, J. (1991) Influence of soil macroporosity on environmental quality. *Advances in Agronomy* **46**, 1–37

Bouyoucos, G.J. (1926) Estimation of the colloidal material in soils. *Science* **64**, 362.

Bradford, J.M. (1986) Penetrability. In: Klute, C.A. (Ed.) *Methods of Soil Analysis. Part 1. Agronomy*, **9**, American Society of Agronomy Inc. Madison, Wisconsin, USA. pp. 463-478.

Bronick, C.J. & Lal, R. (2005) Soil structure and management: a review. *Geoderma* **124**, 3-22.

Caravaca, F., Hernández, T., García, C. & Roldán, A. (2002) Improvement of rhizosphere aggregate stability of afforested semiarid plant species subjected to mycorrhizal inoculation and compost addition. *Geoderma* **108**, 133-144.

Cárdenas, L.M., Hawkins, J.M.B., Chadwick, D. & Scholefield, D. (2003) Biogenic gas emissions from soils measured using a new automated laboratory incubation system. *Soil Biology & Biochemistry* **35**, 867-870.

Clancy, V.P. & Willis, S. (2003) Second intercomparison for nutrients in seawater. NAOO Technical Memo 158. http://ccmaserver.nos.noaa.gov/ [May 2005].

Clayden, B. (1971) *Memoirs of the Soil Survey of Great Britain: Soils of the Exeter District; Sheets 325 and 339*. Rothamsted Experimental Station, Harpenden.

Clayden, B. & Hollis, J.M. (1984) *Criteria for differentiating soil series*. Soil Survey Technical Monograph No. 17. Rothamsted Experimental Station, Harpenden.

Condron, L.M., Cameron, K.C., Di, H.J., Clough, T.J., Forbes, E.A., McLaren, R.G. & Silva, R.G. (2000) A comparison of soil and environmental quality under organic and conventional farming systems in New Zealand. *New Zealand Journal of Agricultural Research* **43**, 443-466.

Cresswell, A., Hamilton, N.S., Thomas, H., Charnock, R.B., Cookson, A.R. & Thomas, B.J. (1999) Evidence for root contraction in white clover (*Trifolium repens* L.). *Annals of Botany* **84**, 359-369.

Cuttle, S.P., Scurlock, R.V. & Davies B.M.S. (1998) A 6-year comparison of nitrate leaching from clover/grass and N-fertilised grass grazed by sheep. *Journal of Agricultural Science* **131**, 39-50.

Czarnes, S., Hallett, P.D., Bengough, A.G. & Young, I.M. (2000) Root- and microbial-derived mucilages affect soil structure and water transport. *European Journal of Soil Science* **51**, 435-443.

Dabire, K.R., Duponnois, R. & Mateille, T. (2001) Indirect effects of the bacterial soil aggregation on the distribution of *Pasteuria penetrans*, an obligate bacterial parasite of plant-parasitic nematodes. *Geoderma* **102**, 139-152.

Dathe, A. (2001) Fractal dimensions of soil properties as measured by image analysis. *Soil Structure, Water and Solute Transport. IRD International Symposium.* Bondy, France. pp. 64-66.

Davidson, D.T. (1965) Penetrometer Measurements. In: Black, C.A. (Ed.) *Methods of Soil Analysis. Part 1. Agronomy*, **9**, American Society of Agronomy Inc., Madison, Wisconsin, USA. pp. 472-484.

Davidson, D.A. & Grieve, I.C. (2006) Relationships between biodiversity and soil structure and function: Evidence from laboratory and field experiments. Applied Soil *Ecology* **33**, 176-185.

Davies, B., Eagle, D. & Finney, B. (1993) *Soil Management.* Farming Press.

Davis, J.L. & Chudobiak, W.J. (1975) In-situ meter for measuring relative permittivity of soils. *Geological Survey of Canada* **75**, 75-79.

Davis, J.L. & Annan, A.P. (1977) Electromagnetic detection of soil moisture: Progress report I. *Canadian Journal of Remote Sensing* **3**, 76-86.

Dawoudu, W. (2004) *The British Survey of Fertiliser Practise: Fertiliser use on farm crops for crop year 2003.* BSFP Authority, UK.

Day, P.R. (1965) Particle fractionation and particle-size analysis. In: Black, C.A. (Ed.) *Methods of Soil Analysis. Part 1. Agronomy*, 9, American Society of Agronomy Inc., Madison, Wisconsin, USA. pp. 545-567.

Deeks, L.K., Williams, A.G., Dowd, J.F. & Scholefield, D. (1999) Quantification of pore size distribution and the movement of solutes through isolated soil blocks. *Geoderma* 90, 65-86.

DEFRA (2001) *White Clover*. (WWW) http://www.defra.gov.uk [August 2002].

DEFRA (2002) (WWW) http://www.defra.gov.uk [March 2006].

DEFRA (2006) (WWW) http://www.defra.gov.uk [March 2006].

De Gryze, S., Jassogne, L., Bossuyt, H., Six, J. & Merckx, R. (2006) Water repellence and soil aggregate dynamics in a loamy grassland soil as affected by texture. *European Journal of Soil Science* 57, 235-246.

Denef, K., Six, J., Bossuyt, H., Frey, S.D., Elliott, E.T., Merckx, R. & Paustian, K. (2001) Influence of dry – wet cycles on the interrelationship between aggregate, particulate organic matter, and microbial community dynamics. *Soil Biology and Biochemistry* 33, 1599-1611.

Dexter, A.R. (1988) Advances in characterization of soil structure. *Soil and Tillage Research* 11, 199-238.

Dexter, A.R. (2004) Soil physical quality: Part III: Unsaturated hydraulic conductivity and general conclusions about S-theory. *Geoderma* 120, 227-239.

Dhanoa, M.S., Siddons, R.C., France, J. & Gale, D.L. (1985) A multicompartmental model to describe marker excretion patterns in ruminant faeces. *British Journal of Nutrition* 53, 663-671.

Diaz-Zorita, M., Perfect, E. & Grove, J.H. (2002) Disruptive methods for assessing soil structure. *Soil and Tillage Research* 64, 3-22.

Didden, W.A.M., Marinissen, J.C.Y. & Kroesbergen, B. (1991) A method to construct artificial soil cores from field soil with a reproducible soil structure. *Agriculture, Ecosystems and Environment* **34**, 329-333.

Diestel, H. (1993) *Saturated Flow and Soil Structure*, Springer-Verlag, Berlin.

Droogers, P., Stein, A., Bouma, J. & De Boer, G. (1998) Parameters for describing soil macroporosity derived from staining patterns. *Geoderma* **83**, 293-308.

Drummond, L. & Maher, W. (1995) Determination of phosphorus in aqueous-solution via formation of the phosphoantimonymolybdenum blue complex – reexamination of optimum conditions for the analysis of phosphate. *Analytica Chimica Acta* **302**, 69-74.

Duiker, S.W., Rhoton, F.E., Torrent, J., Smeck, N.E & Lal, R. (2003) Iron (hydr)oxide crystallinity effects on soil aggregation. *Soil Science Society of America Journal* **67**, 606-611.

Duke, J.A. (1981) *Handbook of Legumes of World Economic Importance*. Plenum Press, NewYork.

Edwards, A.C. & Withers, P.J.A. (1998) Soil phosphorus management and water quality: A UK perspective. *Soil Use and Management* **14**, 124-130.

Eggleston J.J. & Peirce, J.J. (1995) Dynamic programming analysis of pore space. *European Journal of Soil Science* **46**, 581-590.

Eriksen, J. (2001) Nitrate leaching and growth of cereal crops following cultivation of contrasting temporary grasslands. *Journal of Agricultural Science* **136**, 271-281.

Eriksen J., Vinther F.P. & Søegaard K. (2004) Nitrate leaching and N2-fixation in grasslands of different composition, age and management. *Journal of Agricultural Science* **142**, 141-151.

Ersahin, S., Papendick, R.I., Smith, J.L., Keller, C.K. & Manoranjan, V.S. (2002) Macropore transport of bromide as influenced by soil structure differences. *Geoderma* **108**, 207-223.

Estela, J.M. & Cerdá, V. (2005) Flow analysis techniques for phosphorus: An overview. *Talanta* **66**, 307-331.

Ewing, R.P. & Horton, R. (1999 a) Discriminating dyes in soil with colour image analysis. *Soil Science Society of America Journal* **63**, 18-24.

Ewing, R.P. & Horton, R. (1999 b) Quantitative colour image analysis of agronomic images. *Agronomy Journal* **91**, 148-153.

Fergusson, J.E. (1982) *Inorganic Chemistry and the Earth. Chemical Resources, Their Extraction, Use and Environmental Impact.* Pergamon Press.

Ferree, M.A. & Shannon, R.D. (2001) Evaluation of a second derivative UV/visable spectroscopy technique for nitrate and total nitrogen analysis of waste water samples. *Water Research* **35**, 327-332.

Findlay, D.C., Colborne, G.J.N., Cope, D.W., Harrod, T.R., Hogan, D.V. & Staines, S.J. (1984) *Soil survey of England and Wales bulletin No. 14: Soils and Their Use in South West England.* Rothamsted Experimental Station, Harpenden.

FitzPatrick, E.A. (1983) 2nd ed. *Soils their formation, classification and distribution.* Longman, London.

FitzPatrick, E.A. (1986) 2nd ed. *An Introduction to Soil Science.* Longman, London.

Flury, M., Flühler, H., Leuenberger, J. & Jury, W.A. (1994) Susceptibility of soils to preferential flow of water: a field study. *Water Resour. Res.* **30**, 1945-1954.

Flury, M. & Flühler, H. (1995) Tracer characteristics of brilliant blue FCF. *Soil Science Society of America Journal* **59**, 22-27.

Flury, M. (1996) Experimental evidence of transport of pesticides through field soils – a review. *Journal of Environmental Quality* **25**, 25-45.

Forrer, I., Papritz, A., Kasteel, R., Flühler, H. & Luca, D. (2000) Quantifying dye tracers in soil profiles by image processing. *European Journal of Soil Science* **51**, 313-322.

Frame, J. & Newbould, P. (1986) Agronomy of white clover. *Advances in Agronomy* **40**, 1-88.

Franzluebbers, A.J. (2002) Water infiltration and soil structure related to organic matter and its stratification with depth. *Soil & Tillage Research* **66**, 197-205.

Gardiner, M.J. and Ryan, P. (1971) *Soils of Co. Wexford.* Soil Survey Bulletin No. 1. National Soil Survey of Ireland, Dublin.

Gardner, W.H. (1965) Water content. In: Black, C.A. (Ed.) *Methods of Soil Analysis. Part 1. Agronomy*, **9**, American Society of Agronomy Inc., Madison, Wisconsin, USA. pp. 82-127.

Gardner, C.M.K., Bell, J.P., Cooper, J.D., Dean, T.J. & Hodnett, M.G. Soil Water Content. In: Mullins, C.E. & Smith, K.A. (Eds.) (1991) *Soil Analysis: Physical Methods*. Marcel Decker. pp 1-73.

Gardolinski, P.C.F.C., Hanrahan, G., Achterberg, E.P., Gledhill, M., Tappin, A.D., House, W.A. & Worsfold, P.J. (2001) Comparison of sample storage protocols for the determination of nutrients in natural waters. *Water Research* **35**, 3670–3678.

Geeves, G.W., Cresswell, H.P. & Murphy, B.W. (1998) Division S-6-soil and water management & conservation. *Soil Science Society of America Journal* **62**, 223-232.

Ghodrati, M. & Jury, W.A. (1992) A field study of the effects of soil structure and irrigation method on preferential flow of pesticides in unsaturated soil. *Journal of Contaminant Hydrology* **11**, 101-125.

Gjettermann, B., Nielsen, K.L., Petersen, C.T., Jensen, H.E. & Hansen, S. (1997) Preferential flow in sandy loam soils as affected by irrigation intensity. *Soil Technology* **11**, 139-152.

Greco, R. (2002) Preferential flow in macroporous swelling soil with internal catchment: model development and applications. *Journal of Hydrology* **269**, 150-168.

Grieve, I.C., Davidson, D.A. & Bruneau, P.M.C. (2005) Effects of liming on void space and aggregation in an upland grassland soil. *Geoderma* **125**, 39-48.

Gülser, C. (2006) Effect of forage cropping treatments on soil structure and relationships with fractal dimensions, *Geoderma* **131**, 33-44.

Hall, D.G.M., Reeve, M.J., Thomasson, A.J. & Wright, V.F. (1977). *Water retention, porosity and density of field soils.* Soil Survey Technical Monograph No. 9. Rothamsted Experimental Station, Harpenden.

Hallett, P.D., Bird, N.R.A., Dexter, A.R. & Seville, J.P.K. (1998) Investigation into the fractal scaling of the structure and strength of soil aggregates. *European Journal of Soil Science* **49**, 203-211.

Hawkins, J.M.B. & Scholefield, D. (1996) Molybdate-reactive phosphorus losses in surface and drainage waters from permanent grassland. *Journal of Environmental Quality* **25**, 727-732.

Haygarth, P.M., Hepworth, L. & Jarvis, S.C. (1998 a) Forms of phosphorus transfer in hydrological pathways from soils under grazed grassland. *European Journal of Soil Science* **49**, 65-72.

Haygarth, P.M., Chapman, P.J., Jarvis, S.C. & Smith, R.V. (1998 b) Phosphorus budgets for two contrasting grassland farming systems in the UK. *Soil Use and Management* **14**, 160-167.

Haygarth, P.M. & Jarvis, S.C. (1999) Transfer of phosphorus from agricultural soils. *Advances in Agronomy* **66**, 195-249.

Haygarth, P.M., Wood, F.L., Heathwaite, A.L. & Butler, P.J. (2005) Phosphorus dynamics observed through increasing scales in a nested headwater-to-river channel study. *Science of the Total Environment* **344**, 83-106.

Haynes, R.J. & Beare, M.H. (1997) Influence of six crop species on aggregate stability and some labile organic matter fractions. *Soil Biology and Biochemistry* **29**, 1647-1653.

Heilman, P. & Norby, R.J. (1998) Nutrient cycling and fertility management in temperate short rotation forest systems. *Biomass and Bioenergy* **14**, 361-370.

Herridge, D.F. & Danso, S.K.A. (1995) Enhancing legume N_2 fixation through selection and breeding. *Plant and Soil* **174**, 51-82.

Hewitt, E.J. (1966) Sand and water culture methods used in the study of plant nutrition. Technical Communication of the Commonwealth Agriculture Bureau of Horticulture and Plant Crops, 22.

Hillel, D. (1980) *Introduction to Soil Physics.* Academic Press, London.

Hillel, D. (1998) *Environmental Soil Physics.* Academic Press, London.

Hoagland D.R., & Arnon D.I. (1950). The water culture method of growing plants without soil. *California Agricultural Experiment Station* Circular No. 347.

Hofman, G. & Van Cleemput, O. (1992) Nitrogen cycling in agricultural systems. In: Francois, E., Pithan, K. and Bartiaux-Thill, N. (Eds) *Agriculture: Nitrogen Cycling and Leaching in Cool and Wet Regions of Europe*, pp. 1-7, Commission of the European Communities, European Cooperation in the Field of Scientific and Technical Research.

Hodgson, J.M. (1974) (Ed) *Soil Survey Field Handbook.* Technical Monograph No. 5. Rothamsted Experimental Station, Harpenden.

Holden, N.M., Scholefield, D., Williams, A.G. & Dowd, J.F. (1995 a) A large soil block for in situ real-time fine spatial and temporal resolution of measurement of preferential flow. In: Więzik (Ed.) Proceedings of the International Conference on *Hydrological Processes in the Catchment*, Institute of Water Engineering & Water Management and Cracow University of Technology. Cracow, Poland. pp 239-247.

Holden, N.M., Scholefield, D., Williams, A.G. & Dowd, J.F. (1995 b) The simultaneous use of three common hydrological tracers for fine spatial and temporal resolution investigation of preferential flow in a large soil block. In: Proceedings of a Boulder Symposium, *Tracer Technologies for Hydrological Systems*, IHAS Publication **229**, pp 77-85.

Holden, N.M. (2001) Description and classification of soil structure using distance transform data. *European Journal of Soil Science* **52**, 529-545.

Huang, G. & Zhang, R. (2005) Evaluation of soil water retention curve with the pore-solid fractal model. *Geoderma* **127**, 52-61.

Hubble, D.S. & Harper, D.M. (2000) A revised method for nitrate analysis at low concentrations. *Water Research* **34**, 2598-2600.

Hunter & Goldspink (1956) Unknown, from a paper supplied courtesy of Skalar Analytical, Wheldrake, York, UK.

Isensee, A.R. & Sadeghi, A.M. (1992) Laboratory Apparatus for studying pesticide leaching in intact soil cores. *Chemosphere* **25**, 581-590.

Isermann, K. (1990) Share of agriculture in nitrogen and phosphorus emissions into the surface waters of Western Europe against the background of their eutrophication. Cited In: Misslebrook *et al.* (1995)

Jarvis, M.G., Allen, R.H., Fordham, S.J., Hazelden, J., Moffat, A.J. & Sturdy, R.G. (1984) *Soil survey of England and Wales bulletin No. 15: Soils and Their Use in South East England.* Rothamsted Experimental Station, Harpenden.

Jarvis, S.C. (2000) Progress in studies of nitrate leaching from grassland soils. *Soil Use and Management* **16**, 152-156.

Jarvis, N.J., Zavattaro, L., Rajkai, K., Reynolds, W.D., Olsen, P.A., McGechan, M., Mecke, M., Mohanty, B., Leeds-Harrison, P.B. & Jacques, D., (2002) Indirect estimation of near-saturated hydraulic conductivity from readily available soil information. *Geoderma* **108**, 1-17.

Jastrow, J.D. & Miller, R.M. (1991) Methods for assessing the effects of biota on soil structure. *Agriculture, Ecosystems and Environment* **34**, 279-303.

Jastrow, J.D. (1996) Soil aggregate formation and the accrual of particulate and mineral-associated organic matter. *Soil Biology and Biochemistry* **28**, 665-676.

Jastrow, J.D., Miller, R.M. & Lussenhop, J. (1998) Contributions of interacting biological mechanisms to soil aggregate stabilization in restored prairie. *Soil Biology and Biochemistry* **30**, 905-916.

Javaux, M. & Vanclooster, M. Three-dimensional structure characterization and transient flow modeling of a variably saturated heterogeneous monolith. *Journal of Hydrology.* In Press.

Johnson, A., Roy, I.M., Matthews, G.P. & Patel, D. (2003 a) An improved simulation of void structure, water retention and hydraulic conductivity in soil with the Pore-Cor three-dimensional network. *European Journal of Soil Science* **54**, 477-489.

Johnson, A., Mathews, T.J., Matthews, G.P., Patel, D., Worsfold, P.J. & Andrew, K.N. (2003 b) High-resolution laboratory lysimeter for automated sampling of tracers through a 0.5m soil block. *Journal of Automated Methods & Management in Chemistry* **25**, 43-49.

Johnson, A. (2004) Aqueous & non-aqueous phase tracer migration through differing soil textures. *PhD Thesis*, University of Plymouth, UK.

Juma, N.G. (1994) A conceptual framework to link carbon and nitrogen cycling to soil structure formation. *Agriculture, Ecosystems and Environment* **51**, 257-267.

Kasteel , R., Vogel, H.-J. & Roth, K. (2000) From Hydraulic properties to effective transport in soil. *European Journal of Soil Science* **51**, 81-91.

Kay, P., Blackwell, P.A. & Boxall, A.B.A. (2005) A lysimeter experiment to investigate the leaching of veterinary antibiotics through a clay soil and comparison with field data *Environmental Pollution* **134**, 333–341.

Ketcham, R.A. & Carlson, W.D. (2001) Acquisition, optimization and interpretation of X-ray computed tomographic imagery: applications to the geosciences. *Computers & Geosciences* **27**, 381–400.

Klocke, N.L. & Hergert, G.W. (1996) *How soil holds water.* (WWW) hppt://www.ianr.un/edu/pubs/Fieldcrops [August, 2002].

Kramer, K.J.M. (1998) Inorganic certified reference materials in 'water' – What do we have, what do we need? *Analyst* **123**, 991-995.

Kung, K.J.S., Steenhuis, T.S., Kladivko, E.J., Gish, T.J., Bubenzer, G. & Helling, C.S. (2000) Impact of preferential flow on the transport of adsorbing and non-adsorbing tracers. *Soil Science Society of America Journal* **64**, 1290-1296.

Lal, R. (2004) Soil carbon sequestration to mitigate climate change. *Geoderma* **123**, 1-22.

Langner, H.W., Gaber, H.M., Wraith, J.M., Huwe, B. & Inskeep, W.P. (1999) Preferential flow through intact soil cores: Effects of matric head. *Soil Science Society of America Journal* **63**, 1591-1598.

Larsson, M.H., Jarvis, N.J., Torstensson, G. & Kasteel, R. (1999) Quantifying the impact of preferential flow on solute transport to tile drains in a sandy field soil. *Journal of Hydrology* **215**, 116-134.

Le Bissonnais, Y. (1996). Aggregate stability and assessment of soil crustability and erodibility. I. Theory and methodology. *European Journal of Soil Science* **47**, 425-437.

Ledgard, S.F. (1991) Transfer of fixed nitrogen from white clover to associated grasses in swards grazed by cows, estimated using ^{15}N method. *Plant and Soil* **113**, 215-223.

Legout, C., Leguèdois, S & Le Bissonnais, Y. (2005) Aggregate breakdown dynamics under rainfall compared with aggregate stability measurements. *European Journal of Soil Science* **56**, 225-237.

Lesturgez, G., Poss, R., Noble, A., Grünberger, O., Chintachao, W. & Tessier, D. (2006) Soil acidification without pH drop under intensive cropping systems in Northeast Thailand. *Agriculture, Ecosystems & Environment* **114**, 239-248.

Letey, J. (1991) The study of soil structure—Science or art. *Australian Journal of Soil Research* **29**, 699-707.

Lewis, T.E., Blasdell, B. & Blume, L.J. (1990) Collection of intact cores from a rocky desert and a glacial till soil. *Soil Science Society of America Journal* **54**, 938-940.

Li, Y. & Ghodrati, M. (1995) Transport of nitrate in soils as affected by earthworm activities. *Journal of Environmental Quality* **24**, 432-438.

Li, Q.P., Zhang, J-Z., Millero, F.J. & Hansell, D.A. (2005) Continuous colorimetric determination of trace ammonium in seawater with a long-path liquid waveguide capillary cell. *Marine Chemistry* **96**, 73-85.

Logsdon, S.D. (2002) Determination of preferential flow model parameters. *Soil Science Society of America Journal* **66**, 1095-1103.

Loiseau, P., Carrere, P., Lafarge, M., Delpy, R. & Dublanchet, J. (2001) Effect of soil-N and urine-N on nitrate leaching under pure grass, pure clover and mixed grass/clover swards. *European Journal of Agronomy* **14**, 113-121.

Luxmoore, R.J. (1991) A source sink framework for coupling water, carbon and nutrient dynamics of vegetation. *Tree Physiology* **9**, 267-280.

MacDuff, J.H., Jarvis, S.C. & Roberts, D.H. (1990) Nitrates: leaching from grazed grassland systems. In: Calvert, R. (Ed.) *Nitrates-Agriculture-Eau*, Paris INRA. pp. 405-410.

McBratney, A.B. & Moran, C.J. (1990) A rapid method of analysis for soil macropore structure: II. Stereological model, statistical analysis and interpretation. *Soil Science Society of America Journal* **54**, 509-515.

McBratney, A.B., Moran, C.J., Stewart, J.B., Cattle, S.R. & Koppi, A.J. (1992) Modifications to a method of rapid assessment of soil macropore structure by image analysis. *Geoderma* **53**, 255-274.

McBratney, A.B., Minasny, B., Cattle, S.R. & Vervoort, R.W. (2002) From pedotransfer functions to soil inference systems. *Geoderma* **109**, 41-73.

McDowell, R.W., Sharpley, A.N., Condron, L.M., Haygarth, P.M. & Brookes, P.C. (2001) Processes controlling soil phosphorus release to runoff and implications for agricultural management. *Nutrient Cycling in Agroecosystems* **59**, 269-284.

Ma, Q., Hook, J.E. & Ahuja, L.R. (1999) Influence of three-parameter conversion methods between vanGenuchten and Brooks-Corey function on soil hydraulic properties and water-balance predictions. *Water Resources Research* **35**, 2571-2578.

Macdonald, L.A. (2000) Sub-surface migration of an oil pollutant into aquifers. *PhD Thesis*, University of Plymouth, UK.

Mackney, D. (1986) *Soils in Buckinghamshire/Berkshire 1; Sheet SU88 (Marlow)*. Soil Survey Record No 92. Rothamsted Experimental Station, Harpenden.

Mannetje, L.'t & Jarvis, S.C. (1990) Nitrogen flows and losses in grazed grasslands. Cited In: Sprent & Mannetje (1996)

Marshall, T.J., Holmes, J.W. & Rose, C.W. (1996) 3rd ed. *Soil Physics*. Cambridge University Press.

Mayr, T. & Jarvis, N.J. (1999) Pedotransfer functions to estimate soil water retention parameters for a modified Brooks-Corey type model. *Geoderma* **91**, 1-9.

Meneffe, E. & Hautala, E. (1978) Soil stabilisation by cellulose xanthate. *Nature* **275**, 530-532.

Miller, J.C. & Miller, J.N. (1992) *Statistics for Analytical Chemistry*. Ellis Horwood Limited, Chichester, UK.

Miller, R.M. & Jastrow, J.D. (1990) Hierarchy of root and mycorrhizal fungal interactions with soil aggregation. *Soil Biology and Biochemistry* **22**, 579-584.

Miller, R.M. and Jastrow, J.D. (1996) Contributions of legumes to the formation and maintenance of soil structure. In: Younie, D. (Ed.) *Legumes in Sustainable Farming Systems. British Grassland Society Occasional Symposium* No. 30. BGS. pp. 105-112.

Misslebrook, T.H., Pain, B.F., Stone, A.C. & Scholefield, D. (1995) Nutrient run-off following application of livestock wastes to grassland. *Environmental Pollution* **88**, 51-56.

Molope, M.B., Grieve, I.C. & Page, E.R. (1987) Contributions by fungi and bacteria to aggregate stability of cultivated soils. *Journal of Soil Science* **38**, 71-77.

Mooney, S.J. (2002) Three-dimensional visualization and quantification of soil macroporosity and water flow patterns using computed tomography. *Soil Use and Management* **18**, 142-151.

Mooney, S.J. & Nipattasuk, W. (2003) Quantification of the effects of soil compaction on water flow using dye tracers and image analysis. *Soil Use and Management* **19**, 356-363.

Moorcroft, M.J., Davis, J. & Compton, R.G. (2001) Detection and determination of nitrate and nitrite: A review. *Talanta* **54**, 785-803.

Moran, C.J. & McBratney, A.B. (1992) Acquisition and analysis of three-component digital images of soil pore structure I. Method. *Journal of Soil Science* **43**, 541-550.

Morris, C. & Mooney, S.J. (2004) A high-resolution system for the quantification of preferential flow in undisturbed soil using observations of tracers. *Geoderma* **118**, 133-143.

Mualem, Y. (1976) A new model for the predicting the hydraulic conductivity of unsaturated porous media. *Water Resources Research* **12**, 513-522.

Mullins, C.E. and Fraser, A. (1980) Use of the drop cone penetrometer on undisturbed and remoulded soils at a range of soil-water tensions. *Journal of Soil Science* **31**, 25-32.

Murphy, C.P., Bullock, P. & Turner, R.H. (1977 a) The measurement and characterisation of voids in soil thin sections by image analysis. Part I. Principles and techniques. *Journal of Soil Science* **28**, 498-508.

Murphy, C.P., Bullock, P. & Biswell, K.J. (1977 b) The measurement and characterisation of voids in soil thin sections by image analysis. Part II. Applications. *Journal of Soil Science* **28**, 509-518.

Murphy, J. & Riley, J.P. (1962) A modified single solution method for the determination of phosphate in natural water. *Analytica Chimica Acta* **27**, 31-36.

Mytton, L.R., Cresswell, A. & Colbourn, P. (1993) Improvement in soil structure associated with white clover. *Grass and Forage Science* **48**, 84-90.

Neal, C., Neal, M. & Wickham, H. (2000) Phosphate measurement in natural waters: Two examples of analytical problems associated with silica interference using phosphomolybdic acid methodologies. *The Science of the Total Environment* **251/252**, 511-522.

Niewczas, J. & Witkowska-Walczak, B. (2005) The soil aggregates stability index (ASI) and its extreme values. *Soil & Tillage Research* **80**, 69-78.

Nunan, N., Ritz , K., Rivers, M., Feeney, D.S. & Young, I.M. (2006) Investigating microbial micro-habitat structure using X-ray computed tomography. *Geoderma* **133**, 398-407.

Oades, J.M. (1984) Soil organic matter and structural stability: mechanisms and implications for management. *Plant and Soil* **76**, 319-337.

Oades, J.M. (1993) The role of biology in the formation, stabilization and degradation of soil structure. *Geoderma* **56**, 377-400.

Oliver, D.M., Clegg, C.D., Haygarth, P.M. & Heathwaite, A.L. (2005) Assessing the potential for pathogen transfer from grassland soils to surfaces waters. *Advances in Agronomy* **85**, 125-180.

O'Neill, P. (1993) 2nd ed. *Environmental Chemistry*. Chapman and Hall, London.

Pachepsky, Y., Yakovchenko, V., Rabenhorst, M.C., Pooley, C. & Sikora, L. (1996) Fractal parametres of pore surfaces as derived from micromorphological data: Effects of long term management practices. *Geoderma* **74**, 305-319.

Pachepsky, Y.A. & Rawls, W.J., (2003) Soil structure and pedotransfer functions. *European Journal of Soil Science* **54**, 443-451.

Pachepsky, Y.A., Rawls,W.J. & Lin, H.S. (2005) Hydropedology and pedotransfer functions. *Geoderma* In Press.

Packham, R.F. (1996) Drinking water quality and health. In: Harrison, R.M. (Ed.) 3rd ed. *Pollution: Causes, Effects and Control*, pp. 52-65. The Royal Society of Chemistry.

Pagliai, M., Vignozzi, N. & Pellegrini, S. (2004) Soil structure and the effect of management practices. *Soil & Tillage Research* **79**, 131–143.

Papadopoulos, A., Mooney, S.J. & Bird, N.R.A. (2006) Quantification of the effects of contrasting crops in the development of soil structure: an organic conversion. *Soil Use and Management* **22**, 172-179.

Parsons, A.J., Orr, R.J., Penning, P.D. & Lockyer, D.R. (1991) Uptake, cycling and fate of nitrogen in grass-clover swards continuously grazed by sheep. *Journal of Agricultural Science* **116**, 47-61.

Peat, D.M.W., McKelvie, I.D., Matthews, G.P., Haygarth, P.M. & Worsfold, P.J. (1997) Rapid determination of dissolved organic phosphorus in soil leachates and runoff waters by flow injection analysis with on-line photo-oxidation. *Talanta* **45**, 47-55.

Peat, D.M.W. (1998) Modelling and monitoring of phosphorus transport and speciation in soil. *PhD Thesis*, University of Plymouth, UK.

Peat, D.M.W., Matthews, G.P., Worsfold, P., Jarvis, S.C. (2000) Simulation of water retention and hydraulic conductivity in soil using a three dimensional network. *European Journal of Soil Science* **5**, 65-81.

Pederson, G.A. (1995) White Clover and Other Perennial Clovers. In: Barnes, R.F., Miller, D.A. & Nelson, C.J.(Eds.) *Forages Volume 1: An Introduction to Grassland Agriculture.* Iowa State University Press, USA. pp. 227-236.

Peoples, M.B., Herridge, D.F. & Ladha, J.K. (1995 a) Biological nitrogen fixation: An efficient source of nitrogen for sustainable agricultural production? *Plant and Soil* **174**, 3-28.

Peoples, M.B., Ladha, J.K. & Herridge, D.F. (1995 b) Enhancing legume N_2 fixation through plant and soil management. *Plant and Soil* **174**, 83-101.

Piccolo, A., Pietramellara, G. & Mbagwu, J.S.C. (1997) Use of humic substances as soil conditioners to increase aggregate stability. *Geoderma* **75**, 267-277.

Pierret, J., Prasher, S.O., Kantzas, A. & Langford, C. (1999) Three-dimensional quantification of macropore networks in undisturbed soil cores. *Soil Science Society of America Journal* **63**, 1530-1543.

Pierret, A., Capowiez, Y., Belzunces, L. & Moran, C.J. (2002) 3D reconstruction and quantification of macropores using X-ray computed tomography and image analysis. *Geoderma* **106**, 247-271.

Piotrowski, J.S., Denich, T., Klironomos, J.N., Graham, J.M. & Rillig, M.C. (2004) The effects of arbuscular mycorrhizas on soil aggregation depend on the interaction between plant and fungal species. *New Phytologist* **164**, 365-373.

Pires, L.F., Bacchi, O.O.S. & Reichardt, K. (2005) Gamma ray computed tomography to evaluate wetting/drying soil structure changes. *Nuclear Instruments and Methods in Physics Research B* **229**, 443-456.

Plante, A.F. & McGill, W.B. (2002) Intraseasonal soil macroaggregate dynamics in two contrasting field soils using labeled tracer spheres. *Soil Science Society of America Journal* **66**, 1285-1295.

Porporato, A., Odorico, P.D., Laio, F. & Rodriguez-Iturbe, I. (2003) Hydrologic controls on soil carbon and nitrogen cycles. I. Modeling scheme. *Advances in Water Resources* **26**, 45-58.

Powlson, D.S. (1998) Phosphorus, agriculture and water quality. *Soil Use and Management* **14**, 123.

Powlson, D.S. (2000) Tackling nitrate from agriculture. *Soil Use and Management* **116**, 141.

Puget, P., Chenu, C. & Balesdent, J. (1995) Total and young organic matter distributions in aggregates of silty cultivated soils. *European Journal of Soil Science* **46**, 449-459.

Pulleman, M.M., Six, J., Van Breemen, N. & Jongmans, A.G. (2005) Soil organic matter distribution and microaggregate characteristics as affected by agricultural management and earthworm activity. *European Journal of Soil Science* **56**, 453-467.

Quisenberry, V.L., Smith, B.R., Phillips, R.E., Scott, H.D. & Nortcliffe, S. (1993) A soil classification system for describing water and chemical transport. *Soil Science* **156**, 355-373.

Quisenberry, V.L., Phillips, R.E. & Zeleznik, J.M. (1994) Spatial distribution of water and chloride macropore flow in a well-structured soil. *Soil Science Society of America Journal* **58**, 1294-1300.

Radojević, M. & Bashkin, V.N. (1999) *Practical Environmental Analysis*. The Royal Society of Chemistry, UK.

Reid, J.B. & Goss, M.J. (1981) Effect of living roots of different plant species on the aggregate stability of two arable soils. *Journal of Soil Science* **32**, 521-541.

Reid, J.B. & Goss, M.J. (1982) Interactions between soil drying due to plant water use and decreases in aggregate stability caused by maize roots. *Journal of Soil Science* **33**, 47-53.

Rhodes, I. (2001) *In Clover. A farmer's guide to the use of white and red cloves in sustainable livestock agriculture.* An IGER publication. (WWW) http://www.iger.bbsrc.ac.uk [October 2002]

Rillig, M.C., Wright, S.F. & Eviner, V.T. (2002) The role of arbuscular mycorrhizal fungi and glomalin in soil aggregation: comparing effects of five plant species. *Plant & Soil* **238**, 325–333.

Ringrose-Voase, A.J. & Bullock, P. (1984) The automatic recognition and measurement of soil pore types by image analysis and computer programmes. *Journal of Soil Science* **35**, 673-684.

Ringrose-Voase, A.J. (1987) A scheme for the quantitative description of soil macrostructure by image analysis. *Journal of Soil Science* **38**, 343-356.

Ringrose-Voase, A.J. (1996) Measurement of soil macropore geometry by image analysis of sections through impregnated soil. *Plant and Soil* **183**, 27-47.

Robards, K., Mckelvie, I.D., Benson, R.L., Worsfold, P.J., Blundell, N.J. & Casey, H. (1994) Determination of carbon, phosphorus, nitrogen and silicon species in waters. *Analytical Chimica Acta* **287**, 147-190.

Robinson, G.S. & Jacques, W.A. (1958) Effect of pure sowing of some grasses and clovers on the structure of a Tokomaru silt loam. *New Zealand Journal of Agricultural Research* **1**, 199-216.

Rowell, D.L. (1994) *Soil Science: Methods and Applications.* Longman Scientific and Technical, Harlow, UK.

Rudeforth, C.C. (1970) *Memoirs of the Soil Survey of Great Britain: Soils of North Cardiganshire; Sheets 163 and 178.* Rothamsted Experimental Station, Harpenden.

Rudeforth, C.C., Hartnup, R., Lea, J.W., Thompson, T.R.E. & Wright, P.S. (1984) *Soil survey of England and Wales bulletin No. 11: Soils and Their Use in Wales.* Rothamsted Experimental Station, Harpenden.

Sallberg, J.R. (1965) Shear Strength. In: Black, C.A. (Ed.) *Methods of Soil Analysis. Part 1. Agronomy*, **9**, American Society of Agronomy Inc., Madison, Wisconsin, USA. pp. 431-433.

Santos, D., Murphy, S.L.S., Taubner, H., Smucker, A.J.M. & Horn, R. (1997) Uniform separation of concentric surface layers from soil aggregates. *Soil Science Society of America Journal* **61**, 720-724.

Sarah, P. (2005) Soil aggregation response to long- and short-term differences in rainfall amount under arid and Mediterranean climate conditions. *Geomorphology* **70**, 1-11.

Schils, R.L.M., Boxem, Tj., Jagtenberg, C.J. & Verboon, M.C. (2000) The performance of white clover-based dairy system in comparison with a grass/fertilizer-N system. II. Animal production, economics and environment. *Netherlands Journal of Agricultural Science* **48**, 305-318.

Schjønning, P., Thomsen, I.K., Møberg, J.P., de Jonge, H., Kristensen, K. & Christensen, B.T. (1999) Turnover of organic matter in differently textured soils: I. Physical characteristics of structurally disturbed and intact soils. *Geoderma* **89**, 177-198.

Schoen, R., Gaudet, J.P. & Bariac, T. (1999) Preferential flow and solute transport in a large lysimeter, under controlled boundary conditions. *Journal of Hydrology* **215**, 70-81.

Scholefield, D., Tyson, K.C., Garwood, E.A., Hawkins, J. & Stone A.C. (1993) Nitrate leaching from grazed grassland lysimeters: Effects of fertiliser input, field drainage, age of sward and patterns of weather. *Journal of Soil Science* **44**, 601-613.

Scholefield, D. & Titchen, N.M. (1995) Development of a rapid field test for soil mineral nitrogen and its application to grazed grassland. *Soil Use and Management* **11**, 33-43.

Scholefield, D., Lord, E.I., Rodda H.J.E. & Webb, B.W. (1996) Estimating peak nitrate concentrations from annual nitrate loads. *Journal of Hydrology* **186**, 355-373.

Scholefield, D., Chadwick, D. & Macey, N. (1998) Design criteria for effective buffer zones. In: Proceedings of the 17th General Meeting of the European Grassland Federation. Debrecen, Hungary. pp 587-591.

Scholefield, D., Halling, M., Tuori, M., Isolahti, M., Soelter, U. & Stone, A.C. (2001) Assessment of nitrate leaching from beneath forage legumes. In: Wilkins, R.J. & Paul, C. (Eds.) *Legumes Silages for Animal Production.* FAL Agricultural Research, Special Issue No. 234. Braunschweig, Germany. pp 17-25.

Scholefield, D., Le Goff, T., Braven, J., Ebdon, L., Long, T. & Butler, M. (2005 b) Concerted diurnal patterns in riverine nutrient concentrations and physical conditions. *Science of the Total Environment* **344**, 201-210.

Scholefield, D., Cresswell, C., Mytton, L. & Wood, F. (2005) BBSRC Report D15329.

Schröder, J.J., Scholefield, D., Cabral, F. & Hofman, G. (2004) The effects of nutrient losses from agriculture on ground and surface water quality: The position of science in developing indicators for regulation. *Environmental Science & Policy* **7**, 15-23.

Sharpley, A.N. (1995) Soil phosphorus dynamics: Agronomic and environmental impacts. *Ecological Engineering* **5**, 261-279.

Six, J., Elliott, E.T. & Paustian, K. (2000) Soil macroaggregate turnover and microaggregate formation: A mechanism for C sequestration under no-tillage agriculture. *Soil Biology and Biochemistry* **32**, 2099-2103.

Six, J., Bossuyt, H., De Gryze, S. & Denef, K. (2004) A history of research on the link between (micro)aggregates, soil biota, and soil organic matter dynamics. *Soil and Tillage Research* **79**, 7-31.

Sowers, G.F. (1965) Consistency. In: Black, C.A. (Ed.) *Methods of Soil Analysis. Part 1. Agronomy,* **9**, American Society of Agronomy Inc., Madison, Wisconsin, USA. pp. 391-399.

Spaccini, R., Mbagwub, J.S.C., Igwe, C.A., Conte, P. & Piccolo, A. (2004) Carbohydrates and aggregation in lowland soils of Nigeria as influenced by organic inputs. *Soil & Tillage Research* **75**, 161-172.

Sprent, J.I. & Mannetje, L.'t (1996) The role of legumes in sustainable farming systems: Past, present and future. In: Younie, D. (Ed.) *Legumes in Sustainable Farming Systems. British Grassland Society Occasional Symposium* No. 30. BGS. pp. 2-14.

Stockdale, E.A., Lampkin, N.H., Hovi, M., Keatinge, R., Lennartsson, E.K.M., Macdonald, D.W., Padel, S., Tattersall, F.H., Wolfe, M.S. & Watson, C.A. (2000) Agronomic and environmental implications of organic farming systems. *Advances in Agronomy* **70**, 261-327.

Stutter, M.I., Deeks, L.K. & Billett, M.F. (2003) Transport of conservative and reactive tracers through a naturally structured upland podzol field lysimeter. *Journal of Hydrology* **300**, 1-19.

Tindall, J.A., Hemmen, K. & Dowd, J.F. (1992) An improved method for field extraction and laboratory analysis of large, intact soil cores. *Journal of Environmental Quality* **21**, 259-263.

Tisdall, J.M. & Oades, J.M. (1979) Stabilization of soil aggregates by the root system of ryegrass. *Australian Journal of Soil Research* **17**, 429-441.

Tisdall, J.M. & Oades, J.M. (1982) Organic matter and water-stable aggregates in soils. *Journal of Soil Science* **33**, 141-163.

Topp, G.C., Davis, J.L. & Annan, A.P. (1980) Electromagnetic determination of soil-water content – measurements in coaxial transmission lines. *Water Resources Research* **16**, 574-582.

Towner, G.D. (1973) An examination of the fall-cone method for the determination of some strength properties of remoulded agricultural soils. *Journal of Soil Science* **24**, 470-479.

Traoré, O., Groleau-Renaud, V., Plantureux, S., Tubeileh, A. & Bœuf-Tremblay, V. (2000) Effect of root mucilage and modelled root exudates on soil structure. *European Journal of Soil Science* **51**, 575-581.

Tyson, K.C., Scholefield, D., Jarvis, S.C. & Stone A.C. (1997) A comparison of animal output and nitrogen leaching losses recorded from drained fertilised grass and grass/clover pasture. *Journal of Agricultural Science* **129**, 315-323.

van Genuchten, M.T., (1980) A closed-form equation for predicting the hydraulic conductivity of unsaturated soils. *Soil Science Society of America Journal* **44**, 892-898.

Vogel, H.-J. & Kretzschmar, A. (1996) Topological characterization of pore space in soil - sample preparation and digital image-processing. *Geoderma* **73**, 23-38.

Vogel, H.-J. (1997) Morphological determination of pore connectivity as a function of pore size using serial sections. *European Journal of Soil Science* **48**, 365-377.

Vogel, H.-J. & Roth, K. (2001) Quantitative morphology and network representation of soil pore structure. *Advances in Water Resources* **24**, 233-242.

Vogel, H.-J. & Roth, K. (2003) Moving through scales of flow and transport in soil. *Journal of Hydrology* **272**, 95-106.

Wardlaw, N.C., Li, Y. & Forbes, D., (1987) Pore-throat size correlation from capillary pressure curves. *Transport in Porous Media* **2**, 597-614.

Wetzel R. G. and Likens G. E. (1991) *Limnological Analyses*, 2nd ed. Springer-Verlag, New York, pp. 84-87. Cited In: Hubble & Harper (2000).

Whalley, W.R., Leeds-Harrison, P.B., Clark, L.J. & Gowing, D.J.G. (2005) Use of effective stress to predict the penetrometer resistance of unsaturated agricultural soils. *Soil & Tillage Research* **84**, 18-27.

White, R.E. (1997) 3rd ed. *Principles and Practice of Soil Science, Soil as a Natural resource.* Blackwell Science, London.

Whitehead, R. (1999) *The UK Pesticide Guide 1999.* CABI Publishing University Press, Cambridge.

Williams, A., Scholefield, D., Dowd, J., Holden, N. & Deeks, L. (2000) Investigating preferential flow in a large intact soil block under pasture. *Soil Use and Management* **16**, 264-269.

Williams, A.G., Dowd, J.F., Scholefield, D., Holden, N.M. & Deeks, L.K. (2003) Preferential flow variability in a well-structured soil. *Soil Science Society of America Journal* **67**, 1272-1281.

Williams, I. (2001) *Environmental Chemistry: A Modular Approach.* John Wiley & Sons Ltd, Chichester, UK.

Withers, P.J.A., Edwards, A.C. & Foy, R.H. (2001) Phosphorus cycling in UK agriculture and implications for phosphorus loss from soil. *Soil Use and Management* **17**, 139-149.

Witty, J.F. (1998) A rapid method for measuring the porosity of soils and other materials. Patent Application to be submitted by Urquhart-Dykes and Lord.

Wood, M. (1996) Nitrogen fixation: How much and at what cost? In: Younie, D. (Ed.) *Legumes in Sustainable Farming Systems. British Grassland Society Occasional Symposium* No. 30. BGS. pp. 26-35.

Worsfold, P.J., Gimbert, L.J., Mankasingh, U., Omaka, O.N., Hanrahan, G., Gardolinski, P.C.F.C., Haygarth, P.M., Turner, B.L., Keith-Roach, M.J. & Mckelvie, I.D. (2005) Sampling, sample treatment and quality assurance issues for the determination of phosphorus species in natural waters and soils. *Talanta*, **66**, 273-293.

Wright, S.F. & Upadhyaya, A., (1998) A survey of soils for aggregate stability and glomalin, a glycoprotein produced by hyphae of arbuscular mycorrhizal fungi. *Plant & Soil* **198**, 97–107.

Wright, A.L. & Hons, F.M. (2005) Tillage impacts on soil aggregation and carbon and nitrogen sequestration under wheat cropping sequences. *Soil & Tillage Research* **84**, 67-75.

Young, I.M., Crawford, J.W. & Rappoldt, C. (2001) New methods and models for characterising structural heterogeneity of soil. *Soil and Tillage Research* **61**, 33-45.

Young, I.M. & Crawford, J.W. (2004) Interactions and self-organisation in the soil–microbe complex. *Science* **304**, 1634–1637.

Zehe, E. & Flühler, H. (2001) Preferential transport of isoproturon at a plot scale and a field scale tile-drained site. *Journal of Hydrology* **247**, 100-115.

Zhang, J-Z. (1997) Distinction and quantification of carry-overand sample interaction in gas segmented continuous flow analysis. *Journal of Atomic Chemistry* **19**, 205-212.

Zhang, J-Z., Fischer, C.J. & Ortner, P.B. (1999) Optimisation of performance and minimization of silicate interference in continuous flow phosphate analysis. *Talanta* **49**, 293-304.

Zhang, J-Z. (2000) Shipboard automated determination of trace concentrations of nitrite and nitrate in oligotrophic water by gas-segmented continuous flow analysis with a liquid waveguide capillary flow cell. *Deep-Sea Research* **47**, 1157-1171.

Zhang, B., Horn, R. (2001) Mechanisms of aggregate stabilization in Ultisols from subtropical China. *Geoderma* **99**, 123-145.

Zhu, J.T., Mohanty, B.P., Warrick, A.W. & van Genuchten, M.T. (2004) Correspondence and upscaling of hydraulic functions for steady- state flow in heterogeneous soils. *Vadose Zone Journal* **3**, 527-533.

COPYRIGHT STATEMENT

This copy of the thesis has been supplied on condition that anyone who consults it is understood to recognise that its copyright rests with its author and that no quotation from the thesis and no information derived from it may be published without the author's prior consent.
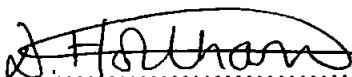
AUTHOR'S DECLARATION

At no time during the registration for the degree of Doctor of Philosophy has the author been registered for any other University award.

This study was financed with the aid of a studentship from both the University of Plymouth and the Institute of Grassland and Environmental Research.

Seminars and conferences were regularly attended throughout the period of study at which research was regularly presented. Consultation with other institutions occurred and several publications are to be prepared.

<div align="right">Word Count: 45,253</div>

Signed..

<div align="right">Deborah Anne Lydia Holtham

July, 2006</div>

DEDICATION

Dedicated to my father, my mentor, my coach, my idol, my hero, my family's teacher, my mum's best friend and the funniest man I have ever known. I miss you everyday, but always try to make you proud.

PROFESSIONAL DEVELOPMENT

COURSES AND TRAINING

Laboratory based Teaching Methods and Practice (ENV 5101), Dr Dave Harwood, University of Plymouth, November 2000, Plymouth, UK.

Research Skills (IMS 5101), 2000-2001, University of Plymouth, UK.

Research Methods (EAR 5101), 2000-2001, University of Plymouth, UK.

Technical Writing, Dr David Cooke, ADAS, 10-12 September 2001, IGER, Aberystwyth, UK.

Presentational Skills, Dr David Cooke, ADAS, 12-14 September 2001, IGER, Aberystwyth, UK.

Database Training, Steve Smith, IGER Librarian, 25 October 2001, IGER, North Wyke, UK.

Statistical Methods, Dr Hayley Randle, University of Plymouth, Seale-Hayne Faculty, 15 November – 13 December 2001, IGER, North Wyke, UK.

Excel (Advanced), Jez Fairclough, Dependon Quality Solutions, 17-18 December 2001, Bristol, UK.

Personal Effectiveness, Bob Mawer, BBSRC Training Officer, 10 January 2002, IGER, North Wyke, UK.

First Aid, British Red Cross, 10 April 2002, IGER, North Wyke, UK.

Bioinformatics, Dr Helen Ougham, Cell Biology, IGER, Aberystwyth, 18 April 2002, IGER, North Wyke, UK.

Manual Handling, Mr Roger Field, Technical Services, IGER, North Wyke, 15 May 2002, IGER, North Wyke, UK.

Trailers and Towing, Mr Chris Pope, Devon County Council, Devon Drivers Centre, 24 May 2002, IGER, North Wyke, UK.

4 x 4 Vehicle Training, Devon County Council, Devon Drivers Centre, 9 July 2002, IGER, North Wyke, UK.

Kinetic Handling, Mr John Studley, J.H.W. Training, 14 November 2002, IGER, North Wyke, UK.

Animal Handling, 14 November 2002, IGER, North Wyke, UK.

Soil Coring, 14 November 2002, IGER, North Wyke, UK.

Microsoft Outlook, Mr Tom Morgan, T.C. & P. Consultancy Ltd., 18 November 2002, IGER, North Wyke, UK.

Microsoft Word (Intermediate), Mr Tom Morgan, T.C. & P. Consultancy Ltd., 21 November 2002, IGER, North Wyke, UK.

Microsoft Word (Advanced), Mr Tom Morgan, T.C. & P. Consultancy Ltd., 22 November 2002, IGER, North Wyke, UK.

All Terrain Vehicles, Lantra Awards 31 January 2003, IGER, North Wyke, UK.

Visual Basic, 8-9 April 2003, IGER, North Wyke, UK.

Data-logging, Ian Oaks Green, Campbell Scientific, Inc., 15-16 April 2003, IGER, North Wyke, UK.

Soil Ecology: Linking Theory to Practice, Wageningen Graduate Schools Functional Ecology (FE), Socio-Economic and Natural Sciences of the Environment (SENSE) and Production Ecology and Resource Conservation (PE & RC), 15-21 June 2003, Wageningen, The Netherlands.

Laboratory Training Skills, Michael Gilford, Plymouth College of Further Education, 4-5 September 2003, Plymouth, UK.

CONFERENCES, SEMINARS AND PRESENTATIONS

University of Plymouth Coursework, *Research Skills* (IMS 5101), 7 November 2000, Plymouth, UK. **Oral Presentation.**

University of Plymouth Coursework, *Laboratory based Teaching Methods and Practice* (ENV 5101), November 2000, Plymouth, UK. **Laboratory Demonstration.**

IGER Workshop, *Modelling and Scaling*, 5-6 December 2000, Aberystwyth, UK. **Attended.**

International conference organised by Scottish Executive Rural Affairs Dept and the British Society of Soil Science, *Environmental Flows: are there key scales for solute and pollutant transport?* 26-27 March 2001, Westpark Centre, Dundee, UK. **Attended.**

University of Plymouth Environmental Research Centre, Aquatic and Fluid Monitoring and Modelling Seminars, 16 May 2001, Plymouth, UK. **Oral Presentation.**

International symposium organised by Institut de Recherche pour le Développement (IRD), in memoriam of Michel Rieu, *Soil Structure, water and solute transport*, 8-10 October 2001, Paris, Ile de France, Paris, **Attended.**

Society of Chemical Industry (SCI), Agriculture and Environment Group conference, *Soil fertility in organic farming*, 13 November 2001, London, UK. **Poster Presentation.**

IGER, Annual Tour of Experiments, 26 November 2001, North Wyke, UK. **Glasshouse Demonstration.**

IGER / Silsoe Colloquium, 12 December 2001, Silsoe Research Institute, Silsoe, UK. **Oral Presentation.**

North Wyke Research Station Winter Seminars, 7 February 2002, IGER, North Wyke, UK. **Oral Presentation.**

University of Plymouth Environmental Research Centre, Aquatic and Fluid Monitoring and Modelling Seminars, 28 February 2002, Plymouth, UK. **Oral Presentation.**

Aquatic and Fluid Monitoring and Modelling Seminars, *Journal Review Club*, 14 March 2002, University of Plymouth Environmental Research Centre, Plymouth, UK. **Oral Presentation.**

Visit from Dr John Sherlock, Science Directorate, DEFRA, 2 July 2002, IGER, North Wyke. **Glasshouse Demonstration.**

Fourth International Symposium on Ecosystem Behaviour – *BIOGEOMON*, 17-21 August 2002, University of Reading. 23 August 2002, North Wyke, UK. **Glasshouse Demonstration.**

British Society of Soil Science September conference, *Soils and Environmental Quality*, Seale-Hayne Faculty, University of Plymouth, and North Wyke Research Station, 9-11 September 2002, Newton Abbot, UK. **Oral Presentation.**

British Society of Soil Science, September conference, *Soils and Environmental Quality*, Seale-Hayne Faculty, University of Plymouth, and North Wyke Research Station, 10 September 2002, North Wyke, UK. **Glasshouse Demonstration.**

British Society of Soil Science, September conference, *Soils and Environmental Quality*, Seale-Hayne Faculty, University of Plymouth, and North Wyke Research Station, 11 September 2002, *Soil Degradation under intensive management in Devon and Somerset*, lead by Dr Tim Harrod, National Soils Resources Institute (NSRI) and The Environment Agency. **Attended Field Visit.**

IGER Post-Graduate Seminar Day, 13 November 2002, North Wyke, UK. **Oral Presentation.**

School of Earth, Ocean and Environmental Sciences Research Seminars, University of Plymouth, 20 November 2002, Plymouth, UK. **Oral Presentation.**

British Soil Water Physics Group meeting, *Investigation and Manipulation of Soil Structure*, 1 May 2003, Plymouth, UK. **Oral Presentation.**

A meeting for the Environment Agency, 3 July 2003, North Wyke, UK. **Glasshouse Demonstration.**

A meeting for stakeholders, LEGGRAZE, *Role of legumes in sustainable farming*, 10 July 2003, North Wyke, UK. **Glasshouse Demonstration.**

A meeting for IGER stakeholder, 28 July 2003, North Wyke, UK. **Glasshouse Demonstration.**

Seventh BGS Research Conference, British Grassland Society and Germinal Holdings Ltd., 1-3 September 2003, University of Wales, Aberystwyth, UK. **Poster Presentation.**

Seventh BGS Research Conference, British Grassland Society and Germinal Holdings Ltd., 3 September 2003, Aberystwyth, UK. **Attended Farm Visit.**

South West Modelling Group meeting, *Environmental interests in the South West in all three media – water, land and air*, 15 October 2003, University of Plymouth, UK. **Poster Presentation.**

Society of Chemical Industry (SCI), Agriculture and Environment Group conference, *Practical Soil Management*, 21 October 2003, London, UK. **Poster Presentation.**

Special reception organised by Science, Engineering and Technology for Europe, NERC and EPSRC, *Taking UK Chemistry Research and R & D to Parliament – Britain's Younger Chemists, Chemical Engineers and Technologists,* 10 November 2003, House of Commons, London, UK. **Poster Presentation.** *(Included in the best top ten presentations, research to be included in publication/flyer).*

South-East England Soil Discussion Group Winter Meeting, *Soil Health and Quality,* 18 December 2003, Rothamsted, UK. **Oral Presentation.**

IGER Germinal Holdings Ltd. meeting, 13-14 January 2004, North Wyke, UK. **Glasshouse Demonstration.**

School of Earth, Ocean and Environmental Sciences Inter-subject Research Group Forum, *Diffuse Pollution.* 4 February 2004. Nutrient leaching beneath white clover. The implications for organic farming. **Oral Presentation.**

South West England Soils Discussion Group, *Soils and microbial contaminants – soil quality and transfers from soil to water,* 18 February 2004, Seale-Hayne Campus, University of Plymouth, Newton Abbot, UK. **Attended.**

University of Plymouth Modelling seminars, 24 March 2004, Plymouth, UK. **Oral Presentation.**

British Society of Soil Science, Easter meeting, *Recent Advances in Soil Science,* 5-7 April 2004, University of Nottingham, Sutton Bonington Campus, UK. **Oral Presentation.**

ESRC/NERC Marine and Coastal Policy Research Group Meeting, *The analysis of societal causes and impacts on the marine environment, Seminar Two: Agriculture,* 17-18 May 2004, Plymouth, UK. **Oral Presentation**

Plant Genetics and Nitrogen Leaching Workshop, 10-11 November 2004, IGER, Aberystwyth, UK. **Oral Presentation.**

BBSRC New Scientists Conference, *BBSRC at 10 – The Next Generation,* 22-23 November 2004, London, UK. **Attended.**

IGER/CSG legume project, *Plant genetics of clover and nitrogen leaching,* 11 November 2004. **Oral Presentation.**

South West England Soils Discussion Group, *Soil Function, Quality and Indicators – Useful Concepts?,* University of Plymouth, 3 February 2006. **Attended**

MISCELLANEOUS ACHIEVEMENTS

Laboratory based Teaching Methods and Practice Coursework (ENV 5101), 30 November 2000, University of Plymouth, UK.

Research Monitoring: 6 monthly reviews, 2001 - 2004, Dr Bob Clements, Deputy Head of North Wyke Research Station, IGER, North Wyke, UK.

Lecturer and assistant to lecturer for 1st year Environmental Science B.Sc. laboratory practical sessions. Demonstrated laboratory techniques and marked coursework. February - March 2002, University of Plymouth, Plymouth, UK.

Postgraduate Meeting, 20 February 2002, Annual Meeting, IGER North Wyke.

School's Science Week at IGER, 11-15 March 2002, North Wyke, UK. Demonstrated agricultural practices that cause phosphate water pollution.

Work Experience, July 2002, One-week supervision of two AS level students, IGER North Wyke.

Gold Crest Award, August 2002, Four weeks supervision of AS level student, IGER North Wyke.

Soil Science and Environmental Quality Group Meeting, 27 September 2002, IGER North Wyke and Aberystwyth group members, IGER North Wyke, UK.

Assistant to lecturer for 1st year Environmental Science B.Sc. laboratory practical sessions. Assisted with laboratory practical. October - November 2002, University of Plymouth, Plymouth, UK.

University of Plymouth / Silsoe Colloquium, 11 October 2002, Wrest Park Research Institute, Silsoe, UK.

Wrote conference review for British Society of Soil Science (News letter 42), Ref: Society of Chemical Industry (SCI), Agriculture and Environment Group conference, *Practical Soil Management*, 21 October 2003, London, UK.

Laboratory demonstration to Astra Zeneca, University of Plymouth, 9 February 2004.

South West England Soils Discussion Group, Annual General Meeting, 18 February 2004, Seale-Hayne Campus, University of Plymouth, Newton Abbot, UK.

Participated in 1st year Environmental Science B.Sc. Field Week (EVTQ 102), *Soil analysis at Seale-Hayne Farm, Newton Abbot, UK*. Demonstrated field techniques and assessed presentations. April 2004.

Exeter school visit, GCSE students. 8 May 2004, IGER, North Wyke, UK.

University of Plymouth / Thermo Electron Corporation business meeting, 27 May 2004, Plymouth, UK.

Carlton Television News Broadcast, 22 June 2003. http://www.pore-cor.com/latest_news.htm

Assisted with 3rd year Environmental Science B.Sc. field trip (ENV 311). 12 January 2004. Institute of Grassland and Environmental Research, North Wyke, Okehampton.

Assisted with 1st year Environmental Science B.Sc. field trip (EVTQ 102). 29 March – 1 April 2004. Seale Hayne, University of Plymouth.

Research advice to Plymouth Environmental Geochemistry, University of Plymouth, 29 September 2004.

International Pore-Cor Training Course, University of Plymouth, 6-7 October 2004. Oral presentations and demonstrations of software.

Pore-Cor monthly business meetings, University of Plymouth Enterprise Ltd, November 2004 – Present.

International Pore-Cor Training Course, University of Plymouth, 6-8 April 2005. Oral presentations and demonstrations of software.

International Pore-Cor Training Course, University of Plymouth, 5-7 October 2005. Oral presentations and demonstrations of software.

Interview for "The Furrow" (a John Deere publication), 8 November 2005.

International Pore-Cor Training Course, Interscience Belgium, 13-14 June 2006. Oral presentations and demonstrations of software.

MEMBERSHIP OF PROFESSIONAL ORGANISATIONS

Society of Chemical Industry (SCI)

British Grassland Society (BGS)

British Society of Soil Science (BSSS)

SUPERVISORY TEAM

Dr Peter Matthews

Environmental and Fluid Modelling Group

School of Earth, Ocean and Environmental Sciences

University of Plymouth

Plymouth

Devon

PL4 8AA

UK

Tel: 01752 233021

pmatthews@plymouth.ac.uk

Professor David Scholefield

Soil Science and Environmental Quality

Institute of Grassland and Environmental Research

North Wyke

Okehampton

Devon

EX20 2SB

UK

Tel: 01837 883500

david.scholefield@bbsrc.ac.uk

Dr Ann Cresswell (RETIRED)

Biodiversity Group

Institute of Grassland and Environmental Research

Plas Gogerddan

Aberystwyth

Wales

SY23 3EB

UK